Evolution, competition and cooperation in bacterial populations

Thomas Julou

THOMAS JULOU

EVOLUTION, COMPETITION AND COOPERATION IN BACTERIAL POPULATIONS

THÈSE DE DOCTORAT DE L'ÉCOLE NORMALE SUPÉRIEURE
Spécialité Biologie

École Doctorale Interdisciplinaire Européenne Frontières du Vivant

Présentée par

THOMAS JULOU

pour l'obtention du grade de

Docteur de l'École Normale Supérieure

EVOLUTION, COMPETITION AND COOPERATION IN BACTERIAL POPULATIONS

Soutenue le 9 juin 2011 devant le jury composé de :

Rapporteur	DIDIER CHATENAY, Université Pierre & Marie Curie
Rapporteur	IVAN MATIC, Université Paris Descartes
Examinateur	SAM BROWN, Edinburgh University
Examinateur	PIERRE CORNELIS, Vrije Universiteit Brussel
Invité	NICOLAS DESPRAT, École Normale Supérieure
Directeur de thèse	DAVID BENSIMON, École Normale Supérieure

Final printed version as of June 14, 2011.

ABSTRACT

The interplay of environment, heritability, and stochasticity results in the development of different individuals starting from a given genotype. This phenotypic variability affects how natural selection acts on genetic variability. From a general perspective, I aim at studying the impact of phenotypic variability on adaptive dynamics.

In the first chapter, I report on the design of an evolutionary experiment in a structured environment using *Escherichia coli*. The trait under selection is resistance to high temperature. In particular, we study the effects of high temperature on chemotaxis, as well as the impact of acclimation on growth and survival at high temperature.

The second chapter is about the development of a microbial population measurement device dedicated to diluted populations. This continuous, non-invasive measurement has a low detection limit that depends on the species. For the model species *E. coli*, the limit is ca. $5 \cdot 10^3$ mL^{-1} which represents a 100-fold improvement compared to classical photometric methods.

In the third chapter, we study the distribution of pyoverdine between individuals of a clonal population of *Pseudomonas aeruginosa*. The variability of the concentration of this siderophore is much greater than expected. Although pyoverdine is considered to be a public good, neither spatial heterogeneity nor heritability provide a meaningful description of the variability. Instead we characterize rapid fluctuations in pyoverdine concentration, and propose a model based on a phenotypic switch in pyoverdine metabolism that is in good agreement with the experimental data.

Keywords: adaptation, phenotypic variability, bacteria, high temperature, spatial structure, cell counting, pyoverdine

AFFILIATION

Laboratoire de Physique Statistique
École Normale Supérieure
24, rue Lhomond - 75 005 Paris

RÉSUMÉ

Les différents facteurs que sont l'environnement, l'héritabilité et la stochasticité contribuent au développement d'individus différents à partir d'une information génétique donnée. Cette variabilité phénotypique modifie l'action de la sélection naturelle sur la variabilité génétique. Un fil conducteur de ce travail est l'étude de l'impact de la variabilité phénotypique sur les dynamiques d'adaptation.

Le premier chapitre expose la conception d'une expérience d'évolution de *Escherichia coli* dans un environnement structuré. Le trait sélectionné est la resistance aux hautes températures. En particulier, nous étudions les effets de la température sur le chimiotactisme ainsi que l'impact de l'acclimatation sur la croissance et la survie à haute température.

Le deuxième chapitre porte sur la réalisation d'un dispositif de mesure de population microbienne à basse concentration. Cette mesure est continue et non invasive et sa limite de détection varie selon l'espèce. Pour l'espèce modèle *E. coli*, la limite est environ $5 \cdot 10^3$ mL^{-1} soit une amélioration d'un facteur 100 par rapport à la photométrie classique.

Dans le troisième chapitre, nous étudions la distribution de la pyoverdine entre les individus d'une population clonale de *Pseudomonas aeruginosa*. La variabilité de la concentration de ce sidérophore considéré comme un "bien commun" est beaucoup plus grande que celle attendue et ne peut être expliquée en terme de répartition spatiale ou d'héritabilité. Après avoir caractérisé des fluctuations rapides de la concentration en pyoverdine, nous proposons un modèle de *switch* phénotypique dans le métabolisme de la pyoverdine qui est en très bonne adéquation avec les observations.

Mots clés : adaptation, variabilité phénotypique, bactérie, haute température, structure spatiale, comptage cellulaire, pyoverdine

REMERCIEMENTS

Je suis reconnaissant à Didier Chatenay, Ivan Matic, Sam Brown et Pierre Cornélis d'avoir accepté d'évaluer ce travail, et les remercie pour la pertinence de leurs suggestions et commentaires.

Ces années de thèse constituent une aventure scientifique et humaine très formatrice. A ce titre, je tiens à remercier David Bensimon pour son encadrement empreint de confiance et d'optimisme et Nicolas Desprat, exemple d'enthousiasme et de persévérance. J'ai aussi eu la chance de travailler avec Vincent Croquette qui a eu assez de pédagogie et de patience pour enrichir les horizons du biologiste que je suis d'un peu d'électronique, de conception mécanique, de traitement du signal… et j'en oublie ! Et je remercie tous les membres de l'équipe pour avoir contribué à cette ambiance de travail détendue et chaleureuse si appréciable ; avec une pensée gourmande pour les repas de Noël orchestrés de main de maître par notre chef attitré, Jean-François Allemand.

Plusieurs collaborateurs ont notablement enrichi mon travail de thèse et je les en remercie : Jonathan Saragosti pour les expériences en microfluidique sur le chimiotactisme, Isabelle Schalk et Laurent Guillon pour m'avoir initié aux subtilités du métabolisme de la pyoverdine, et Thierry Mora pour sa contribution à l'interprétation de nos résultats expérimentaux sur la variabilité de la pyoverdine. D'autres personnes m'ont beaucoup aidé en partageant leurs compétences, leurs connaissances et leurs résultats : David Bikard, Nabil Garroum, Stéphane Guyot, José Quintas, Lydia Robert, François Taddéi pour ne citer qu'eux. Ma curiosité et ma culture scientifiques ont aussi été nourries par les échanges avec de nombreux collègues, professeurs et amis ; parmi eux Timothée Flutre, Karim Barkati, Jean-Yves Bansard, Konrad Hinsen et Michel Morange.

Le Centre de Recherches Interdisciplinaires et l'école doctorale qu'il héberge ont été tout au long de ma thèse des lieux privilégiés d'échanges et de rencontres. Que tous ceux qui contribuent à leur donner vie soient ici remerciés !

Je porte une reconnaissance toute particulière à ceux qui m'ont aidé à persévérer en m'offrant une oreille attentive et des conseils enthousiastes dans les moments difficiles, en particulier Grégory Paul, Pascal Hersen et Andrew Murray. Je remercie aussi Boris Shraiman pour m'avoir offert la possibilité de rédiger la première partie de ce manuscrit dans le cadre extrêmement propice de la conférence "Microbial and Viral Evolution" au KITP de Santa Barbara.

Sur le plan personnel, je remercie beaucoup Romaric Rifleu et les amis d'Ameno Uki Ashi qui m'ont aidé à avancer vers un équilibre, du corps et de l'esprit. Un grand merci à mes parents et à mes amis pour les éclats de rire, les bouteilles partagées, et quelques virées inoubliables !

Enfin, je remercie Claire qui enrichit chaque jour et chaque idée de leurs indispensables nuances.

ON THIS THESIS LAYOUT

This thesis was typeset with LaTeX 2ε using the `classicthesis` style by Andre Miede. This typographic style was inspired by Bringhurst's recommendation as presented in *The Elements of Typographic Style*. Most plots have been produced with R using the `ggplot2` package by Hadley Wickham. This is an implementation of *The Grammar of Graphics* from Leland Wilkinson.

I am warmly grateful to the developers of these packages for providing such powerful, elegant, open-source tools.

CONTENTS

LIST OF FIGURES

LIST OF TABLES

ACRONYMS

TECHNICS AND MODELS

CLT	central limit theorem
CTMI	cardinal temperature model with inflexion
GSL	GNU scientific library
OD	optical density
PIV	particle image velocimetry
SEM	standard error of the mean

BIOLOGICAL COMPOUNDS

ECF-σ	extracytoplasmic function sigma factor
GFP	green fluorescent protein
MCP	methyl-accepting chemotaxis protein
NRP	non-ribosomal peptide
NRPS	non-ribosomal peptide synthetase
HSP	heat shock protein

GROWTH MEDIA

CAA	Casamino acids medium
DM	Davis minimal medium
LB	Luria Bertani rich medium
SMM	succinate minimal medium
YNB	yeast nitrogen base
YPD	yeast peptone dextrose

CHEMICALS

GNP	gold nanoparticle
PDMS	polydimethylsiloxane
PI	propidium iodide

ELECTRONICS

ADC	analog-to-digital converter
LED	light emitting diode
PID	proportional-integral-derivative
PWM	pulse-width modulation
TEC	thermoelectric cooler

FOREWORD

In general, the characteristics observed in individuals (*phenotype*) result from the expression of their genes (*genotype*) conditioned by environmental conditions (*environment*) and random effects (*stochasticity*). Importantly, environmental and stochastic effects interact in producing phenotypes out of a given genotype.

The environmental conditions can change in time and/or along space. In fluctuating environments, the phenotype of an individual with a given genotype may vary with time through a process called acclimation. In spatially heterogeneous environments, clonal individuals at different places can potentially express different phenotypes. In addition, in all conditions, the stochasticity of biochemical reactions (e.g. gene expression) is another source of variability between clonal individuals.

The variations in phenotypes, be they stochastic or due to the environment, can be inherited from one generation to the next. Although this is not a long lasting effect, it makes the distribution of phenotypes even more complex since parameters are history-dependent. More generally, the history of individuals, including for instance their interactions with others, can affect their phenotypes. Overall, since natural selection acts on phenotypes, studying these sources of phenotypic variations is central in order to understand better the mechanisms of adaptation.

This thesis is written as three independent chapters. In the first chapter, I report on the design of an evolutionary experiment in a spatially structured environment. A strong emphasis is given to the identification of the different biological issues adressed in the experiment (in particular in terms of acclimation) and to how they can be disentangled. In the second chapter, I describe a new microbial population density measurement device dedicated to diluted populations. This is an extension of the project presented in the first chapter. Finally, in the third chapter, I focus on interactions in microbial populations and study the variability in the access to public goods between individuals.

Chapter 1

ON THE INTERPLAY BETWEEN ACCLIMATION AND ADAPTATION: EVOLUTION IN A TEMPERATURE GRADIENT

1.1 INTRODUCTION

In evolutionary biology, *adaptation* refers to the process occurring as a result of natural selection. Due to random mutations, individuals in a population exhibit slightly different phenotypes and corresponding abilities to reproduce. Given a set of environmental constraints, those with higher reproductive rates will be advantaged and their relative abundance will increase in proportion. Consequently, adaptation occurs over several generations and gives rise to heritable genetic changes that will in turn produce modified phenotypes (Smith, 1998).

In contrast, *acclimation* (sometimes spelled *acclimatization*) refers to reversible, nongenetic changes in phenotype that are induced by specific environmental conditions; it is a particular case of phenotypic plasticity observed in response to environmental changes (Bennett and Lenski, 1997). The phenotypic changes are understood as the result of rapid modifications of metabolic regulations, thanks to modified gene expression or enzymatic activity for instance. It can occur within the individuals lifetime or can last for a few generations when changes are heritable.

A well-known example in humans illustrates these two responses: during short or intermittent exposure to high altitude, variations in blood volume and erythropoietic activity allow to face reduced oxygen availability due to lower atmospheric pressure (Schmidt, 2002). While this response is observed in all populations, similar traits are observed as the result of heritable genetic changes in those who have settled at high altitude (over 4000 m) for long times (Bigham et al., 2010; Yi et al., 2010). Similar adaptation has been analyzed in details in other mammals: in deer mice, balanced polymorphism is reported at duplicated globin genes loci and hemoglobin of deer mice living at higher altitude has higher affinity for oxygen (Storz et al., 2009).

Similarly, when bacteria are exposed to antibiotics, resistance arises both from acclimation and adaptation mechanisms. *Pseudomonas aeruginosa* is naturally resistant to a broad range of antibiotics thanks to very efficient efflux pumps that drive chemicals out of the cell. The expression of certain efflux pumps is inducible and increases in presence of antibiotics (Jeannot et al., 2005). However, heritable resistance can also be acquired by mutation or horizontal gene transfer. These adaptive modifications take place over generations and confer most of the time either a higher constitutive expression of efflux pumps or a new enzymatic function allowing to degrade chemicals (Andersson and Hughes, 2010).

In this study, we focus on microbes and in particular on the most studied bacteria, *Escherichia coli*, as it provides a very powerful model organism for ecological, evolutionary and functional approaches: its rapid growth and small size allow to study large populations over a large number of generations while at the cellular level molecular tools are well de-

veloped. In addition, we choose high temperature as an experimental selective pressure since it has a marked effect on several phenotypic traits in bacteria. As stated by Hickey and Singer (2004),

> "while variations in environmental temperature share many of the characteristics of other environmental variables, temperature is special because of its pervasiveness: it can penetrate physical barriers and can have dramatic effects on the structure of virtually all macromolecules."

From a practical point of view, temperature is easily regulated in culture devices, and linear gradients establish spontaneously by heat diffusion between two sources.

In order to be able to describe accurately adaptation to different temperature regimes, let me introduce the notion of thermal niche in the next paragraphs. Following the concept of ecological niche, a thermal niche is defined as the range of temperatures where a species can maintain itself and reproduce. In microbes, we follow the definition that restricts this notion to the range of temperatures where the species can maintain itself (Bennett and Lenski, 1993). In this case, the thermal niche is summed up by the quantitative dependance of growth rate on temperature. This relationship can be satisfactorily approximated in most cases using three parameters referred to as cardinal temperatures: minimal, maximal and optimal growth temperatures.

Temperature affects bacteria phenotypes in two main ways:

– Within the thermal niche, the dominant effect is the dependance of growth rate on temperature. Several models have been proposed to describe this relationship. The cardinal temperature model with inflexion (CTMI) is a popular one that only takes the cardinal temperatures (T_{min}, T_{max}, T_{opt}) and maximal growth rate at optimal temperature (γ_{opt}) as parameters (Fig. 1.1; Rosso et al., 1993). The maximal growth rate γ at a given temperature T writes

$$\gamma = \max\Big(0, \frac{\gamma_{\text{opt}}(T-T_{\text{max}})(T-T_{\text{min}})^2}{(T_{\text{opt}}-T_{\text{min}})\big((T_{\text{opt}}-T_{\text{min}})(T-T_{\text{min}})-(T_{\text{opt}}-T_{\text{max}})(T_{\text{opt}}+T_{\text{min}}-2T)\big)}\Big).$$

  Interestingly, the optimal growth temperature of *E. coli* isolated from human is higher than 37°C, its host's temperature.

– Above the thermal niche upper limit (that is the maximal growth temperature), temperature challenges survival. Due to high temperature damage, the bacterial population size decreases with time (Fig. 1.2 left); whether the decrease is exponential or not is still debated (Russell, 2003). However, this death rate increases rapidly with temperature (Fig. 1.2 right). In this field, the survival is usually described by two parameters. The decimal reduction time (D-value) is the time required at a given temperature to decrease 10

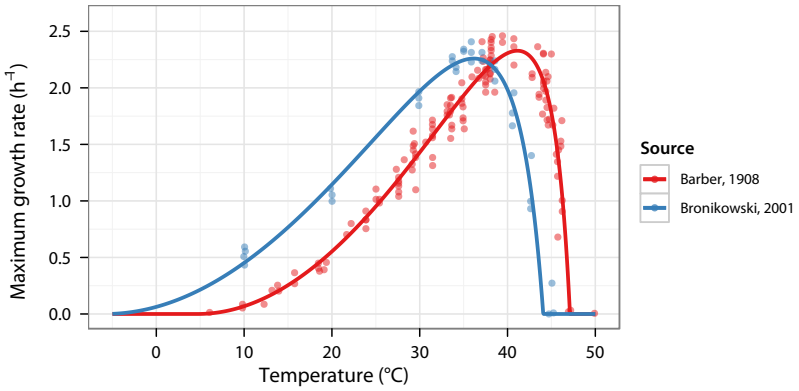

Figure 1.1: Maximum growth rate as a function of temperature in *E. coli*. Bacteria maximum growth rates are reported for a laboratory strain in beef peptone broth (Barber, 1908) and for natural isolates sampled at different seasons in ectothermic turtles and grown in LB (Bronikowski et al., 2001). For both datasets, the relationship is fitted to the CTMI model (Rosso et al., 1993) using the least square method implemented with Rgenoud (Mebane and Sekhon). Such model is very useful to describe adaptation to temperature as it allows to approximate the thermal niche using only four parameters.

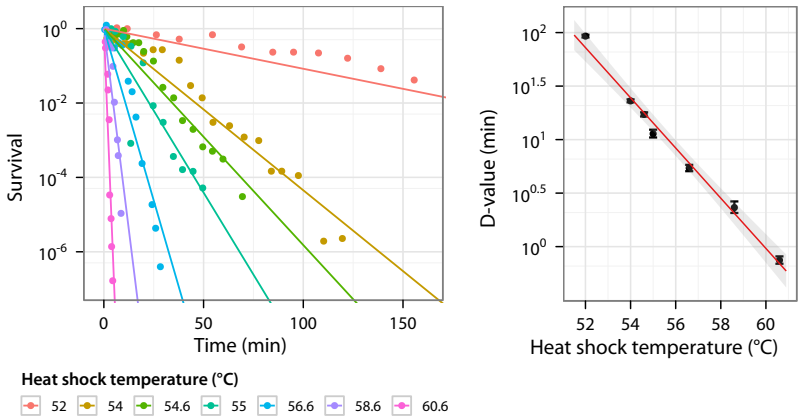

Figure 1.2: Survival of *E. coli* MG1655 at high temperature (using data from Valdramidis et al., 2006). Early stationary phase culture grown in LB is transfered to higher temperature and survival is measured as a function of time. Left: Proportion of surviving cells after transfer to high temperature, fitted exponentially and setting initial survival to 1. Right: Decimal reduction time (D-value) computed from the survival curves and plotted against temperature with an exponential fit.

times the population size. The z-value is the increase of the heat-shock temperature required to decrease 10 times the D-value. The relevance of the z-value is based on the hypothesis that the D-value decreases exponentially with temperature.

With both applied motivations (infection control, food safety, ...) and basic incentives (heat shock as a model of gene regulation), the interest for bacteria resistance to high temperature started as early as the beginning of the twentieth century. The impact of temperature on growth was examined both in mesophiles (Barber, 1908) and thermophiles (Casman and Rettger, 1933), while survival at relatively high temperature was described in *Bacillus* spp. (Elliker and Frazier, 1938). Although more and more descriptions are available and mechanisms are elucidated one after the other, a global understanding of the effects of high temperature on life history is still lacking. Noteworthily, a promising thermodynamics global approach has recently been proposed (Chen and Shakhnovich, 2010).

In broad outline, our project consists in evolving bacteria over a long time in a temperature gradient. Nutrients are delivered at the hottest point of the setup where growth is originally not possible so as to create an adverse nutrient gradient. This results in selection for growth and survival at higher temperature. In order to explicit the relevance of this experimental design, I review in the next sections (i) the importance of spatial structure in ecology and evolution, (ii) the impact of high temperature on bacteria physiology, and results from (iii) adaptation and (iv) acclimation experiments from the literature.

1.1.1 SPATIAL STRUCTURE IN ECOLOGY AND EVOLUTION

1.1.1.1 *Taking spatial structure into account in ecological and evolutionary descriptions*

Although all living systems are scattered over their environment, classic theoretical and modeling approaches do not take it into account when describing population dynamics and interactions. As pointed out by Dieckmann et al. (2000), this corresponds to a mean-field assumption that is most likely to hold as a good approximation when the physicochemical environment of organisms is homogeneous and

- physical forces exist that cause strong mixing of organisms, or
- organisms themselves are highly mobile, or
- organisms interact with others over long distances.

These three interaction conditions are violated in several natural systems, and the physical environment is often structured by patchiness or gradients. Let's review a few examples:

- One of the yeast natural habitats is fruits as they represent a large source of nutrients. While mean-field assumption may be reasonable within an overripe juicy fruit, overall population dynamics at the level of a tree cannot rely on it. Patchy environmental resources are also very common in pathogens and parasites since hosts are generally separated from each other.
- Environmental gradients are common in nature as they appear every time a diffusible resource (nutrient, light, heat, ...) is locally more concentrated. For instance, hot springs are punctual heat sources (Miller et al., 2009) while hydrothermal vents also bring hydrogen sulfide in the environment. Sometimes, the gradient can be produced by living organisms themselves as for light gradient observed in forests where the canopy layer intercepts most light and reduces light available for photosynthesis at the understory layer. Gradients can also occur when stress varies over space (heat, radiations, ...) as observed in desertification gradients.
- Several types of ecosystems do not fulfill the interaction conditions formulated above. In plant communities, individuals can only disperse from one generation to the next which results in a long lasting spatial organization. In microbial biofilms, individuals are part of large colonies developing on surfaces thanks to extracellular polymeric substance secretion. Consequently cells are no longer motile nor affected by medium flows.

As illustrated above, the spatial structure of the environment and that of communities are shaping each other. In general, at the level of individuals this results in increased local competition for resources and in repeated interactions between neighbours that must be taken into account to give an accurate ecological description. This can qualitatively change the nature of interactions over long times and thus affect evolutionary dynamics: while local competition between relatives can be detrimental to cooperation (Buckling et al., 2007), repeated interactions can contrarily favor it (Doebeli and Hauert, 2005).

It is noteworthy that taking spatial structure into account is even more important when considering long term dynamics, since rare events (long range dispersal, mutations in the interaction system, ...) may happen that can result in qualitatively different outcomes. This may be a caveat for theoretical approaches where evolutionary dynamics are derived from ecological dynamics: the ecological description may be relevant over short periods but misses some important features that are shaping the adaptive sequence in nature.

1.1.1.2 *Spatial structure in evolutionary experiments*

As far as experimental evolution is concerned, spatial structure is rarely taken into account as most experiments are run in well-mixed environments. It is probably considered to be an additional source of variability that is better kept as small as possible. Adaptation to minimal medium over 1000 generations has been compared between liquid medium and plates in *Comamonas* sp., revealing more diversity and higher divergence between replicates in structured environment (Korona et al., 1994). These differences are significant although of limited magnitude.

In addition, recent advances in microfluidics have allowed to manipulate the spatial availability of nutrients and have brought unexpected results on the ecological dynamics of *E. coli* stationary phase cultures (Lambert et al., 2011). This emphasizes the need to study evolutionary dynamics in spatially complex environments.

The most notable study of evolution in structured environments focuses on diversification in *Pseudomonas fluorescens*. When grown in static medium, *P. fluorescens* rapidly diversifies into three morphs specialized in different ecological niches (Rainey and Travisano, 1998). This has become a model system for the study of adaptive radiation (Jessup et al., 2004).

1.1.1.3 *Environmental gradients as a special case of spatial structure*

Allopatric speciation refers to individuals becoming two distinct species due to geographical isolation. By contrast, sympatric speciation occurs in the same habitat. It is common in bacteria due to horizontal gene transfers.

Among the various types of spatial structure, gradients are a special case that received particular attention (Ackermann and Doebeli, 2004; Doebeli and Dieckmann, 2003; Mizera and Meszena, 2003). In the study of geographical aspects of speciation, gradients are not a case of allopatric speciation but rather facilitate sympatric speciation. Models predict that this allows diversification when it would not occur in non-spatial models (Doebeli and Dieckmann, 2003). In this study, the slope of the gradient, i.e. the rate of temperature variation along space, appears as a critical parameter for facilitation, with intermediate slope being the most favorable for speciation. Moreover, natural populations of the cyanobacterium *Mastigocladus laminosus* sampled at different points of a temperature gradient around a geyser show clear signs of lineages differentiation indicating that sympatric diversification does occur along ecological selection gradients in nature (Miller et al., 2009).

SITE	DAMAGE
Outer membrane	Affected to some extent by high temperature
Cytoplasmic (inner) membrane	Severe damage (heat stability varies with melting point of cell lipids); cells become leaky; leakage precedes death
Ribosomes and ribosomal RNA	Degradation; precedes loss of viability
DNA	Single strand breaks, partly a consequence of nuclease activity; repaired in radiation-resistant but not -sensitive bacteria
Proteins	Denaturation, especially at high temperatures (possible aggregation)
Enzymes	Inactivation, especially at high temperatures

Table 1.1: Sites of damage in non-sporulating Gram-negative bacteria exposed to high temperature (after Russell, 2003).

1.1.2 IMPACT OF HIGH TEMPERATURE ON BACTERIA PHYSIOLOGY

In order to study the interplay between acclimation and adaptation to high temperature, it is important to know about the molecular mechanisms that are affected by temperature. Good starting points are the physiological differences observed when bacteria are grown at various temperatures or upon heat shock. In this section, I focus on *E. coli* to examine how bacterial components and metabolism are affected during acclimation and/or adaptation to high temperature.

1.1.2.1 *Effects of high temperature on cellular components*

When temperature is higher than the optimal growth temperature, both the cell envelope ensuring cell integrity and cytoplasmic molecules are affected. The main alterations are listed in Table 1.1 and reviewed in a clear and concise manner in Russell (2003). So far, there is no clear evidence for which damage is primarily responsible for cell death, if any. This may vary depending on temperature and other environmental conditions.

As we are interested in populations able to grow, we only consider the case of moist heat while the effects of dry heat may be notably different (Russell, 2003).

In bacteria, the cell envelope consists in one or two lipid membranes strengthened by a peptidoglycan cell wall and has a tightly regulated permeability. Temperature may affect various physical properties of this enveloppe such as its fluidity, its permeability and the bilayers conforma-

tional states (bilayer, inverted micelle, ...) as well as its chemical composition.

In heat shock experiments, the membrane fluidity increases with temperature as shown by measuring the lateral diffusion coefficients of lipids (Lindblom et al., 2002). Moreover sugars as trehalose form hydrogen bonds with lipid polar heads and stabilize the bilayer structure (Crowe et al., 1988), as do membrane proteins by increasing the rigidity of phospholipids alkyl chains (Denich et al., 2003). From a mechanical viewpoint, a temperature shift to 55°C damages the cell envelope of *E. coli* W3110 as surface blebs are observed, mainly at the septa of dividing cells. This results primarily in the destruction of the outer membrane permeability barrier and in the release of periplasmic molecules (Katsui et al., 1982; Tsuchido et al., 1985).

In *E. coli* grown at different temperatures, saturated phospholipids are more abundant at higher temperature (Marr and Ingraham, 1962). This results in higher packing of phospholipids and consequently balances the increase in membrane permeability expected due to higher temperature (Haest et al., 1969). In addition, as suggested by Morein et al. (1996), bacteria adjust their membrane composition depending on the temperature in order to keep a suitable structure. In particular, the protein content of the outer membrane differs between growth at 30°C and 42°C (Lugtenberg et al., 1976).

Proteins are another type of cellular components strongly affected by temperature: the conformation of proteins changes when temperature increases as hydrogen bonds formed with surrounding water molecules weaken (Vogt et al., 1997). For most proteins, unfolding is a reversible process that occurs already at temperatures lower than optimal growth temperature. Although this process is reversible, the unfolded proteins may be irreversibly inactivated whey they are recruited within large hydrophobic protein aggregates (Fig. 1.3).

Nucleic acids are also affected by high temperature. While ribosomal components are degraded early and probably not primarily involved in cell death, damages on DNA are abundant. Single strand breaks are produced either directly or by acceleration of the action of endogenous nucleases; they are repaired only in radiation-resistant strains.

These modifications of cellular components result both from direct effects of temperature (e.g. protein unfolding, nucleic acids damages, ...) and indirect effects that also involve changes in gene expression. The latter are described in the next section.

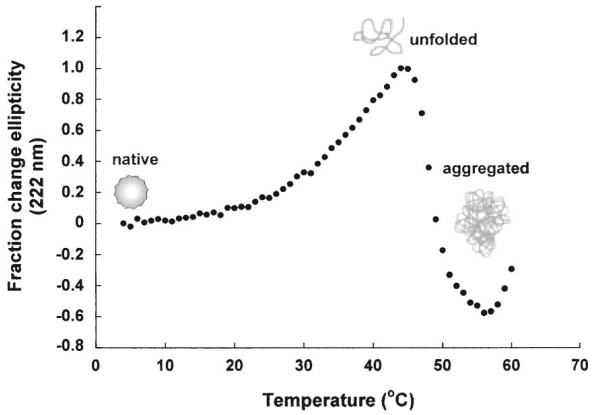

Figure 1.3: Thermostability of *E. coli* homoserine transsuccinylase (after Gur et al., 2002).
Homoserine transsuccinylase folding is strongly affected by temperature. Unfolding starts around 20°C. Above 44°C massive aggregation of this protein has been reported. Homoserine transsuccinylase (metA gene product) is the first enzyme of the methionine biosynthesis pathway. In absence of methionine, it is claimed to be the first enzyme limiting growth at high temperature (Gur et al., 2002) although van Derlinden et al. (2008) did not manage to reproduce this observation.

1.1.2.2 *Effects of high temperature on cellular metabolism and gene expression*

From a biochemical viewpoint, temperature variations affect the kinetics of all chemical reactions. The rate of a reaction k is related to the temperature T (expressed in kelvin) following Arrhenius law:

$$k = Ae^{-E_a/RT}$$

where E_a is the activation energy, R is the gas constant and A is a prefactor. This relationship provides an accurate description of enzymatic activity below the optimal growth temperature. Interestingly, the growth rate of *E. coli* depending on temperature can be described using Arrhenius law below the optimal growth temperature and this relationship is maintained in a number of different nutrient conditions (Monod, 1942). However in this case, the relationship is purely descriptive and should not be interpreted by hypothesizing that one master reaction is limiting growth.

Above the optimal growth temperature, enzymatic activity decreases primarily because of protein denaturation described in the previous section. Putting together the Arrhenius relationship at moderate temperature and the denaturation occurring at high temperature results in a

ACTIVITY	PROTEINS
Chaperone	DnaK, DnaJ, HtpG, ClpB, IbpA, IbpB, GroEL, GroES
Protease	ClpP, ClpX, Lon, ClpY, ClpQ, FtsH (metalloprotease)
Other	GapA (dehydrogenase), PrpA (phosphatase), GrpE (nucleotide exchange factor), σ^{70} (sigma factor), HtrM (epimerase), MetA (homoserine transsuccinylase)

Table 1.2: Major heat shock proteins (HSPs) of the σ^{32} regulon (after Yura et al., 2000). A detailed description of cellular functions is proposed in Riehle et al. (2003).

satisfying approximation of the enzymatic activity dependance to temperature over the thermal niche (Copeland, 2000; Guyot, 2007). The shape of this relationship is very similar to growth rate dependance to temperature (Fig. 1.1), although it can be shifted along the temperature axis depending on enzyme stability.

When exposed to high temperature (transiently or over longer periods), *E. coli* shows a massive change of gene expression. While the detailed mechanism and effectors of this response have been characterized early (Gross, 1996), recent transcriptome studies in different strains (MG1655 and O157:H7) show that expression of hundreds of genes is affected (Carruthers and Minion, 2009; Harcum and Haddadin, 2006). These changes are usually refered to as the "heat shock response".

The changes in gene expression mostly result from the activation of two sigma factors, σ^{32} and σ^{E}, encoded by rpoH and rpoE respectively. This is reviewed very clearly in Yura et al. (2000). σ^{32} controls the transcription of cytoplasmic heat shock proteins (HSPs) while σ^{E} controls that of periplasmic ones; since it is used to signal extracytoplasmic conditions to the cytoplasm, σ^{E} is classified as an extracytoplasmic function sigma factor (ECF-σ). These two transcription factors controlling the expression of similar proteins in cytoplasm and periplasm respectively correspond to an example of overlooked compartmentation in bacteria physiology. HSPs consist primarily in chaperones and proteases (Table 1.2) and are characterized by a consensus sequence in their promoter region. In more details, σ^{32} activates the transcription of DnaK-DnaJ and GroEL-GroES chaperones that help protein folding and are essential for growth above 20°C. σ^{E} activates the transcription of rpoH and its own gene rpoE as well as the transcription of periplasmic proteases and isomerases (assisting protein folding); it is essential for growth at all temperatures.

Interestingly, the heat shock response activation relies on physicochemical alteration of cell compounds (as described in section 1.1.2.1). In particular, the mRNA of σ^{32} exhibits an unusual secondary structure

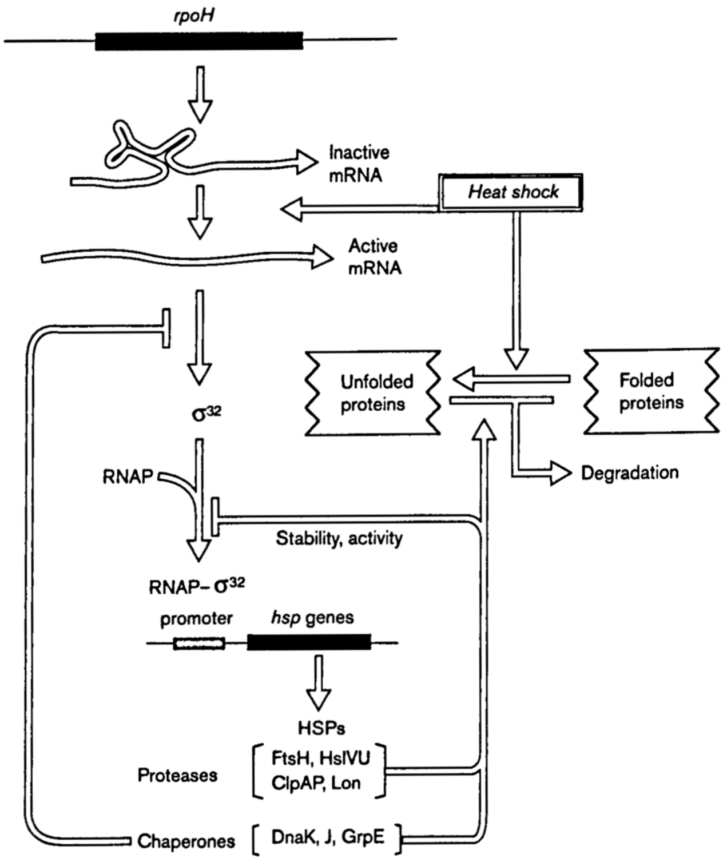

Figure 1.4: Regulatory circuits of the σ^{32} regulon in *E. coli* (after Yura and Nakahigashi, 1999).

with loops that prevents ribosome binding and subsequent translation. At high temperature, the stability of the secondary structure is lower and translation can initiate. It is believed that rpoH mRNA alone acts as a cellular thermometer (Fig. 1.4).

In addition, the σ^{32} regulon temperature-dependent regulation is also based on proteins sensitivity to temperature. Downregulation of the σ^{32} regulon involves DnaK, a chaperone binding to σ^{32} and preventing the formation of the σ^{32}-RNA polymerase active complex. Once bound to DnaK, σ^{32} can be subsequently degraded by the protease FtsH. As DnaK chaperone is mostly implicated in preventing protein misfolding and is present in limited amount, even a slight increase of the pool of misfolded protein will reduce DnaK-σ^{32} interaction and result in activating the heat shock response. This role of DnaK in σ^{32} turnover actually offers another

induction mechanism for the heat shock response. As a consequence, the heat shock response is actually a general stress response (induced among other by ethanol, abnormal protein synthesis, antibiotics, ...). It appears to be widely conserved as such through evolution (Sorensen et al., 2003).

Ultimately, the activation of the heat shock response results not only in the synthesis of a certain numbers of effectors but more generally in a global reorganization of cell structures in a way that limits the damages described previously.

1.1.2.3 *Dynamics and specificity of the heat shock response*

From a dynamic viewpoint, the heat shock response consists in rapid modifications of the bacteria physiology. When *E. coli* is exposed to a sudden change of temperature (30°C to 42°C), the synthesis of HSPs increases and very rapidly reaches the maximum induction (10 to 15 fold after only 5 min where HSPs represent 20 % of total proteins). This is followed by a gradual decrease and reaches a plateau (2 to 3 fold preshift level) after 30 min. If temperature is higher, synthesis of other proteins stops and HSPs are produced as long as the cell can produce proteins (Yura et al., 2000).

This heat shock response has been characterized in the case of rapid temperature increases. Nonetheless, if the rate of temperature increase is sufficiently low, *E. coli* can survive and grow at unexpectedly high temperature, between 50 and 55°C (Guyot, 2007, reported in greater details in section 1.1.4.2). Does this occur thanks to the same mechanisms at play at lower temperature that would be challenged in this case to their upper limit? Or are there other stress resistances that take over in this case? Unexpectedly, neither the level of aggregated proteins nor the level of cytoplasmic chaperones was changed in this experiment suggesting that the heat-shock response was not dominant.

The fact that the so-called heat shock response is not always activated at high temperature is supported by other experiments. It has been proposed that following a heat shock, σ^{32} activation is important mostly in aerobic conditions while σ^{32}-independent mechanisms would be active in anaerobic conditions and in stationary phase (Díaz-Acosta et al., 2006). In line with these observations, *E. coli* transcriptional response has been shown to be different in transient vs. long term responses to elevated temperature (Gunasekera et al., 2008). Together, these results suggest that HSPs may rather act as healing compounds after a heat shock rather than conferring a stress resistance in itself.

Finally, whatever the mechanism, it is likely that growth above the upper thermal limit through acclimation has not be selected for in recent *E. coli* history and that it rather challenges the flexibility of general stress response mechanisms.

1.1.2.4 *Adaptations to high temperature in thermophilic bacteria*

As far as adaptation is concerned, the actual targets of selection will very likely depend on the precise selective pressures (constant or seasonal environment, nutrients availability, uniform or structured environment, ...) and any sequence of adaptive events is difficult to predict since the relative effect of the different damages is not elucidated (Hickey and Singer, 2004). In these conditions, it can be instructive to look at how thermophiles and hyperthermophiles survive at high temperature. As exposed by Russell (2003),

> "enzymes and proteins are much more heat-stable and appear to function optimally at high temperatures as a result of critical amino acid substitution in one of a few locations. They thus appear to fold in a different way and can better cope with the denaturing effects of heat. The heat stability of proteins from thermophiles is increased by the presence of a number of salt bridges, *of disulfide bonds (Beeby et al., 2005) [an]*, and by the densely packed hydrophobic interior nature of the proteins. It must also be pointed out that the ribosomes tend to be thermostable and that thermophilic organisms have membranes that are rich in saturated fatty acids, which form much stronger hydrophobic bonds, thereby conferring stability and functionality at high temperatures."

Importantly, thermophiles' DNA is also protected by high levels of intracellular potassium and polyamines (protecting against bonds degradation), by high reverse gyrase activity generating positive supercoiling (that stabilizes DNA), and by histone-like proteins that increase the degradation temperature (Grosjean and Oshima, 2007). Although the CG content is expected to stabilize DNA, it does not clearly increase with optimal growth temperature and may rather depend on other selective pressures like high recombination rates. Overall, regarding changes observed in thermophiles DNA sequences, it is difficult to disentangle the effects of selection on DNA stability and on RNA and protein stability (Hickey and Singer, 2004).

Finally, from an evolutionary perspective, it is noteworthy that the heat shock response is a general stress response than can in particular be triggered by increased level of abnormal proteins following mutations (Sorensen et al., 2003). Consequently individuals acclimated to high temperature may be more prone to express and fold mutated proteins (thereby limiting the cost of an harmful mutation or taking advantage of a beneficial mutation), extending the range of possible phenotypes offered to selection. This can be interpreted as an increase in robustness or in evolvability: one may consider the ability to express a given phenotype even with a genotype altered by mutations (increased robustness) or

the increased tolerance to unstable proteins caused by mutations possibly conferring a selective advantage despite of lower stability (increased evolvability).

1.1.3 ADAPTATION TO HIGH TEMPERATURE IN EVOLUTIONARY EXPERIMENTS

Although Darwin originally stated that evolution by means of natural selection proceeds in small steps and is a very slow process, he already suggested that the relevant timescale for adaptation is the number of generations (Darwin, 1859). Following this idea, it is possible to study adaptation in controlled laboratory experiments provided the organisms reproduce fast enough. Doing so, one can follow Gould's idea of

> "replaying life's tape. You press the rewind button and, making sure you thoroughly erase everything that actually happened, go back to any time and place in the past. Then let the tape run again and see if the repetition looks at all like the original" (Gould, 1989).

Since unicellular organisms can be kept frozen, the experimental evolution approach has become more and more popular since the 1980's as it allows to store "fossil records" of ancestral states and to revive them in order to compare them with evolved states.

In more details, experimental studies of evolution are conducted in two steps (Elena and Lenski, 2003). In a first time, several populations of interest are grown during a large number of generations (typically ca. 10 per day over a few months) in a controlled environment starting from the same ancestral clone. Selective pressures can be introduced by modifying the environmental conditions relative to the ancestor environment. From time to time, samples are frozen and kept as "fossil records". In a second time, phenotypic modifications due to evolution are assessed by comparing the evolved lines with ancestors or earlier states of evolution revived from frozen samples. As a typical example, the relative fitness of the evolved line relative to the ancestor is assessed by measuring the growth rate ratio of the two lines in a mixed culture; the use of neutral genetic markers allows to distinguish between them.

The most famous study in this field is the "Long Term Evolutionary Experiment" conducted by Lenski's laboratory over more than twenty years (more than 50 000 generations) on the adaptation of *E. coli* to a low-nutrient environment (Lenski, 2004, and `http://myxo.css.msu.edu/` for an exhaustive list of more than 50 articles published on this experiment). This experiment has shed a new light on the evolutionary dynamics of adaptation, showing that relative fitness first increases rapidly and then at a much slower pace (Cooper and Lenski, 2000) while the

number of mutations increases linearly with time (Barrick et al., 2009). Surprisingly, among the twelve replicate lineages, five of them acquired a mutator phenotype within the first 30 000 generations (Sniegowski et al., 1997). For a larger overview including metazoan as well, Garland and Rose (2009) expose methods, concepts and advances of experimental evolution.

It is noteworthy that evolutionary experiments with controlled selective pressure were already designed shortly after the publication of the *Origins of species* (Darwin, 1859). Indeed, communities of unicellular algae with a very short life cycle were evolved during seven years by gradually increasing the temperature. Starting from their usual temperatures of growth (15 °C to 18 °C), 23°C was reached rapidly while consecutive temperature increases (up to 70°C!) required longer time steps (Dallinger, 1887). These long steps could be interpreted nowadays as the time required to fix mutations allowing to increase thermotolerance. In addition, strong trade-offs were reported with strains growing above 60°C being unable to grow at the initial temperature (15°C). Surprisingly, no overall decrease in the tolerable rate of temperature increase was observed (Fig. 1.5). Eventually the setup and evolving lines were destroyed in an accident and although Dallinger claimed he restarted his experiment, no further publication mentions any subsequent observation. At that time, the main interest was to show adaptive evolution in action as a support to Darwin's theory; the description of evolution in this context was then not conceptually different from the one in natural populations. In particular, several species were mixed in the same culture that was not kept sterile and no indication regarding medium renewal or population size are provided.

1.1.3.1 *Adaptation of survival and growth to high temperature*

In addition to Dallinger's early attempt to select for individuals growing at higher temperature than their ancestral niche, more recent experiments have been run in Bennett's laboratory using conditions and strains similar to Lenski's experiment. Adaptation of *E. coli* to a change in temperature was studied both after a temperature shift or in alternated regime: after 2000 generations of adaptation to a low nutrient medium at constant temperature of 37°C, bacteria were propagated by daily serial dilutions in the same medium at 32, 37 or 42°C, or alternating daily between 32 and 42°C (Bennett et al., 1992).

The relative fitness to the ancestor (assessed at the adaptation temperature) increased in all conditions and did so more rapidly at 42°C (Fig. 1.6 left). However the absolute fitness (as estimated by the growth rate) did not significantly change in all conditions and over the whole range of temperature of growth between 12 and 44°C (Fig. 1.6 right; Bennett and

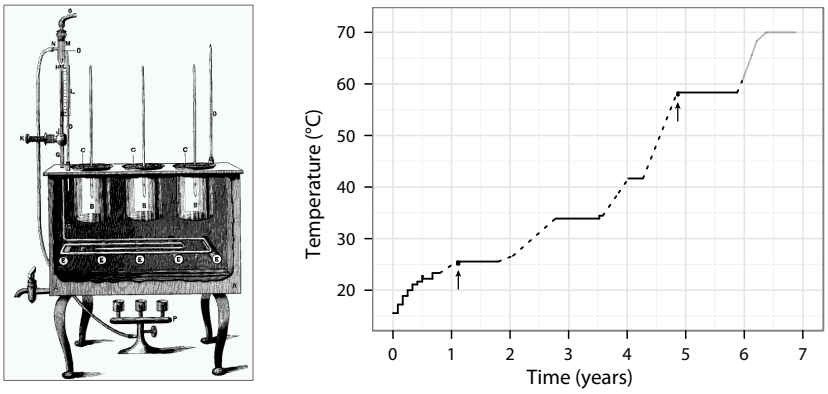

Figure 1.5: Adaptation to high temperature in green algae (after Dallinger, 1887). A mixed community of green algae was propagated during nearly 7 years at its maximum growth temperature. Based on the growth performance of three given species (estimated by microscopical observations), temperature was increased in small steps from 15 to 70°C. Left: Thermostatic water bath devised for this experiment in which the amount of gas provided to the burner is controlled by a mercury column. Temperature accuracy and stability are better than 1°C. Right: Maximal growth temperature dynamics over time. Using Dallinger's description, it is possible to plot the temperature of growth against time during the experiment. When the detailed steps are not mentioned in the text, a dotted line is drawn instead. At the end, the text does not allow to plot the real temporal dynamics as indicated by a grey line. Arrows highlight two events where temperature was modulated by 1°C over several weeks before normal growth could be recovered.

Lenski, 1993). This difference between relative and absolute fitness evolution can be interpreted as an improvement of resource usage with growth rate being unchanged due to physiological constraints.

Not much emphasis was put on survival at higher temperature in this study and no increase of the thermal niche upper limit was observed. However mutants with heritable thermotolerance at 44°C appear more frequently in the lines evolved at 42°C than in other conditions (Mongold et al., 1999). Since survival is estimated over days (as the populations ability to maintain), growth and survival cannot be disentangled as causes of this increased evolvability at the niche limit.

More in line with early Dallinger's experiment, *Pseudomonas pseudoalcaligenes* has been cultivated during 10 months at increasing temperature: starting from 41°C, temperature was raised by 1°C per month up to 44°C and by 1°C every two months up to 47°C. The ancestral strain grows very slowly at 45°C and not at 46°C. After adaptation, evolved bacteria grow

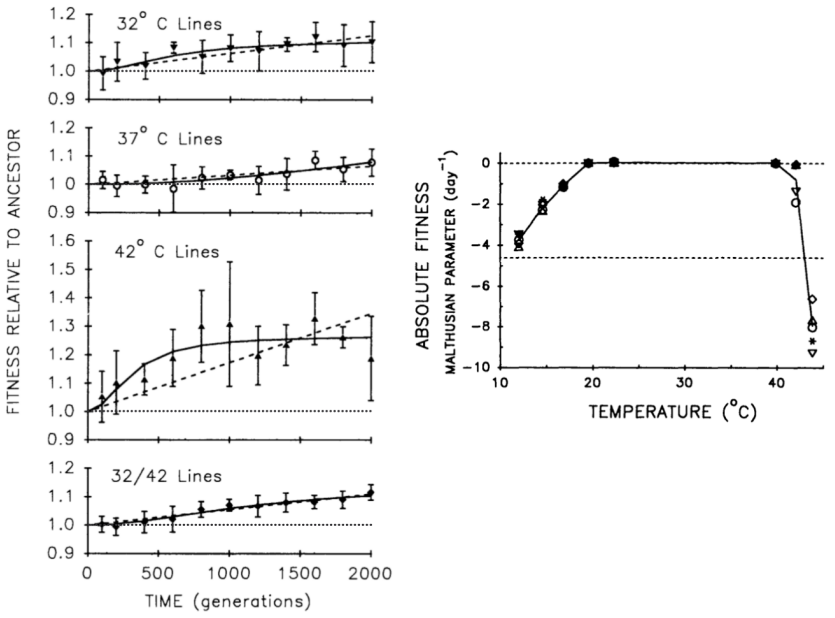

Figure 1.6: Relative and absolute fitness changes in a temperature adaptation experiment with *E. coli* over 2000 generations.
Left (after Bennett et al., 1992): Direct fitness response of each group over 2000 generations of experimental evolution at constant 32, 37, or 42°C or alternating 32/42°C. Fitness is expressed relative to the common ancestor, and was assayed for each group under its own experimental temperature regime. Each point is the mean fitness of six replicate lines; the error bars show the 95 % confidence interval. Dotted lines show the ancestral fitness, dashed lines give the average of the linear regressions for the six replicate lines and solid curves represent a fit of the mean fitness trajectory to a sigmoidal model.
Right (after Bennett and Lenski, 1993): Mean absolute fitnesses of the common ancestor (asterisks), 32°C group (downward triangles), 37°C group (circles), 42°C group (upward triangles), and 32/42°C group (diamonds) between 12 and 44°C. Malthusian parameter equals 0 day^{-1} indicates persistence in daily serial dilution culture; −4.6 day^{-1} corresponds to dilution without any growth or death. Means are calculated from six replicate lines for each condition (except the common ancestor, for which the mean is based on the two marker variants). Absolute fitness did not differ significantly between conditions at any assay temperature.

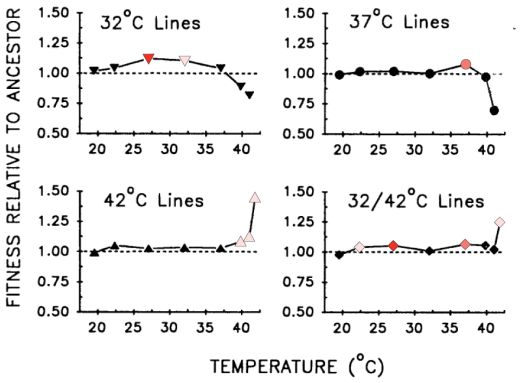

Figure 1.7: Absence of evolutionary trade-offs in *E. coli* adaptation to constant temperatures over 2000 generations (after Bennett and Lenski, 1993).
Mean fitnesses of the evolved groups relative to the common ancestor are assayed by competition experiments at different temperatures. Means are calculated from six replicate lines for each condition and the color indicates whether the mean relative fitness is significantly different from 1 (red for $p < 0.001$, light red for $0.001 < p < 0.01$, pink for $0.01 < p < 0.05$ and black for $p > 0.05$). In constant temperature regimes, no difference appears to be significant at non-adaptive temperature while there is significant adaptation in all conditions, indicating the absence of trade-off.

at 45°C with shorter lag and higher growth rate and yield than the ancestor (Shi and Xia, 2003). Unfortunately, as bacteria have been propagated in solid medium and are of different species and as there is no measure of relative fitness, this study is difficult to relate to results on *E. coli* mentioned earlier in this section.

1.1.3.2 *Trade-offs in adaptation to high temperature*

Bennett and Lenski (1993) reports no significant trade-off in temperature of adaptation after 2000 generations (Fig. 1.7): increase in relative fitness is significant at adaptation temperature but variations (and potential decrease) at other temperatures are not, meaning that the improvement selected at a given temperature does not come at a cost at other temperatures. Similarly, in *P. pseudoalcaligenes*, increase in growth rate at 45°C does not impair growth at 35°C (Shi and Xia, 2003).

However, after 2000 generations of adaptation at 20°C, *E. coli* shows significant trade-off between relative fitness at 20°C (ca. 1.1) and at 40°C (ca. 0.8) (Mongold et al., 1996). This trade-off was confirmed later on although no quantitative association was shown between fitness increase at low temperature and decrease at high temperature (Bennett and Lenski,

2007). Moreover massive trade-offs are reported in a qualitative manner by Dallinger (1887): algae evolved at 70°C are no longer able to grow at 15.5°C while the ancestral line dies if taken from 15.5°C to 65.5°C. Consequently trade-offs may depend on the selective pressure and on the species of interest and are probably more likely to appear along with more substantial changes acquired over long times.

Another kind of trade-off has been considered in these experiments: does adaptation to a given constant temperature affect the ability to adapt to another temperature? It is mentioned above that in Bennett's experiment, thermotolerant mutants are more likely to arise at 44°C than in the 42°C condition. In addition, they investigated why these mutants were not selected at 42°C and showed that they have a lower relative fitness at maximal growth temperature (around 41 – 42°C) than the evolved strain they are derived from (Mongold et al., 1999).

Subsequent experiments showed no growth predisposition or disadvantage of the past temperature selection regime when adapting *E. coli* at 20°C during 2000 generations (Mongold et al., 1996).

In natural thermophile populations, in the water surrounding geysers, trade-offs between growth rate at high and low temperature have been reported. Related lineages of one given cyanobacteria population sampled along a thermal gradient show significant variations in growth rate, with higher values in their thermal niches and lower values elsewhere (Miller et al., 2009).

1.1.3.3 *Genetic modifications following adaptation to high temperature*

While full-genome sequencing analysis of strains adapted to high temperature are still under work, two different genomic approaches give some insight on the genetic basis of adaptation:

- DNA arrays allow to study genome rearrangement. Several duplications were observed repeatedly and interpreted as a way to increase the level of gene expression (Riehle et al., 2001) although this was not confirmed in further studies (Riehle et al., 2003).
- DNA microarrays reveal that 12 % of whole genome expression is modified with 39 genes being modified repeatedly in different replicates. Among those are found stress response and heat-inducible genes (Riehle et al., 2005).

Unfortunately, no dynamics of these changes over time is available. It would be very interesting to see if gradual steps of evolution as reported by Lenski and Travisano (1994) and Elena et al. (1996) for adaptation to low nutrient environment and by Dallinger (1887) for adaptation to high temperature coincide with fixation of new mutations.

A recent molecular evolution study focuses on substitutions during *E. coli* adaptation to increasing temperature from 37°C to 45°C by 2°C steps (Kishimoto et al., 2010). Interestingly, there is a transition from positive to neutral selection of substitutions during the experiment. In addition, even in the positive selection phase, there is no clear correlation between the rate of fitness increase and the rate of substitution fixation.

1.1.3.4 *Alterned selection at different temperatures*

Alternated temperature regimes allow to address two related issues: what drives adaptation toward specialist vs. generalist types? Is it possible to select for more efficient acclimation as one possible generalist strategy?

In the alternated regime of Bennett's experiment, bacteria were switched daily from 32 to 42°C over 2000 generations. Compared with constant temperature regimes, these evolved lines show significant relative fitness increase along all the range of temperatures of growth (notably at 27 and 37°C) while the lines evolved at a constant temperature only show an increase in relative fitness in their own niches (Bennett and Lenski, 1993) (Fig. 1.7). These data suggest that alternated regime selects for generalists while constant selection favors specialists. Interestingly, adaptation was not slowed down by this alternance of selective pressure; although slower adaptation may be expected with goals in opposite directions, alternating selective pressures have rather been proposed to fasten adaptation by reducing the probability to be trapped in a local adaptation optima (Kashtan et al., 2007).

Subsequent analysis of the lines evolved in this alternated regime identified that adaptation occurs mostly at constant temperature and that no or very limited improvement in the ability to face temperature change occurred (Leroi et al., 1994a). It is worth asking how these results would be affected by different alternance frequencies. More frequent transitions could favor selection of improved response to environmental switches themselves.

1.1.4 ACCLIMATION TO TEMPERATURE VARIATIONS: EFFECTS OF TEMPERATURE HISTORY

Although it has been overlooked for long times, bacteria growth and survival at high temperature depend on the previous temperatures experienced by the cells. This additional parameter, referred to as *temperature history*, is critical as it shapes how much acclimation occurs. In this section, I review experiments addressing the impact of acclimation on survival and growth at high temperature, which special attention to tem-

perature history. Emphasis is given to strains and growth conditions as they may partly explain the contrasted results reported here.

1.1.4.1 *Acclimation & survival at high temperature*

Survival to high temperature depends on the physiological state of bacteria, in particular it is lower in exponential phase than in stationary phase. In *E. coli* H-52 grown in milk, this difference in survival between exponential and stationary phases is stronger when bacteria are grown below the optimal growth temperature at 28°C than above it at 38.5°C (Elliker and Frazier, 1938). In another experiment, exponentially growing *E. coli* MC4100 cells treated at 43°C during 20 min survive a 30 min heat shock at 50°C while cells in exponential phase growing at 37°C die (Shigapova et al., 2005). In stationary phase, more detailed descriptions are available:

- Survival to heat shock at 57.5°C increases with temperature of growth (6-fold increase between 10 and 42°C) in *E. coli* W3110 grown in tryptone soya broth supplemented with yeast extract (Cebrián et al., 2008). No acclimation is observed below 30°C.
- *E. coli* H-52 grown in milk survive better to a 30 min heat shock at 53°C when preliminarily incubated above the optimal growth temperature than below: survival reaches almost 70 % at 38.5°C while it is as low as 15 % at 28°C (Elliker and Frazier, 1938).
- Survival to heat shock at 50°C is almost twice higher for bacteria grown at 41.5°C than at 32°C with *E. coli* B in Davis minimal medium (DM) (Leroi et al., 1994b).
- Survival to heat ramp from 30 to 55°C for *E. coli* MG1655 grown in Brain Heart Infusion broth is claimed to be accurately described from heat shock survival data assuming (i) no growth occurs, (ii) inactivation by temperature starts from 49.5°C and (iii) heat resistance does not increase due to gradual temperature change (from 0.15 to 1.64°C/min) (Valdramidis et al., 2006). This is interpreted as a demonstration of limited acclimation to heat stress in stationary phase. However, direct survival rate estimation using their data suggests that death rate increases with slope and almost doubles between 0.15 to 1.64°C/min.
- *E. coli* MM28 grown in Luria Bertani rich medium (LB) at 30°C survive better a one hour heat shock at 50°C when temperature increases slowly (0.5°C/min) than after instantaneous heat shock (Guyot et al., 2010). This is a marked effect as survival rate is 90 × higher. Interestingly the primary cause of mortality is the loss of envelope integrity as shown by permeability and membrane fluidity measurements. Moreover this increase relies on protein synthesis during the heat treatment resulting in higher membrane stabil-

ity rather than in expression of heat-inducible chaperones and proteases.

Beyond the strain and media differences, the contrasted results reported by the latter studies are worth commenting: differences are likely due to the different target temperatures and also to the different temperature variation rates considered. This suggests that above a certain temperature, acclimation is of limited help for the cell and that it is a very rapid response, occurring in less than 15 min (as shown by 1.64°C/min increase from 30 to 55°C).

Interestingly, the acquisition of thermotolerance can be induced by other stresses. For instance, *Salmonela typhimurium* survival after heat shock at 50°C is markedly increased when grown at high osmolarity with 0.3 M NaCl (Fletcher and Csonka, 1998). Similarly, in exponentially growing *E. coli*, acclimation to high temperature can be obtained with benzyl alcohol, an amphiphilic molecule that fluidize the membrane. This occurs quicker than required for benzyl alcohol to activate σ^{32} and the heat shock response (Shigapova et al., 2005). It is interpreted as a non-transcriptional regulation mechanism in which membrane fluidization (by chemical or heat) may be sufficient to induce a rapid remodeling of membrane composition conferring short-term bacterial thermotolerance.

1.1.4.2 *Acclimation & growth at high temperature*

In a non-lethal temperature range, during competition at 32°C, acclimation to this temperature confers a competitive advantage over acclimation to 41.5°C. However, the contrary is not true: bacteria acclimated at 41.5°C are outcompeted at this temperature by bacteria acclimated at 32°C (Leroi et al., 1994b). This results obtained with *E. coli* B grown in DM are interpreted in terms of cost of heat-inducible proteins synthesis that would be disadvantageous at low temperature.

Probably due to the complex interplay of death and growth at high temperature, very little is known about growth of mesophile bacteria at high temperature. When pre-heated during 24 hours at 45°C, *E. coli* MG1655 achieves exponential growth up to 46°C while it grows exponentially only up to 44°C when precultured at 37°C (van Derlinden et al., 2008).

More striking acclimation has been reported when using very slow temperature ramps. When grown in LB with daily 10 × serial dilution and temperature increasing from 37°C at 2°C/day, *E. coli* MM28 grows repeatedly up to 50°C and occasionally up to 54°C; above this temperature, growth is too slow to compensate dilution (Guyot, 2007). In contrast, in absence of acclimation, growth is not possible above 42°C. This growth at high temperature is likely to be due to acclimation rather than

adaptation since it occurs over a short period (less than 25 generations) and it is lost after freezing. Even if mutations are selected and partly responsible for growth at high temperature in this experiment, they are not sufficient to confer this ability and acclimation appears to be also required. Unexpectedly, neither the level of aggregated proteins nor the level of cytoplasmic chaperones was changed.

Although very limited data are available, it is possible that acclimation plays a role in the previously reported Dallinger's experiments since algae are always maintained at high temperature. Adaptation of algae to high temperature is accompanied by a loss of growth ability at ancestral temperature. This can be interpreted in terms of trade-offs, in which case mutations allowing to grow at high temperature would prevent algae to grow at their ancestral temperature. As a result, it is likely that acclimation and adaptation are intertwined in a complex manner in this experiment.

RESEARCH OUTLINE

In the next sections, I report our efforts toward running an evolution experiment in a structured environment. This project is primarily motivated by the strong impact of spatial structure on ecological and evolutionay dynamics and the lack of such experiments. Environmental gradients have been hypothesized to facilitate diversification and are likely to be advantageous for individuals able to acclimate to a broad range of conditions. We propose to test this experimentally by evolving *E. coli* in a temperature gradient.

Actually, environmental gradients appear to be an interesting study case for acclimation: when individuals move, they respond to environmental changes first by acclimation while selection of advantageous mutations possibly occurs only later, over generations. Consequently, we aim at addressing how genetic adaptation that takes place on the long run is affected by prior physiological acclimation. Overall, due to the continuous spatial variation of the environment, this project is very different from other evolutionary experiments in well-mixed environments where environmental conditions are modified over time.

After summarising the progress on the core experiment and the main difficulties encountered, I will propose two lines of experiments in order to disentangle the issues addressed in this project. First, I study the interplay of chemotaxis and temperature, as well as thermotaxis properly speaking. In addition, I focus on the effects of acclimation on growth and survival at high temperature by controlling the temperature history experienced by liquid cultures.

1.2 ADAPTATION AND ACCLIMATION TO A TEMPERATURE GRADIENT IN A CHEMOSTAT

In this section, I report my efforts to devise an automated setup for evolutionary experiments in a structured environment.

1.2.1 EXPERIMENTAL DESIGN

1.2.1.1 *Setup principle*

The major goal of this project is to understand how organisms colonize and adapt to new ecological niches, and what role this plays in adaptive evolution. For that purpose we designed a chemostat so as to generate a temperature gradient adverse to the nutrient gradient. Chemostats are continuous culture devices where fresh medium is provided at the same rate at which culture medium (also containing individuals and waste) is removed. This allows to control the population growth rate as it is set by the dilution rate. By feeding *E. coli* bacteria from the higher non-permissive temperature we create a steady-state gradient of ecological niches where growing at higher temperature is expected to be advantageous thanks to reduced competition for nutrients in empty niches at higher temperature (Fig. 1.8).

In order to illustrate the expected steady state concentrations in the chemostat, let us write a simple one-dimensional reaction diffusion model, where B and N read the bacterial and nutrient concentrations respectively:

$$\begin{aligned} \frac{\partial B}{\partial t} &= \underbrace{c \cdot \frac{\partial B}{\partial x}}_{\text{flow}} + \underbrace{D_B \cdot \frac{\partial^2 B}{\partial x^2}}_{\text{diffusion}} + \underbrace{\gamma \cdot B(\alpha \cdot \frac{N}{N+N_0})}_{\text{growth / uptake}} \\ \frac{\partial N}{\partial t} &= \underbrace{c \cdot \frac{\partial N}{\partial x}}_{\text{flow}} + \underbrace{D_N \cdot \frac{\partial^2 N}{\partial x^2}}_{\text{diffusion}} - \underbrace{\gamma \cdot B(\frac{N}{N+N_0})}_{\text{growth / uptake}} \end{aligned} \tag{1.1}$$

where c denotes the flow velocity, D_B and D_N the diffusion coefficients of bacteria and nutrients respectively, γ the growth rate (as a function of temperature defined in (Rosso et al., 1993)) and α the metabolic yield. As shown by simulations, a nutrient gradient is created by bacteria uptake, adverse to the temperature gradient (Fig. 1.8). One can identify a front of growing bacteria at the upper limit of the thermal niche which is the population of interest.

The original intention was to replicate such a design and to run several experiments in parallel over a few months. During and after this evolution round, adaptive events were to be studied by various means with increasing finesse:

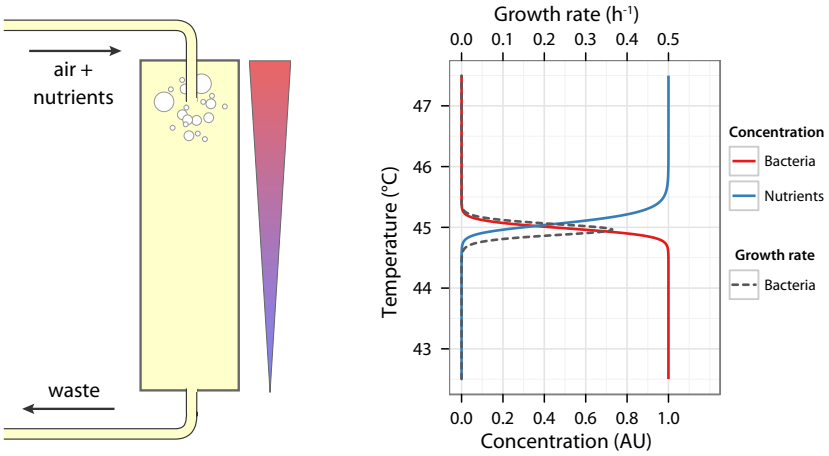

Figure 1.8: Spatially structured chemostat setup principle.
Left: Two opposite gradients are established in the culture chamber in order to study a non-uniform selective pressure: temperature is regulated and nutrient gradient is established thanks to the medium flow and to bacterial uptake.
Right: Expected dynamics from numerical integration of a simple reaction diffusion model of the chemostat (Eq. 1.1). The population of interest has a positive growth rate (between 44.5 and 45.5°C in this example). Numerical integration was run in R using the package deSolve (Soetaert et al., 2010) assuming a 40 – 50°C temperature gradient. Steady state concentrations are shown at time 11.5 days in the region between 42.5°C and 47.5°C. Parameters used in Eq. 1.1 are $c = 10^{-2}$ cm/s, $D_B = 7 \cdot 10^{-6}$ cm²/s, $D_N = 5 \cdot 10^{-5}$ cm²/s, $\alpha = 1$ and $N_0 = 0.3$; γ dependance to temperature is computed using the CTMI with $T_{min} = 4.7$°C, $T_{max} = 47.1$°C, $T_{opt} = 41.1$°C and $\mu_{opt} = 2\,\text{h}^{-1}$ (Rosso et al., 1993).

- Detecting colonization events of new ecological niches using a custom cell counting device allowing to monitor low cell density in real time (finally developed as an independent project presented in the next chapter).
- Estimating relative fitness of the various populations using competition experiments between ancestral and evolved lines at various temperatures.
- Estimating minimal, maximal and optimal growth temperatures as phenotypical traits of first interest to describe the possible diversification occurring in each chemostat (as exposed in introduction and Fig. 1.1).

– Screening for molecular changes in evolved lines using DNA sequencing and 2D proteins gels to describe two different levels of molecular events (genetic and phenotypic).

1.2.1.2 *Maintaining spatial structure in a long term evolution experiment*

Although spatial structure is a theoretically exciting issue, several experimental difficulties are to be taken into account in order to run long term experiments. In particular, the environment must be kept stable over time so that only spatial variations account for the observed changes.

As the environment is likely to be modified by living organisms, it is important to ensure that this does not cancel the selective pressure maintained on the environment. In our case, we use a chemostat since it allows to maintain continuously growth. However, long-term cultures are known to rapidly form biofilms on their walls that perturb the flow and more crucially introduce an uncontrolled history sensitive parameter in the experiment. Indeed, wall populations are not outcompeted by strains from the liquid phase even if the latter are fitter (Chao and Ramsdell, 1985). Here we propose to use another kind of chemostat specially devised for evolutionary experiments (de Crécy-Lagard et al., 2001). In its simpler form it consists of a classical chemostat in which biofilms are periodically cleaned with caustic soda (while temporarily sequestering the bacterial population), allowing the evolution of a bacterial population to be monitored in steady state conditions over many months.

In classical evolutionary experiments, cultures are repeatedly diluted. Such serial dilution protocols allow for further growth once stationary phase is reached. In contrast, our approach has the great advantage that it can be automatized (thus reducing the maintenance work and limiting contamination). However, a possible drawback is that it may lower adaptation speed (Patwa and Wahl, 2008). There is no direct experimental test of this prediction, and evolutionary experiments in chemostat have shown pronounced diversification even in constant environments (Maharjan et al., 2006).

1.2.2 BUILDING THE SETUP

Our chemostat dedicated to evolutionary experiments with a temperature gradient is composed of the following main parts (Fig. 1.9):

– Two interconnected culture chambers, one of which has a gradient temperature regulation and an optical measurement device. The temperature gradient is generated by regulating temperature at the ends of metal bars surrounding the square glass culture tube. Power

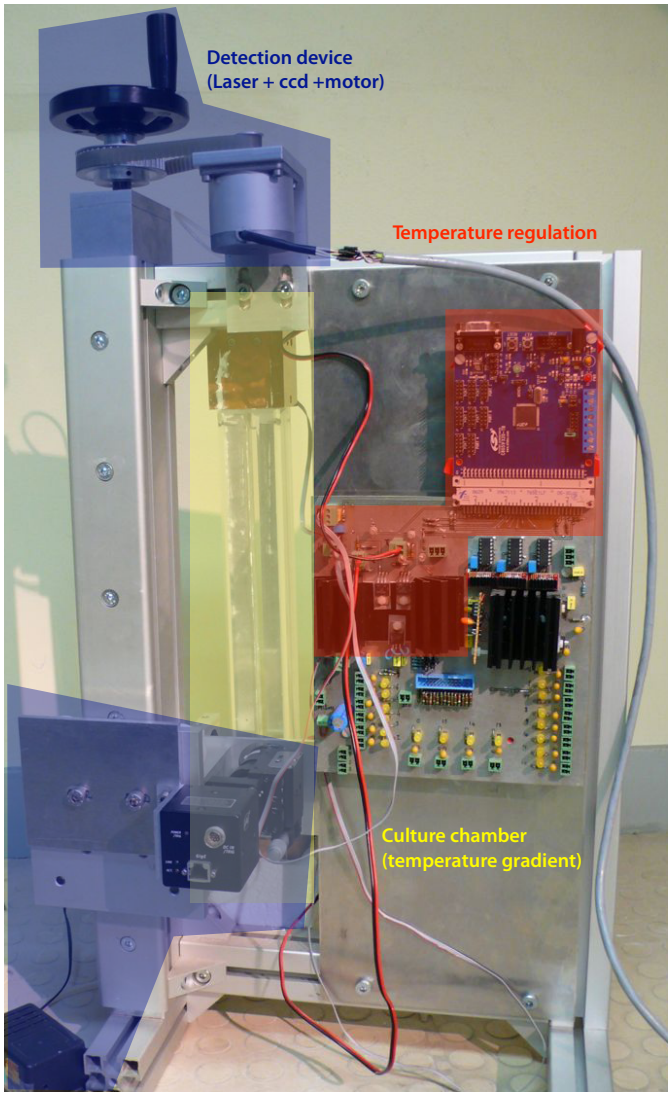

Figure 1.9: Picture of the chemostat prototype. At this intermediate state of development, only one culture chamber is used and all tubing and electrovalves have been replaced by minimalist autoclavable inlets and outlets. Main components are highlighted in color: culture chamber and metal bars used to control a temperature gradient in yellow, temperature regulation electronics (including the global microcontroller) in red, detection device allowing to measure OD or convection intensity along the gradient in blue.

resistors bring heat at hot end while thermoelectric coolers (TECs) are used at the other end to cool the metal. The other chamber is a simple flask used to store the population while biofilms are cleaned within the main chamber.
- Three inlets (air and nutrients for cell culture, soda for washing) and one outlet for waste removal are connected to large volume tanks. An additional uptake device is dedicated to biological sampling.
- A set of electrovalves are used to move liquids from one chamber to the other and to wash all parts of the setup.
- A microcontroller controls the electrovalves and is also in charge of the temperature regulation and of all measurements.

The temperature is regulated thanks to a custom proportional-integral-derivative regulation based on thermistors located close to power resistors or TECs. Temperature is measured from the thermistors by the microcontroller analog-to-digital converters (ADCs) at ca. 1 kHz and averaged. The heating (or cooling) power supplied to the resistors and TECs is modulated using a pulse-width modulation (PWM) and is adjusted every second. The stability is on the order of 0.002°C over 1 min and of 0.01°C over 1 h.

In addition, in order to meet the requirements of our experiment, the chemostat is designed with these specifications:
- All tubing, valves and fittings are soda-proof (namely in Teflon).
- The tanks volume (10 L) allows long-term autonomy (weekly maintenance only, to be compared with daily serial dilutions in classical evolution experiments).
- Stability against environmental hazards is optimized. Power consumption is kept as low possible in order to rely on a battery. Fluid flow is generated by air pressure rather than pumps. Overall, in case of power failure, the setup will remain stable over several hours except for the temperature gradient.

A much more detailed technical description of the setup is given in appendix A.1.

When I started being in charge of this project, the prototype was built but was not properly functional. After failing to use it in real experimental conditions, I spent the first year rebuilding it part by part: designing new electronic printed circuits, recoding microcontroller program, changing all valves and fittings, and finally, designing a sampling device.

In addition, I calibrated the apparatus. I defined the different states (growth by default but also inoculation, washing, uptake, …) that is the corresponding flow routes and the corresponding precise durations (allowing enough washing while not being to long). To this end, flow rates in different parts of the setup were precisely characterized and controlled. Also, the number of rinsing steps required to neutralize soda was mea-

sured as two to three when using a buffered growth medium. Contamination tests were replicated: soda sterilization is quite efficient but not total (surviving contaminants are visible after 4 to 5 days).

As it was difficult to do modifications with one prototype only, I built a second one including all the improvements and new features developed previously. This allowed myself to turn the first one into a very simple version that can be simply sterilized by autoclave (shown in Fig. 1.9). This much simpler sterilization process allowed me to run the first biological tests, i.e. to study short term ecological dynamics of colonization within the chemostat. Finally, in order to measure bacterial density in real-time, a classical optical density measurement was devised and mounted on a motorized vertical axis.

1.2.3 SHORT-TERM ECOLOGICAL DYNAMICS

1.2.3.1 *Gradient colonization by motile bacteria*

Early tests were conducted to check that imposing temperature gradient and delivering nutrients at the hottest point led to a bacterial density gradient as expected from our assumptions (Fig. 1.8 right). Default conditions were *E. coli* MG1655 grown in M9 minimal medium with 0.4 % glucose in a 35 – 58°C temperature gradient. Inoculation was uniform over the growth chamber at an equivalent OD of 10^{-4} AU. Our observable was the optical density along the vertical growth chamber.

More on the relevance of optical density as a biomass estimate is to be found in chapter 1.5.4.3.

The first inoculation trials showed unexpected dynamics of optical density profile. After uniform inoculation, optical density increased independently of the temperature and reached saturation at high uniform optical densities (data not shown)! This was interpreted as the result of two mixed effects. Optical density measures biomass of both alive and dead cells. As death can occur at high temperature, optical density can lead to overestimating the population size. In addition, any convective flow within the chamber would homogenize the culture and disrupt the spatial structure.

1.2.3.2 *Identifying colonization forces*

After the stability of the temperature gradient had been improved and limited convection supposedly confirmed, two kinds of subsequent experiments were attempted:

– Monitoring the growth of bacteria depraved of flagella after inoculation at an equivalent OD of 10^{-4} AU. While the only source of movement was diffusion, I observed uniform growth independent of temperature (Fig. 1.10 left).

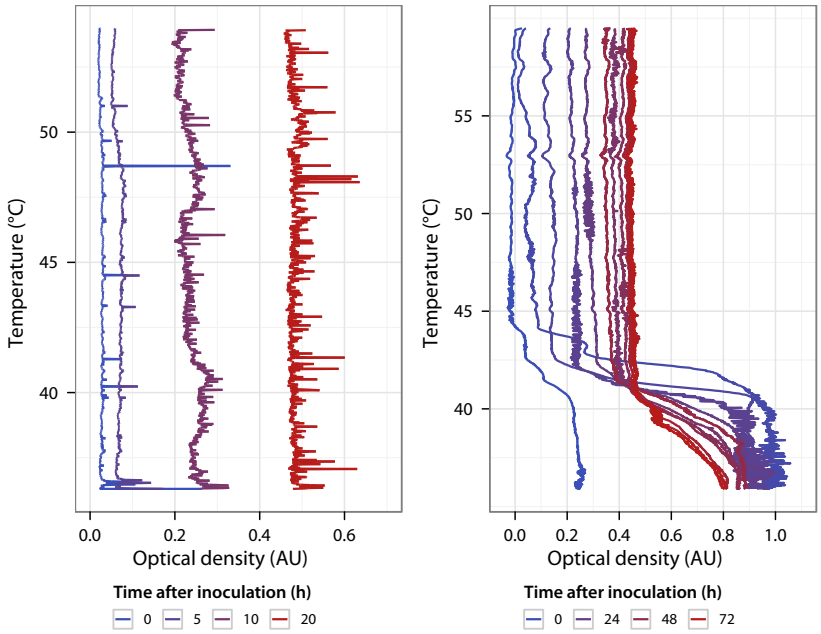

Figure 1.10: Time-lapse optical density profiles after uniform and non-uniform inoculation.
Left: Uniform inoculation with Δ*fliA* flagella-less strain. Each line is a single record, from inoculation to steady state 20 h later. Similar profile is observed after uniform inoculation with wild-type MG1655.
Right: Inoculation at the bottom of the culture chamber with *E. coli* MG1655. Each line is a single record, with 6 h between them.

– Using non-uniform inoculation. I inoculated a bacterial population (at OD $\simeq$ 1) at the chamber bottom in order to observe colonization due to both cell chemotaxis and cell division. Actually, after a lag, I observed uniform growth independent of temperature (Fig. 1.10 right), irrespectively of the strength of the gradient (data not shown).

In addition, uptakes at various heights within the culture chamber allowed to check that the temperature profile of the growth medium was as expected, and to estimate cell mortality as a function of temperature (using both cell plating and microscopy with membrane markers). Though there was a strong decrease in cell density with temperature that was not visible by optical density, bacteria sampled at 56°C were still able to grow when plated at 37°C.

This suggests that convection may occur though we did not detect it at this time. Bacteria would be exposed to different temperatures due

to convective flows moving the population around the chamber. In this case, uniform increase of OD would result from bacteria division in a narrow temperature range followed by population mixing by convection. One can hypothesize that continuous temperature variations give time for acclimation and consequently limit the mortality at high temperature. This is supported by the growth of bacteria sampled at high temperature.

1.2.4 REDUCING CONVECTION

1.2.4.1 *Characterizing convective flows*

Convection in this device is a problem that must be overcome before running any experiment as it breaks down all spatial structure and thus voids the setup principle. In order to characterize it in greater details, we developed a particle image velocimetry (PIV) software that allows to quantify convection from movies of 1 µm polystyrene beads in the chamber illuminated with a laser beam.

Fast convective flows on the order of 100 µm/s occur in the original $10 \times 10\,\mathrm{mm}^2$ chamber when a $30 - 60^\circ\mathrm{C}$ temperature gradient is maintained. However, convection is much weaker without temperature regulation. This strongly suggests that convection is triggered by lateral temperature heterogeneity in the setup: any temperature difference between the two sides of a thin horizontal sheet of liquid produces a difference of density which, integrated over the chamber height, results in a large convective cell. Such convection occurs without threshold, meaning that the faintest difference in temperature will trigger it. This problem could be easily overcome by reducing the chamber to submillimetric size, which we are reluctant to do as we want to keep the evolving populations as large as possible.

1.2.4.2 *Controling convection in the growth chamber*

In order to reduce convection flows below the swimming speed of bacteria, we proceeded to successive improvements of our setup, basically consisting in two metal bars at the end of which temperature is controlled. First the heat source at each end was made unique to limit lateral inhomogeneities, and the insulation was considerably improved. This stage of development is shown on Fig. 1.11 left. These changes did not significantly reduce the intensity of convection in the chamber.

Later on, the square section of the chamber ($10 \times 10\,\mathrm{mm}^2$) was changed to a thin rectangular section of similar area (Fig. 1.11 right). Two prototypes with section of $2 \times 50\,\mathrm{mm}^2$ and of $2.5 \times 80\,\mathrm{mm}^2$ have been built and give similar results. A 1 cm wide observation slit is opened on

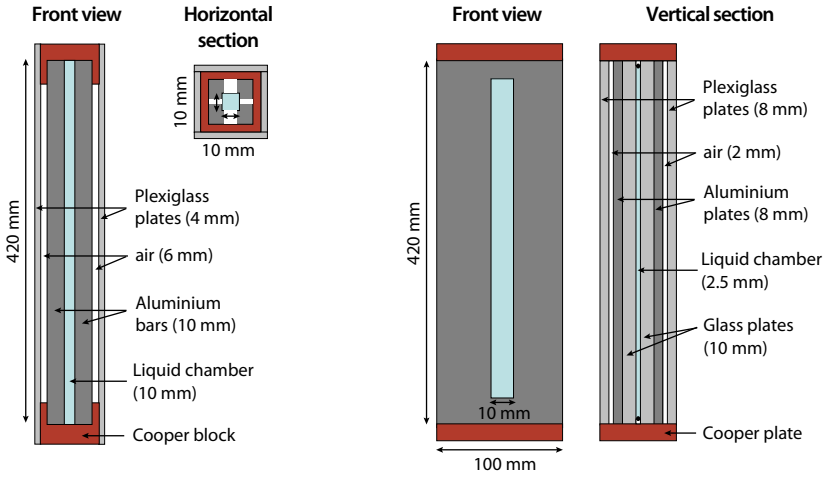

Figure 1.11: Improvement of the growth chamber geometry.
The initial growth chamber has a square $10 \times 10\,\text{mm}^2$ section and is heated by metal bars with large slits (left). The design has been improved by using a thin rectangular $2.5 \times 80\,\text{mm}^2$ section that lowers convection intensity. See text for details.

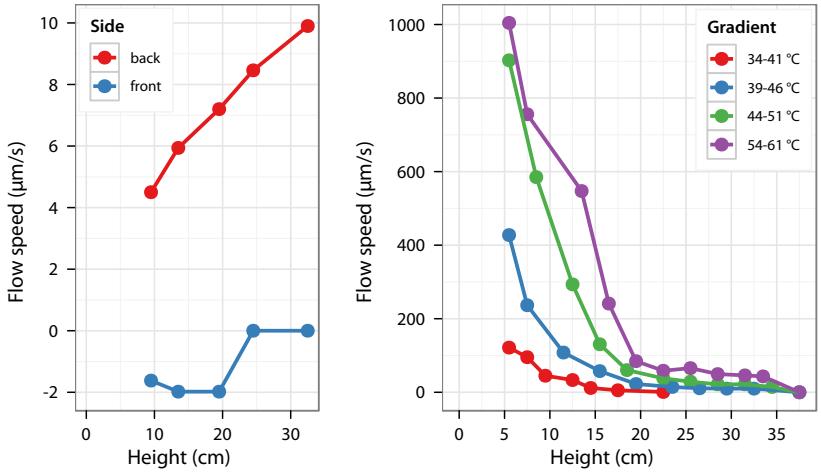

Figure 1.12: Convection intensity in a thin rectangular chamber. Positive speed indicates that flow goes up.
Left: With a $30 - 60^\circ\text{C}$ temperature gradient, the flow speed is measured on the front and the back along the chamber height using a PIV software. Right: Flow speed as a function of height for different gradients of same magnitude (7°C).

the front. Convection in this chamber geometry has been characterized with the help of T. Imine during his undergraduate internship in the lab.

The speed of the convective flow measured with a 30 – 60°C gradient, initially on the order of 100 µm/s, is notably reduced in the thin rectangular chamber, to less than 10 µm/s (Fig. 1.12 left). Interestingly, the flow goes up on the back (positive speed) and down on the front (slightly negative speed). This indicates that a thin convective cell is established in this direction (i.e. the setup depth), probably due to the loss of heat linked to the observation window. The chamber has been modified to be symmetric with two opposite observation windows: the flow goes down on the front and on the back (data not shown), suggesting that a convective cell established in the orthogonal direction (i.e. the setup width), with warmer regions on the lateral sides of the slit. This confirms that heat is lost through the observation window; its width was reduced to less than 1 mm but this did not reduce markedly the convection intensity. However, as bacteria are supposed to move freely in this device, we still need to lower it to approximately 1 µm/s.

In addition, without gradient, there is no more convective flow. Interestingly, for a given temperature difference between the two ends (7°C), the speed of the flow depends on the absolute temperature of the setup. It increases continuously with temperatures varying from 34 – 41°C to 54 – 61°C (Fig. 1.12 right). In addition, in all conditions, the convection is much stronger in the lower part of the chamber. This is interpreted as the effect of heat loss due to the imperfect insulation: when the absolute temperature are higher than room temperature, the coldest point of the setup is in the middle, far from the heating elements. Consequently the lower half of the chamber is very unstable with colder liquid being on top of warmer one. In the case of a 30 – 60°C gradient, this effect does not occur as the heat flow is larger and no cold point establishes between the two ends (Fig. 1.12 left).

Although all this has been unexpected as the difference of density (cold at the bottom, hot at the top) was supposed to stabilize the flow, it is not in contradiction with the theory. The flow in a thin chamber of infinite length, with a small temperature difference between the two walls can be estimated analytically. It scales with l^3 and $1/\eta$, where l is the chamber thickness and η the viscosity. Numerically, this predicts that to keep the flow under 10 µm/s with a 2 mm wide chamber filled with water, one must prevent temperature differences larger than 0.01°C between the two walls! This is in agreement with finite-elements simulations run in Comsol by Nabil Garroum, research engineer in the lab.

The challenge is to guarantee temperature uniformity, not stability over time…

As building such tightly regulated setup is challenging, another strategy would be to increase the viscosity of the growth medium. Actually this is supposed to linearly decrease the flow speed, while bacteria motion is not impaired very much (less than 50 % decrease) by a 10 ×

increase of growth medium viscosity from 1 to 10 cP (Schneider and Doetsch, 1974). This could be done using for instance methyl-cellulose, a polymer which increases viscosity even at low concentration and thus does not affect too much osmolarity. However, the variation of viscosity with temperature is to be considered carefully, and adding such polymers to the growth medium would represent an uncontrolled source of nutrients.

As time was running out, I decided in February 2010 to concentrate on shorter term projects described in following chapters. Hopefully this experiment will be running one day…

We have successfully built an evolutionary chemostat modified in order to impose a temperature gradient on the culture chamber. Maintaining a spatially structured growth medium with a temperature gradient appears to be very difficult due to convection. Lateral temperature inhomogeneities trigger convective flows on the order of bacteria swimming speed. This might be overcome by increasing the medium viscosity but has prevented us from running any adaptation experiment up to now. However, preliminary experiments have pointed out the probable importance of acclimation in such an experiment.

1.3 INTERPLAY OF CHEMOTAXIS AND TEMPERATURE

In the overall project development, the first biologically relevant step is to describe the colonization of the chamber by a bacterial population, which implies thermotaxis, growth and survival. In addition, chemotaxis has been shown to play also an important role in similar ecological contexts where a nutrient gradient is created by bacteria uptake. As devising a large scale non-convective setup happened to take so long, we decided to address this ecological aspect at a much smaller scale where convection issues vanish. In collaboration with Jonathan Saragosti (Pascal Silberzan & Axel Buguin's lab, Institut Curie), we transposed our design at the microscopic scale, taking advantage of his experience of bacterial chemotaxis in microchannels (Saragosti, 2010) and of my experience of temperature gradient regulation.

1.3.1 MICROCHANNELS SETUP PRINCIPLE

The setup consists in a polydimethylsiloxane (PDMS) microchannel (20 mm long × 500 µm high × 100 µm wide) sealed at both ends, in which temperature is regulated between 35°C and 55°C. Bacteria inoculated at

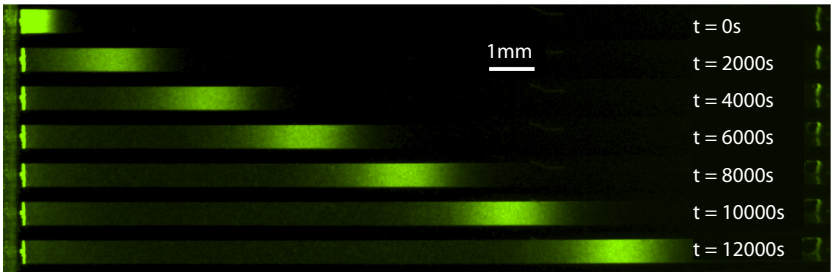

Figure 1.13: Setup principle of microchannel used for collective motion experiments (after Saragosti, 2010).
After inoculation, channels are sealed at both ends using epoxy and centrifugated at low force which results in a sedimentation with a characteristic length $\simeq 100\,\mu m$. This time-lapse shows the front progression of *E. coli* RP437 (bearing a plasmid confering constitutive GFP expression) in M9 medium at 37°C after inoculation at $5 \cdot 10^8\ mL^{-1}$. Average front velocity is $1.2\,\mu m/s$.

$5 \cdot 10^8\ mL^{-1}$ are slowly centrifuged toward the cool end before the experiment. Starting from this asymmetric initial condition, the colonization of the channel is monitored using time-lapse imaging with a binocular. The small size of the device guarantees that there is no convection and allows to run 16 replicates in parallel on a single microfluidic chip.

In these experiments, we use *E. coli* RP437 expressing high levels of green fluorescent protein (GFP) from pGFPmut2 and bacteria are grown in M9 medium with 0.4 % glucose and 0.1 % casamino acids as this corresponds to the control condition well characterized with uniform temperature at 30°C (Saragosti, 2010).

1.3.2 COLLECTIVE MOTION OF BACTERIA IN A TEMPERATURE GRADIENT

1.3.2.1 *Collective motion at uniform temperature*

As mentioned above, a key advantage of this system is its extensive characterization at constant temperature where only chemotaxis is supposed to take place: at 30°C, after inoculation and centrifugation, a bacteria front starts to propagate at constant speed toward the empty end of the channel. When bacteria are inoculated at $5 \cdot 10^8\ mL^{-1}$, the front velocity is ca. $1.2\,\mu m/s$ (Fig. 1.13 bottom). This front is interpreted as a consequence of chemotaxis, driving bacteria toward higher nutrient concentration. These macroscopic travelling pulses are very reproducible and can be accurately modeled based on the mesoscopic run and tumble behaviour of bacteria (Saragosti et al., 2010).

1.3.2.2 *Collective motion in a temperature gradient*

When a 35 – 55°C temperature gradient is maintained, the early colonization of the channel is very similar: high bacteria concentration at one end triggers a front propagation, in this case toward higher temperature. Surprisingly, in a large temperature range the speed of the front peak is independent of the temperature and identical to the speed measured at 30°C (Fig. 1.14). This has been observed in two independent experiments, that is more than 15 channels (a small proportion of the channels can not be analysed due to evaporation at high temperature).

In elevated temperature range (43 to 45.5°C), front velocity decreases with temperature. This can be seen as the result of opposite chemotaxis and thermotaxis effects or as chemotaxis being modulated by temperature. The decrease is unexpectedly weak and appears at very high temperature (around the upper limit of the thermal niche). It is noteworthy that growth conditions are likely to prevent thermoresponse in this case: Maeda and Imae (1979) showed that the thermoresponse is inhibited by excess of methyl-accepting chemotaxis protein (MCP) analogs, above 0.1 mM in the case of serine. In comparison, 0.1 % casamino acids used here in M9 medium corresponds to approximately 0.31 mM serine (Nolan, 1971).

Above a certain temperature around 45.5°C, the front stops. This can be interpreted either as a manifestation of thermotaxis (an internal signal preventing chemotaxis if temperature increases too much) or of damages due to high temperature.

1.3.2.3 *Disentangling temperature damages and negative thermotaxis*

To distinguish between the thermotaxis and the temperature damage hypothesis, we ran the same experiment, bringing temperature back to 30°C as soon as the front's speed decreased (around 45°C). However, no further chemotaxis to the empty part of the channel was observed, indicating that in these conditions chemotaxis had overcome thermotaxis and had lead to cellular damages.

This interpretation in terms of damages is supported by the filamentous shape of all bacteria observed in the channel after 20 h (Fig. 1.15): while thermotolerance can be increased by DnaK chaperone overexpression, Δ*dnaK* mutants exhibit a similar filamentous phenotype in rich medium even without stress (Rockabrand et al., 1995). Consequently, increased level of damaged proteins due to high temperature could exceed chaperones maximum activity and in turn result in filamentous bacteria as observed when DnaK is knocked out.

Whether this can lead to population extinction or whether bad swimmers remain safe at the bottom of the gradient is still an open question.

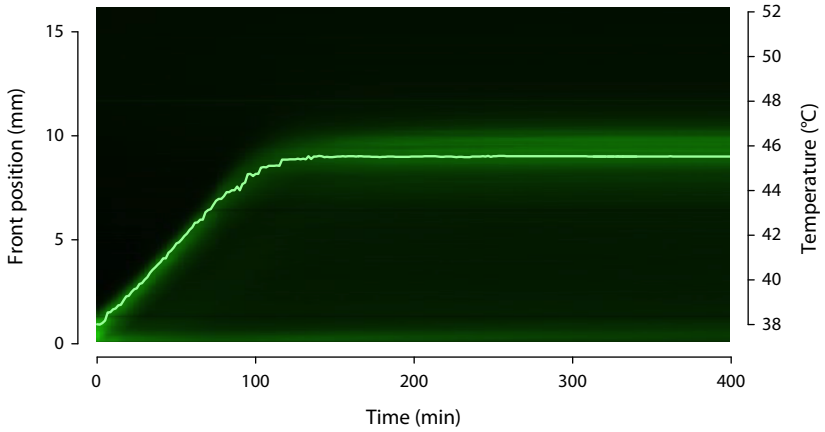

Figure 1.14: Collective chemotactic motion of *E. coli* RP437 in a microchannel with a temperature gradient. Bacteria (bearing a plasmid confering constitutive GFP expression) are centrifugated to the low temperature end after inoculation in M9 medium. The line shows the position of the intensity maximum against time while the background image is a chimograph of the average intensity (over the channel width) depending on time (horizontal) and position (vertical).

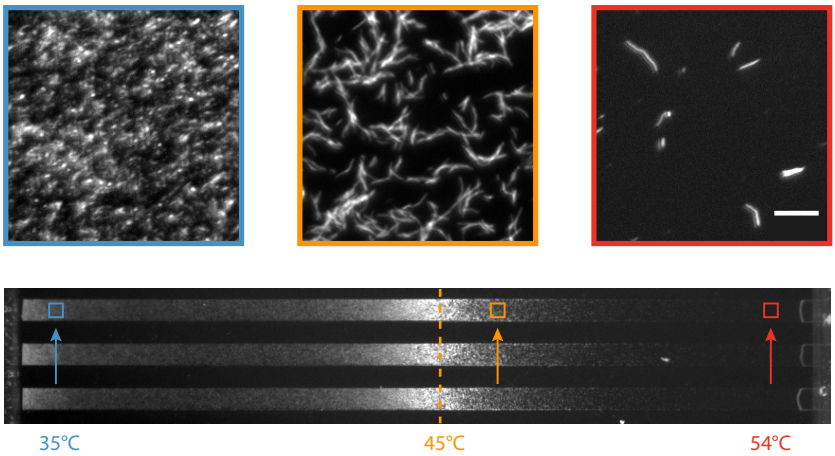

Figure 1.15: Morphological changes of *E. coli* RP437 after migration in a microscopic temperature gradient. The bottom picture shows the channel density profile after equilibrium has been reached. Small coloured frames indicate gradient regions where higher magnification pictures have been taken. At the front tail (35°C), bacteria are motile and their morphology is not affected. At the front head (47°C), bacteria are filamentous and are not motile any more. Only few bacteria colonize the higher temperature niches; at time of observation they are not motile any more. How they reach such high temperature is not elucidated.

1.3.3 CHARACTERIZATION OF THERMOTAXIS

Since the observations in microchannels reported above are new and relevant to the initial project of evolution to high temperature in a structured environment, we decided to design these experiments in a more general way and to address the issue of the interplay between chemotaxis and thermotaxis. This represents a nice example of how living systems react to contradictory environmental signals.

1.3.3.1 *Overlap of chemotaxis and thermotaxis machinery*

In the literature, the molecular basis of thermotaxis in *E. coli* is understood as very similar to the one of chemotaxis (Mizuno and Imae, 1984; Nara et al., 1996), based on methylation of membrane receptors called MCPs. This has two main implications: on the one hand, chemotaxis and thermotaxis are expected to be tightly coupled; on the other hand, this means that all mutants produced to study chemotaxis, one of the best characterized bacterial sensing system, are readily available to study thermotaxis. Unfortunately, although the chemotaxis signalling pathway has been shown to be robust to temperature variations within the thermal niche (Oleksiuk et al., 2011), the effects of high temperature on this pathway have not been characterized yet.

Before undertaking these experiments, we had in mind to follow two lines:

- Characterize a control condition of thermotaxis, in a thermal gradient without nutrient inoculated with a uniform concentration of bacteria, which consists in reproducing the results obtained for instance by Maeda et al. (1976). Consequently, using chemical analogs of serine and aspartate that triggers MCP methylation (Mesibov and Adler, 1972) should allow to study how thermotaxis depends on the level of methylation of MCPs.
- Address the issue of the interplay between thermotaxis and chemotaxis at the population level by using a moderate temperature gradient (for instance 25 – 45°C) and an adverse serine or aspartate analog concentration gradient. Provided thermotaxis has been characterized in absence of chemoattractant, such experiment would show which response is dominant when bacteria encounter adverse signals.

As shown by Salman and Libchaber (2007), the chemotactic and thermotactic responses depend strongly on the level of the two major MCPs, Tsr and Tar. The former is more abundant in early exponential phase (driving bacteria to warmer regions) while the latter takes over in stationary phase (driving bacteria to cooler regions where metabolism is slowed down). The relative level of expression of both proteins depend-

ing on the medium and growth phase has not been well characterized yet, which could make our approach more difficult.

1.3.3.2 *Thermotactic collective motion*

Over repeated trials, we did not manage to observe thermotaxis using *E. coli* RP437 strain grown beforehand in M9 medium at 34°C and inoculated in mobility buffer (Maeda et al., 1976) within a 25 – 45°C gradient. After inoculation, the distribution remains uniform except for very faint fronts propagating from the ends, which were interpreted as due to the channel sealing compound (epoxy glue). Consecutive attempts to use another strain or to change the growth medium (in order to use glycerol medium as in Maeda et al. (1976) supplemented with the appropriate amino acids for *E. coli* RP437 growth) have been unsuccessful.

Difficulties to establish a well characterized control condition for thermotaxis prevented us from further studying its interplay with chemotaxis.

Although Salman et al. (2006) claimed to observe thermotaxis at the beginning of their experiment in similar microfluidic design, this effect is very weak and has not been characterized in detail as the authors focused on chemotaxis-driven collective motion. The clearest evidence for thermotaxis in *E. coli* is the accumulation of cells in a laser-heated region at 30°C in a 18°C setup; this is observed in early exponential phase, while later in growth the reverse behaviour is reported (Salman and Libchaber, 2007). Most other recent studies on thermotaxis have been done at the single cell level with temperature variations in time (Paster and Ryu, 2008). Consequently, one can question whether seminal results reported by Maeda et al. (1976) are partly artifactual: within a glass capillary, a marked oxygen gradient can form and trigger a strong chemotactic response that would dominate the thermoresponse. This does not happen in PDMS channels thanks to PDMS permeability.

At this point, two directions may be easily explored:

- Characterize the possible role of oxygen in macroscopic thermotaxis experiments, for instance by comparing our results with similar experiments where PDMS is sealed in order to prevent oxygen diffusion.
- Explore the effect of acclimation to high temperature in the collective motion experiments: by changing the inoculation concentration, it is possible to modulate the front speed and consequently acclimation duration, i. e.the time spent at high temperature before reaching the irreversible limit.

Using microchannels (whose size prevents convection) we have studied the colonization by *E. coli* of a new environment with a temperature gradient. In this setup, colonization in absence of temperature gradient has been described to occur by front propagation due to nutrient uptake by bacteria themselves. Surprisingly, adding a temperature gradient does not affect the front speed until bacteria reach damage-inducing temperature. As motility is not recovered at lower temperature and morphology becomes filamentous, bacteria arrest is likely to be due to irreversible damages rather than negative thermotaxis lowering motility.

1.4 EFFECT OF TEMPERATURE HISTORY ON GROWTH AND SURVIVAL

The results obtained in structured environments highlight the importance of temperature history, that refers to the previous temperatures bacteria encountered before experiencing a high temperature stress. In this part, I aim at characterizing survival and growth of *E. coli* at high temperature depending on the temperature history. The farseeing perspective is to evolve populations under different regimes of acclimation in order to monitor how far acclimation (i.e. physiological adaptation) to a given selective pressure affects genetic adaptation.

For the sake of feasibility, these experiments are done in well-mixed environments. The variable condition consists in different temperature regimes, where rapid heat shocks (referred to as "steps") are compared with long temperature "ramps" offering continuous variation of the temperature (Fig. 1.17 bottom). At the time I did these experiments, we did not know about other previously reported studies of kinetics effects on survival (Guyot et al., 2010) nor about other attempts to grow bacteria at high temperature using acclimation (Guyot, 2007).

1.4.1 SURVIVAL TO HEAT SHOCK

A prerequisite in order to interpret acclimation experiments with temperature ramp is to characterize the survival kinetics of *E. coli* during heat shocks at different temperatures. To test for a possible effect of the physiological state on survival, these experiments are done both with bacteria in exponential and stationary phase at the time of heat shock.

1.4.1.1 *Experimental procedure*

The survival of *E. coli* MG1655 is measured in M9 medium supplemented with 0.1 % glucose, 1 % casamino acids and 2 mM magnesium

sulfate. A 100 × dilution of an overnight culture in LB at 37°C is inoculated into fresh M9 medium and grown at 37°C. Bacteria are grown in 5 mL culture, in 50 mL Falcon tubes incubated in Infors Multitron shaker.

Once exponential or stationary phase are reached (respectively after 2.5 h or overnight growth), temperature steps from 37°C to 50°C, 55°C and 60°C respectively are performed on 1 mL samples. This heat shock is done in a water bath using small 14 mL culture tubes in order to allow faster temperature increase of the medium. After 15 min, tubes are transferred into an incubator set at the heat shock temperature. Survival is monitored by colony counting after dilution, plating and growth at 37°C on LB agar.

For each condition, two replicates are run in parallel in order to estimate variability; heat shock at 55°C has been run one more time to catch longer term dynamics. Some replicates have been performed by H. Bosc-Ducros during his undergraduate internship in the lab.

1.4.1.2 *Results*

When exposed to temperature steps above 50°C, *E. coli* exhibits mortality both in exponential and stationary phase. Death kinetics are exponential (Fig. 1.16), in accordance with the literature (Russell, 2003). The survival decreases rapidly above a certain temperature, between 50°C and 55°C, as already reported in different growth conditions (Valdramidis et al., 2006).

Although there is a fair amount of variability in certain conditions, survival is higher in stationary phase than in exponential phase at each temperature (Fig. 1.16 bottom). This difference ranges from 1.7 to 3.3 times and decreases with temperature. It could be due to the expression of stress resistance genes in stationary phase (possibly independent of the heat shock response as proposed by Díaz-Acosta et al. (2006)), resulting for instance in the synthesis of chaperone proteins or in lower membrane permeability.

1.4.2 ACCLIMATION AND GROWTH AT HIGH TEMPERATURE

In order to characterize the effect of acclimation on growth at high temperature, temperature is gradually increased from 37°C to 50°C. This target temperature is chosen so that it prevents growth after a heat shock but has a limited effect on mortality as demonstrated in the previous section (1.4.1).

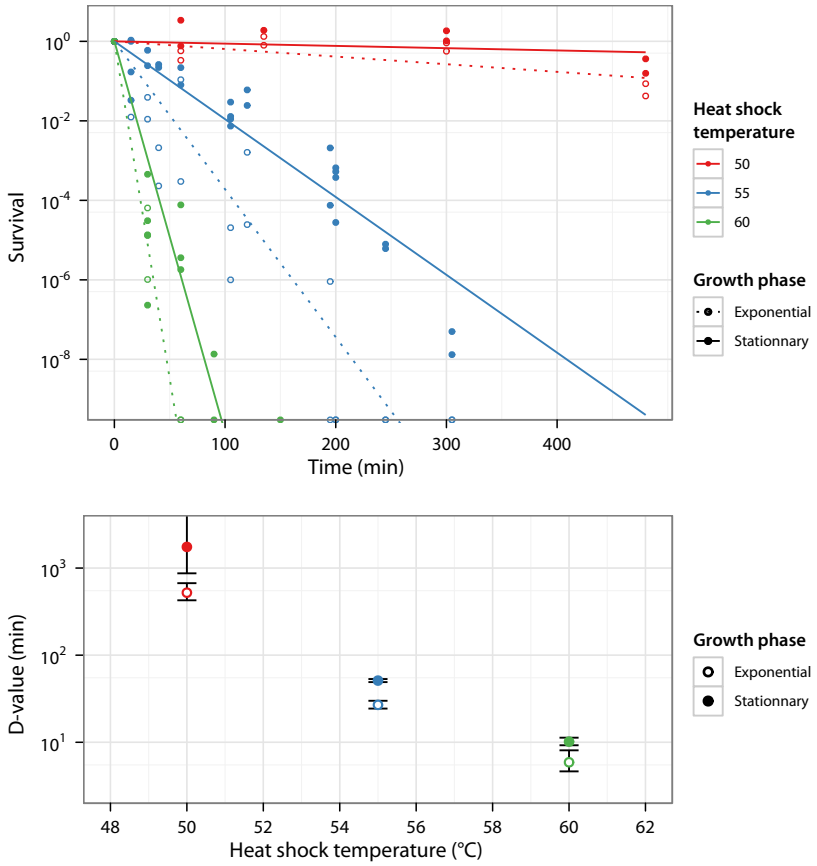

Figure 1.16: Survival of *E. coli* MG1655 at high temperature in M9 minimal medium. Bacteria in exponential or stationary phase (open and plain circles respectively) are heat shocked in a water bath and survival is estimated by colony counting after dilution and plating. Top: Surviving proportion of the initial concentration against time. Bottom: Decimal reduction time (D-value) estimation and confidence intervals.
Initial concentration at the beginning of heat shock is within $4 \cdot 10^6$ and $2.9 \cdot 10^8$ cfu/mL for exponential phase condition, and within $2.4 \cdot 10^8$ and $3.6 \cdot 10^9$ cfu/mL for the stationary phase condition. Lines correspond to robust linear regression with concentration at origin being 1.

1.4.2.1 *Experimental procedure*

Growth at high temperature is studied using similar protocols as in survival experiments reported in the previous section (1.4.1.1). A dilution of an overnight culture in LB at 37°C is inoculated into fresh M9 medium and grown at 37°C. Three treatments are used: (i) growth at temperature increasing gradually from 37°C to 50°C, (ii) growth at 37°C followed by a heat shock (at the end of the ramp), and (iii) growth at 37°C as a control. The experiments have been run in three conditions, with ramps lasting 70 min, 140 min and 240 min respectively.

Gradual temperature increase is achieved thanks to a custom program, developed for these experiments allowing to remotely control the temperature of the incubator. Growth is monitored by OD at 600 nm (measured with an Eppendorf Biophotometer) every 30 min. For each condition, two replicates are run in parallel in order to estimate variability. Some of these have also been performed by H. Bosc-Ducros.

1.4.2.2 *Results*

In all conditions, some growth is achieved at 50°C, both after heat shock or ramp (Fig. 1.17). Once 50°C is reached, growth is better in the "ramp" condition for the 70 min and 140 min ramps (3.5-fold and 2.4-fold OD increase respectively), but the effect does not last more than 3 h after the end of the ramp. In addition, considering the 240 min ramp condition, growth is slightly better in the corresponding "step" condition (1.8-fold vs. 1.32-fold OD increase) (Fig. 1.18).

These observations are difficult to interpret as changes in OD reflect both transient increase in growth rate (optimal growth temperature is higher than 37°C) and damages occurring when temperature increases in the ramp. Moreover, this protocol results in bacteria experiencing high temperature at different stages of their exponential phase (Fig. 1.17); this is likely to affect both survival (as shown in Fig. 1.16) and acclimation ability.

Although experimental conditions have been chosen so that mortality is low, the measurement of such a slow growth suggests that mortality is likely to play an important role. Indeed the growth in long temperature ramp is difficult to estimate as death occurs before the target temperature is reached and dead cell still account in OD measurements. In survival experiments, death rate estimated at 50°C in exponential phase corresponds to 50 % survival after 200 min and 20 % after 400 min. If less than half of the (living and dead cells) population is actively dividing, the apparent growth rate will be much lower than the actual one. Consequently mortality happening below and at 50°C could hide a possible growth of cells acclimated to high temperature.

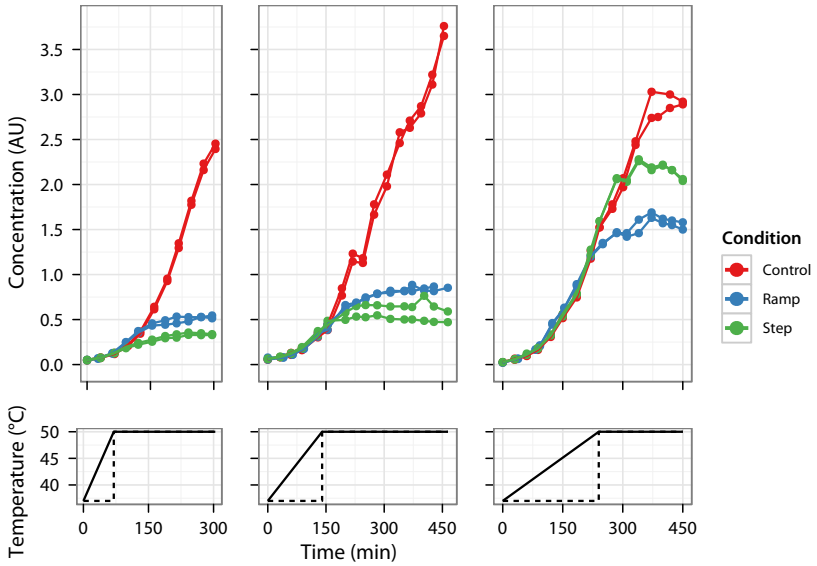

Figure 1.17: Growth of *E. coli* MG1655 in temperature ramps of decreasing slopes. Two conditions (heat shock in a water bath vs. temperature ramp) are compared to a control condition (growth at 37°C) using optical density measurements. After 180 min, concentration is estimated after a 2 × dilution which notably perturbs measurements of the control condition. Two replicates are run for each condition. Bottom panels indicate the temperature history (plain line: ramp; dash line: step).

Finally, in heat shock conditions, the effect of temperature shift is stronger in early exponential phase when bacteria are growing very fast (at 70 min) than later in growth (Fig. 1.18).

Using heat shock experiments, we showed that *E. coli* MG1655 survival at high temperature decreases very rapidly above 50°C. Death rates depend on bacteria physiological state, being higher in exponential than in stationary phase.
Using continuous temperature increase from 37°C to 50°C, there is no long-lasting acclimation effect of the rate of temperature increase on growth at 50°C in all tested conditions (rates above 0.054°C/min). In addition, ramps shorter than 140 min (above 0.093°C/min) tend to allow better growth than heat shock.

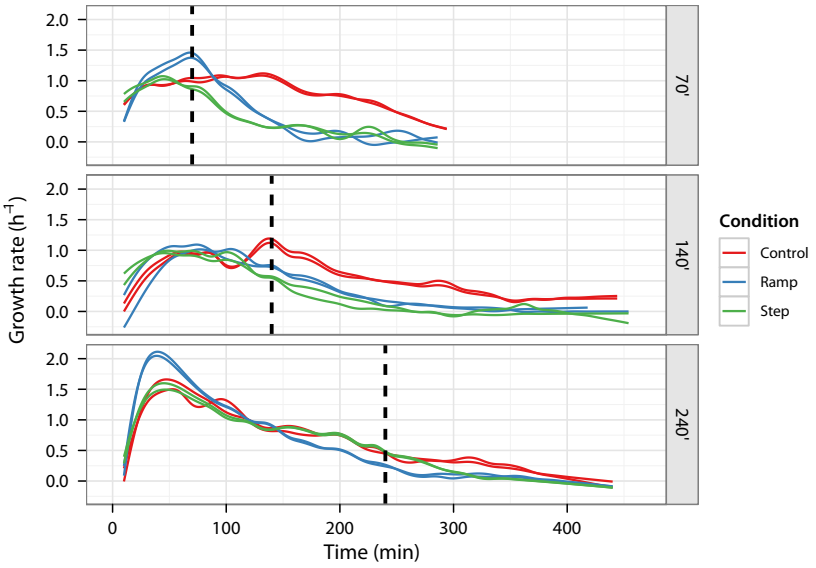

Figure 1.18: Instantaneous growth rate of *E. coli* MG1655 in temperature ramps of decreasing slopes. Instantaneous growth rate is estimated using a 20 min time window after local polynomial interpolation of the experimental growth curve shown in Fig. 1.17. Top, middle and bottom panels correspond to heating ramps lasting 70 min, 140 min and 240 min respectively. Vertical dash lines show the end of heating ramp which also corresponds to heat shock time.

1.5 DISCUSSION

1.5.1 CHALLENGES OF EVOLUTIONARY EXPERIMENTS IN A SPATIAL TEMPERATURE GRADIENT

This work was initiated as an attempt to run an adaptation experiment in a spatially structured environment. As reported, this proved to be experimentally difficult due mostly to convection issues. This prevented us from running evolution experiments properly speaking. Nonetheless, I managed to disentangle several biological effects possibly at play in these ecological conditions.

First, when designing the experiment, we hypothesized that only growth rate depended on temperature and death above the maximal growth temperature was implicitly assumed. I pointed out that survival to high temperature is possible above the maximal growth temperature. In addition, I identified that temperature history critically affects growth and survival at high temperature. This magnifies the role of acclimation in this experiment.

Second, we initially vastly underestimated the importance of chemotaxis. At microscopic scale, bacteria uptake of nutrients can result in nutrient gradients. In this case, ecological dynamics are governed by chemotaxis-driven collective motion. We showed that in a temperature gradient this effect is stronger than thermotaxis. Although the relevance of such dynamics remains to be established at larger scales, there is no simple argument to claim that it should vanished. Consequently, ecological dynamics are likely to be much more complicated than proposed in equation 1.1. For instance, a front could propagate due to chemotaxis just after inoculation bringing most of the population to irreversible damages; in this case a steady state could be reached where bacteria grow at the tail of the front. In another scenario, similar fronts could be initiated repeatedly after nutrients are consumed by growing bacteria, leading to periodic dynamics.

Third, we came to undermine the magnitude of thermotaxis: in a temperature gradient without nutrients, no clear thermotaxis was observed. As argued previously (in section 1.3.3.2), this questions the current understanding of thermotaxis. Anyhow, the large overlap between chemotaxis and thermotaxis molecular machineries makes thermotaxis likely to depend very much on nutrient conditions.

Other unexpected effects are likely to make this evolutionary experiment more difficult to run and/or to interpret than we thought, but have not been explored in detail yet. The experiment design was based on the assumption that nutrient consumption would create a gradient that would drive selection toward higher temperature niches. Although sugars are regarded here as primary nutrients in minimal medium, the same reasoning stands for other metabolites like oxygen. Consequently, which gradient will make growth at higher temperature advantageous is not clearly identified at that point and can change during the experiment depending on metabolic adaptations.

Finally, another instability that is likely to occur is also due to nutrients consumption. As bacteria grow, the nutrients concentration in the medium decreases and causes density to decrease as well. In our design, higher niches are empty which is likely to trigger convection as denser fluid will be on top. Preliminary tests with inoculation at the bottom and constant temperature show clear plume patterns indicating a Rayleigh-Taylor instability already reported by Benoit et al. (2008). However, we have not characterized yet what magnitude of temperature gradient can compensate this density difference.

1.5.2 ON THE NATURE OF ACCLIMATION

As exposed in the introduction, acclimation is a particular case of phenotypic plasticity induced by specific environmental conditions. Historically, the concept of phenotypic plasticity was first coined in developmental biology in order to describe the variability of adult forms for a given genotype depending on environmental conditions. These changes, generally referred to as developmental switches, occur during early stages of the life cycle, most of the time in an irreversible manner. Nowadays, the notion of phenotypic plasticity has been extended to describe "the general effect of the environment on phenotypic expression" (Scheiner, 1993). In the case of acclimation, one refers precisely to phenotypic modifications occurring during the life cycle in response to gradual environmental changes. In general, it is considered to be reversible.

Another interesting aspect of phenotypic plasticity is that modifications can sometimes be transmitted across generations (Huey and Berrigan, 1996), giving rise to more complex acclimation dynamics for instance.

In the case of developmental switches, reaction norms are used to describe difference between phenotypes for a given genotype depending on growth conditions (most often constant over time). Such a simplistic description is impossible for acclimation as it occurs in response to gradual changes and is intrinsically history-dependent. Among the difficult questions are when does the acclimation process start and how it is affected by the rate and overall magnitude of environmental changes. Consequently, accurate descriptions should take into account a large number of parameters although this is very difficult to put into practice.

This raises the question of the nature of acclimation. As acclimation ability can vary depending on the condition, it is tempting to consider it as a phenotypic trait. However, phenotypic traits such as growth rate at a given temperature are usually considered to depend on individuals history. Consequently, one can wonder whether acclimation ability also depends on individuals history and can be considered as a phenotypic trait or whether one should follow the terminology used to describe evolvability and consider acclimation ability as a "second order phenotype".

1.5.3 COSTS AND BENEFITS OF ACCLIMATION IN BACTERIA

Until the 1990's, acclimation was interpreted following the implicit "beneficial acclimation hypothesis" phrased and challenged by Leroi et al. (1994b). This viewpoint consists in assuming that acclimation will increase individual performance and ultimately fitness thanks to appropriate physiological changes. However, this omits the possible costs of ac-

climation that can make it ultimately detrimental as reported in bacteria. In addition, when physiological constraints make it impossible to acclimate to a new stressful environment, survival depends primarily on the time spent under stress. In this case, gradual changes may be more detrimental than rapid ones if they result in longer time spent in stressful conditions. This has been shown in yeast where survival is optimal at intermediate temperature increase rates (Gervais and de Marañon, 1995).

Hereafter, I discuss the costs and benefits of acclimation to temperature in mesophile bacteria, in relation with our experiments.

Firstly, it is important to notice that the thermal niche of mesophile species is generally asymmetric: the optimal growth temperature is shifted toward the upper limit, while growth rate decreases much more rapidly with temperature increase than with decrease (Fig. 1.1). In addition, at the niche boundary, irreversible damages occur much more rapidly at high temperature than at low temperature (respectively 45 and 5°C in *E. coli*). Interestingly, trade-offs asymmetry observed during adaptation to constant temperature could result from this niche asymmetry: *E. coli* lines adapted during 2000 generations at 42°C experience no decrease in fitness at lower temperature (Fig. 1.7; Bennett and Lenski, 1993) while those adapted at 20°C are 20 % less fit than the ancestor at 42°C (Mongold et al., 1996).

As far as acclimation is concerned, this niche asymmetry suggests that the costs and benefits of acclimation are different at the lower and upper limits of the thermal niche.

In our ramp experiments (reported in section 1.4.2), we observed limited acclimation of growth and survival at high temperature. In line with the beneficial acclimation hypothesis, our working hypothesis was that prior exposure to high temperature improves survival at high temperature and possibly allows growth. Consequently, a gradual temperature increase was supposed to confer the best acclimation to high temperature. However, our data rather suggest that the time spent at high temperature is the dominant factor shaping survival thus rejecting this idea that longer acclimation is more beneficial. Unfortunately, when the duration of acclimation changes, bacteria experience slightly different growth conditions. As a result, it is very difficult to distinguish the effect of acclimation duration from an hypothetical effect of physiological state (exponential vs. stationary phase) on acclimation to high temperature. Finally, the observation that longer acclimation is not beneficial could be explained by the temperature increase being still too fast. This could also be due to acclimation mechanisms being different for growth and survival as suggested by results obtained with slower ramps (Guyot, 2007). In the latter explanation, damages accumulating with the time spent under thermal

stress would be compensated by the improvement in growth allowed by slow acclimation.

Even more unexpected is our observation in microchannels reported in section 1.3.2. While bacteria were moving freely in the temperature gradient, very limited acclimation occurred and bacteria finally lost motility around 45.5°C. Although the current setup does not allow it, it would be informative to know whether bacteria are still alive or experience lethal damages, using for instance propidium iodide labeling. Although mortality is supposedly very low at this temperature, we showed in section 1.4.1 that high level of metabolic activity increased the susceptibility to heat shock. Anyhow, this suggests either that such situation where chemotaxis drives bacteria toward damaging conditions was very uncommon in *E. coli* past life history or that the cost/benefit ratio of acclimation was too high for it to be selected.

1.5.4 INTERPLAY BETWEEN ACCLIMATION AND ADAPTATION IN EVOLUTION EXPERIMENTS

1.5.4.1 *Acclimation as a target of selection*

The interplay between acclimation and adaptation could also be studied in bacteria response to antibiotics where both persistence and resistance are distinguished (Balaban et al., 2004).

In Bennett's experiment, inducible thermotolerance to 50°C after acclimation at 41°C was shown to be higher in the lines evolved at 42°C than in the ancestor (Riehle et al., 2003). This shows that acclimation ability is an evolvable trait, probably selected here as a by-product of selection for growth at high temperature. Unfortunately, it was not reported whether survival without acclimation evolved during the experiment.

In order to propose a selective mechanism for acclimation, it is important to disentangle whether it acts as a reactive or anticipatory process. In the first case, environmental change is interpreted as a steady state cue: "it's hotter, let's adapt to it and perform better!". In the latter, it is interpreted as a dynamic cue: "it's getting hotter, let's get protected before it becomes even hotter…" (Huey et al., 1999). In both cases, the type of acclimation to be expected is not the same (improving respectively either growth and survival, or mostly survival as detailed in the previous section 1.5.3). It is likely that both types of acclimation have been selected depending on the past life history of species.

In particular, considering the differences between the lower and upper limits of the thermal niche (exposed previously in section 1.5.3), several types of acclimation can be envisaged:

- Acclimation of growth performance at a non-stressful temperature.
- Acclimation of survival at a lethal temperature, possibly induced by earlier temperature of growth or transient heat shock.
- Acclimation of growth and survival following a gradual variation from non-stressful to stressful temperature.

The first and last cases correspond to acclimation as a reactive process, while the second is a case of acclimation as anticipatory process.

1.5.4.2 *Acclimation to the adaptation environment is the most beneficial*

The beneficial acclimation hypothesis states that acclimation is advantageous for growth in a given environment. As explained previously, this view omits the possible costs of acclimation. For instance in Bennett's experiment, after 2000 generations of adaptation at constant temperature, *E. coli*'s relative fitness is higher when measured after acclimation at its evolution temperature than at the competition temperature (Bennett and Lenski, 1997). This suggests that the benefit of acclimation in terms of growth is less than its related costs. No systematic study has tested whether this is true also for survival.

More generally, this raises the question of fitness estimation. In evolutionary experiments with microbes, it is usually assimilated to the relative growth rate compared to the ancestor during competition. This proved to bring great explanatory power in a number of experiments. However, this corresponds to selective pressures where either growth or survival is challenged. In nature and over long time, it is likely that the fitness of free-living species results from a mixture of both, alternating between periods of competition for growth and periods of prolonged survival. This supports the view of acclimation as an anticipatory process in which it may be advantageous in the long run to reduce growth in order to increase later survival. Occurrence of sporulation in bacteria, the best-studied case of a developmental switch in these species, corroborates that such strategy can be selected.

1.5.4.3 *Acclimation ability can be lost during selection in constant environment*

In Bennett's temperature adaptation experiment, no trade off was observed between the growth advantage at the adaptation temperature and the growth ability at other temperatures. This suggests that acclimation mechanisms are maintained during adaptation, even in constant environment. Adaptation to other stressful environments gives valuable insights on the generality of the dynamics observed with temperature.

When adapted to a variable environment with controlled pH (either periodic or random changes), *E. coli* B tends to become generalist and acclimation ability is likely not much changed. However, when adapted to a constant environment with controlled pH, specialists showing only limited adaptation are selected. Interestingly, in the acid and basic conditions, *E. coli* loses the ability to acclimate to the other environment (Hughes et al., 2007).

In three different strains of *E. coli*, asymmetry of time to division between sister cells is reported to be higher in rich medium than in nutrient-limited medium. This difference is no longer observed after 1000 generations of adaptation to a constant environment, be it rich or poor medium (Lele et al., 2011).

The loss of acclimation ability during adaptation to a constant environment can be interpreted in at least two nonexclusive ways. First, if the cost of acclimation is high, it is likely to be counter selected provided its components are expressed in constant environment, even at low level. Second, acclimation is a complex trait likely to involve a large number of components. In this case, acclimation has a higher chance to be lost by genetic drift as each component can be inactivated independently of the others. Finally, the loss of acclimation reported for pH tolerance and division asymmetry contrasts with Bennett's experiment where acclimation ability is maintained, as shown by the absence of trade-off. This difference highlights how much the adaptive dynamics depends on the underlying physiological constraints.

A parallel can be established between the repeated loss of acclimation ability during adaptation experiments to constant conditions and the fact that acclimation ability is rarely selected in adaptation experiments with a fluctuating environment. Regarding the cost of acclimation, this suggests that in general the cost/benefit ratio of acclimation is low. In addition, the difficulty to predict whether or not an intermittent regime of selection will select for improved acclimation implies that acclimation ability is a complex trait depending heavily on physiological constraints.

Another strategy that can be selected for in a fluctuating environment is bet-hedging based on stochastic phenotypic switching. As a proof of principle, yeasts have been engineered to express a synthetic bistable gene circuit with adjustable switching frequency. Fast switching phenotypes have a growth advantage in an environment fluctuating at high frequency and *vice versa* (Acar et al., 2008). Interestingly, a similar bet-hedging mechanism has been selected in *P. fluorescens* evolved in an environment alternating between spatially structured (static) and well-mixed (shaken) condition. Instead of selecting for advantageous mutations at each change, a small part of the population switches spontaneously toward the other phenotypic state independently of environmental conditions. This strain appeared to be selected in quickly varying environment although it is less fit in each static condition (Beaumont et al., 2009). Why and in which case bet-hedging is selected instead of improved acclimation remains an open question.

In this respect, it would be interesting to run an adaptation experiment in which individuals repeatedly experience acclimation due to a gradual temperature increase. This was the purpose of the work reported in section 1.4. However, we failed to identify conditions of pronounced accli-

mation. Using results obtained with 2°C/day ramps (Guyot, 2007), this could now be envisaged as a way to select for improved acclimation. Another alternative is to rely on a spatial gradient as we originally intended to.

As a matter of conclusion, let us elaborate on one possible implication of acclimation regarding adaptation. By its nature, acclimation is an history-dependant process. As strains acclimated to high temperature are expressing a different phenotype, they may be selected for, in particular in the case where survival is critical making the cost of acclimation secondary. This is likely to make evolutionary trajectories history-dependent as well.

This effect would contribute to contingency in adaptation, that is also driven by the constraints on succession of mutational events. This has been shown using combinatorially engineered antibiotic-resistant mutants (Weinreich et al., 2006) as well as in Lenski's experiment. In the latter, it appears to be critical for evolutionary innovation, in this case the acquisition of a new metabolic function (Blount et al., 2008).

BIBLIOGRAPHY

M. Acar, J. T. Mettetal, and A. van Oudenaarden. 2008. Stochastic switching as a survival strategy in fluctuating environments. *Nature Genetics*, 40(4):471–475.

M. Ackermann and M. Doebeli. 2004. Evolution of niche width and adaptive diversification. *Evolution*, 58(12):2599–612.

D. I. Andersson and D. Hughes. 2010. Antibiotic resistance and its cost: is it possible to reverse resistance? *Nature Reviews. Microbiology*, 8(4):260–271.

N. Q. Balaban, J. Merrin, R. Chait, L. Kowalik, and S. Leibler. 2004. Bacterial persistence as a phenotypic switch. *Science (New York, N.Y.)*, 305(5690):1622–1625.

M. A. Barber. 1908. The rate of multiplication of Bacillus coli at different temperatures. *The Journal of Infectious Diseases*, 5(4):379–400.

J. E. Barrick, D. S. Yu, S. H. Yoon, H. Jeong, T. K. Oh, D. Schneider, R. E. Lenski, and J. F. Kim. 2009. Genome evolution and adaptation in a long-term experiment with Escherichia coli. *Nature*, 461(7268):1243–1247.

H. J. E. Beaumont, J. Gallie, C. Kost, G. C. Ferguson, and P. B. Rainey. 2009. Experimental evolution of bet hedging. *Nature*, 462(7269):90–93.

M. Beeby, B. D. O'Connor, C. Ryttersgaard, D. R. Boutz, L. J. Perry, and T. O. Yeates. 2005. The genomics of disulfide bonding and protein stabilization in thermophiles. *PLoS Biology*, 3(9):e309.

A. Bennett and R. Lenski. 1993. Evolutionary adaptation to temperature. 2. Thermal niches of experimental lines of Escherichia coli. *Evolution*, 47(1):1–12.

A. Bennett and R. Lenski. 1997. Evolutionary adaptation to temperature. 6. Phenotypic acclimation and its evolution in Escherichia coli. *Evolution*, 51(1):36–44.

A. Bennett and R. Lenski. 2007. An experimental test of evolutionary trade-offs during temperature adaptation. *Proceedings of the National Academy of Sciences of the United States of America*.

A. Bennett, R. Lenski, and J. Mittler. 1992. Evolutionary adaptation to temperature. 1. Fitness responses of Escherichia coli to changes in its thermal environment. *Evolution*, 46(1):16–30.

M. R. Benoit, R. B. Brown, P. Todd, E. S. Nelson, and D. M. Klaus. 2008. Buoyant plumes from solute gradients generated by non-motile Escherichia coli. *Physical Biology*, 5 (4):46007.

A. Bigham, M. Bauchet, D. Pinto, X. Mao, J. M. Akey, R. Mei, S. W. Scherer, C. G. Julian, M. J. Wilson, D. L. Herráez, T. Brutsaert, E. J. Parra, et al. 2010. Identifying signatures of natural selection in Tibetan and Andean populations using dense genome scan data. *PLoS Genetics*, 6(9):e1001116.

Z. D. Blount, C. Z. Borland, and R. E. Lenski. 2008. Inaugural Article: Historical contingency and the evolution of a key innovation in an experimental population of Escherichia coli. *Proceedings of the National Academy of Sciences of the United States of America*.

A. Bronikowski, A. Bennett, and R. Lenski. 2001. Evolutionary adaptation to temperature. 8. Effects of temperature on growth rate in natural isolates of Escherichia coli and Salmonella enterica from different thermal environments. *Evolution*, 55(1):33–40.

A. Buckling, F. Harrison, M. Vos, M. A. Brockhurst, A. Gardner, S. A. West, and A. Griffin. 2007. Siderophore-mediated cooperation and virulence in Pseudomonas aeruginosa. *FEMS microbiology ecology*, 62(2):135–41.

M. D. Carruthers and C. Minion. 2009. Transcriptome analysis of Escherichia coli O157:H7 EDL933 during heat shock. *FEMS Microbiology Letters*, 295(1):96–102.

E. Casman and L. Rettger. 1933. Limitation of Bacterial Growth at Higher Temperatures. *Journal of Bacteriology*, 26(1):77–123.

G. Cebrián, N. Sagarzazu, R. Pagán, S. Condón, and P. Mañas. 2008. Resistance of Escherichia coli grown at different temperatures to various environmental stresses. *Journal of Applied Microbiology*, 105(1):271–8.

L. Chao and G. Ramsdell. 1985. The effects of wall populations on coexistence of bacteria in the liquid phase of chemostat cultures. *Journal of General Microbiology*, 131(5):1229–36.

P. Chen and E. I. Shakhnovich. 2010. Thermal adaptation of viruses and bacteria. *Biophysical Journal*, 98(7):1109–1118.

V. Cooper and R. Lenski. 2000. The population genetics of ecological specialization in evolving Escherichia coli populations. *Nature*, 407(6805):736–739.

R. A. Copeland. 2000. *Enzymes: a practical introduction to structure, mechanism, and data analysis*. John Wiley & Sons Inc, 2nd revised edition.

J. H. Crowe, L. M. Crowe, J. F. Carpenter, A. S. Rudolph, C. A. Wistrom, B. J. Spargo, and T. J. Anchordoguy. 1988. Interactions of sugars with membranes. *Biochimica et Biophysica Acta*, 947(2):367–384.

W. Dallinger. 1887. The President's address. *Journal of the Royal Microscopical Society*, 7:185–199.

C. Darwin. 1859. *On the origin of species by means of natural selection*. John Murray.

V. A. de Crécy-Lagard, J. Bellalou, R. Mutzel, and P. Marlière. 2001. Long term adaptation of a microbial population to a permanent metabolic constraint: overcoming thymineless death by experimental evolution of Escherichia coli. *BMC biotechnology*, 1:10.

T. J. Denich, L. A. Beaudette, H. Lee, and J. T. Trevors. 2003. Effect of selected environmental and physico-chemical factors on bacterial cytoplasmic membranes. *Journal of Microbiological Methods*, 52(2):149–182.

U. Dieckmann, R. Law, and J. A. J. Metz. 2000. *The Geometry of Ecological Interactions*. Cambridge Studies in Adaptive Dynamics. Cambridge University Press.

M. Doebeli and U. Dieckmann. 2003. Speciation along environmental gradients. *Nature*, 421(6920):259–264.

M. Doebeli and C. Hauert. 2005. Models of cooperation based on the Prisoner's Dilemma and the Snowdrift game. *Ecology Letters*, 8(7):748–766.

A. Díaz-Acosta, M. L. Sandoval, L. Delgado-Olivares, and J. Membrillo-Hernández. 2006. Effect of anaerobic and stationary phase growth conditions on the heat shock and oxidative stress responses in Escherichia coli K-12. *Archives of Microbiology*, 185 (6) : 429–438.

S. Elena and R. Lenski. 2003. Evolution experiments with microorganisms: The dynamics and genetic bases of adaptation. *Nature Reviews Genetics*, 4(6) : 457–469.

S. Elena, V. Cooper, and R. Lenski. 1996. Punctuated evolution caused by selection of rare beneficial mutations. *Science*, 272(5269) : 1802–1804.

P. Elliker and W. Frazier. 1938. Influence of Time and Temperature of Incubation on Heat Resistance of Escherichia coli. *Journal of Bacteriology*, 36(1) : 83–98.

S. A. Fletcher and L. N. Csonka. 1998. Characterization of the induction of increased thermotolerance by high osmolarity in Salmonella. *Food Microbiology*, 15(3) : 307–317.

T. Garland and M. R. Rose, editors. 2009. *Experimental evolution: Concepts, methods, and applications of selection experiments*. University of California Press, Berkeley.

P. Gervais and I. M. de Marañon. 1995. Effect of the kinetics of temperature variation on Saccharomyces cerevisiae viability and permeability. *Biochimica et Biophysica Acta - Biomembranes*, 1235(1) : 52–56.

S. J. Gould. 1989. *Wonderful life: the Burgess shale and the nature of history*. W. W. Norton & Company.

H. Grosjean and T. Oshima. 2007. How nucleic acids cope with high temperature. In C. Gerday and N. Glansdorff, editors, *Physiology and Biochemistry of Extremophiles*, pages 39–56. ASM Press, Washington D.C.

C. A. Gross. 1996. Function and regulation of the heat shock proteins. In F. C. Neidhardt, editor, *Escherichia coli and Salmonella: cellular and molecular biology*, page 1382–1399. ASM Press, Washington D.C., second edition.

T. S. Gunasekera, L. N. Csonka, and O. Paliy. 2008. Genome-wide transcriptional responses of Escherichia coli K-12 to continuous osmotic and heat stresses. *Journal of Bacteriology*, 190(10) : 3712–3720.

E. Gur, D. Biran, E. Gazit, and E. Ron. 2002. In vivo aggregation of a single enzyme limits growth of Escherichia coli at elevated temperatures. *Molecular Microbiology*, 46(5) : 1391–1397.

S. Guyot. 2007. *Influence de la cinétique d'un stress thermique sur la physiologie cellulaire*. PhD thesis, Université de Bourgogne, Dijon.

S. Guyot, L. Pottier, E. Ferret, L. Gal, and P. Gervais. 2010. Physiological responses of Escherichia coli exposed to different heat-stress kinetics. *Archives of Microbiology*, 192(8) : 651–661.

C. W. Haest, J. de Gier, and L. L. van Deenen. 1969. Changes in the chemical and the barrier properties of the membrane lipids of E. coli by variation of the temperature of growth. *Chemistry and Physics of Lipids*, 3(4) : 413–417.

S. W. Harcum and F. T. Haddadin. 2006. Global transcriptome response of recombinant Escherichia coli to heat-shock and dual heat-shock recombinant protein induction. *Journal of Industrial Microbiology & Biotechnology*, 33(10) : 801–814.

D. A. Hickey and G. A. C. Singer. 2004. Genomic and proteomic adaptations to growth at high temperature. *Genome Biology*, 5(10):117.

R. B. Huey and D. Berrigan. 1996. Testing evolutionary hypotheses of acclimation. In I. A. Johnston and A. F. Bennett, editors, *Animals and temperature: phenotypic and evolutionary adaptation*. Cambridge University Press.

R. B. Huey, D. Berrigan, G. W. Gilchrist, and J. C. Herron. 1999. Testing the adaptive significance of acclimation: a strong inference approach. *American Zoologist*, 39(2): 323 –336.

B. S. Hughes, A. J. Cullum, and A. F. Bennett. 2007. An experimental evolutionary study on adaptation to temporally fluctuating pH in Escherichia coli. *Physiological and Biochemical Zoology*, 80(4):406–421.

K. Jeannot, M. L. Sobel, F. E. Garch, K. Poole, and P. Plésiat. 2005. Induction of the MexXY efflux pump in Pseudomonas aeruginosa is dependent on drug-ribosome interaction. *Journal of Bacteriology*, 187(15):5341–5346.

C. M. Jessup, R. Kassen, S. E. Forde, B. Kerr, A. Buckling, P. B. Rainey, and B. J. M. Bohannan. 2004. Big questions, small worlds: microbial model systems in ecology. *Trends in Ecology & Evolution (Personal Edition)*, 19(4):189–197.

N. Kashtan, E. Noor, and U. Alon. 2007. Varying environments can speed up evolution. *Proceedings of the National Academy of Sciences of the United States of America*.

N. Katsui, T. Tsuchido, R. Hiramatsu, S. Fujikawa, M. Takano, and I. Shibasaki. 1982. Heat-induced blebbing and vesiculation of the outer membrane of Escherichia coli. *Journal of Bacteriology*, 151(3):1523–1531.

T. Kishimoto, L. Iijima, M. Tatsumi, N. Ono, A. Oyake, T. Hashimoto, M. Matsuo, M. Okubo, S. Suzuki, K. Mori, A. Kashiwagi, C. Furusawa, et al. 2010. Transition from positive to neutral in mutation fixation along with continuing rising fitness in thermal adaptive evolution. *PLoS Genetics*, 6(10):e1001164.

R. Korona, C. H. Nakatsu, L. J. Forney, and R. E. Lenski. 1994. Evidence for multiple adaptive peaks from populations of bacteria evolving in a structured habitat. *Proceedings of the National Academy of Sciences of the United States of America*, 91(19): 9037–9041.

G. Lambert, D. Liao, S. Vyawahare, and R. H. Austin. 2011. Anomalous spatial redistribution of competing bacteria under starvation conditions. *Journal of Bacteriology*, 193(8):1878–1883.

U. N. Lele, U. I. Baig, and M. G. Watve. 2011. Phenotypic plasticity and effects of selection on cell division symmetry in Escherichia coli. *PLoS ONE*, 6(1):e14516.

R. Lenski. 2004. Phenotypic and genomic evolution during a 20,000-generations experiment with the bacterium Escherichia coli. *Plant Breeding Reviews*, 24(2):225–265.

R. Lenski and M. Travisano. 1994. Dynamics of adaptation and diversification - A 10,000-generation experiment with bacterial-populations. *Proceedings of the National Academy of Sciences of the United States of America*, 91(15):6808–6814.

A. Leroi, R. Lenski, and A. Benn. 1994. Evolutionary adaptation to temperature. 3. Adaptation of Escherichia coli to a temporally varying environment. *Evolution*, 48 (4):1222–1229.

A. M. Leroi, A. F. Bennett, and R. E. Lenski. 1994. Temperature acclimation and competitive fitness: an experimental test of the beneficial acclimation assumption. *Proceedings of the National Academy of Sciences of the United States of America*, 91(5): 1917–1921.

G. Lindblom, G. Orädd, L. Rilfors, and S. Morein. 2002. Regulation of lipid composition in Acholeplasma laidlawii and Escherichia coli membranes: NMR studies of lipid lateral diffusion at different growth temperatures. *Biochemistry*, 41(38): 11512–11515.

B. Lugtenberg, R. Peters, H. Bernheimer, and W. Berendsen. 1976. Influence of cultural conditions and mutations on the composition of the outer membrane proteins of Escherichia coli. *Molecular and General Genetics*, 147(3): 251–262–262.

K. Maeda and Y. Imae. 1979. Thermosensory transduction in Escherichia coli: inhibition of the thermoresponse by L-serine. *Proceedings of the National Academy of Sciences of the United States of America*, 76(1): 91–95.

K. Maeda, Y. Imae, J. I. Shioi, and F. Oosawa. 1976. Effect of temperature on motility and chemotaxis of Escherichia coli. *Journal of Bacteriology*, 127(3): 1039–1046.

R. Maharjan, S. Seeto, L. Notley-McRobb, and T. Ferenci. 2006. Clonal Adaptive Radiation in a Constant Environment. *Science*, 313(5786): 514–517.

A. G. Marr and J. L. Ingraham. 1962. Effect of temperature on composition of fatty acids in Escherichia coli. *Journal of Bacteriology*, 84(6): 1260–1267.

W. R. Mebane and J. S. Sekhon. rgenoud: R version of GENetic Optimization Using Derivatives. `http://cran.r-project.org/web/packages/rgenoud/`.

R. Mesibov and J. Adler. 1972. Chemotaxis toward amino acids in Escherichia coli. *Journal of Bacteriology*, 112(1): 315–326.

S. R. Miller, C. Williams, A. L. Strong, and D. Carvey. 2009. Ecological specialization in a spatially structured population of the thermophilic cyanobacterium Mastigocladus laminosus. *Applied and Environmental Microbiology*, 75(3): 729–734.

F. Mizera and G. Meszena. 2003. Spatial niche packing, character displacement and adaptive speciation along an environmental gradient. *Evolutionary Ecology Research*, 5(3): 363–382.

T. Mizuno and Y. Imae. 1984. Conditional inversion of the thermoresponse in Escherichia coli. *Journal of Bacteriology*, 159(1): 360.

J. Mongold, A. Bennett, and R. Lenski. 1996. Evolutionary adaptation to temperature. 4. Adaptation of Escherichia coli at a niche boundary. *Evolution*, 50(1): 35–43.

J. Mongold, A. Bennett, and R. Lenski. 1999. Evolutionary adaptation to temperature. 7. Extension of the upper thermal limit of Escherichia coli. *Evolution*, 53(2): 386–394.

J. Monod. 1942. *Recherches sur la croissance des cultures bactériennes*. Hermann, Paris.

S. Morein, A. Andersson, L. Rilfors, and G. Lindblom. 1996. Wild-type Escherichia coli cells regulate the membrane lipid composition in a "window" between gel and non-lamellar structures. *The Journal of Biological Chemistry*, 271(12): 6801–6809.

T. Nara, I. Kawagishi, S. Nishiyama, M. Homma, and Y. Imae. 1996. Modulation of the thermosensing profile of the Escherichia coli aspartate receptor tar by covalent modification of its methyl-accepting sites. *Journal of Biological Chemistry*, 271(30): 17932.

R. A. Nolan. 1971. Amino acids and growth factors in vitamin-free casamino acids. *Mycologia*, 63(6):1231–1234.

O. Oleksiuk, V. Jakovljevic, N. Vladimirov, R. Carvalho, E. Paster, W. S. Ryu, Y. Meir, N. S. Wingreen, M. Kollmann, and V. Sourjik. 2011. Thermal robustness of signaling in bacterial chemotaxis. *Cell*, 145(2):312–321.

E. Paster and W. S. Ryu. 2008. The thermal impulse response of Escherichia coli. *Proceedings of the National Academy of Sciences of the United States of America*, 105(14): 5373–5377.

Z. Patwa and L. M. Wahl. 2008. Fixation probability for lytic viruses: the attachment-lysis model. *Genetics*, 180(1):459–470.

P. B. Rainey and M. Travisano. 1998. Adaptive radiation in a heterogeneous environment. *Nature*, 394(6688):69–72.

M. M. Riehle, A. F. Bennett, and A. D. Long. 2001. Genetic architecture of thermal adaptation in Escherichia coli. *Proceedings of the National Academy of Sciences of the United States of America*, 98(2):525–530.

M. M. Riehle, A. F. Bennett, R. E. Lenski, and A. D. Long. 2003. Evolutionary changes in heat-inducible gene expression in lines of Escherichia coli adapted to high temperature. *Physiological genomics*, 14(1):47–58.

M. M. Riehle, A. F. Bennett, and A. D. Long. 2005. Changes in gene expression following high-temperature adaptation in experimentally evolved populations of E. coli. *Physiological and Biochemical Zoology: PBZ*, 78(3):299–315.

D. Rockabrand, T. Arthur, G. Korinek, K. Livers, and P. Blum. 1995. An essential role for the Escherichia coli DnaK protein in starvation-induced thermotolerance, H2O2 resistance, and reductive division. *Journal of Bacteriology*, 177(13):3695.

L. Rosso, J. R. Lobry, and J. P. Flandrois. 1993. An unexpected correlation between cardinal temperatures of microbial growth highlighted by a new model. *Journal of Theoretical Biology*, 162(4):447–63.

A. D. Russell. 2003. Lethal effects of heat on bacterial physiology and structure. *Science Progress*, 86(1-2):115–137.

H. Salman and A. Libchaber. 2007. A concentration-dependent switch in the bacterial response to temperature. *Nature Cell Biology*, 9(9):1098–1100.

H. Salman, A. Zilman, C. Loverdo, M. Jeffroy, and A. Libchaber. 2006. Solitary Modes of Bacterial Culture in a Temperature Gradient. *Physical Review Letters*, 97(11):118101–4.

J. Saragosti. 2010. *Chimiotactisme collectif de Escherichia coli*. PhD thesis, Université Pierre et Marie Curie, Paris, Paris.

J. Saragosti, V. Calvez, N. Bournaveas, A. Buguin, P. Silberzan, and B. Perthame. 2010. Mathematical description of bacterial traveling pulses. *PLoS Computational Biology*, 6(8).

S. M. Scheiner. 1993. Genetics and evolution of phenotypic plasticity. *Annual Review of Ecology and Systematics*, 24(1):35–68.

W. Schmidt. 2002. Effects of intermittent exposure to high altitude on blood volume and erythropoietic activity. *High Altitude Medicine & Biology*, 3(2):167–176.

W. R. Schneider and R. N. Doetsch. 1974. Effect of viscosity on bacterial motility. *Journal of Bacteriology*, 117(2):696–701.

B. Shi and X. Xia. 2003. Changes in growth parameters of Pseudomonas pseudoalcaligenes after ten months culturing at increasing temperature. *FEMS Microbiology Ecology*, 45(2):127–134.

N. Shigapova, Z. Török, G. Balogh, P. Goloubinoff, L. Vígh, and I. Horváth. 2005. Membrane fluidization triggers membrane remodeling which affects the thermotolerance in Escherichia coli. *Biochemical and Biophysical Research Communications*, 328(4):1216–1223.

J. M. Smith. 1998. *Evolutionary genetics*. Oxford University Press, 2 edition.

P. D. Sniegowski, P. J. Gerrish, and R. E. Lenski. 1997. Evolution of high mutation rates in experimental populations of E. coli. *Nature*, 387(6634):703–5.

K. Soetaert, T. Petzoldt, and R. W. Setzer. 2010. Solving differential equations in R: package deSolve. *Journal of Statistical Software*, 33(9):1–25.

J. Sorensen, T. Kristensen, and V. Loeschcke. 2003. The evolutionary and ecological role of heat shock proteins. *Ecology Letters*, 6(11):1025–1037.

J. F. Storz, A. M. Runck, S. J. Sabatino, J. K. Kelly, N. Ferrand, H. Moriyama, R. E. Weber, and A. Fago. 2009. Evolutionary and functional insights into the mechanism underlying high-altitude adaptation of deer mouse hemoglobin. *Proceedings of the National Academy of Sciences of the United States of America*, 106(34):14450–14455.

T. Tsuchido, N. Katsui, A. Takeuchi, M. Takano, and I. Shibasaki. 1985. Destruction of the outer membrane permeability barrier of Escherichia coli by heat treatment. *Applied and Environmental Microbiology*, 50(2):298–303.

V. Valdramidis, A. Geeraerd, K. Bernaerts, and J. van Impe. 2006. Microbial dynamics versus mathematical model dynamics: The case of microbial heat resistance induction. *Innovative Food Science & Emerging Technologies*, 7(1-2):80–87.

E. van Derlinden, K. Bernaerts, and J. F. van Impe. 2008. Dynamics of Escherichia coli at elevated temperatures: effect of temperature history and medium. *Journal of Applied Microbiology*, 104(2):438–453.

G. Vogt, S. Woell, and P. Argos. 1997. Protein thermal stability, hydrogen bonds, and ion pairs. *Journal of Molecular Biology*, 269(4):631–643.

D. M. Weinreich, N. F. Delaney, M. A. Depristo, and D. L. Hartl. 2006. Darwinian evolution can follow only very few mutational paths to fitter proteins. *Science*, 312 (5770):111–114.

X. Yi, Y. Liang, E. Huerta-Sanchez, X. Jin, Z. X. P. Cuo, J. E. Pool, X. Xu, H. Jiang, N. Vinckenbosch, T. S. Korneliussen, H. Zheng, T. Liu, et al. 2010. Sequencing of 50 human exomes reveals adaptation to high altitude. *Science*, 329(5987):75–78.

T. Yura and K. Nakahigashi. 1999. Regulation of the heat-shock response. *Current Opinion in Microbiology*, 2(2):153–158.

T. Yura, M. Kanemori, and M. T. Morita. 2000. The heat shock response: regulation and function. In G. Storz and R. Hengge-Aronis, editors, *Bacterial stress responses*, page 3–18. ASM Press, Washington D.C.

Chapter 2

MICROBIAL POPULATION DYNAMICS AT LOW DENSITIES

2.1 INTRODUCTION

2.1.1 CONTEXT AND AIMS

Pathogenicity of a variety of microbial species drove the early times of microbiology. Nonetheless, being able to characterize precisely infection dynamics, in particular at early stages is still a relevant issue. Moreover, microbial populations are important model systems in ecology and evolution, used to address a variety of topics such as population dynamics (Balagaddé et al., 2008; Fru et al., 2011; Varon and Zeigler, 1978), ecological interactions (Foster, 2011), and adaptation (Elena and Lenski, 2003). The advantages and limits of microbial experimental systems in ecological studies are discussed in detail by Jessup et al. (2005).

In this chapter, I report the development of a high sensitivity microbial concentration measurement device that was initially imagined in order to monitor in real-time colonization events in a growth chamber with a temperature gradient as presented in the previous chapter. Beforehand, I review existing technics of microbial concentration measurements. All considerations in this chapter are restricted to liquid cultures as they represent the most widely used experimental system. Microbes detection and concentration measurements in aerosol are discussed in details in Henningson et al. (1997). This restriction brings us to use either "concentration" or "population size" assuming that we are considering a known volume of culture solution.

Finally, two important distinctions have to be highlighted. First, in certain applications such as food safety, the critical issue is detection of microbes presence while their precise concentration is of little interest. Several methods have been developed for this purpose. In contrast, we are here interested in concentration measurements. Second, concentration measurements generally focus on living bacteria. Identification methods of living bacteria depend on assumptions on the detrimental process causing death. For instance, in mutagenic conditions, death is generally assessed as bacteria that are not able to divide and grow a colony anymore due to lethal mutations in indispensable genes; this is referred to as "genetic death". If structural damages are caused to cells as in the case of heat stress discussed in the previous chapter, it is more common to consider physiological death as the ability to maintain a permeability barrier at the cell enveloppe; this can be identified using dyes that are not membrane permeable and produce a much stronger stain on cells with damaged membranes and wall. Our method is designed to allow the identification of this kind of damages.

2.1.2 METHODS TO MEASURE MICROBIAL POPULATION SIZE

In this section, I review the existing methods dedicated to measure microbial population size in liquid cultures, with an emphasis on their sensitivity at low concentration. Their main characteristics are summarised in Table 2.1.

2.1.2.1 *Manual counting methods*

Historically, microbial population sizes were measured by manual counting. These methods consist in making the microbes visible to the experimenter eyes, either based on colony growth or on microscopy.

COLONY FORMING UNIT This method relies on the fact that single microbes in solidified rich medium grow by binary fission and can form a colony visible by eye. Practically, it consists in preparing solutions at different dilutions from the microbial culture and plating these diluted solutions on petri dishes poured with solid growth medium (usually LB mixed with agar). This process is called serial dilution. After growth, the number of colonies (the so-called colony forming units) are counted at the dilution giving 30 to 400 colonies per plate. This method was introduced by Koch in the second part of the nineteenth century and is reports alive bacteria. Rapidly, microbiologists have considered possible artefacts as spatial growth inhibition between close colonies (Wilson, 1922), or plating effects that may prevent growth of certain microbes (e.g. due to desiccation). Another possible bias is that some bacteria may not separate completely during the sample preparation process (e.g. *Staphylococcus*, *Streptococcus*). Overall, although this method has raised a lot of criticism regarding its accuracy in estimating growth (see for instance Monod, 1942, p. 27), it is still widely used and is sometimes referred to as the Miles and Misra method (Miles et al., 1938). While dilution errors due to sampling and pipetting are limited (typically on the order of 5 – 10 % as estimated by Hedges, 2002), experimental errors can be larger in practice due to all artefacts mentioned above.

Regarding the estimation of growth rate at low density, this method is appealing as there is no lower limit of concentration estimation. However as mentioned above, this concentration measurement has limited precision. One possible extension at low density is based on the "most probable number": highly diluted samples are grown in microwells such that growth occurs in certain wells and not in others, and concentration is inferred from the proportion of growing wells (Taylor, 1962). Although this method reduces certain biases (plating effect, spatial competition), it is still

impaired by cell clumping and random sampling in serial dilutions.

MICROSCOPE COUNTING Another way of counting microbes by hand is to magnify them using a microscope. Bacteria are observed in an evaluation chamber (e.g. a Petroff-Hausser counting chamber similar to an hemocytometer but ten times thiner). Bacteria which are not moving too fast can be individually distinguished under white light (phase contrast, dark field, ...) and counted (Wilson, 1922). However, as the observation volume is limited, this method is not well suited for low concentration (in a $30 \times 30 \times 20\,\mu m^3$ chamber, less than 20 bacteria are expected in average in the chamber below $10^6\ mL^{-1}$). In addition, only non-motile strains can be studied. This method is rarely used nowadays for concentration estimation.

These counting methods have two major drawbacks: they are invasive (as culture sampling is required) and are very time consuming (both for sample preparation and counting). Nowadays, image analysis softwares are proposed to automate them, but no robust solution is available for unstained cells. As a result, microbiologists tend to use cell staining which considerably improves automated analysis. In most cases, direct counting tends to be replaced by flow cytometry presented below. Nonetheless, when additional individuals traits are measured as well, microscopy can be used since it provides higher sensitivity than flow cytometry.

2.1.2.2 *Photometric methods*

The development of electronics in the first part of the twentieth century gave rise to new approaches to measure microbial population size. In particular with the rise of photometry, i.e. the measurement of light intensity, microbial concentration could be estimated after light diffusion by cells. Light diffusion can be detected in two ways, either by measuring scattered light intensity or by measuring the decrease in transmitted light due to diffusion (multiple scattering). A great semantic confusion reigns in this domain, with turbidimetry referring alternatively to one method or the other. Hereafter, I refer to the former as nephelometry and to the latter as turbidimetry.

NEPHELOMETRY Etymologically, a nephelometer measures the cloudiness of a solution. It does so by measuring the light intensity diffused at 90° by cells or particles (Faguet, 1935; Forrest and Stephen, 1965). Consequently, the measurement depends on the light path (slit size, distance between sample and sensor, ...) and is expressed in arbitrary units that cannot be compared between setups. Only relative measurements can be performed, and concentration can be obtained from calibrations. Despite these limitations, this

method has proven to be useful for some work: Monod's thesis and diauxy characterization was based on the linearity of nephelometry over one order of magnitude (Monod, 1942). Nowadays, nephelometry is mostly used for the study of aerosols, that are gaseous suspensions of particles.

TURBIDIMETRY This method consists in measuring the attenuation of a light beam by a liquid solution (also called absorbance or optical density of the solution), estimated as the logarithm of the ratio of the light intensity measured through a blank solution and the sample. In the case of microbial cultures, absorbance is due to light diffusion (i.e. multiple scattering, which is stronger at higher visible wavelengths) and to absorption (which is stronger at lower visible wavelengths). Consequently, the optical density of a culture is expressed in absorbance units and is usually measured at high visible wavelength, typically 600 nm. Theoretically, absorbance is a linear function of the concentration and the sample thickness as stated by the Beer Lambert law. Consequently, at a given wavelength and sample thickness, it could be considered to be an absolute measurement of concentration, although in practice calibration is required. In addition, although absorbance takes into account any other absorbing source present along the path (Forrest and Stephen, 1965), the fact that it is normalized with a blank solution makes it much more robust to small variations of the light path than nephelometry.

$OD = \log(I_0/I)$ where OD is the optical density, I_0 the light intensity measured through blank, I the light intensity measured through the sample.

Absorbance has been shown to be closer to biomass than to cell number (Koch, 1961) and this technics has been slightly improved in various ways (see for instance Fujita and Nunomura, 1968 for variable sample thickness and Byrne et al., 1989 for a continuous measure device operating at 950nm with real-time calibration). As far as low populations sizes are concerned, the sensitivity at low concentrations (below 10^6 mL^{-1}) is not good and indirect methods have been proposed to measure low concentrations based on repeated measurements (Dekel and Alon, 2005; Novak et al., 2009).

Nowadays, turbidimetry is the most widely used method for microbial concentration measurements and is satisfactory in an intermediate concentration range. However, it is not satisfactory at low concentration and cannot be taken as a population size estimation method but rather as a biomass estimate. Moreover, it cannot be used in solvents with high turbidity (sediments, proteins, micelles).

Recently devices relying both on the intensity of diffused light at 90° and attenuation of transmission have been proposed and are claimed to provide better stability over long times in demanding applications such as space experiments (van Benthem et al., 2002).

METHOD	LOWER LIMIT	DURATION	INVASIVE	PROS	CONS
Colony Forming Unit	10^3 mL^{-1}	10 to 20 min (over 2 days)	Yes	Distinction between cell types.	Sample manipulation. High experimental error. Potential plating effect.
Microscope counting	10^6 mL^{-1}	5 to 10 min	Yes	Distinction between cell types. Direct observation.	Sample manipulation. Experimenter bias.
Turbidimetry	10^6 mL^{-1}	2 s	No	Robust to light path perturbations.	Depends on cell size, shape, and index (biomass measurement).
Nephelometry	10^5 mL^{-1}	2 s	No	Better sensitivity than turbidimetry at low concentrations.	Sensitive to light path. Depends on cell size, shape, and index (biomass measurement).
Coulter counter	10^3 mL^{-1}?	1 min	Yes (no sampling required)	Absolute measurement.	Sensitive to pollution in sample at low concentration.
Flow cytometry	10^4 mL^{-1}	1 to 3 min	Yes	Distinction between cell types.	Sample manipulation. Low reproducibility. Cost of the apparatus.
Digital in-line holographic microscopy	10^3 mL^{-1}	5 to 10 min	No	High sensitivity. Spatial localisation of individuals.	No detection of fluorescence.

Table 2.1: Comparison of bacteria concentration measurement methods for liquid cultures

2.1.2.3 *Particle detection methods*

In the second part of the twentieth century, several microscopic particle counting methods have been devised among which certain proved to be efficient for microbes as well.

COULTER COUNTER This device was initially dedicated to blood cells analysis. It consists in two liquid compartments filled with an electrolyte that are connected through a microscopic hole. Electrodes in the two compartments allow to measure variations of the impedance of the setup. Every time a particle (larger than 0.5 µm) passes through the hole, this creates a transient increase in impedance, the amplitude of this peak being proportional to the particle volume. This has been successfully used to measure low bacteria concentration (Smither, 1975; Swanton et al., 1962) and gave rise to elegant studies such as growth rate measurements in small populations at low glucose concentration (Shehata and Marr, 1971). Although this method gives a population size rather than a biomass measurement, it is affected by inert particles in the solution as is turbidimetry.

FLOW CYTOMETRY This method consists in passing the solution of interest in a capillary excited with a laser. Transmitted and scattered lights are collected using photomultipliers. Although this has been designed for the characterization of eukaryotic cells, the principle is suitable for microbes counting. In practice, it is not widely used due to the cost of the apparatus, intensive samples handling, and difficult precise calibration. However, it is used in environmental microbiology (for instance with phytoplankton; Tijdens et al., 2008; Veldhuis and Kraay, 2008) where it provides several advantages: large volume samples can be analyzed, several types of cells can be distinguished based on their size and light scattering, and fluorescent stains allow to discriminate between microbes and inert particles or to characterize phenotypic traits such as membrane integrity (Gunasekera et al., 2000; Hammes et al., 2008).

Recently, another method of cell detection has been proposed based on digital in-line holographic microscopy. A two-dimensional interference image of the culture solution is produced with a coherent light source and subsequently used to reconstruct a three-dimensional image of the population (Frentz et al., 2010). This approach brings several improvements over existing technics, in particular the position of microbes can be studied which can be of great interest in certain studies. Its main drawbacks are that it is limited by the computation time required to reconstruct the image from the hologram (400 s below 10^5 mL^{-1}, more for higher concentrations) and that it cannot discriminate between different

fluorescent properties of the individuals (compared to flow cytometry for instance).

RESEARCH OUTLINE

An ideal measurement device would work in real-time and be accurate in a wide range of concentrations. It would also be minimally invasive, meaning that no sampling is required and that physical constraints (observation window, contact with the liquid, ...) are as limited as possible. Finally, it should also allow to distinguish between several populations mixed in the same culture based on their fluorescent properties.

In this chapter, I report on the development of a new method of microbial concentration measurement dedicated to diluted populations. After explaining the method principle, I present two independent validations based on stochastic simulations and on serial dilutions of gold nanoparticles (GNPs). In the last section, I describe the method accuracy on biological samples and use it to address practical cases of microbial growth at low density.

2.2 DEVICE MONITORING MICROBIAL GROWTH AT LOW DENSITY

2.2.1 PRINCIPLE AND SETUP

2.2.1.1 *Principle of measurement*

In contrast, nephelometry consists in measuring the total intensity of diffused light.

The method we propose is based on the fact that particles with optical index different from that of water, e.g. bacteria or microscopic beads, diffuse light. By focusing a laser beam in the solution and imaging it orthogonally, individual particles can be detected provided that the volume fraction of particles is small enough (Fig. 2.1). Taking advantage of convection, or stirring the solution, a large volume can be sampled in a reasonable time. The particles signal can be analyzed in two ways to estimate a concentration:

POISSON METHOD (or λ_0 method) When the concentration is low, the presence of a particle in the excitation volume is a rare event and thus follows a Poisson distribution. As the Poisson parameter λ is equal to the mean of the distribution (and again the volume is constant), we can use it as an estimate of the concentration. Let us write n the number of particles in the excitation volume: $P(n=0) = e^{-\lambda}$, thus $\lambda = -\ln(P(n=0))$ (referred to as λ_0). This means that we can estimate the concentration out of the proportion of time where there is no particle in the sampling volume. However,

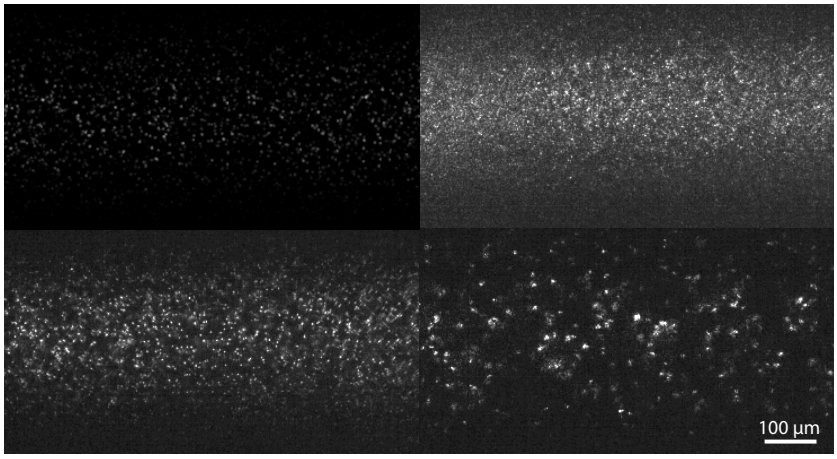

Figure 2.1: Typical diffused light pictures obtained from simulation and experiments.
Top left: result of stochastic simulation for a solution at $3 \cdot 10^7$ mL^{-1} (cf section 2.2.2.1). Bottom left: gold nanoparticle (GNP) in water at $7 \cdot 10^7$ mL^{-1}. Top right: *E. coli* in magnesium sulfate (10 × dilution of an overnight culture in LB). Bottom right: *S. cerevisiae* in magnesium sulfate (10 × dilution of an overnight culture in YNB glucose). All pictures are at the same scale; contrast has been adjusted on each picture, thus darker background corresponds to higher signal to noise ratio.

this method requires longer acquisition when the concentration decreases and is not expected to work when the concentration is too high.

CLT METHOD (or λ_m method) According to the central limit theorem (CLT), the sum of n (independent and identically distributed) random variables with the same mean μ and the same (not null) variance σ^2 follows a Gaussian distribution of mean $m = n\mu$ and variance $s^2 = n\sigma^2$ for large n. Consequently, $m^2/s^2 = n$. Taking the intensity of diffused light of single particles as random variables, the sum of these variables i.e. the total intensity per image is expected to follow a gaussian distribution of mean m and variance s^2. As the excitation volume is constant, this means that the concentration is proportional to $\lambda_m = m^2/s^2$. However, this method requires that the concentration is high enough so that the mean and variance of the signal can be estimated accurately.

In these two methods, the measured parameter (hereafter referred to as estimation or estimated concentration) is proportional to the concentration. Therefore, the relationship between the estimation and the absolute concentration requires a calibration as described below.

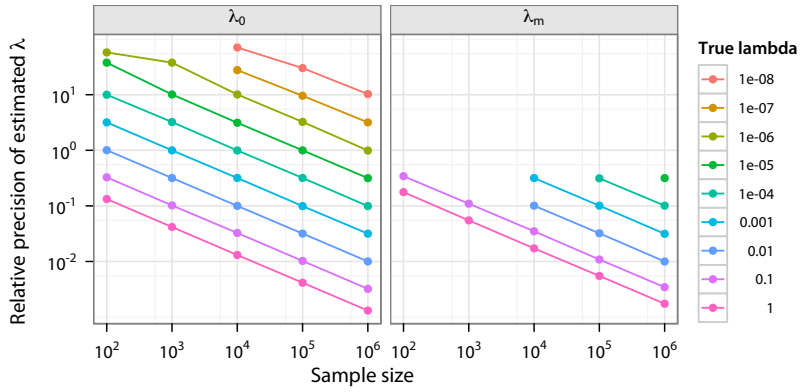

Figure 2.2: Relative precision of λ estimation (standard deviation divided by mean) depending on λ true value and on the sample size. The Poisson method (λ_0) is shown on the left plot, while the right plot shows the CLT method (λ_m). Missing values indicate that λ was estimated equal to 0: it occurs at higher λ for the CLT method suggesting that it is less appropriate at low concentration.

The statistical errors of these methods was estimated by simulations for intensity distributions assumed to be poissonian (Fig. 2.2). The error depending on the sample size n and on the real parameter value λ can be approximated as $\sigma \simeq \sqrt{\lambda_{th}/n}$ where σ is the standard deviation of the parameter estimations.

This statistical error stands for uncorrelated events in absence of other experimental errors and is thus considered as a lower bound for errors. In fact, events observed at intermediate to high image acquisition frequencies are not independent anymore which increases the errors. Overall, experimental errors are the most critical in this case and are estimated empirically based on repeated measurements.

As far as calibration is concerned, serial dilutions are appropriate: a $10^6 \times$ dilution using successive $10 \times$ dilutions results in less than 7 % error (estimated by the coefficient of variation; Hedges, 2002).

Finally, our approach can in principle be implemented using both scattered light and emitted fluorescence. This makes it general, working for instance on natural isolates as well as being suitable to distinguish between living and dead bacteria using fluorescent dyes, or between two strains with one being fluorescent.

2.2.1.2 *Setup description and data processing*

A dedicated setup has been built for this experiment, featuring a spectroscopy cuvette in a custom temperature-controlled holder, illuminated

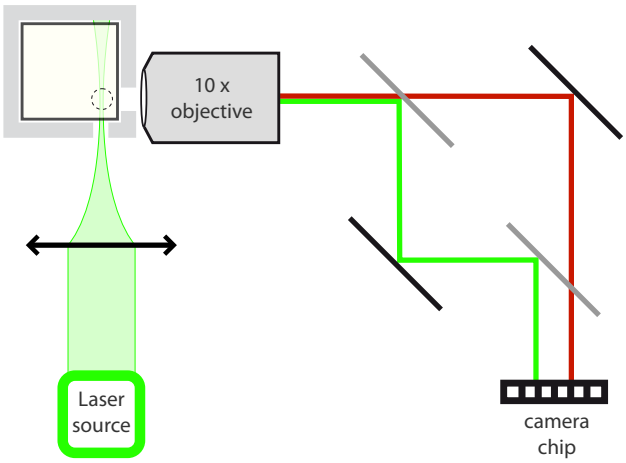

Figure 2.3: Schematic of the cell counting setup. Band pass filters, tube lens and aperture diaphragm are not shown. Using a 50 mm tube lens with a 18 mm effective focal length objective (10 ×) yields approximately a 2.77 × magnification.

with a 532 nm diode-pumped solid-state laser. At the focal point, typical beam width is 80 µm (estimated as two standard deviations of the gaussian light intensity profile) and total power is adjusted to ca. 5 mW. The laser beam is imaged orthogonally using a camera behind a 10 × infinity-corrected objective (Fig. 2.3). A magnetic stirrer is included in the holder, so to move the particles and homogenize the solution, and is remotely controlled by the acquisition software.

In order to be able to distinguish two populations with different fluorescent properties in the same sample, this setup has been built as a dual-view with dichroic mirrors reflecting light above 550 nm, so to image both diffused light and fluorescence on the same camera. Coupled with the 532 nm excitation, this is suitable for propidium iodide (PI) or mOrange imaging and allows to estimate at the same time the total population and the fluorescent population (Fig. 2.3). PI is a cell death marker which stains cells with permeabilized membranes (100-fold fluorescence increase; López-Amorós et al., 1997). mOrange is a fluorescent protein that is at 50 % of excitation at 532 nm and which emission peak is at 562 nm.

Disposable cuvettes in polystyrene with four optical sides are used in order to reduce as much as possible sample pollution by dust. All dilution solutions are filtered using 0.2 µm disposable filters.

The camera image is treated in real time with the following algorithm: (i) the current image background is attenuated by subtracting a mean black image acquired using the same parameters but without illumina-

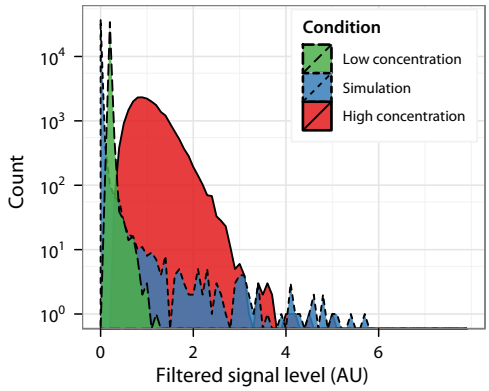

Figure 2.4: Typical histogram of intensity obtained after signal filtering. Low and high concentrations correspond to GNPs at $7.0 \cdot 10^4$ mL^{-1} and $7.0 \cdot 10^7$ mL^{-1} respectively. Histograms are accumulated during 60 s at 2 Hz. Simulation is run in conditions similar to low concentration, over 128 frames at $1.97 \cdot 10^4$ mL^{-1}.

tion; (ii) the region of interest (approximately 5 laser beam σ width) is split into 16×16 px² images with 2 px overlap on each edge; (iii) these small images are band-pass filtered in order to remove the low-frequency variations; (iv) the root mean square of the intensity at the center of filtered images (to avoid treating overlapping area twice) is computed and stored in an accumulated histogram (Fig. 2.4); (v) the histogram statistics (in particular λ estimation) are updated on screen in real time. Acquisition and treatment are written in C, using the lab custom API and user interface xVin.

As images are processed in real-time, the primary record of an experiment is the accumulated histogram of intensities. Typical distributions are shown for diluted solutions (GNP and simulation) and concentrated solutions (GNP only; Fig. 2.4). At low concentration, the rapid decrease of the histogram is in agreement with the shape of the distribution of intensities expected from single particles in a gaussian beam ($\propto 1/I$).

2.2.2 VALIDATING THE APPROACH

In this section, I describe two methods developed to validate this measurement technics. Stochastic simulations are used to study the effects of various parameters on sampling errors and on saturation. In addition, measurements with solutions of GNPs of known concentrations allow to validate the setup and to estimate experimental errors.

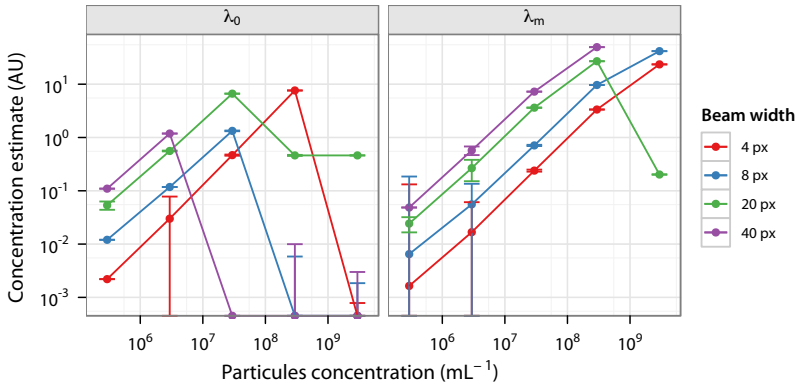

Figure 2.5: Validation of the cell counting method using stochastic simulations. Ten short movies of 32 frames are simulated for each concentration and beam width condition. Poisson method (left) and CLT method (right) are used to calculate the estimated concentration on each movie. Dots and error bars show mean and SEM of ten replicates respectively. Beam width refers to the standard deviation of the gaussian excitation profile. Using the λ_0 method, the estimation saturates at high concentration (points on the bottom line) as the probability not to observe a particle vanishes. See text for details.

2.2.2.1 *Validation by stochastic simulations*

In order to validate these methods, I wrote stochastic simulations which output a picture (Fig. 2.1 top left) that is analyzed using the same algorithm as camera images, so as to produce an intensity histogram and concentration estimations. The simulations are written in C, using GNU scientific library (GSL) for random number generators and xVin API and user interface.

In greater details, simulation is run in a finite size parallelepiped. The intensity profile of the laser beam is assumed to be gaussian. For a given concentration, the corresponding number of particles are randomly spread over space. For each particle, a radius is chosen from a normal distribution. The intensity of the gaussian spot produced by a particle on the picture is computed from the size of the particule and its position in the gaussian beam. The width of this spot is assumed to follow a gaussian distribution independent on the size of the particle (due to the diffraction limit reached for small particles).

All gaussian spots produced by the particles population are added to a picture of low-level gaussian gray-levels accounting for picture background. As only particles solutions of low volumic fraction are considered, overlapping particles are treated as independent: since this case is statistically very rare, it is supposed not to affect the simulation outcome.

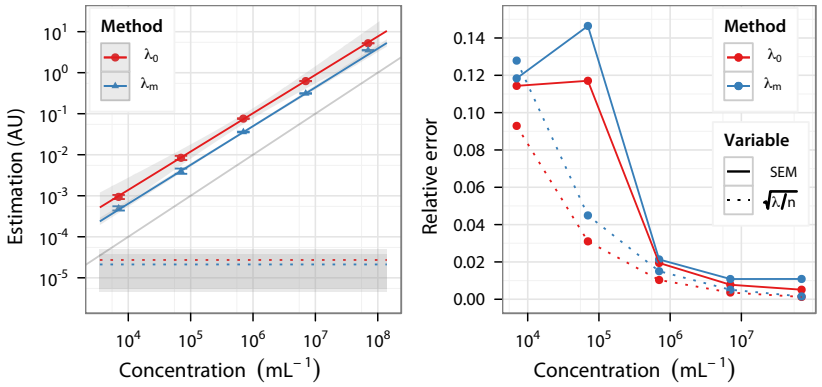

Figure 2.6: Validation of the cell counting method using gold nanoparticles. Concentration of serially diluted solutions of 200 nm GNP is estimated ten times (during 1 min each) for each dilution.
Left: Relationship between the absolute concentration and λ estimated by both Poisson (red) and CLT (blue) methods. Points and error bars are mean and SEM respectively, dashed lines and greyed areas indicate the background level measured in water.
Right: Relative errors depending on the concentration, estimated as sampling errors (see details in section 2.2.1.1) or experimental errors (SEM over ten replicates)

These simulations confirm the linear relationship between the estimation and the concentration (Fig. 2.5). In addition, the comparison between Poisson and CLT methods is instructive: as expected the Poisson method is more precise at low concentration but happens to work at surprisingly high concentrations if the excitation volume is small enough. In addition, although the technics was designed with the idea of a small excitation volume in mind, estimation using the CLT method and a large excitation volume shows very limited saturation at high concentration while it brings lower errors at low concentration. In this respect, the best compromise is to use the CLT method with a large beam.

2.2.2.2 *Experimental validation using gold nanoparticles*

Microbes are variable in size, shape and optical properties. In this first step, inert particles are used to validate the approach and setup. As 1 µm wide polystyrene beads produce very pronounced diffraction rings that perturb the image analysis algorithm, 200 nm wide GNPs (BBInternational, Cardiff, UK) were chosen as they produce a $2 \times 2\,px^2$ clean and strong scattered light signal (corresponding to $4.3 \times 4.3\,\mu m^2$) which is very similar to the bacteria signal.

Estimated concentration of serially diluted solutions shows a linear dependence to the actual concentration over five orders of magnitude (Fig. 2.6 left). Interestingly, this linear dependence is observed with both Poisson and CLT methods. The detection saturates below 10^3 mL^{-1} where the estimation becomes independent of the concentration (data not shown). This also corresponds to the background level measured with clean water. As expected, saturation at high concentration occurs when using Poisson method (data not shown). However errors are not larger at low concentration with CLT method contrary to expectations and results obtained with simulations.

Regarding errors, repeated measurements allow to estimate experimental errors (Fig. 2.6 right). As expected, experimental errors are higher than theoretical sampling errors and satisfactorily of the same order of magnitude. Above $5 \cdot 10^5$ mL^{-1}, errors are below 5 %; higher errors of the order of 10 – 15 % can be lowered by increasing the duration of acquisition.

2.2.2.3 *Parameters sensitivity*

During the conception of this device, we tested the effects of several parameters on the estimation of the concentration. Although they can be adjusted, they are usually kept constant at a convenient value chosen after tests with GNPs, *E. coli* and *S. cerevisiae*.

BACKGROUND THRESHOLD The camera dark current produces a background signal after filtering. Determining a relevant background threshold is crucial as the Poisson method is based on distinguishing presence and absence of particles. Practically, this threshold must be higher than the highest intensity detected without illumination. Variations of the threshold above this limit have limited effect on estimation linearity: higher threshold lowers the estimated concentration as the effective excitation volume is smaller. Among other advantages, spatial band-pass filtering ensures that background is reasonably independent of illumination conditions (beam intensity, exposure time, …).

BEAM WIDTH As already mentioned, this technics was proposed with a small beam width in mind. As shown with simulations, using a larger beam width is supposed to increase the dynamic range of this technics with limited side effects. This has been confirmed with GNPs and bacteria. Typically, the beam gaussian profile has a standard deviation of 40 px, that is ca. 85 µm.

BEAM INTENSITY & EXPOSURE TIME Illumination conditions are adjusted depending on the type of particles, so that to use all the dynamic range of the camera while limiting saturation (less than

0.1 %). In practice, illumination intensity is adjusted so that exposure is shorter than 5 ms thus preventing blurry images of particles.

DEPTH OF FIELD Although several configurations have been tried by varying aperture using a diaphragm, 10 × objectives offer a depth of field that is large enough to image all particles in the beam. In addition, reducing the aperture imposes to increase the beam intensity while we try to keep it as low as possible to prevent hypothetical light-induced damages.

ACQUISITION FREQUENCY The acquisition frequency is theoretically limited by real time processing duration. In practice, acquisition is run at a much lower frequency in order to image different particles from one frame to the next, that is to acquire independent images. Typically, acquisition is run at 2 Hz to 7 Hz and pixels autocorrelation over a stack is computed to check the absence of correlation between frames.

PARTICLES VELOCITY The technics relies on the fact that particles are moving in the liquid, allowing to sample a large effective volume while the beam is fixed. However, rapid liquid flows prevent acquisition of sharp images of particles. In practice convection triggered by temperature heterogeneity (as in section 1.2.4) provides an appropriate flow speed. An alternative for making the technics faster would be to move the beam through the sample although this would be much more complicated to implement.

CUVETTE The choice of the sample container is critical as it takes part in the optical path and as its cleanness set the background level. Quartz cuvette used for preliminary tests was very long to clean properly and was advantageously replaced by disposable plastic cuvettes with 4 optical sides. The custom cuvette holder was designed to ensure repeatable positioning of the cuvette. The effect of cuvette rotation has been tested and is not detectable.

2.3 BIOLOGICAL APPLICATIONS

2.3.1 METHODS

Calibration and subsequent growth experiments are run on:

– *E. coli* MG1655 used as model bacteria. Calibrations are performed using an overnight culture in LB at 37°C, resuspended and serially diluted in 10 mM magnesium sulfate. In growth experiments, bacteria are grown at 30°C in M9 medium supplemented with 0.4 % glucose and 2 mM magnesium sulfate.

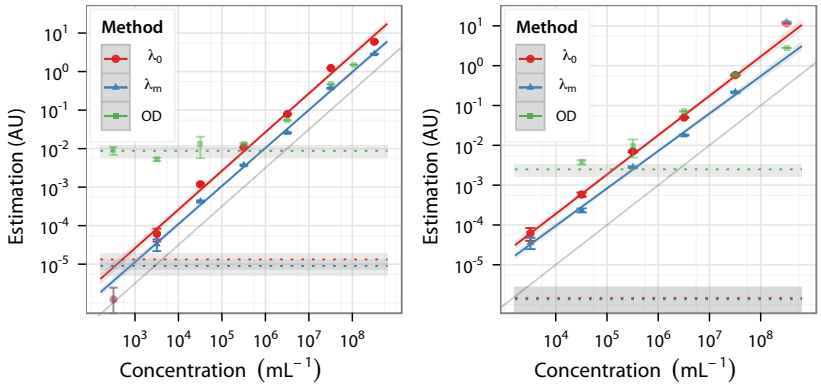

Figure 2.7: Calibration with bacteria *E. coli* MG1655 (left) and yeast *S. cerevisiae* S288C (right) following our default protocol described in section 2.3.1. OD values are plotted for comparison. Points and error bars are mean and SEM of ten repeated measurements (four in the case of OD), dashed lines and greyed areas indicate the background level measured in magnesium sulfate. Outliers corresponding to saturation are greyed out and are not used in linear fits.

– Haploid *S. cerevisiae* S288C used as a model unicellular eukaryote. Calibrations are performed using an overnight culture in yeast peptone dextrose (YPD) medium at 30°C, resuspended and serially diluted in 10 mM magnesium sulfate. In growth experiments, yeasts are preliminary grown overnight at 30°C in YNB medium supplemented with 80 mM glucose.

Typically, during calibration the signal is acquired during 1 min for each measurement. In growth experiments, it is acquired during 3 min and the solution is stirred during 15 s (followed by 15 s delay for the flow speed to decrease) between each measurement.

During calibrations, a diluted solution of the overnight culture is plated on LB-agar for *E. coli* and YPD-agar for *S. cerevisiae*. The dilution factor is chosen so as to count 30 to 200 colonies per plate after growth at 37°C for *E. coli* and 30°C for *S. cerevisiae*.

OD is measured at 600 nm using an Eppendorf Biophotometer.

2.3.2 CALIBRATIONS WITH MICROBES

The device has been tested in a large range of concentrations with the two most common model organisms: *E. coli*, a rod-shaped bacteria which is ca. $3 \times 1 \times 1\,\mu m^3$ or slightly smaller, and *S. cerevisiae*, a round-shaped unicellular eukaryote typically 5 µm in diameter.

2.3.2.1 *Calibration with* E. coli

The concentration is estimated on serial dilutions of a stationary phase *E. coli* culture. In addition, the absolute concentration is estimated by plating and colony counting. The estimated concentration shows a linear dependence to the actual concentration over five orders of magnitude (Fig. 2.7 left). Interestingly, this linear dependence is observed with both Poisson and CLT methods. The lower limit of detection, around $5 \cdot 10^3\,\mathrm{mL}^{-1}$ is set by the background level measured in a clean magnesium sulfate solution. No clear saturation is observed at high concentration, but the linearity of the estimation is better for the CLT method than for the Poisson method. In addition, as observed with GNPs, errors are not larger at low concentration with CLT method contrary to our initial expectations.

In comparison, OD measurements can not be used below $10^6\,\mathrm{mL}^{-1}$. Consequently our device constitutes a 100-fold improvement of the lower detection limit, with an extended dynamic range of almost five orders of magnitude.

2.3.2.2 *Calibration with* S. cerevisiae

The same type of calibration is run with stationary phase *S. cerevisiae* cultures. Similar results are obtained, with OD reaching its lower limit around $5 \cdot 10^5\,\mathrm{mL}^{-1}$ while our device is above the background signal until at least $5 \cdot 10^3\,\mathrm{mL}^{-1}$. Surprisingly, both methods overestimate the concentration above $10^8\,\mathrm{mL}^{-1}$. In addition, the linearity of the estimation based on the CLT method is not as good as for GNPs or *E. coli*, which suggests that a numerical correction may improve our estimation in biological experiments with yeast.

2.3.3 POPULATION DYNAMICS

2.3.3.1 *Growth of* E. coli

We monitor growth of *E. coli* starting from a diluted population. After dilution, stationary phase *E. coli* grow in a typical manner, showing a lag phase followed by exponential growth and finally entry in stationary phase (Fig. 2.8). Overall, the device allows to monitor exponential growth over four orders of magnitude. As the initial dilution corresponds to ca. $5000\,\mathrm{mL}^{-1}$, the long lag phase seen in the plot (at least 4 h) is likely to relate the mixed effects of the biological lag and the low accuracy of the detection at these low concentrations (below $10^4\,\mathrm{mL}^{-1}$). In addition, there is no clear evidence yet whether the faint departure from exponential growth (observed between 8 and 20 h is a biological effect or an artefact of the measurement.

2.3.3.2 *Sucrose metabolism & density dependence in* S. cerevisiae *growth*

Growth experiments have been conducted with yeast in order to test the device at low concentration. Stationary phase cultures are diluted 30 × and grown during 4 h. After being rinsed twice in YNB, the exponential phase culture is diluted to an equivalent OD of $5 \cdot 10^{-5}$ AU in this medium supplemented with sucrose. Subsequent growth is monitored in the counting device. In *S. cerevisiae*, sucrose is not imported as such by the cells but rather hydrolyzed to glucose and fructose by the invertase, an enzyme secreted by the cells in the extracellular environment. At low cell density, the production of invertase is limited and sucrose hydrolysis limits yeast growth. When the population grows, the extracellular concentration of invertase increases which in turn increases growth rate (thanks to higher nutrients availability). This is expected to result in a density-dependence of growth rate. All yeast strains have been provided by J. Koschwanez from A. Murray's lab.

In our experiment, the lag phase is very long (more than 10 h) and the reproducibility between replicates is not as good as with *E. coli* (Fig. 2.9). At this point of the work, it is difficult to decipher whether the increase in growth rate observed after the lag phase is due to an experimental artefact or to this biological effect. The sucrose concentration is not a critical parameter.

2.3.3.3 *Population dynamics of mixed populations*

As explained in the introduction, we aim at monitoring several populations with fluorescent properties mixed in the same culture. Preliminary tests on heat-killed bacteria stained with PI show that the fluorescent signal is strong enough to be detected in our setup. Moreover, growth with or without PI have been compared over 8 hours and exhibit no difference neither in LB nor in M9 as measured with optical density (data not shown). In principle, this will allow us to use PI to estimate mortality during growth in our setup.

In practice, the initial setup was based on a camera (IDS UI-1225LE-M) that was not sensitive enough to distinguish accurately fluorescent particles from background. The device has been modified to use a more sensitive camera (JAI BM141-GE) with much higher signal to noise ratio but tests with fluorescent particles have not been run yet.

2.3.4 DISCUSSION AND PERSPECTIVES

In this chapter, I have described a new method for the measurement of microbial cultures concentration. This method works well in a wide

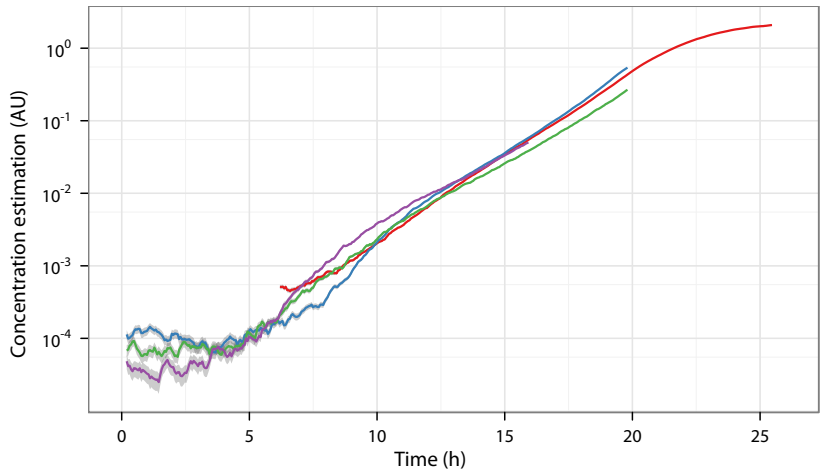

Figure 2.8: Growth of *E. coli* MG1655 in M9 with 0.1 % glucose at 30°C. Stationary phase culture are diluted $2 \cdot 10^5 \times$ and grown in the cell counting device. The measurement is averaged over 15 min; grey area shows the SEM. Different colours show independent replicates. Since the initial dilution factor was 20 times lower, the red line has been shifted in time to align it with the other curves. According to Fig. 2.7 (left), 1 AU corresponds to ca. $1.0 \cdot 10^8$ mL^{-1}.

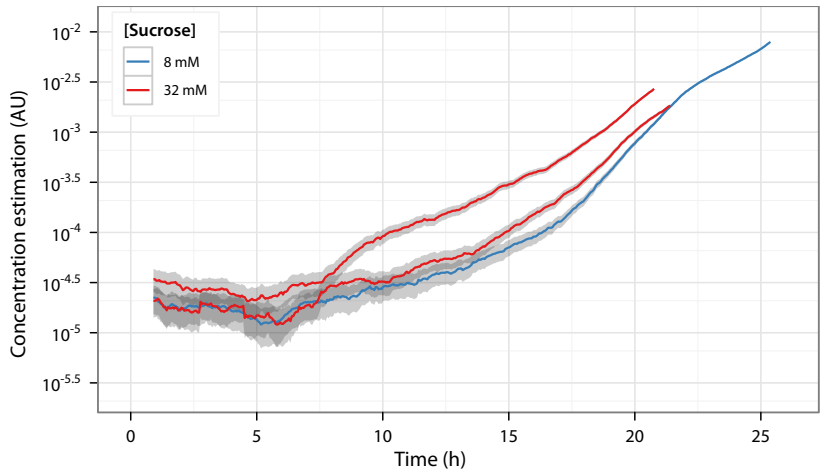

Figure 2.9: Growth of *S. cerevisiae* S288C in YNB with sucrose at 30°C. Stationary phase culture are diluted to an equivalent OD of $5 \cdot 10^{-5}$ AU and grown in the cell counting device. The measurement is averaged over 90 min; grey area shows the SEM. Three independent replicates are shown with two different sucrose concentrations indicated in colour. According to Fig. 2.7 (right), 1 AU corresponds to ca. $3.0 \cdot 10^8$ mL^{-1}.

range of concentrations, from 10^3 mL^{-1} to 10^8 mL^{-1}. In addition, it does not require sampling and can be performed in a continuous manner to monitor microbial growth. In principle, it can be extended to the identification of two sub-populations with different fluorescence properties.

Several specific points can be discussed. First, although the CLT method was implemented for the intermediate to high concentrations, it gives satisfactory estimations in a large range of concentrations, even for the lower ones. This observation is still to be explained. Second, regarding the comparison between the precision of our method and OD measurements (Fig. 2.7), the signal is averaged over a much longer time in our device (10×1 min) than in the spectrophotometer (4×1 s). It would be interesting to modify the setup so that OD can be integrated over the same duration. Third, nonlinearity is observed in certain conditions (e.g. calibrations with yeast). We tried to verify whether this could be due to the aggregation of some particles that would decrease the number of events and add some high intensity ones (as the intensity is supposed to increase very rapidly with the particle size). No clear result has been obtained yet. In particular, experiments with a mixture of GNPs of different diameters were not conclusive since all sizes of GNPs do not bring a linear relationship between the actual concentration and the estimation. Fourth and last, the generality of our approach is still to be confirmed on different microbial species. Preliminary tests with a smaller bacteria, *P. aeruginosa*, do not show such a good linearity of the estimation with concentration as observed in *E. coli* and *S. cerevisiae*. This may be due to the fact that light scattering by smaller particles is lower.

From a personal viewpoint, developing a new measurement technics has been very enriching. In addition to giving me the opportunity to acquire new skills, it changed my view on the use of existing technics. It is tempting to convert measurements directly into physical or biological quantities of interest while they should rather be compared directly, with physical or biological explanations being developed to explain the observed differences. Regarding the practical side, I learnt that it is more efficient to validate the relevance of a new technics using standard, reliable hardware than taking other constraints into account at first (e.g. size and cost). Using cheap and/or compact building blocks at first can bring unexpected difficulties due to their usually low reliability. In this work, I changed the compact laser since it was not monomodal and the low-cost camera since it was not sensitive enough.

Finally, compared to the recently proposed digital in-line holographic microscopy, our method has comparable dynamic range, acquisition duration, and cost: the choice to use one rather than the other will depend on the particular requirement of an experiment. In particular, digital in-line holographic microscopy allows to determine the position of microbes. In contrary, our method relies on a continuous displacement of

the particles (by convection or stirring) that is used to scan a larger effective volume of liquid. This limit could be overcome by moving the laser beam within the camera and objective fields for instance by rotating a plane parallel plate. Nonetheless, our method is easier to implement and much less computer intensive, and can be extended to detect fluorescent microbes. Finally, it is difficult to compare the linearity of the estimation obtained with the two methods as the calibration plot given by Frentz et al. (2010) spans less than one order of magnitude.

In summary, microbial growth is routinely monitored using either time-lapse microscopy in solid medium (for less than 1000 cells) or photometry in liquid medium (above 10^6 mL^{-1}, or 10^5 mL^{-1} using repeated measurements). In between, colony forming unit counting or flow cytometry can be used, but they require population sampling and are not appropriate to continuous measurements. Both our method and digital in-line holographic microscopy represent new tools to fill this gap in the description of diluted liquid populations.

BIBLIOGRAPHY

F. K. Balagaddé, H. Song, J. Ozaki, C. H. Collins, M. Barnet, F. H. Arnold, S. R. Quake, and L. You. 2008. A synthetic Escherichia coli predator-prey ecosystem. *Molecular Systems Biology*, 4:187.

P. O. Byrne, T. S. J. Elliott, P. R. Sisson, P. D. Oliver, and H. R. Ingham. 1989. An optical probe for the enumeration of bacteria in liquid media. *Journal of Physics E: Scientific Instruments*, 22(3):146–150.

E. Dekel and U. Alon. 2005. Optimality and evolutionary tuning of the expression level of a protein. *Nature*, 436(7050):588–592.

S. Elena and R. Lenski. 2003. Evolution experiments with microorganisms: The dynamics and genetic bases of adaptation. *Nature Reviews Genetics*, 4(6):457–469.

M. Faguet. 1935. Etude photométrique de la multiplication microbienne. *Comptes Rendus de l'Académie des Sciences*, 200:498.

W. W. Forrest and V. A. Stephen. 1965. A simple recording nephelometer for studies of bacterial growth. *Journal of Scientific Instruments*, 42(8):664–665.

K. R. Foster. 2011. The sociobiology of molecular systems. *Nature Reviews. Genetics*, 12 (3):193–203.

Z. Frentz, S. Kuehn, D. Hekstra, and S. Leibler. 2010. Microbial population dynamics by digital in-line holographic microscopy. *Review of Scientific Instruments*, 81(8): 084301.

E. C. Fru, I. D. Ofiţeru, V. Lavric, and D. W. Graham. 2011. Non-linear population dynamics in chemostats associated with live-dead cell cycling in Escherichia coli strain K12-MG1655. *Applied Microbiology and Biotechnology*, 89(3):791–798.

T. Fujita and K. Nunomura. 1968. New turbidimetric device for measuring cell concentrations in thick microbial suspensions. *Applied Microbiology*, 16(2):212–215.

T. S. Gunasekera, P. V. Attfield, and D. A. Veal. 2000. A flow cytometry method for rapid detection and enumeration of total bacteria in milk. *Applied and Environmental Microbiology*, 66(3):1228–1232.

F. Hammes, M. Berney, Y. Wang, M. Vital, O. Köster, and T. Egli. 2008. Flow-cytometric total bacterial cell counts as a descriptive microbiological parameter for drinking water treatment processes. *Water Research*, 42(1-2):269–277.

A. J. Hedges. 2002. Estimating the precision of serial dilutions and viable bacterial counts. *International Journal of Food Microbiology*, 76(3):207–214.

E. W. Henningson, M. Lundquist, E. Larsson, G. Sandström, and M. Forsman. 1997. A comparative study of different methods to determine the total number and the survival ratio of bacteria in aerobiological samples. *Journal of Aerosol Science*, 28(3): 459–469.

C. M. Jessup, S. E. Forde, and B. J. Bohannan. 2005. Microbial experimental systems in ecology. In *Population dynamics and laboratory ecology*, volume 37 of *Advances in Ecological Research*, pages 273–307. Academic Press.

A. L. Koch. 1961. Some calculations on the turbidity of mitochondria and bacteria. *Biochimica Et Biophysica Acta*, 51:429–441.

R. López-Amorós, S. Castel, J. Comas-Riu, and J. Vives-Rego. 1997. Assessment of E. coli and Salmonella viability and starvation by confocal laser microscopy and flow cytometry using rhodamine 123, DiBAC4(3), propidium iodide, and CTC. *Cytometry*, 29(4):298–305.

A. A. Miles, S. S. Misra, and J. O. Irwin. 1938. The estimation of the bactericidal power of the blood. *The Journal of Hygiene*, 38(6):732–749.

J. Monod. 1942. *Recherches sur la croissance des cultures bactériennes*. Hermann, Paris.

M. Novak, T. Pfeiffer, M. Ackermann, and S. Bonhoeffer. 2009. Bacterial growth properties at low optical densities. *Antonie Van Leeuwenhoek*, 96(3):267–274.

T. E. Shehata and A. G. Marr. 1971. Effect of Nutrient Concentration on the Growth of Escherichia coli. *Journal of Bacteriology*, 107(1):210–216.

R. Smither. 1975. Use of a Coulter counter to detect discrete changes in cell numbers and volume during growth of Escherichia coli. *The Journal of Applied Bacteriology*, 39(2):157–165.

E. M. Swanton, W. A. Curby, and H. E. Lind. 1962. Experiences with the Coulter counter in bacteriology. *Appl. Environ. Microbiol.*, 10(5):480–485.

J. Taylor. 1962. The estimation of numbers of bacteria by tenfold dilution series. *Journal of Applied Microbiology*, 25(1):54–61.

M. Tijdens, H. L. Hoogveld, M. P. K. van Agterveld, S. G. H. Simis, A. Baudoux, H. J. Laanbroek, and H. J. Gons. 2008. Population dynamics and diversity of viruses, bacteria and phytoplankton in a shallow eutrophic lake. *Microbial Ecology*, 56(1):29–42.

R. C. van Benthem, D. V. D. Assem, and J. Krooneman. 2002. Compact optical sensor for real-time monitoring of bacterial growth for space applications. *Annals of the New York Academy of Sciences*, 974:541–555.

M. Varon and B. P. Zeigler. 1978. Bacterial predator-prey interaction at low prey density. *Applied and Environmental Microbiology*, 36(1):11–17.

M. J. Veldhuis and G. W. Kraay. 2008. Application of flow cytometry in marine phytoplankton research: current applications and future perspectives. *Scientia Marina*, 64 (2).

G. S. Wilson. 1922. The proportion of viable bacteria in young cultures with especial reference to the technique employed in counting. *Journal of Bacteriology*, 7(4):405–446.

Chapter 3

DISTRIBUTION OF SIDEROPHORES IN CLONAL POPULATIONS

3.1 INTRODUCTION

Iron is essential to a number of biochemical processes since it is a common enzyme cofactor. For instance, it is found in proteins involved in DNA replication and repair (ribonucleotide proteases, primases, helicases, ...), in protein synthesis (translation initiation), in energy production (mitochondrial electron transport chain), etc. The iron concentration required for cell metabolism is estimated to be on the order of micromolar.

In solution, iron can be found as ferrous iron Fe(II) and as ferric iron Fe(III). While Fe^{2+} is soluble in water, Fe^{3+} has a much lower solubility and precipitates as iron hydroxyde. Due to the abundance of dioxygen on Earth, most Fe^{2+} is oxidized to Fe^{3+}. As a result, soluble iron concentration is very low in most environments: at pH close to 7, the maximum Fe^{3+} concentration is estimated to be about 10^{-18} M (Spiro, 1977). The big discrepancy between cellular needs and iron availability results in competition for iron as a limiting nutrient in a number of environments. In particular, pathogens and parasites compete for iron with their hosts (Fischbach et al., 2006).

To fulfill their iron needs, nearly all cells have developed the same strategy, which consists in secreting molecules (siderophores) that chelate iron in the extracellular environment. The cells can then retrieve some of the diffusing pool of molecules bound to iron. A well-studied example of bacterial siderophores is pyoverdines of pseudomonads: it is a family of diffusible green-fluorescent molecules with very high affinity for ferric iron. In *Pseudomonas aeruginosa*, the association constant of the iron-pyoverdine complex has been estimated to be around 10^{32} M^{-1} (Albrecht-Gary et al., 1994). From a functional viewpoint, pyoverdine has been shown to act as a siderophore (i.e. to facilitate iron acquisition by bacteria) using radioactive labeling of iron in *P. fluorescens* (Meyer and Hornsperger, 1978).

Siderophores can be seen as a "public good" (as reviewed for pyoverdine by Buckling et al., 2007). Public goods are characterized by the fact that, although their production is costly, they are secreted in the extracellular environment and can thus be used by other individuals. Consequently, their production is a cooperative trait, and producers are susceptible of exploitation by non-producers. Classical examples of public goods in microbes include extracellular enzymes (amylase, sucrose invertase, etc) or nutrient-chelating molecules such as siderophores.

The maintenance of cooperation in nature is a difficult issue as it involves different levels of selection (Okasha, 2006). From the cooperator viewpoint, the cooperative trait is by definition costly; however at the level of the population or group, it provides a benefit. The frequent occurrence of stable cooperation is in apparent contradiction with natural

selection theory that is based on individuals maximising their own reproduction. Several non-exclusive mechanisms have been proposed so far to sort out this issue (Nowak, 2006; West et al., 2007).

DIRECT RECIPROCITY is a simple explanation in cases where interactions are repeated between two individuals, as in classical game theory (reviewed in Hofbauer and Sigmund, 1998). If they can perform two actions either cooperating or defecting, non-cooperators will ultimately invade if only pure strategies are considered. A conditional strategy consists in choosing the action performed at a round n depending on the outcome at the previous round $n-1$. It has been shown that conditional strategies allowing for direct reciprocity are evolutionarily stable and consequently promote the maintenance of cooperators in the population (Axelrod and Hamilton, 1981). This explanation can be extended to "spatial reciprocity" or "network reciprocity" when considering multiple individuals in a spatially-structured environment or on a graph respectively. In this context, cooperation is maintained if the benefits to costs ratio of cooperating is large compared to the average number of neighbours.

KIN SELECTION is a genotype-centered formalism stating that the cost of cooperation can be compensated by the benefits it provides to relatives. To this end, the inclusive fitness of a cooperative individual is defined as a decomposition of its fitness in terms of direct effects (individual fitness in the absence of recipients) and indirect effects (fitness of the recipients due to the presence of the cooperator weighted by the relatedness between them) (Hamilton, 1964a). The sum of both can be positive. In this view, as the product of cooperation is directed towards the kin, its members must bear markers to be recognized and profit from the cooperation (Hamilton, 1964b). Such recognition mechanisms have been identified in birds and in insects, based on songs or cuticle chemicals respectively. Higher benefits for relatives can also occur passively if individuals dispersion is low since the offsprings will be located around their parents. In this context, one expects cooperative traits to be heritable.

Among other arguments against group selection, the group reproduction rate would be much lower than that of individuals making selection on the group secondary to selection on individuals.

GROUP SELECTION considers populations as groups of individuals that are selected on the basis of their collective properties. Cooperative traits could be selected in unrelated individuals provided they confer a reproductive advantage to the group. Although the biological relevance of group selection was highly debated in the 1960's and 1970's, recent experimental evidences support a comeback under the vocable multi-level selection.

Interestingly, in these three explanations, spatial structure is a key parameter setting what interactions can occur. In general, spatially structured environments are likely to stabilize cooperation since it favors repeated interactions and interactions between relatives by limiting individuals dispersion, and it makes group selection more likely to occur by allowing the formation of spatial groups. The positive effect of spatial structure on the evolution of cooperation has also been shown in evolutionary games as prisoner's dilemma (Nowak and May, 1992; Nowak et al., 1994).

See also section 1.1.1 for a general introduction on spatial structure in ecology and evolution.

Finally, public goods games are special cases of cooperation where a beneficial resource produced at a cost by individuals is shared with others, be they producers or not. The interactions are no longer considered between pairs of individuals: in well-mixed environments, each individual interacts with the average of the population, while in structured environments, it interacts with the average of its neighbours. The former explanations for the maintenance of cooperation can also be considered in this case. However, the difference between individuals dispersion range and public good diffusion can result in more complex dynamics.

Unexpected detrimental effects of spatial structure on the emergence of cooperation in evolutionary game models has been identified when cost-to-benefit ratio is high (Hauert and Doebeli, 2004).

At first glance, limited dispersal of public goods appears as a stabilizing factor for cooperation (Doebeli and Hauert, 2005). In this context, spatial clustering of public goods producers (likely to have higher public goods concentration) and heritability of the level of production (leading also to spatial clustering when individuals dispersion is limited) are expected to stabilize cooperative dynamics. Nevertheless, this argument is counterbalanced by the local competition for the resources between cooperators (Griffin et al., 2004), as described in greater details in the next section.

In the next sections, I first review the experimental evidence that pyoverdine is a relevant model of public good in *P. aeruginosa*, as well as evolutionary issues that have been investigated using this system. In a second time, I present the current knowledge of pyoverdine metabolism in *P. aeruginosa*.

3.1.1 BACTERIAL SIDEROPHORES: A MODEL SYSTEM TO STUDY PUBLIC GOODS GAMES

Although their production is costly, bacterial siderophores are secreted in the extracellular environment and can thus be used by other individuals: they constitute a public good. In the ecological and evolutionary studies of microbial siderophores, most efforts have focused on *P. aeruginosa* and on its main siderophore pyoverdine since it is naturally fluorescent. This property allows to estimate public goods concentration very easily using simple photometry. It is noteworthy that pyoverdine

fluorescence is quenched by iron. Therefore this measure informs about the concentration of apo pyoverdine only (i.e. of iron-free pyoverdine) which is an acceptable approximation as it is supposed to be much more abundant than ferric pyoverdine.

Consequently, this section deals only with this particular case of bacterial siderophore. In most studies of siderophores as public good, producers and non-producers are usually identified *a priori* as cooperators and cheats. Let me point out that I will not follow this terminology. Though it is relevant and valuable for the interpretation of social interactions, using it *a priori* in experimental reports may bias what questions are adressed in data analysis and interpretation. Specifically, identifying a production characteristic with a cooperative strategy suggests that pyoverdine has been selected mainly as a cooperative trait while I believe evolutionary forces at play may be more complex.

3.1.1.1 *Pyoverdine production is a cooperative trait and can be exploited*

In bacteria, yield is the total growth achieved in a given environment.

The effects of pyoverdine production have been studied by comparing the yields of producers and non-producers in pure and mixed cultures, in different environments where pyoverdine is produced or not (Griffin et al., 2004; Meyer et al., 1996). In particular, in King's medium B where low pyoverdine synthesis is reported, pure cultures of producers and non-producers achieve the same yield. In contrast, in Casamino acids medium (CAA) where less iron is available and pyoverdine is produced, the producers yield is lower than that of non-producers; this difference in yield indicates the cost of pyoverdine production. When an iron chelator (with lower affinity for iron than pyoverdine), human transferin, is added to CAA, iron becomes limiting for *P. aeruginosa* growth and producers consequently achieve higher yield than non-producers; this indicates that pyoverdine production is beneficial in iron-poor environments. Finally, when producers and non-producers are grown in mixed culture in CAA with human transferin, non-producers yield is higher than that of producers; this is interpreted as non-producers being able to take advantage of pyoverdine present in the environment without payout the cost of production.

In a subsequent study, various mutants with lower levels of pyoverdine production have been characterized and compared with the corresponding producer genotypes. As expected, the mutants absolute fitness in pure culture is positively correlated with their level of pyoverdine production while their relative fitness in mixed cultures with wild-type is negatively correlated with this trait (Jiricny et al., 2010). These results indicate that this cooperative trait is continuous rather than discrete (producer / non-producer) and that the level of pyoverdine production itself is likely to be under selection.

Interestingly, although kin selection predicts that the inclusive fitness of cooperators should not vary with their frequency, several studies have shown frequency-dependent selection in microbes. In particular, the relative fitness of pyoverdine non-producers has been shown to be negatively correlated with their frequency (Harrison et al., 2006). Ross-Gillespie et al. (2007) have proposed that the dependance of total population growth on the level of cooperation may account for this frequency-dependent selection and have tested this hypothesis experimentally by shortening the duration of population growth.

Another particularity of this system compared with other model systems of cooperation is that pyoverdine is long-lasting: even when it used for iron uptake, half-life is on the order of 20 h (as estimated from data in Kümmerli and Brown, 2010). Consequently, individuals fitness at a given time does not only depend on the levels of production in the population at that time, but rather on the overall concentration in the population that depends on past production levels. Using models, extended durability of public goods has been proposed to reduce the selection for cheating provided the public good production is regulated. In fact, although pyoverdine durability has been shown to decrease more rapidly with time when it is used as a siderophore (in presence of iron and bacteria recycling it), there are some evidence that increase in pyoverdine durability is negatively correlated with non-producer fitness (Kümmerli and Brown, 2010). However, these evidences are only indirect as pyoverdine durability is not manipulated as such but rather mimicked by pyoverdine supplementation.

3.1.1.2 *Cooperative traits and spatial structure*

As highlighted in the introduction, spatial structure is a key parameter in the description of cooperative systems in general, and of microbial interactions in particular. Although not properly addressing the issue of cooperation, two interesting experiments compared the production of diffusible toxins in liquid medium and on plates: in mixed culture of colicin producers and non-producers, producers advantage is frequency-dependent in liquid medium while it is not on plates (Chao and Levin, 1981). Later on, a three partners community with non-transitive interactions was studied in these two environments. It consists in a colicinogenic and resistant strain, outcompeted by a resistant only strain, itself outcompeted by a sensitive strain but that can be killed by the first colicinogenic (and resistant) strain. In this system, the maintenance of the three types was largely facilitated when interactions were local, as demonstrated by both models and experiments (Kerr et al., 2002).

Regarding cooperation in *P. aeruginosa*, the relative fitness of pyoverdine non-producers is negatively correlated with the viscosity of the

growth medium, when viscosity varies from almost liquid to 1 % agarose i.e. a viscoelastic medium (Kümmerli et al., 2009). In this case, changes of the medium viscosity are used to modify the range of interactions between individuals. This result is interpreted in terms of greater indirect benefits for relatives and greater direct benefits for the producer in viscous environments, i.e. when interactions are local. The argument of the direct benefits is interesting as it suggests that pyoverdine production can be a more or less cooperative trait depending on environmental conditions.

In addition to the already exposed explanations for the beneficial effect of spatial structure in cooperation, recent models suggest that limited access to nutrients in spatially-structured environments can favour the spontaneous segregation of cell lines (Nadell et al., 2010), for instance separating in this case pyoverdine producers and non-producers.

3.1.1.3 *Kin selection & local competition*

The principle of kin selection has been presented in the introduction: it explains the stability of cooperation in spite of its cost by the advantage it confers on genetically related organisms. Although it is a seducing idea, one of the difficulties encountered is that interactions between relatives is likely to come at the price of increased competition for resources between them. What matters here is not only the intensity of competition (i.e. the amount of resources available for a given population), but rather its scale (i.e. the fact that resources are shared globally or within small parts of the environment).

In order to disentangle these two effects, experiments with *P. aeruginosa* have been designed to manipulate relatedness and the scale of competition independently from each other (Fig. 3.1 left; Griffin et al., 2004). Relatedness is defined in this case with respect to the cooperative trait i.e. pyoverdine production rather than across the whole genome, and the scale of competition is manipulated by different rules of clones sampling between consecutive growth episodes. As expected, increased relatedness favors pyoverdine producers. In the other hand, local competition (i.e. increased competition between relatives) disadvantages them when competed with non-producers during several rounds (Fig. 3.1 right). In addition, there is a significant interaction between these two parameters.

This work represents a significant contribution to the understanding of the evolutionary forces driving the selection of cooperative traits. Nonetheless, it is not to be confused with experimental evolution: this is rather a case of experimental population dynamics where no adaptation is required to explain the changes in producers frequency. In the local competition and high relatedness condition, there is no mix between producers and non-producers so their ratio is expected to be constant;

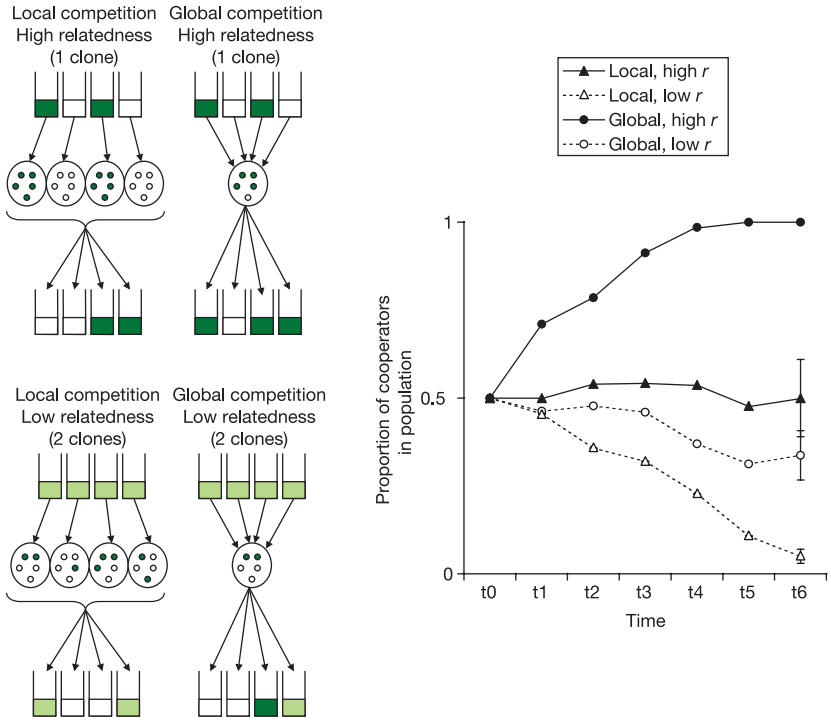

Figure 3.1: Relatedness & scale of competition in *P. aeruginosa* (after Griffin et al., 2004).
Left: The experimental design is such that the scale of competition is manipulated by changing the number of colony picked per plate (n per plate in the local competition regime vs. N in total in the global competition regime). The relatedness is manipulated by growing bacteria in pure or mixed liquid cultures (high and low relatedness respectively).
Right: The production of pyoverdine producers is plotted against time for four different treatments. Each treatments was replicated four times, and standard errors are shown for the final time point. Time is measured as transfers, between which cultures were allowed to grow for 24 h.

in the global competition and high relatedness condition, the spread of producers is likely to be due to growth differences in pure culture; in the local competition and low relatedness condition, the invasion by non-producers is probably due to their growth advantage in mixed culture; finally, in the global competition and low relatedness condition, the invasion by non-producers is probably limited by the higher yield of producers.

A similar approach has been used to demonstrate that repression of competition within a group favours cooperation. Here also, no repression of competition was evolved but it was rather imposed by the experimental procedure (Kümmerli et al., 2010). A notable exception to this experimental population dynamics approach is a study of the effect of mutation rate on the emergence of non-producer strains where *P. aeruginosa* is evolved during 30 days (Harrison and Buckling, 2005).

In microbial species, the occurrence of situations where relatives interact depends very much on each species lifestyle and on corresponding population histories. Another mechanism of cooperation maintenance based on population history has been demonstrated in a very elegant study using *E. coli* genetically engineered so that it produces a public good. In brief, if the reproductive success of a mixed population of producers and non-producers is negatively correlated with the initial proportion of non-producers, then the overall proportion of producers in a collection of populations (of sufficiently variable composition) can increase although their proportion will decrease in each population. This unexpected dynamics is known as the Simpson's paradox (Chuang et al., 2009). Such a scenario is likely to occur in natural populations experiencing frequent and strong bottlenecks as the Poisson distribution of types in newly founded populations makes their composition sufficiently variable.

3.1.1.4 *Public goods dynamics and metabolic regulations*

The study reported in the previous section where pyoverdine durability affects the outcome of competition between producers and non-producers (Kümmerli and Brown, 2010) highlights that costs and benefits of cooperation depend on molecular details, which can modulate the conditions of cooperation maintenance. Interestingly, theoretical work has demonstrated that changing the durability of public goods can transform the type of social dilemmas and also affect their dynamics (Brown and Taddei, 2007).

Another case where the outcome of cooperative interactions has been shown to depend on molecular subtleties is sucrose metabolism in yeast. The relationship between growth rate and glucose availability (produced from sucrose by invertase, an exoenzyme that is a public good in this

case) is highly nonlinear. This nonlinearity and the slightly higher glucose concentration experienced by invertase producers (due to the fact that some part of the invertase is retained in the vicinity of each producer) allow these producers to maintain while they would be outcompeted by non-producers otherwise (Gore et al., 2009).

In *P. aeruginosa*, in addition to pyoverdine which is the best studied public good, another type of public good has been described recently. Large amounts of rhamnolipid biosurfactants can be secreted and allow bacteria to swarm and explore new environments. Although in wild type strains the production of this compound is regulated so that non-producers do not have a growth advantage over producers, a regulation mutant producing it constitutively is outcompeted by non-producers (Xavier et al., 2011). This highlights how the molecular regulations underlying phenotypic traits can affect the outcome of cooperative dynamics.

These three examples illustrate the diversity of the physiological constraints impairing the evolution of public goods. In particular, it is clear that metabolic regulations are likely to change drastically the nature of these social interactions, allowing for instance to reduce the cost of exploitation by non-producers. In line with this prediction, I review the current knowledge about pyoverdine metabolism in the next section.

3.1.2 PYOVERDINE METABOLISM IN *PSEUDOMONAS AERUGINOSA*

The high affinity of pyoverdine for iron results from its molecular structure. Though very diverse between different species and even between strains of a given species, pyoverdines are all composed of three parts (Ravel and Cornelis, 2003): (i) a conserved fluorescent dihydroxyquinoline chromophore, (ii) an acyl side chain bound on the chromophore and (iii) a peptide chain bound to another group of the chromophore and featuring non-standard amino acids (D-serine, ornithine, ...). In *P. aeruginosa*, three types of pyoverdine have been reported so far (Visca et al., 2007b), which differ in their peptide chain composition. These types are produced by different strains that also produce the pyoverdine receptor corresponding to their own type.

In this work, we focus on *P. aeruginosa* PAO1 in which the pyoverdine metabolism has been best described. By pyoverdine metabolism, I refer to pyoverdine synthesis, maturation and export, as well as uptake and recycling mechanisms (as depicted on Fig. 3.2). The strain PAO1 produces type I pyoverdine.

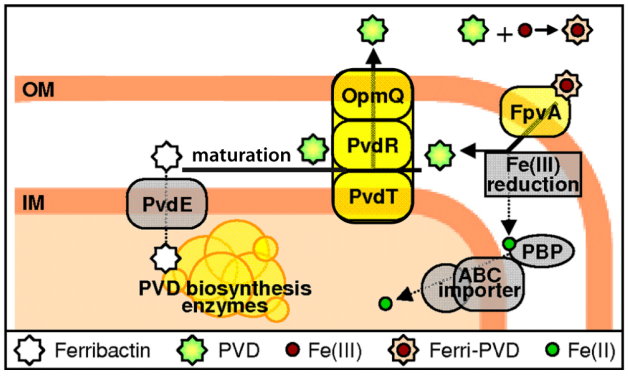

Figure 3.2: Simplified scheme of pyoverdine metabolism (modified from Imperi et al., 2009).
The synthesis of pyoverdine involves the production of ferribactin in the cytoplasm. It is exported and matured to pyoverdine in the periplasm. The uptake of extracellular pyoverdine relies on a dedicated transporter, and iron is dissociated in the periplasm. The secretion of newly synthesized and recycled pyoverdine occur through the same efflux pump. Importantly, only matured pyoverdine not bound to iron is fluorescent.

3.1.2.1 *Pyoverdine is a non-ribosomal peptide matured in the periplasm*

Pyoverdine results from the production of ferribactin, a non-fluorescent precursor, further matured in the periplasm. Ferribactin is not synthesized by translation from an mRNA template. In contrary, its synthesis involves non-ribosomal peptide synthetases (NRPSs) which are large modular enzymatic complexes catalyzing the addition of amino acids to a peptide chain. Each amino acid is added by a dedicated enzyme or enzyme domain. The enzymatic complexes are organized so that the product of one enzyme reaction is passed as substrate to the next enzyme, thereby enhancing the rate of synthesis.

In the cytoplasm, PvdL, PvdI, PvdJ and PvdD NRPS catalyze the synthesis of ferribactin. To this end, they rely on prior amino acids modifications by PvdA, PvdF and PvdH. All corresponding genes are required in order for *P. aeruginosa* to be able to synthesise pyoverdine. This complex synthesis process is reviewed in greater details by Visca et al. (2007b).

The precursor ferribactin is exported in the periplasm by PvdE (Yeterian et al., 2010a), that was early characterized as an ABC transporter required for pyoverdine synthesis (McMorran et al., 1996). PvdN, PvdO, PvdP and PvdQ contribute to the final maturation of the chromophore which results in a fluorescent and active compound.

Secretion of matured pyoverdine to the extracellular environment has been characterized only recently and involves an efflux pump formed by

PvdR, PvdT and OpmQ (hereafter abbreviated as PvdRTQ; Hannauer et al., 2010b).

3.1.2.2 *Pyoverdine uptake and recycling*

In the extracellular environment, its high affinity for iron makes apo pyoverdine likely to bind Fe^{3+}. The receptor of pyoverdine FpvA binds both apo and ferric pyoverdine. As apo pyoverdine is much more abundant, this would be the default ligand of the receptor. In presence of ferric pyoverdine, apo pyoverdine bound to FpvA is replaced by ferric pyoverdine (Schalk et al., 2001). While apo pyoverdine is not imported, ferric pyoverdine is imported thanks to a conformational change of FpvA; this energy-dependent process is powered by TonB, a protein that is coupled to the electrochemical gradient of the cytoplasmic membrane (Schalk et al., 2004). Interestingly, although FpvA is composed of a barrel and a plug domain, the plug is never removed from the barrel during the uptake cycle (Nader et al., 2011). Recent findings showing that pyoverdine interacts with a large variety of metallic ions suggest that apo pyoverdine is rarer than initially expected and that pyoverdine that is not bound to iron is rather bound to other ions (Braud et al., 2009b). Taking this into account, the uptake process scenario described in this paragraph can be slighlty rephrased. FpvA would import pyoverdine bound to different metals. Iron would be dissociated from pyoverdine and the resulting apo pyoverdine would be recycled. In addition, the pool of pyoverdine bound to other metals would be recycled directly to the extracellular environment.

Although FpvA is usually referred to as a receptor *due to its specificity for pyoverdine, it should rather be seen as a* specific transporter *since it mediates the entry in the periplasm of pyoverdine and other molecules as pyocins.*

Iron is released from pyoverdine in the periplasm and further transported to the cytoplasm. The release process involves iron reduction (Greenwald et al., 2007). Although not finely characterized yet, iron release requires FpvC, FpvD, FpvE and FpvF. In particular, deletion of *fpvC* completely abolishes iron uptake by the cell, even in presence of pyoverdine (Meksem et al., 2011). As pyoverdine is imported in the periplasm even when bound to other ions, the iron-specificity of pyoverdine-mediated uptake would come from the metal dissociation step (Braud et al., 2009b).

Interestingly, imported siderophores can also be recycled after iron dissociation (Greenwald et al., 2007). This recycling occurs only through the periplasm and involves the same efflux pump PvdRTQ as the export of newly synthesized pyoverdine (Imperi et al., 2009; Yeterian et al., 2010b). The role of this pump in export following synthesis was discarded by Imperi et al. (2009) but confirmed by Hannauer et al. (2010b).

The characterization of pyoverdine metabolic pathways is complicated by the overlap between redundant pathways. For instance, although PvdRTQ was proposed early to be involved in export, early experiments

reported that its inactivation by mutation did not prevented pyoverdine secretion (Imperi et al., 2009; Lamont and Martin, 2003). This misanalysis is probably due to the fact that other secretion systems are involved though they have not been identified yet (Hannauer et al., 2010b; Visca et al., 2007b). The multidrug efflux pump MexAB-OprM was proposed to be another possible candidate for pyoverdine secretion, although this hypothesis has been discarded recently (Imperi et al., 2009). As far as pyoverdine uptake is concerned, a second receptor specific of type I pyoverdine, FpvB, has been identified which makes this part of the metabolism redundant as well (Ghysels et al., 2004).

3.1.2.3 *Iron homeostasis in* P. aeruginosa

In *P. aeruginosa*, pyoverdine is considered to be produced in response to iron-depleted conditions thus participating to iron homeostasis in the cell. This is inferred by the fact that its synthesis is repressed when iron concentration is higher than 5 µM (Meyer and Abdallah, 1978). In this case, iron is supposed to enter the cell passively and to repress the global regulatory protein Fur (ferric uptake regulator), the main regulator of iron metabolism. Fur conformational changes upon iron binding prevent it from binding to the promoters and consequently from inhibiting the expression of iron-related genes (Escolar et al., 1999). The detailed mechanism of Fur-mediated regulation is reviewed in Visca et al. (2007a). Surprisingly, although the expression of more than hundred genes is modulated by iron concentration, only a minority of these genes contain a Fur-binding sequence.

In the case of pyoverdine-related genes, an iron starvation box is found instead of a Fur-binding sequence at the promoter region. This box is typically recognized by PvdS, an alternative sigma factor of the extracytoplasmic function sigma factor (ECF-σ) family. The presence of three Fur-binding boxes in *pvdS* promoter and the control of the expression of pyoverdine-related genes by PvdS explain that these genes are overall iron-regulated.

The signal transduction pathway leading from changes in extracellular iron concentration to changes in gene expression has been studied in great details. When the main pyoverdine receptor FpvA is bound to apo pyoverdine, the antisigma molecule FpvR sequesters ECF-σ like PvdS thus preventing pyoverdine-related gene expression. Upon ferric pyoverdine binding to FpvA, the interaction between FpvA and FpvR changes and ECF-σ are released. Consequently, the expression of pyoverdine-related genes is triggered by PvdS interaction with their promoters (Fig. 3.3). PvdS also controls the expression of other types of genes among which are virulence factors such as exotoxin A and PrpL protease (Lamont et al., 2002) and most probably quorum sensing genes as well (Ochsner

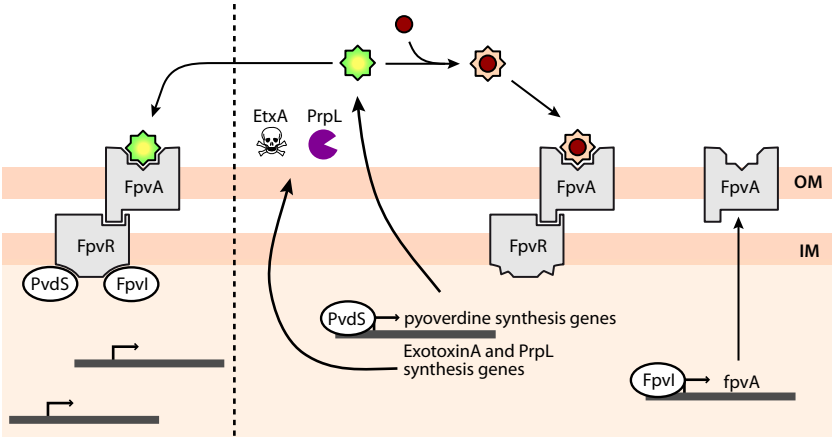

Figure 3.3: Divergent signalling pathways activated by pyoverdine receptor (modified from Beare et al., 2003).
The specific transporter of pyoverdine FpvA is coupled to an anti-sigma molecules. Depending on the interaction of ferric pyoverdine with FpvA, this antisigma regulates the free pool of two ECF-σ controlling pyoverdine-related genes as well as virulence genes expression.

et al., 2002). Finally, the details of the FpvA-FpvR-mediated transduction mechanism is not fully understood yet. In particular, the interaction between FpvA and the energy-transducing protein TonB1 has been shown to be required which suggests that the transduction mechanism is energy-dependent (Shirley and Lamont, 2009).

A distinctive feature of this transduction pathway is that FpvR anti-sigma interacts with two different ECF-σ. In fact, FpvI is another sigma factor that is also regulated by FpvR and that controls the expression of *fpvA* (Beare et al., 2003). These divergent signalling pathways are also reviewed in details in Visca et al. (2007a).

As a result, the expression of most pyoverdine-related genes is controlled directly by PvdS ECF-σ. PvdS expression in turn depends on intracellular iron concentration due to Fur regulation, while its activity is modulated by extracellular iron concentration thanks to the FpvA-FpvR-mediated signalling pathway. This global scheme corresponds to a positive feedback in pyoverdine synthesis regulation at low iron concentration since the synthesis is enhanced by the uptake of ferri pyoverdine by FpvA. The details of genes and operons regulation is shown on Fig. 3.4. This regulation scenario is inferred from pyoverdine metabolism of different mutants and is consequently difficult to test directly. Nonetheless, the first study based on RNAP purification analysis supports this view where PvdS activity is modulated primarily by its interaction with other proteins rather than by the level of its synthesis (Tiburzi et al., 2008).

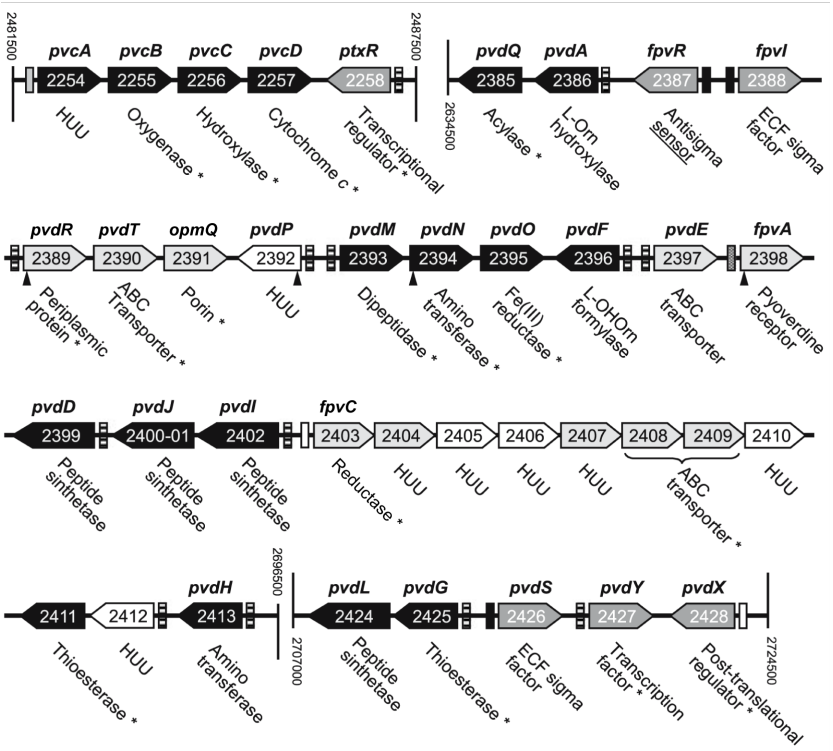

Figure 3.4: Pyoverdine-related genes in *P. aeruginosa* PAO1 (from Visca et al., 2007a).

Genes (not drawn to scale) are oriented according to the direction of transcription. Gene numbers and map positions are according to the Pseudomonas Genome Project (www.pseudomonas.com). Gene names and function (if known) are also shown; asterisks denote protein functions inferred from *in silico* prediction. Uncharacterised gene products are indicated as HUU (hypothetical, unclassified, unknown). The grey scale differentiates predicted or confirmed protein functions, as follows: black, biosynthetic enzymes; dark grey, regulatory proteins; grey, membrane or transport proteins; white, HUU. Binding sites for Fur repressor protein are shown as black boxes, PvdS-dependent promoters as dashed boxes, the PtxR-dependent promoter as a grey box, the FpvI-dependent promoter as a dotted box, and uncharacterised promoters as white boxes. Note that PA2403–PA2410 is transcribed from an iron-regulated promoter lacking an obvious IS box.

3.1.2.4 *Other siderophores used by* P. aeruginosa

The growth of pyoverdine mutants of *P. aeruginosa* in scarce iron conditions indicates that these bacteria can uptake iron thanks to pyoverdine-independent mechanisms. In fact, although pyoverdine is considered as the main siderophore of all fluorescent *Pseudomonas*, most of these species produce secondary siderophores (Cornelis, 2010). In *P. aeruginosa*, the secondary siderophore is pyocheline which forms a complex with ferric iron in a 2 : 1 stoichiometry and has a much lower affinity for this ion than pyoverdine, around $2 \cdot 10^5\,M^{-1}$ (Cox and Graham, 1979). Although this relatively low affinity makes pyocheline unlikely to be involved in iron uptake when pyoverdine is present, pyocheline allows pyoverdine mutants to grow at low iron concentration.

In pyoverdine producing strains, pyocheline has been proposed to play a role in other metal uptake (Co(II), Ga(III), Mo(VI), etc) although the efficiency of these processes has been shown to be too low to consider them as biologically relevant (Braud et al., 2009a). Other biological roles like induction of secondary metabolites have been identified (Vinayavekhin and Saghatelian, 2009) and are reviewed by Cornelis (2010).

In addition to the synthesis of secondary siderophores, fluorescent *Pseudomonas* use a very remarkable strategy: they are able to express a variety of receptors (up to more than forty!) specific for different siderophores produced by other bacterial and fungal species, thus referred to as xenosiderophores (Cornelis, 2010). This mechanism involves a dedicated receptor, an ECF-σ and an antisigma for each type of xenosiderophore. As noticed by Hannauer et al. (2010a),

> "*P. aeruginosa* is also capable of utilizing numerous siderophores secreted by other microorganisms: pyoverdines from other pseudomonas, enterobactin, cepabactin, mycobactin and carboxymycobactin, fungal siderophores (ferrichrome; deferrioxamines; and desferrichrysin, desferricrocin, and coprogen), and natural occurring chelators such as citrate."

The use of xenosiderophore by *P. aeruginosa* is reviewed by Poole and McKay (2003) and more recently by Cornelis et al. (2009).

The ability to use siderophores that are not produced by the cell can lead to intraspecific or interspecific competition. In a study with *P. aeruginosa*, the gene of the second receptor of type I pyoverdine, *fpvB*, is found to be present in 93 % of more than 300 natural isolates although only 49 % of them bear type I *fpvA* (and consequently are likely to produce type I pyoverdine) (Bodilis et al., 2009). The occurrence of interspecific competition for iron is clearly indicated by *Pseudomonas* ability to express receptor of xenosiderophores as described above.

RESEARCH OUTLINE

In this study, we propose to describe pyoverdine concentration in bacteria as a continuous trait. Doing so, we question whether the exploitation of producers by non-producers can be extended to the distinction between high level producers and low level producers. En route, we aim at characterizing the relative importance of the different parts of pyoverdine metabolism (production, uptake, secretion) in this social interaction.

The long term perspective is to provide a more precise description at the individuals level of pyoverdine dynamics in clonal populations of producers as well as in mixed population of producers and non-producers.

Although most studies on pyoverdine are done in pyocheline mutant strain, we choose to study a wild type PAO1 strain in conditions where pyoverdine production is high. Consequently, pyocheline role as a siderophore is likely to be negligible while all regulation pathways are fully functional.

3.2 METHODS AND RESULTS

3.2.1 PROTOCOLS

3.2.1.1 *Strains, medium and protocols*

Phenotypic variability of pyoverdine metabolism is studied primarily in *P. aeruginosa* PAO1. All mutants strains are derived from this ancestral strain. Strains, purified pyoverdine and protocols have been obtained from I. Schalk's lab (Strasbourg Univ.).

The standard growth protocol with succinate minimal medium (SMM) has been chosen in order to maximise pyoverdine expression (Meyer and Abdallah, 1978). It is noteworthy that although these conditions trigger pyoverdine production, the low iron concentration is not limiting growth: the growth of a pyoverdine deficient mutant is comparable to PAO1 growth. SMM is prepared with 6 g of KH_2PO_4, 3 g of K_2HPO_4, 1 g of $(NH_4)_2SO_4$, 0.2 g of $MgSO_4 \cdot 7\,H_2O$, and 4 g of succinic acid in 1 L purified H_2O; pH is adjusted to 7 using concentrated NaOH and the solution is sterilized by filtration at 0.2 µm.

Strains are stored in glycerol stocks at −80°C. They are inoculated from stocks in LB and grown overnight at 37°C. The next day, the culture is washed in SMM, diluted 100× in fresh SMM and grown overnight at 28°C. On the third day, bacteria are ready to be diluted for subsequent growth in liquid medium or on a microscope slide.

For microscopic observations, slides are prepared with a gel pad (1 % agarose in SMM). Image acquisition is done with a Hamamatsu Orca-R^2 CCD camera, mounted on an Olympus IX81 inverted microscope with a 100 × phase objective. Objective and stage temperatures are regulated at 30°C using a custom controller. A mercury vapor light source (EXFO X-Cite 120Q) is used for fluorescence imaging, and pyoverdine fluorescence is excited with a 390(40) nm filter and monitored with a 475(64) nm filter behind a beamsplitter at 405 nm.

3.2.1.2 *Measuring fluorescence distributions*

Distributions of pyoverdine concentration are obtained for PAO1 in different growth conditions and for various mutants. Following standard growth protocol described above, 2 µL of a 30 × dilution of the SMM overnight culture are poured on a microscope slide prepared as described above. After drying is complete, bacteria are sealed behind a coverslip; holes are prepared in agarose and tape in order to prevent anaerobic conditions. When pyoverdine synthesis mutants are studied, they are supplemented with 850 nM HPLC-purified pyoverdine.

After 7 h incubation at 30°C, phase contrast and fluorescence images are acquired using µManager software (Edelstein et al., 2010). Fluorescence exposure time is adjusted depending on growth conditions so that mean intensity is about a third of the 16-bit dynamic range.

Subsequent image analysis consists in bacteria identification in phase contrats images (using band-pass filtering and Otsu thresholding) and in measuring each bacteria fluorescence using this mask. Custom ImageJ macros have been developed to this end.

In order to estimate intracellular pyoverdine concentration from fluorescence intensity, the average background fluorescence is measured on each picture in a 100 × 100 px^2 square and subtracted from cells average fluorescence on the corresponding picture. This ensures to take only into account the intracellular pyoverdine contribution to the fluorescence signal. We assume that the concentration is proportional to the fluorescence signal.

The intracellular level of pyoverdine is variable from one replicate to the next. When comparing pyoverdine distribution in different mutants or conditions, the concentration is normalized per observation field by dividing it by the average intracellular concentration in the field.

3.2.1.3 *Measuring fluorescence dynamics*

Fluorescence dynamics are monitored using time lapse microscopy. Following standard growth protocol described above, 2 µL of a 10^4 × dilution of the SMM overnight culture are poured on a microscope slide as explained above. After 3 h incubation at room temperature, the slide

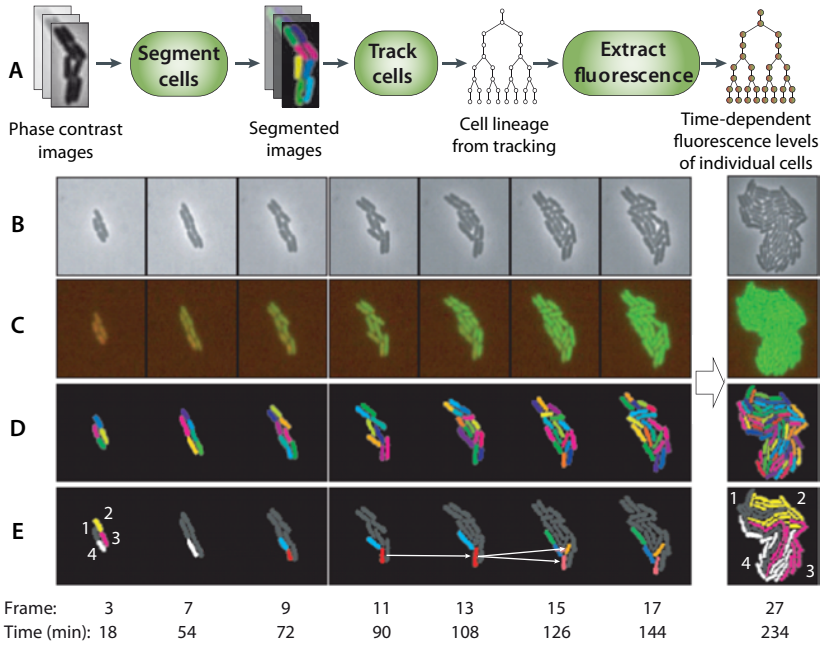

Figure 3.5: Analysis scheme used in Schnitzcell software (from Locke and Elowitz, 2009).
The analysis consists in three steps: bacteria segmentation, bacteria tracking, and fluorescence extraction (A); segmentation and tracking are manually checked and corrected. In more details, phase contrast images (B; or our custom images) are used to produce masks (D) by segmenting bacteria on each frame. These masks are used to track bacteria from one frame to the next (as shown with colours on E). After the genealogy is reconstructed, the intensity of each cell on each frame is extracted from fluorescence images (C).

is transfered onto the temperature-regulated microscope stage where images are automatically acquired during 20 h using a custom LabView program developed by N. Desprat. Instead of using phase contrast, a custom white light imaging method has been developed that provides higher signal to noise ratio, in particular for small objects as *P. aeruginosa* cells (typically 30 % smaller than *E. coli* cells).

The period of acquisition is 5 min during 5 h and 3 min later on; this change in acquisition period allows to get more information on the fluorescence dynamics once the colony features several hundreds of cells, while limiting pyoverdine bleaching in early colony growth.

Time-lapse movies are analyzed using Schnitzcell software developed in Matlab (Rosenfeld et al., 2005, ; kindly provided by M. Elowitz) in order to segment bacteria on each frame and to track them from one frame to the next (Fig. 3.5). We modified the segmentation algorithm

so that it takes our custom images instead of phase contrast images as input to compute the segmentation mask. After manual verification and editing, these genealogical data are analysed using custom scripts in R. Cellular pyoverdine concentration is estimated from fluorescence intensity as described in the previous section. When required, concentration is normalized per frame.

3.2.2 DYNAMIC VARIABILITY OF PYOVERDINE CONCENTRATION WITHIN A CLONAL MICROCOLONY

In this section, I report on the variability of pyoverdine concentration between cells of a clonal microcolony. After a detailed quantitative description, I examine different possible origins of this variability, such as spatial structure, heritability, and metabolic regulation. When referring to pyoverdin concentration in cells, I use indistinctly the words concentration and fluorescence as I refer to the cell contribution to the fluorescence signal which is linear with concentration as mentioned in the previous section.

3.2.2.1 *Heterogeneity of pyoverdine distribution*

Variability of bacteria growth can be used to characterize the reproducibility between replicates. As already reported for rod-shaped bacteria, cell length increases exponentially during all the cell cycle (not shown). The cell doubling time inferred from elongation rate is 43.0 ± 1.5 min (mean and SEM over 10 replicates). This is a reasonable value in minimal medium and the variability is satisfyingly low.

Pyoverdine diffusion coefficient in water is approximately $2 \cdot 10^{-6}$ cm^2/s *as estimated after its molecular weight. Preliminary tests showed that pyoverdine diffusion is not much slower in* 1 % *agarose gel than in water.*

During the growth of *P. aeruginosa* microcolony, pyoverdine fluorescence increases both within cells and outside the microcolony (Fig. 3.6). The fluorescence increase in the surrounding environment is the result of pyoverdine secretion by the microcolony of interest and by all other colonies on the slide. The rapid diffusion of pyoverdine in agarose lowers the spatial variations of its concentration between different regions of the slide. The increase of bacteria fluorescence (and in turn of background fluorescence) is interpreted as the result of the positive feedback in the pyoverdine synthesis pathway (reported in section 3.1.2.3).

At each time of the colony growth, and for all replicates, a large variability of fluorescence is observed between cells of a microcolony (Fig. 3.7 top). In order to characterize this distribution independently from its mean value (varying very fast due to the positive feedback), pyoverdine concentration is normalized on each frame by dividing cell concentrations by the average concentration in the colony (Fig. 3.7 bottom). In addition to its large standard deviation, the concentration distribution is also biased toward high values, resulting in a positive skewness.

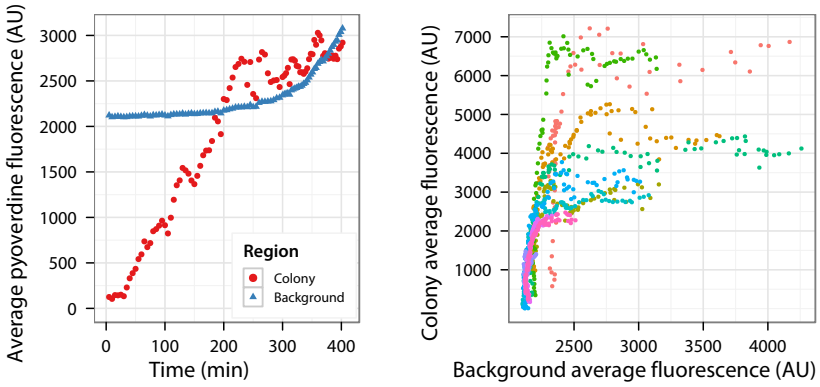

Figure 3.6: Overall pyoverdine fluorescence during microcolony growth.
Left: Pyoverdine fluorescence in the microcolony (red) or in the surrounding medium (blue) are plotted during time. The fluorescence of the colony is corrected by subtracting the background in order to indicate the cells contribution to the fluorescence signal.
Right: Average pyoverdine fluorescence in the colony against the pyoverdine fluorescence in the background region. Each movie is plotted in a distinct colour.

In preliminary experiments, the number of pyoverdine molecules per cell has been estimated to be on the order of 500 to 5000 by measuring the fluorescence of a thin layer of pyoverdine solution of known concentration. To do so, pyoverdine diluted in 10 % polyvinyl alcohol (at 7 µM, 14 µM and 28 µM) is spin-coated on a coverslip and the thickness of the gel layer is measured with a mechanical profilometer for each sample (between 680 nm and 2200 nm).

For a large number n of molecules per cell (with random uncorrelated fluorescence intensities), the mean cell fluorescence is expected to be proportional to n and the standard deviation to $\sqrt{n}$. Consequently, the coefficient of variation of the fluorescence per cell (i.e. its standard deviation divided by its mean) is expected to be proportional to $1/\sqrt{n} \simeq 1\%$.

Unexpectedly in our experiments, the standard deviation of the raw concentration is linearly related to its mean (Fig. 3.8). The slope of this relationship, i.e. the coefficient of variation of the fluorescence, is ca. 30 % which is much higher than expected.

Finally, although pyoverdine is a model of public good and its intracellular concentration is interpreted as the benefits taken from the production in the population, cells growth rate is not correlated with their average pyoverdine concentration (data not shown).

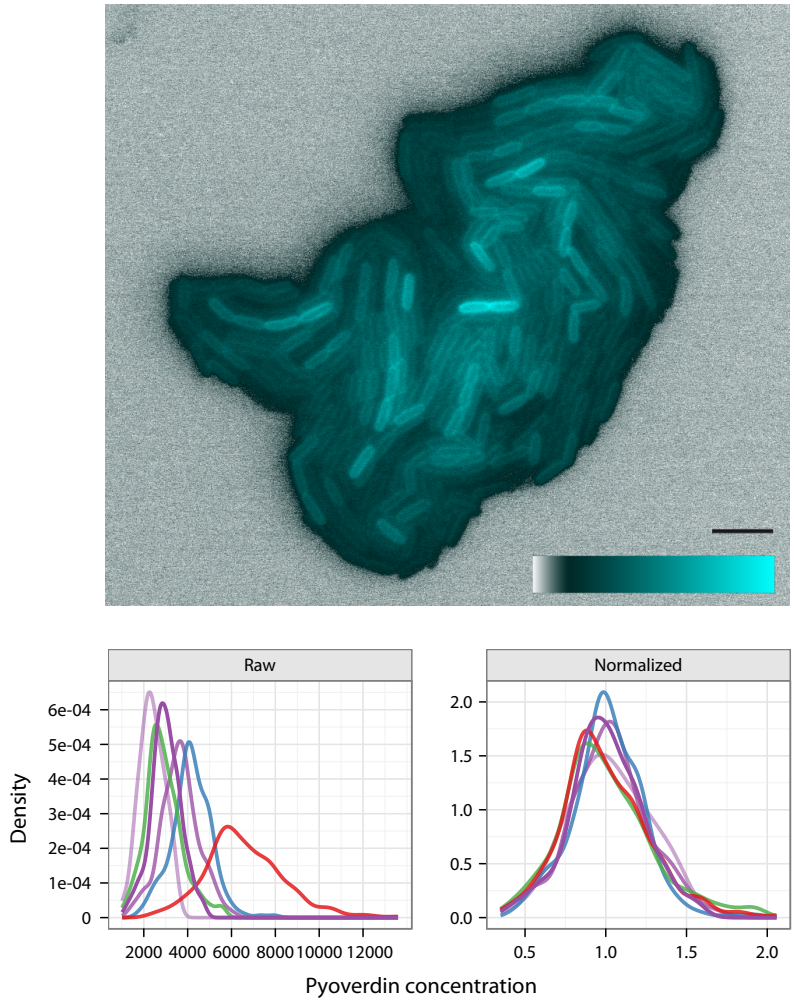

Figure 3.7: Pyoverdine distribution within a clonal microcolony.
Top: Picture of pyoverdine fluorescence in a microcolony grown in SMM with 1 % agarose. Variability between cells is visible by eye. Color scale is shown at the bottom, increasing from left to right. Scale bar is 5 µm.
Bottom: Distribution of average pyoverdine concentration per cell. Each line is the distribution on one frame of one movie; only a small representative subset is shown. The distribution of raw concentrations varies between movies (different colors represent different movies at the stage of 300 cells) and also during time of a given movie. Three purple lines represent the distribution of the same movie at the stages 50, 250 and 415 cells (light, medium and dark purple respectively). In this study, such distributions are compared to each other by focusing on concentration normalized by the average concentration in the colony on the frame of interest.

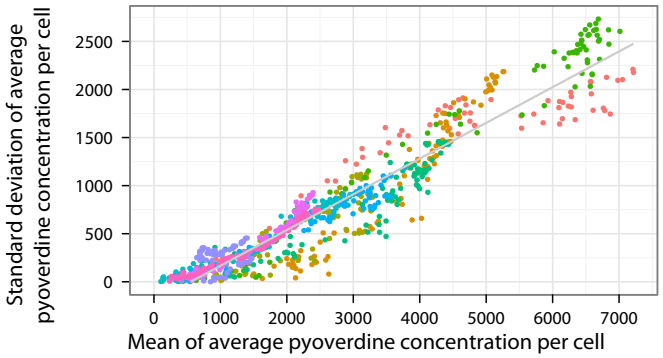

Figure 3.8: Pyoverdine distribution as a function of mean concentration. During colony growth the mean level of pyoverdine concentration per cell increases. Following this increase, the standard deviation is linearly related to the mean, while the null hypothesis (CLT) predicts a square root relationship. Mean and standard deviation are computed on each frame of each movie and are weighted by cell area. A different colour is used for each movie.

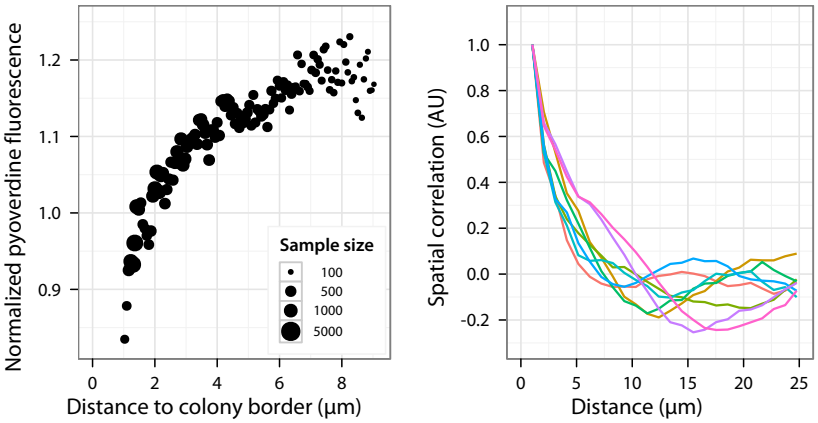

Figure 3.9: Variations in space of pyoverdine concentration.
Left: Pyoverdine concentration dependance on the distance to the colony border. The distance is measured between the cell barycenter and the nearest colony edge. This effect is visible by eye on Fig. 3.7 top. Only the peripheral cell are shown as no clear effect is visible in center of the colony (for $d > 9\,\mu m$).
Right: Spatial correlation of pyoverdine concentration within microcolonies. For each movie, the correlation is computed at stage 300 cells and normalized to 1 for the shortest distance. For distance longer than 25 µm, the correlation increases rapidly in certain movie due to positive correlation between low level cells on the edge (as shown on left plot).

3.2.2.2 *Spatial distribution of pyoverdine*

Pyoverdine is a diffusible molecule that is secreted and imported by bacteria, and also regulates its own synthesis. Consequently, one can expect a non-uniform spatial distribution within the colony.

First, we report that pyoverdine relative concentration is lower near the edges of the colony. This edge effect is weak and affects mostly the two first rows of cells (Fig. 3.9 left).

In order to identify possible patterns in the repartition of concentration within the microcolony, the spatial correlation of pyoverdine concentration between cells is computed at stage 300 cells, for all pairs of cells on the frame. This correlation is monotonically decreasing to zero with a characteristic length of 3 µm to 5 µm (3.9 right). This indicates that no long-scale patterns are present within the microcolony (but the edge effect reported above), and that only short-range interactions between proximate neighbours are directly visible.

Regarding the lower fluorescence of cells near the edges, the proportion of cells in the first two rows decreases when colony grows and our data are dominated by the last frames with more cells. Consequently, this effect is not likely to explain all the reported variability. Another argument is that the variability we observe is coupled with rapid changes in time as detailed in the next section.

Overall, the high variability of pyoverdine concentration between cells of a microcolony does not originate from spatial heterogeneity.

3.2.2.3 *Dynamics of pyoverdine concentration variability*

While the distribution of pyoverdine concentration is a property of the population, a more precise description of pyoverdine metabolism implies to analyse the data at the single-cell level, that is to be able to monitor the concentration of each cell over time. In order to do so, it is critical to take into account cell division which leads to a study of the lineages within the microcolony.

The genealogical tree of a microcolony is drawn with normalized pyoverdine concentration in colour (Fig. 3.10). This shows no clear long-lasting heredity pattern (that would result in subtrees with homogeneous colours) but rather rapid fluctuations of pyoverdine concentration along each branch.

Studying the time series of normalized pyoverdine fluorescence in each branch allows to better characterize these fluctuations in time. After a transient increase in fluorescence variability (until the colony grows to a significant number of cells), fluorescence fluctuates along each branch (Fig. 3.11 left). Interestingly, the power spectrum of these fluctuations

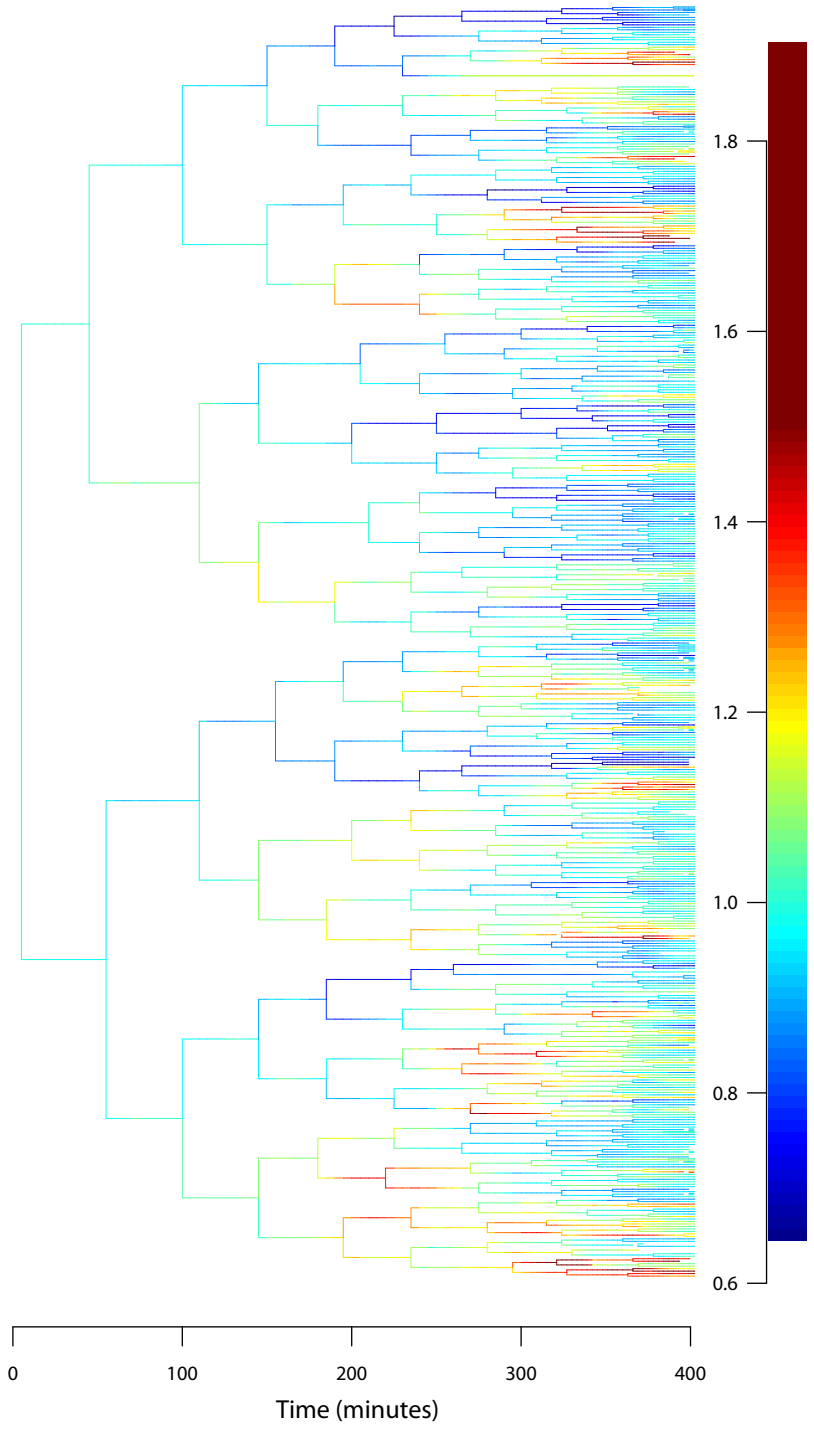

Figure 3.10: Genealogical tree of normalized pyoverdine concentration in a microcolony. The colour scale is saturated at the higher end for easier visualization of the fluctuations.

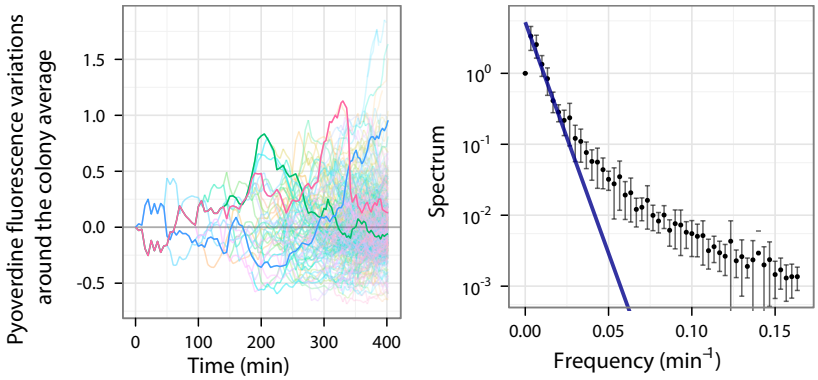

Figure 3.11: Temporal fluctuations of pyoverdine concentration.
Left: Time series of pyoverdine fluorescence for all branches of a genealogical tree in a microcolony. The number of branches increases with time as cell division occur. Three representative branches are highlighted to illustrate fluctuations.
Right: Power spectrum of fluctuations. Spectrum is computed for each branch shown on the left plot and averaged over all branches. Points and error bars show mean and SEM of the average spectrum of 10 replicates.

is monotonically decreasing: low frequencies are preponderant and no typical fluctuation period is characterized (Fig. 3.11 right).

Therefore, the temporal fluctuations of pyoverdine concentration can not be explained by a simple heritability or oscillatory model.

Another interesting aspect of single-cell description is the analysis of asymmetry between sisters. In this study, we define asymmetry as $\frac{\text{trait}_{\text{new}}-\text{trait}_{\text{old}}}{\text{trait}_{\text{new}}+\text{trait}_{\text{old}}}$ where the old pole cell is the cell that inherited the existing pole at the last division and the new pole cell is the cell in which septation occurred at the last division (Fig. 3.12). Although the morphology of sisters is apparently symmetrical, previous studies reported that global traits such as growth rate are asymmetric between sisters (Lindner et al., 2008; Stewart et al., 2005) and this has been interpreted as a mark of ageing (Chao, 2010).

In our experiments, no significant asymmetry is observed in growth rate; this can be due to differences in growth conditions compared to previous studies, possibly resulting in a lower level of damages. In contrast, the concentration of pyoverdine is higher in the new pole cell; this 2 % difference is significantly different from 0 (inset of Fig. 3.13 left). Interestingly, this difference between sisters increases with time after division. If asymmetry comes from a bias in repartition at division, it is supposed to be constant until the next division; in contrary here, the increase of asym-

metry during the cell cycle suggests that the metabolism of pyoverdin is different in the two sisters which can be seen as a functional asymmetry (Fig. 3.13 left).

In order to characterize the integrated effects of asymmetry, it is possible to define an age measure for the cell: following Stewart et al. (2005), bacteria age is defined as the number of consecutive divisions as old or new pole cell that the bacteria just underwent (denoted as negative and positive pole age respectively, Fig. 3.13). The normalized pyoverdine concentration decreases with old pole age (red points on Fig. 3.13 right); this can be interpreted as the cumulative effects of functional asymmetry between sister cells described above. Unexpectedly, the normalized pyoverdine concentration also decreases with new pole age (blue points on Fig. 3.13 right). A tentative interpretation is proposed in the discussion.

3.2.2.4 *Characterization of a stochastic switch in pyoverdine metabolism*

Although no characteristic period of pyoverdine fluctuations can be identified, rapid changes occur during the life cycle. In particular, rapid decreases of pyoverdine metabolism can be seen by eye (Fig. 3.14 left). This highlights that the changes in cellular pyoverdine concentration are not only the result of different levels of synthesis but involve other aspects of the metabolism as uptake and secretion (potentially of both newly synthesized and recycled pyoverdine).

In order to account for these rapid changes in pyoverdine metabolism, we hypothesize the existence of a phenotypic switch between a state where cellular pyoverdine concentration increases (*hoarding*) and a state where it decreases (*dumping*). Fluorescence time series are approximated using robust local quadratic regression (Loader, 1997; Loader and Liaw, 2010) and switches are identified by detecting sign changes of the fitted derivative (Fig. 3.14 right). The smoothing parameters in the regression have been adjusted in order to identify a reasonable number of switches per generation (ca. 0.3 to 3).

Using this switch detection algorithm, it is possible to characterize the phenotypic switch in a quantitative manner. The probability of switching between the two states at a given pyoverdine concentration is estimated by comparing the number of switches at this concentration to the total number of observations at this concentration. Surprisingly the probability of switching between phenotypes appears to depend more clearly on the normalized pyoverdine concentration x in the bacterium than on the absolute one c (with $x = c/\langle c \rangle$ where $\langle c \rangle$ is the colony average; Fig. 3.15

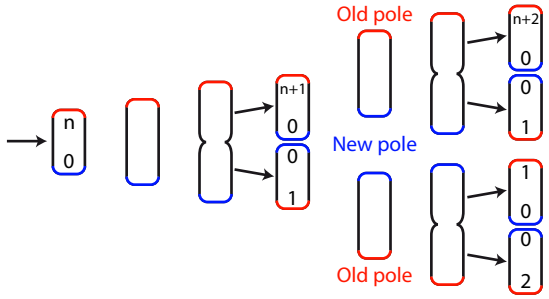

Figure 3.12: Notion of old pole age in symmetrically dividing bacteria.
Although the two sisters appear identical, one of the two poles is newly created at each division (new pole in blue). Following the definition proposed by Stewart et al. (2005), old pole age is defined as the number of consecutive divisions as old pole cell that the bacteria just underwent (≥ 1). The age of the old pole of the cell initiating the colony is unknown. However if the population is growing exponentially, it has probability 0.5 to be of age 1, probability 0.25 to be of age 2, etc. Finally, this notion can be extend to new pole; in this case, old pole age is indicated as negative while new pole age is written as positive.

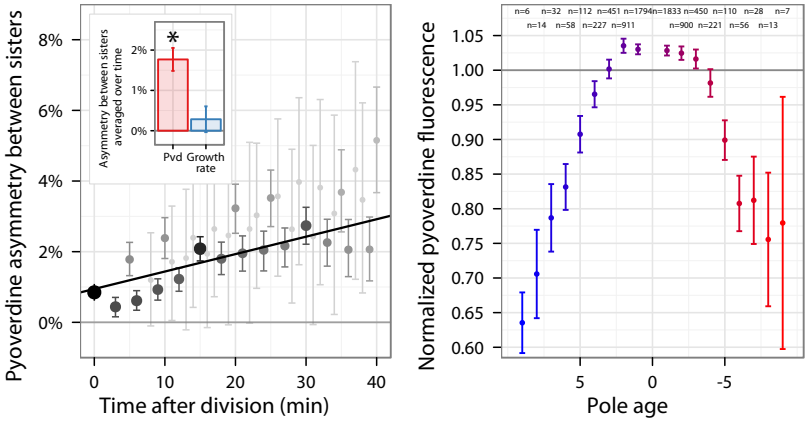

Figure 3.13: Asymmetry of pyoverdine concentration between sister cells.
Left: Pyoverdine concentration asymmetry between sister cell is defined as $\frac{[\text{pvd}]_{\text{new}}-[\text{pvd}]_{\text{old}}}{[\text{pvd}]_{\text{new}}+[\text{pvd}]_{\text{old}}}$. Points and error bars show mean and SEM over 10 replicates.
Right: Pyoverdine normalized concentration as a function of pole age. Pole age is defined as consecutive division at the same (old or new) pole. Negative values (in red) is the number of consecutive division at the old pole, while positive values (in blue) is the number of consecutive division at the new pole.

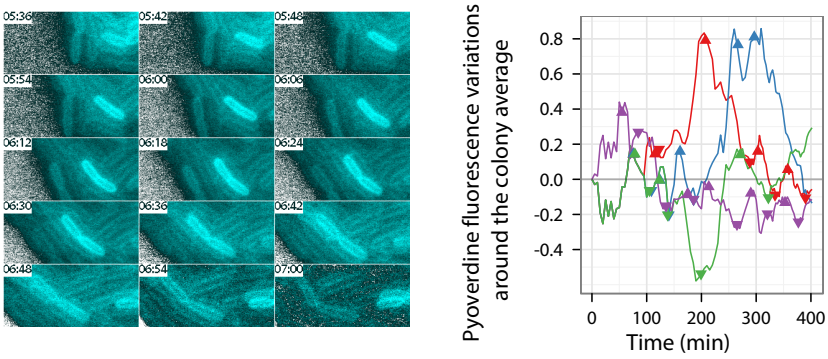

Figure 3.14: Rapid fluctuations of pyoverdine concentration. These fluctuations can be described by assuming a phenotypic switch between a state where pyoverdine concentration increases (hoarding) or decreases (dumping).
Left: Enlargement of a microcolony movie highlighting rapid changes in pyoverdine fluorescence. Period between two frames is 6 min.
Right: Time series of pyoverdine fluorescence. Switches detected in the analysis are highlighted by plain triangles; the triangle direction indicates the type of switch.

left). The switching rate k_{hd} from a *hoarding* to a *dumping* phenotype can be fitted to a Hill curve defined by

$$k_{hd} = \frac{k_h^0}{1 + (x/x_h^0)^m} \tag{3.1}$$

with $k_h^0 = 0.24\ \text{min}^{-1}$, $x_h^0 = 3.80$ and $m = 1.26$. Similarly the switching rate from *dumping* to *hoarding* phenotype can be fitted by

$$k_{dh} = \frac{k_d^0}{1 + (x_d^0/x)^n} \tag{3.2}$$

with $k_d^0 = 0.09\ \text{min}^{-1}$, $x_d^0 = 0.86$ and $n = 2.86$ (Fig. 3.15 left). Parameter estimation after experimental data is done by minimizing least square with Rgenoud (R-GENetic Optimization Using Derivatives; Mebane and Sekhon).

In order to integrate these observations and to model this phenotypic switch, we propose to describe the dynamics as a two states equilibrium:

$$\text{H} \underset{k_{dh}}{\overset{k_{hd}}{\rightleftharpoons}} \text{D}$$

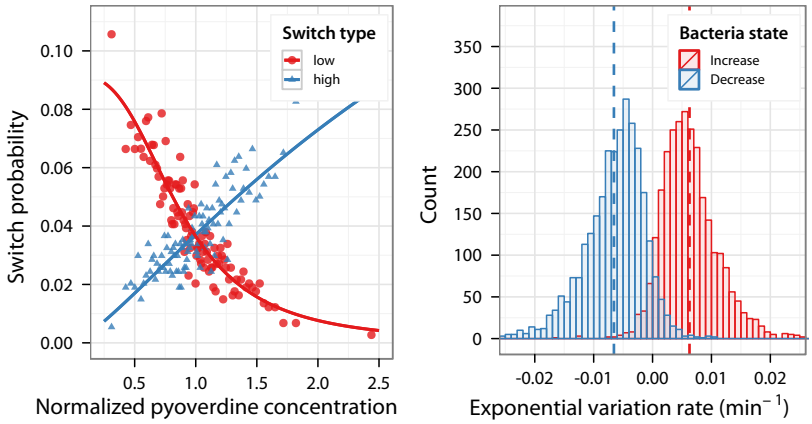

Figure 3.15: Characterization of the phenotypic switch in pyoverdine metabolism.
Left: The probability of switch depends on the normalized pyoverdin concentration: blue points correspond to *hoarding* to *dumping* switches, and red points to *dumping* to *hoarding* switches. Points are the average probability for centiles of the distribution, lines are least square fits with Hill functions: k_{hd} in blue (Eq. 3.1) and k_{dh} in red (Eq. 3.2).
Right: Distribution of the exponential rates of pyoverdine concentration hoarding (red) and dumping (blue). The average value has the same magnitude in the two states, around 0.006 min^{-1}.

where k_{hd} and k_{dh} are switching rates following Eq. 3.1 and Eq. 3.2 respectively. Between two switches, the raw concentration c is assumed to vary exponentially with $\frac{\mathrm{d}c}{\mathrm{d}t} = r_h c$ in *hoarding* state and $\frac{\mathrm{d}c}{\mathrm{d}t} = -r_d c$ in *dumping* state. In the experiments, the magnitudes of variations rates are similar in the two states, with *hoarding* occurring at rate $r_h = 0.0063\,\mathrm{min}^{-1}$ and *dumping* at rate $r_d = 0.0065\,\mathrm{min}^{-1}$ (Fig. 3.15). It is worth noticing that this description of the phenotypic switch has no adjustable parameter.

Interestingly, the distribution of concentrations at equilibrium predicted by this model can be calculated analytically (as pointed out by T. Mora). The evolution of the probabilities of being in either state is given by

$$\begin{cases} \dfrac{\partial P_h}{\partial t} + r_h c \dfrac{\partial P_h}{\partial c} = -k_{hd} P_h + k_{dh} P_d \\ \dfrac{\partial P_d}{\partial t} - r_d c \dfrac{\partial P_d}{\partial c} = +k_{hd} P_h - k_{dh} P_d \end{cases} \tag{3.3}$$

where P_h and P_d are the probabilities for a cell to be in *hoarding* or *dumping* state respectively.

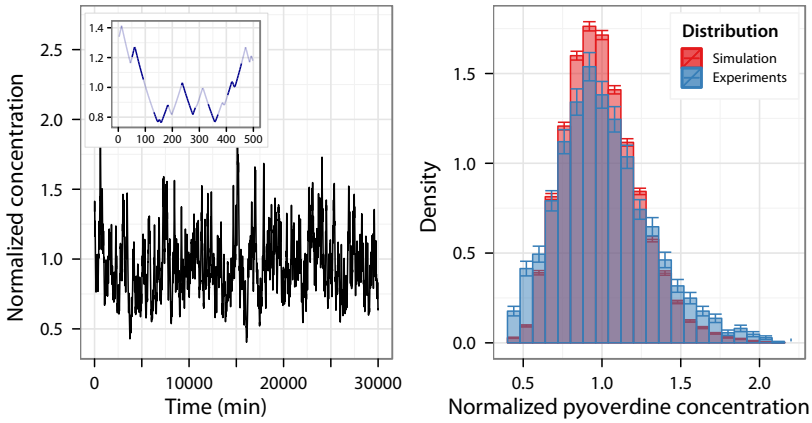

Figure 3.16: Simulations of the phenotypic switch model. All parameters in the simulations are estimated from experimental data (as shown on Fig. 3.15).
Left: Time series of pyoverdine concentration in a simulation. The inset shows the approximative duration of a movie, with cell division indicated with different colours. The number of switches per generation is in agreement with experimental observations (Fig. 3.14 right).
Right: Distribution of pyoverdine concentrations observed in experimental data (pooled over all movies) and in the simulation shown on the left plot.

At steady state, we have $r_h P_h = r_d P_d$ and the probability $P(x) = P_h(x) + P_d(x)$ of observing a bacteria with normalized pyoverdine concentration x satisfies

$$x\frac{\partial P}{\partial x} = \left(\frac{k_{dh}(x)}{r_d} - \frac{k_{hd}(x)}{r_h}\right)P \tag{3.4}$$

Stochastic simulations based on this model are run using parameters estimated in the experiment: using constant time steps, pyoverdine concentration varies exponentially between consecutive steps and the cell state (*hoarding* or *dumping*) can change at each step if a random number (drawn from a uniform distribution between 0 and 1) is higher than the switch probability at this concentration. The simulated concentration fluctuates in a range and with a temporal rate of switching that are similar to experimental data (Fig. 3.16 left). The concentration distribution (Fig. 3.16 right) are also in good agreement with experimental data. Although the spectrum of fluctuations decreases faster in the simulation than in the experiments, it is a qualitatively similar, monotonically decreasing spectrum (Fig. 3.17). Overall, this simplistic model of a stochas-

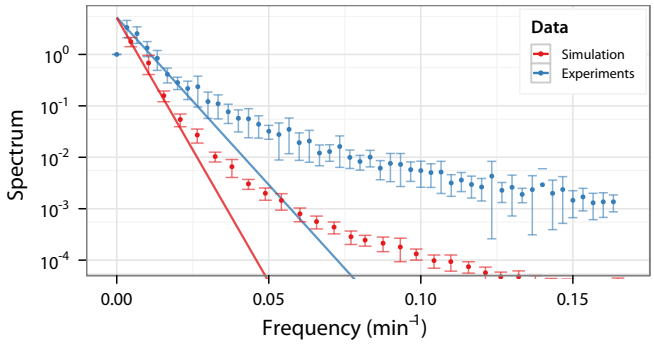

Figure 3.17: Power spectrum of experimental and simulated pyoverdine fluctuations.
Although the spectrum is decreasing faster in the simulation (in red) than in experimental data (in blue; similar to Fig. 3.11 right), they are qualitatively similar, monotonically decreasing spectra. No characteristic frequency of fluctuation is observed.

tic switch provides a satisfying description of the dynamics of the complex pyoverdine metabolic pathway.

An article on this phenotypic switch in *P. aeruginosa* is in preparation. A very preliminary draft in proposed in appendix A.3.

We showed that variability in pyoverdine concentration between clonal individuals of a microcolony is unexpectedly high. There is no sign of exploitation of high level producers by low level producers such as spatial heterogeneity or marked heritability effects. In fact, rapid fluctuations occurring during the lifespan of bacteria have been identified and modeled assuming the existence of a stochastic phenotypic switch between two states in pyoverdine metabolism.

3.2.3 MOLECULAR MECHANISMS UNDERLYING PYOVERDINE VARIABILITY

In this section, I report our effort to identify the molecular mechanism(s) underlying the wide distribution of pyoverdine concentration in clonal microcolonies. Ultimately, we aim at understanding the basis of the phenotypic switch described in the previous section.

3.2.3.1 *Pyoverdine variability in pyoverdine-related mutants*

As emphasized in the previous section, the large coefficient of variation (ca. 30 %) reported in PAO1 was not expected. We hypothesized

that this variability could be linked to one particular component of pyoverdine metabolism (e.g. production, uptake, secretion), in which case the corresponding mutants would be less variable. We tested

- PAO1Δ*pvdF* as a production mutant,
- PAO1Δ*fpvC* as an uptake mutant,
- PAO1Δ*pvdR*, PAO1Δ*pvdT*, PAO1Δ*opmQ* and PAO1Δ*pvdRTopmQ* as secretion mutants,
- PAO1Δ*pvdD*Δ*pvdRTopmQ* as a double production and secretion mutant,
- PAO1Δ*fpvR* as regulation mutant (receptor-coupled antisigma knockout).

None of these mutants showed a marked decrease in the standard deviation of their normalized pyoverdine concentration (i.e. in the coefficient of variation of pyoverdine concentration between cells). Satisfactorily, the value obtained for PAO1 in time-lapse movies (reported in the previous section) and following this slightly different analysis (as explained in section 3.2.1.2) are identical. The variability in pyoverdine concentration of the production, and uptake mutants as well as of the double production and secretion mutant is slightly lower than that of PAO1, around 25 %. On the contrary, all secretion mutants show a moderate increase in this variability, reaching 35 % (Fig. 3.18 top).

In addition, the distribution of pyoverdine in PAO1 is also characterized by its asymmetry, resulting in a positive skewness. All but the secretion (and the double secretion and import) mutants exhibit a significant positive skewness in their pyoverdine distributions. In the secretion mutants, the skewness is more variable between replicates and is not significantly different from 0 anymore (Fig. 3.18 bottom). Finally, the double production and secretion mutant is negatively skewed; the reproducibility of this last observation is still to be confirmed.

The slightly higher variability of export mutants compared to the double production and secretion mutant suggest that they have different pyoverdine metabolism. One notable difference in the protocol is that the double mutant is supplemented with purified pyoverdine while the secretion mutant produces it but cannot export it outside efficiently. Consequently, we expect the extracellular concentration to be much lower in the secretion mutant than in the double mutant. As we cannot easily compare intensity (due to differences between replicates), we study the ratio of extracellular to intracellular concentrations. As expected, it is lower in the secretion mutants than in the double mutant (Fig. 3.19). The double production and secretion mutant can thus increase its intracellular pyoverdine concentration by uptake. Since the extracellular concentration is low in the secretion mutants, it is likely that their increase in pyoverdine concentration is due to production more than to uptake. This sug-

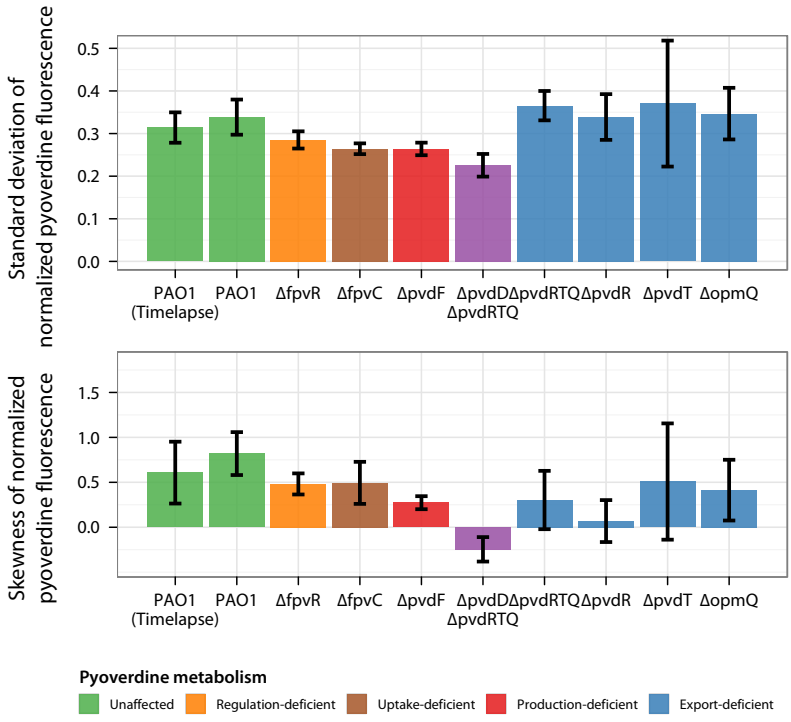

Figure 3.18: Distribution of pyoverdine concentration in various mutants of pyoverdine metabolism.
Points and error bars are mean and sem over more than 10 fields per condition (in 3 independent replicates).

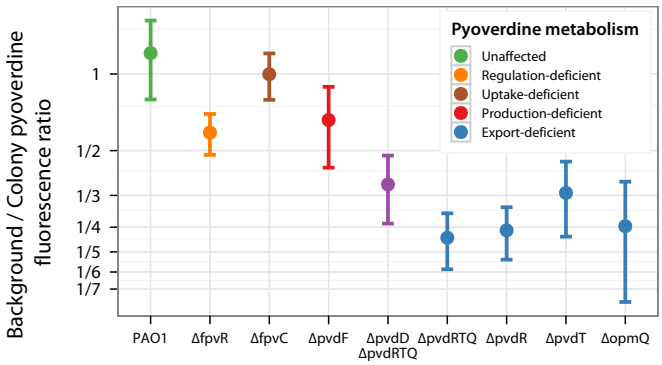

Figure 3.19: Pyoverdine secretion in various mutants of pyoverdine metabolism.
Primary data are the same as in Fig. 3.18. Points and error bars are mean and sem over more than ten fields per condition (in three independent replicates).

gests that the high variability observed in these secretion mutants could be the result of fluctuations in the production of pyoverdine.

3.2.3.2 *Dynamics of pyoverdine variability in import, export and production mutants*

In order to decipher whether the large variability observed in various mutants is also the result of the phenotypic switch characterized in PAO1, analyzing the concentration dynamics is required. This is currently under work.

Unfortunately, it is very difficult to characterize such dynamics by eye, even in a qualitative manner, and the image analysis procedure is very long. The only thing that can easily be distinguished is the occurrence of rapid decreases of intracellular pyoverdine concentration (referred to as *bursts*). Moreover, several strains of *P. aeruginosa* are able to swarm, that is to move slowly between the gel pad and the coverslip which makes cell tracking impossible.

At this time, we have analyzed two movies of uptake mutants, and acquired one movie of the production mutant growing with exogenous pyoverdine. The repeated attempts to monitor the secretion mutant (PAO1Δ*pvdRTQ*) have been unsuccessful due to cell swarming. Rapid fluctuations of pyoverdine concentration (similar to 3.14 left) are observed both in uptake and production mutants. No clear difference of pyoverdine heritability compared to PAO1 can be seen by eye.

3.2.3.3 *Pyoverdine variability and iron availability*

Another parameter that is likely to affect the variability of pyoverdine concentration between cells is iron availability. When iron is rare, pyoverdine becomes a public good and competition for it is expected to increase. In order to characterize pyoverdine variability depending on iron availability, PAO1 is grown with 1.25 µM to 2.5 µM human transferin (an iron chelator with lower affinity for iron than pyoverdine) and 20 mM sodium bicarbonate. These preliminary experiments have been done by A.Decrulle during a Master internship in the lab.

In agreement with the literature, PAO1Δ*pvdF* grows poorly in SMM with 5 µM transferin (20 % of the yield measured in SMM), while PAO1 grows to 90 % of its yield in SMM in these conditions. Normal growth is restored in the mutant by supplementing either 50 µM purified pyoverdine or 100 µM iron chloride (large excess).

In PAO1, the synthesis of pyoverdine increases markedly in presence of transferin as shown by the increase of the extracellular environment fluorescence (Fig. 3.20 left). However, the coefficient of variation of intracellular pyoverdine concentration does not change significantly with the transferin concentration (Fig. 3.20 right). This preliminary result has

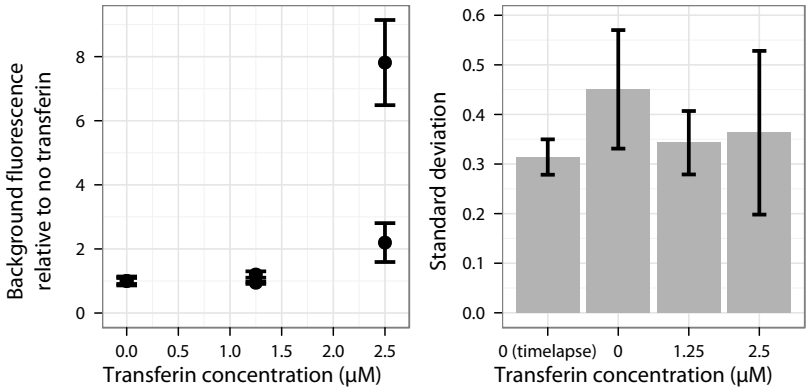

Figure 3.20: Pyoverdine distribution and iron availability.
Left: Relative background fluorescence compared to the condition without transferin (left point). Points and error bars are mean and SEM over the different fields of two independent replicates.
Right: Standard deviation of normalized pyoverdine fluorescence with different transferin concentrations added to the growth medium. Bars height and error bars are mean and SEM of different fiels in two independent replicates.

been observed twice and must be replicated further. In addition, the dynamics of pyoverdine is also being characterized in presence of transferin.

We showed that no mutants of pyoverdine metabolism has a lower variability in pyoverdine concentration between clonal individuals than the wild-type PAO1 strain. In these mutants, fluctuations of pyoverdine concentration are also observed. In addition, the high variability and rapid fluctuations of pyoverdine concentration observed in PAO1 occur in scarce iron conditions as well.

3.3 DISCUSSION

3.3.1 IMPLICATIONS OF A PHENOTYPIC SWITCH IN PYOVERDINE METABOLISM

In this chapter, we have characterized an unexpectedly high variability in pyoverdine concentration between bacteria of a clonal microcolony. Time-lapse microscopy was used to measure concentration fluctuations in cell lineages. Unexpectedly, the variability does not originate from spatial heterogeneity or from heritability effects. Instead rapid fluctuations

occur during the lifespan of bacteria. We have modeled these fluctuations assuming the existence of a stochastic phenotypic switch between two states in pyoverdine metabolism: *P. aeruginosa* bacteria alternate between episodes of pyoverdine accumulation and release (coined as *hoarding* and *dumping* states). Surprisingly, the probability of switching from one state to the next is governed by the cell relative pyoverdine concentration (compared to the colony average) rather than by the absolute concentration.

In this manuscript, the estimation of model parameters is based on a rather naive analysis of the switches in pyoverdine metabolism using quadratic local fitting to approximate concentration fluctuations. In particular, the number of switches identified per generation depends strongly on the smoothing parameter. A more refined analysis of our experimental data dataset based on a hidden Markov model has been done recently by T. Mora. Interestingly, if the rate of pyoverdine concentration variation is assumed to be constant in each state, the outcomes of both analyses are very similar. However, if no parameter is fixed, the likelihood maximization algorithm tends to predict infinite rates of switching and of concentration variation. This could be interpreted as the fact that the fluctuations would be better described using a random walk model rather than a two states stochastic switch model. In our opinion, the rapid and large amplitude changes in pyoverdine concentration indicate that at least a part of the population follows a two states dynamics, while the rest could follow a random walk dynamics. The distinction between these sub-populations could underlie some division of labor regarding pyoverdine metabolism within this bacterial population, a tempting but understudied idea (Shapiro, 1998).

The fact that the regulation of the phenotypic switch in pyoverdine metabolism depends on the relative pyoverdine concentration (rather than on the absolute one) can seem unlikely at first. Nonetheless, such a dependance on relative values of physical quantities is reminiscent of chemotaxis adaptation where the steady-state tumbling frequency in a homogeneous ligand environment is insensitive to the value of ligand concentration (Alon et al., 1999; Barkai and Leibler, 1997). In the case of pyoverdine, we have not identified yet how the average colony concentration is sensed by the cell. A simple hypothesis would be that the extracellular concentration is correlated with the colony average. However, in our experiments, this relationship is not linear at all as shown on Fig. 3.6 (right). Another possible sensing mechanism would be that each cell is able to measure the concentrations of its neighbours; its switching probability would be adjusted accordingly. In this case, cells on the edge of the colony would sense a lower total concentration in the neighbourhood as they have less neighbours. As the dynamics of the two states model is such that in average the cell concentration is equal to the perceived

concentration, this would result in lower concentration relative to the colony average in cells near the edge as seen on Fig. 3.9 (left). It is worth noting that the assumption that the cellular concentration is linked with the extracellular local one cannot account for the edge effect reported in our experiments: the characteristic diffusion length of pyoverdine is expected to be much longer than the scale of the reported variations.

In our experiments, we do not observe any correlation between pyoverdine concentration and cell growth rate, nor spatial clustering of cells with high levels of pyoverdine (expected both from the diffusion of this molecule enhancing its own production and from heritability effects). In fact, iron is not limiting in our experimental conditions and so pyoverdine is not expected to be a public good. Nonetheless, we think that it is reasonable to assume that pyoverdine is likely to have been selected as a public good in recent *P. aeruginosa* evolutionary history. In this cooperation-oriented view, the intracellular concentration of pyoverdine is likely to be a good proxy of the benefits taken from the public goods production in the population. In the next steps of this work, it will be important to confirm the generality of the phenotypic switch model, in particular if it holds at higher pyoverdine concentration and in iron-limited conditions. Preliminary observations in presence of human transferin, another iron chelator competing with pyoverdine, indicate that the cellular concentration of pyoverdine fluctuates as well in these conditions. Whether the switching probabilities still depend on pyoverdine relative concentration remains to be determined.

After having characterized this phenotypic switch, we have focused our efforts toward the identification of the molecular mechanism underlying this phenotypic switch. The two simpler (non-exclusive) hypotheses to explain fluctuations in pyoverdine concentration are either variability of production, or of uptake and secretion. In order to identify which component of pyoverdine metabolism was involved, we have characterized the distribution of pyoverdine concentration in various mutants of the pyoverdine metabolism (affected in production, uptake, secretion and regulation). As the variability observed in PAO1 is unexpectedly high, we were looking for mutants with reduced variability. In fact no mutant shows a significant reduction in its variability of pyoverdine concentration, and preliminary observations suggest that the concentration also fluctuates in time.

This robustness of the fluctuations to genetic perturbations is unexpected. Let us review the precise phenotypic effects of these mutations. In the production mutant Δ*pvdF*, no pyoverdine at all is synthesized; its large distribution indicates that the variability is not primarily due to fluctuations of the production rate. The uptake mutant is Δ*fpvC*. Using radioactive labeling, the uptake of iron has been shown to be com-

pletely abolished in the double production and uptake mutant Δ*pvdF* Δ*fpvC* supplemented with exogenous pyoverdine (Meksem et al., 2011). Despite the redundancy in uptake pathway (at least FpvA and FpvB are able to uptake pyoverdine in PAO1), it is likely that all iron uptake mechanisms are blocked in the Δ*fpvC* mutant. The large distribution of pyoverdine concentration in this mutant indicates that the variability is not primarily due to fluctuations of the uptake rate. Δ*fpvR* is a mutant of the antisigma coupled to pyoverdine receptor FpvA, in which the FpvA-mediated signalling is consequently abolished. This inactivation of this part of pyoverdine metabolism regulation does not change the variability in pyoverdine concentration. Finally, all export mutants abolished only partly the secretion of newly synthesized and recycled pyoverdine as shown by the presence of pyoverdine in the extracellular environment (Fig. 3.19). The alternative channels used in pyoverdine secretion are not characterized yet. Their large distribution indicates that the variability is not primarily due to fluctuations of the secretion rate of the PvdRTQ efflux pump. Overall, these observations support that the variability of pyoverdine concentration in PAO1 is not dominated by one aspect of pyoverdine metabolism and possibly involves a yet uncharacterized efflux pump.

As examining the detail of pyoverdine metabolism is not very informative, can we imagine that the phenotypic switch we have characterized is an indirect effect of another regulation mechanism? Interestingly, oscillations of intracellular iron concentration inferred from *ryhB* promoter activity are observed in *E. coli* after an abrupt change in iron availability (resulting from a step of extracellular iron chelator concentration) (Amir et al., 2010). Hypothesizing that the same oscillatory behaviour of the iron regulation network exists in *P. aeruginosa* and that iron homeostasis generates similar damped oscillations of the intracellular concentration of iron, could this result in fluctuations of pyoverdine concentration similar to those reported in our study?

Another interesting line of explanations is the link between the structure of regulatory networks and bistability: in the sporulation gene network of *Bacillus subtilis*, a positive feedback loop has been shown to lead to a bistable cell fate (Veening et al., 2008). In the case of pyoverdine in *P. aeruginosa*, although the global genetic regulation is seen as a positive feedback, the short period between switches as well as the very limited effect of mutations on pyoverdine distribution suggest that a similar effect could result here from modulations of protein activity rather than of genes expression. One can hypothesize that a regulation of uptake and secretion activities could occur at the protein level. This would involve modification enzymes (e.g. of receptors and pumps) in the same manner that chemotaxis is modulated by receptors methylation.

As far as molecular mechanisms are concerned, the asymmetry in pyoverdine concentration between sister cells is another interesting issue, although not directly linked to the phenotypic switch. In this study, we have shown that this asymmetry is not constant during the cell cycle but rather increases threefold. This can be interpreted in two ways. First pyoverdine can be partitioned in a slightly asymmetric manner at division, and this small initial asymmetry could be amplified by a positive feedback mechanism. Another view is that some components of pyoverdine metabolism are segregated asymmetrically which results in a difference of metabolic activity between the sisters. Such a functional asymmetry is reminiscent of the asymmetry in growth rate reported in *E. coli* (Stewart et al., 2005).

The decrease in normalized pyoverdine concentration with old pole age can be explained as the result of this asymmetry in the rate of accumulation of pyoverdine. However, this does not account for the decrease observed with new pole age. The fact that cells inheriting repeatedly a newly formed pole (and the associated proteins) have a low concentration in pyoverdine compared with the rest of the colony suggests that there is a maturation of some components of pyoverdine metabolism during which their rate of activity increases.

Another line of interpretation regarding the asymmetry of pyoverdine concentration would focus on iron storage. It is likely that iron stocks (e.g. coupled to ferritin) are not very mobile elements in the cell, which could result in accumulation at old poles as reported for protein aggregates (Lindner et al., 2008; Winkler et al., 2010). This would result in difference in intracellular iron concentrations between the old and new pole cells which could in turn affect pyoverdine metabolism.

Finally, none of these observations about stochastic switching or functional asymmetry would have been reported in a classical microbial genetics study at the level of the population. Single-cell analysis gives access to a new level of description; up to now, it has been applied mostly to well-understood systems as lac operon or lambda phage in order to validate theoretical predictions such as bistability models. Our study is an example of how this approach can be use to disentangle the dynamics of a yet uncharacterized system.

Although analysis at the single-cell level is difficult to put in practice, it is likely that it will gain in popularity as it allows to characterize noise in biological systems. The functional role of noise in biological systems has drawn increasing attention recently, in particular in metabolic networks coordination, in cell differentiation and as possible target of natural selection (Eldar and Elowitz, 2010).

3.3.2 ON THE EVOLUTION OF PYOVERDINE

3.3.2.1 *On the evolution of pyoverdine as a public good*

As illustrated in introduction, pyoverdine has been shown to consist in a public good under scarce iron conditions and has thus been used as a model system to test various evolutionary hypotheses related to cooperation. This approach relies on the fact that pyoverdine facilitates iron uptake by *P. aeruginosa*. Although this observation is usually justified by invoking pyoverdine high affinity for iron, there is not a single simple scenario of how this chemical property confers its biological function to pyoverdine.

From a diffusion viewpoint, secreting pyoverdine does not help *P. aeruginosa* to uptake iron out of a larger volume as pyoverdine diffusion coefficient is lower than that of iron. In fact, it is even likely to lower iron diffusion once bound to it. Consequently, from an ecological viewpoint, pyoverdine synthesis can be seen as a mean of securing iron resources by preventing its use by other organisms unable to handle pyoverdine. This reduces the interspecific competition to the strains that are able to express the cognate pyoverdine receptor. From a chemical viewpoint, the role of pyoverdine is actually more straightforward: its very high affinity for iron displaces equilibria of other reactions such as iron precipitation or iron binding to other biological ligands (as hemoglobin, transferrin, other microbial and fungal siderophores, etc). Doing so, it binds to more iron than only the soluble ions. Interestingly, these two effects (equilibrium displacement and reduced interspecific competition) are likely to occur simultaneously.

From a public good viewpoint, the very large amount of secreted pyoverdine (up to ca. 200 mM in SMM) is unexpected as it suggests that the cost of pyoverdine production is low. In addition, the dynamics of secretion is surprising: fluorescence first increases in the cells and suddenly increases in the extracellular environment as well (Fig. 3.6 right). As stated in introduction, iron binding quenches pyoverdine fluorescence. This delayed dynamics could be explained by the fact that pyoverdine would be secreted at a constant rate, would first bind to iron and then accumulate once all available iron is chelated. However, this hypothesis is discarded by the fact that the same dynamics is observed with transferin in the growth medium; this iron chelator competes with transferin for iron binding and a pool of apo pyoverdine is thus likely to remain longer.

Considering the physico-chemical properties of pyoverdine is not enough to study it as public good. In this study, we have shown that intracellular concentration of fluorescent pyoverdine is a continuous trait. Assuming that the concentration of ferric pyoverdine (beneficial but non-

fluorescent) is related to the concentration of apo pyoverdine (fluorescent but neutral), this trait is a good proxy of the benefit the individuals gain from public good production in the population. Although we have not studied it yet, we suppose that investment in pyoverdine production is a continuous trait as well. This contrasts with previous studies of *P. aeruginosa* siderophores where producers are compared to non-producers assuming that all producers are identical. The variability of pyoverdine concentration between producers has a different meaning at the level of individuals (those at low levels of production are exploiting the production of the others) and at the level of the population (where it can be seen as a division of labour strategy that can be beneficial). Anyhow this variability between producers is likely to shape the evolution of pyoverdine regulation system.

However, in natural populations, the emergence of non-producers is reported to be frequent (Vos et al., 2001). In this case, the exploitation of some producers by others is likely to be negligible. Provided that the variability of investment between producers does not vanish when pyoverdine is exploited by non-producers, this variability could increase the overall population robustness against cheating by non-producers since individuals producing less would pay a lower cost.

In the rest of this section, I open the discussion and try to bridge the gap between the molecular knowledge on pyoverdine and its evolution, in particular as a public good. Interestingly, genes involved in pyoverdine metabolism constitute the most divergent region of *P. aeruginosa* core genome. Sequences homologies indicate very frequent horizontal gene transfers of central pyoverdine genes between strains of different siderotypes and of different species. Finer variations due to point mutations are identified as the result of selection mostly in two loci, *fpvA* and *fpvC* (Smith et al., 2005; Tümmler and Cornelis, 2005). It is worth to notice that these two genes code for proteins that are directly involved in pyoverdine-mediated iron uptake, the receptor for pyoverdine and a putative reductase involved in iron dissociation respectively. It is likely that these two genes are under selection due to the fact that any favorable modification of the corresponding proteins will confer a growth advantage.

Overall, the public good nature of pyoverdine makes it likely to be the target of different selective pressures: the requirement to maintain differences with others in order not to be exploited favors diversifying selection (ultimately leading to speciation), while the temptation to keep using different types of pyoverdine produced by others favors coevolution (through directional and/or stabilizing selection). Coevolution is also likely to occur with hosts that can develop strategies of bacterial siderophores inactivation (Fischbach et al., 2006).

These antagonistic selective forces driving adaptation can explain the high variability (by horizontal gene transfer and by mutation) at pyoverdine-related loci, all the more so as both horizontal gene transfers and exploitation of xenosiderophores occur not only between strains of a given species but also between different species.

3.3.2.2 *On the evolution of pyoverdine metabolism*

In this last section, I discuss the various biological roles of pyoverdine that have been reported so far, in order to identify the different facets that affect its evolution.

Antagonistic selective pressures acting on pyoverdine-related loci have been exposed in the previous section. As explained, *fpvA* is one of the two genes showing clear indications of natural selection (high dN/dS ratio). In addition to being a receptor of pyoverdine, FpvA is also the channel of entry of pyocin S3, a toxin produced by *P. aeruginosa* itself that is lethal for cells who do not produce the corresponding immunity protein (Tümmler and Cornelis, 2005). More precisely, this other role of FpvA is reported in type II strains, but not in type I and III. Here as well, two opposite traits are selected on the same target: the ability to uptake pyoverdine and the efficient blocking of pyocin entry. This example illustrates how physiological constraints can modulate the evolution of pyoverdine metabolism.

It is noteworthy that pyoverdine can be produced in conditions where it is not required for growth (as in our study using SMM). In this sense, it can be seen as a *conditional* public good. More generally, this observation and the physiological constraints mentioned above question whether pyoverdine has been primarily selected as a public good and/or as a siderophore.

Several lines of evidence help to address this issue:

- In our experiments, neither spatial structure nor heritability constitute a major source of variability in the microcolony. Since this would be expected for molecules that have been selected as public goods, our study suggests that the cooperative aspects of pyoverdine metabolism may not be preponderant in *P. aeruginosa* natural life history.
- An important lifestyle of *P. aeruginosa* is as pathogen where pyoverdine notably enhances its virulence (Lamont et al., 2009; Meyer et al., 1996; Takase et al., 2000). Consequently, pyoverdine is likely to have been selected for increased virulence. This selective pressure is likely intertwined with selection as a siderophore (and probably as a public good) as free iron concentration is very low in hosts.
- Pseudomonads are also found in soil. In fact the concentration of microbial and fungal siderophores is very high in soil and they are

used by plants as well (that express receptors although they do not produce siderophores) to uptake iron. It has been proposed that the very high affinity for iron of pyoverdines may limit iron availability for other species among which plants pathogens (Visca et al., 2007a). The positive effect on plant growth could in turn be beneficial for pseudomonads.

- Recent advances regarding pyoverdine metal specificity in *P. aeruginosa* indicate that it binds not only to iron but to a very wide variety of metallic ions. Only pyoverdine bound to Fe^{3+}, Cu^{2+}, Ga^{3+}, Mn^{2+} and Ni^{2+} is imported by FpvA, and ultimately only iron is uptaked by the cell using the pyoverdine-dependent pathway (Braud et al., 2009b). The fact that pyoverdine binds to several metals and that its synthesis is enhanced by metals for which it is not mediating uptake (as Al^{3+}, Cu^{2+}, Ga^{3+}, Mn^{2+}, Ni^{2+} and Zn^{2+}) suggest that pyoverdine can also represent a protection against toxic metals by chelating them and thus reducing the effective concentration experienced by the cell.
- Pyoverdine metabolism regulation is also affected by quorum sensing, a communication mechanism mediated by diffusible molecules that has been shown to be another social trait in *P. aeruginosa* (Rumbaugh et al., 2009). Although no clear role of pyoverdine has been identified in quorum sensing, quorum sensing regulation mutant (Δ*lasR* and Δ*lasI*) produce at least twice less pyoverdine than a wild type strain (Stintzi et al., 1998). Interestingly pyoverdine and quorum sensing metabolisms could be tightly coupled as suggested by the occurrence of enzymes involved in both of them. For instance, PvdQ is supposably involved in pyoverdine maturation while it is also degrading quorum sensing diffusible molecules (AHLs) (Bokhove et al., 2010).

Hence, even though pyoverdine has not only been selected as a public goods system, it certainly makes sense to address cooperation-related questions using this model, as proved by the fruitful work in this field. Nonetheless, it is crucial to better characterize the interplay between the different evolutionary forces acting on pyoverdine in order to better understand its role as a public good.

BIBLIOGRAPHY

A. Albrecht-Gary, S. Blanc, N. Rochel, A. Z. Ocaktan, and M. A. Abdallah. 1994. Bacterial iron transport: coordination properties of pyoverdin PaA, a peptidic siderophore of Pseudomonas aeruginosa. *Inorganic Chemistry*, 33(26):6391–6402.

U. Alon, M. G. Surette, N. Barkai, and S. Leibler. 1999. Robustness in bacterial chemotaxis. *Nature*, 397(6715):168–171.

A. Amir, S. Meshner, T. Beatus, and J. Stavans. 2010. Damped oscillations in the adaptive response of the iron homeostasis network of E. coli. *Molecular Microbiology*, 76(2):428–436.

R. Axelrod and W. D. Hamilton. 1981. The evolution of cooperation. *Science*, 211(4489):1390–1396.

N. Barkai and S. Leibler. 1997. Robustness in simple biochemical networks. *Nature*, 387(6636):913–917.

P. A. Beare, R. J. For, L. W. Martin, and I. L. Lamont. 2003. Siderophore-mediated cell signalling in Pseudomonas aeruginosa: divergent pathways regulate virulence factor production and siderophore receptor synthesis. *Molecular Microbiology*, 47(1):195–207.

J. Bodilis, B. Ghysels, J. Osayande, S. Matthijs, J. Pirnay, S. Denayer, D. D. Vos, and P. Cornelis. 2009. Distribution and evolution of ferripyoverdine receptors in Pseudomonas aeruginosa. *Environmental Microbiology*, 11(8):2123–2135.

M. Bokhove, P. N. Jimenez, W. J. Quax, and B. W. Dijkstra. 2010. The quorum-quenching N-acyl homoserine lactone acylase PvdQ is an Ntn-hydrolase with an unusual substrate-binding pocket. *Proceedings of the National Academy of Sciences of the United States of America*, 107(2):686–691.

A. Braud, M. Hannauer, G. L. A. Mislin, and I. J. Schalk. 2009. The Pseudomonas aeruginosa pyochelin-iron uptake pathway and its metal specificity. *Journal of Bacteriology*, 191(11):3517–3525.

A. Braud, F. Hoegy, K. Jezequel, T. Lebeau, and I. J. Schalk. 2009. New insights into the metal specificity of the Pseudomonas aeruginosa pyoverdine-iron uptake pathway. *Environmental Microbiology*, 11(5):1079–1091.

S. P. Brown and F. Taddei. 2007. The durability of public goods changes the dynamics and nature of social dilemmas. *PLoS ONE*, 2(7):e593.

A. Buckling, F. Harrison, M. Vos, M. A. Brockhurst, A. Gardner, S. A. West, and A. Griffin. 2007. Siderophore-mediated cooperation and virulence in Pseudomonas aeruginosa. *FEMS microbiology ecology*, 62(2):135–41.

L. Chao. 2010. A model for damage load and its implications for the evolution of bacterial aging. *PLoS Genetics*, 6(8).

L. Chao and B. R. Levin. 1981. Structured habitats and the evolution of anticompetitor toxins in bacteria. *Proceedings of the National Academy of Sciences of the United States of America*, 78(10):6324–6328.

J. S. Chuang, O. Rivoire, and S. Leibler. 2009. Simpson's paradox in a synthetic microbial system. *Science*, 323(5911):272–5.

P. Cornelis. 2010. Iron uptake and metabolism in pseudomonads. *Applied Microbiology and Biotechnology*, 86(6):1637–1645.

P. Cornelis, S. Matthijs, and L. V. Oeffelen. 2009. Iron uptake regulation in Pseudomonas aeruginosa. *Biometals*, 22(1):15–22.

C. D. Cox and R. Graham. 1979. Isolation of an iron-binding compound from Pseudomonas aeruginosa. *Journal of Bacteriology*, 137(1):357–364.

M. Doebeli and C. Hauert. 2005. Models of cooperation based on the Prisoner's Dilemma and the Snowdrift game. *Ecology Letters*, 8(7):748–766.

A. Edelstein, N. Amodaj, K. Hoover, R. Vale, and N. Stuurman. 2010. Computer control of microscopes using μManager. *Current Protocols in Molecular Biology*, Unit 14.20:1–17.

A. Eldar and M. B. Elowitz. 2010. Functional roles for noise in genetic circuits. *Nature*, 467(7312):167–173.

L. Escolar, J. Pérez-Martín, and V. de Lorenzo. 1999. Opening the iron box: transcriptional metalloregulation by the Fur protein. *Journal of Bacteriology*, 181(20):6223–6229.

M. A. Fischbach, H. Lin, D. R. Liu, and C. T. Walsh. 2006. How pathogenic bacteria evade mammalian sabotage in the battle for iron. *Nature Chemical Biology*, 2(3):132–138.

B. Ghysels, B. T. M. Dieu, S. A. Beatson, J. Pirnay, U. A. Ochsner, M. L. Vasil, and P. Cornelis. 2004. FpvB, an alternative type I ferripyoverdine receptor of Pseudomonas aeruginosa. *Microbiology*, 150(Pt 6):1671–1680.

J. Gore, H. Youk, and A. van Oudenaarden. 2009. Snowdrift game dynamics and facultative cheating in yeast. *Nature*.

J. Greenwald, F. Hoegy, M. Nader, L. Journet, G. L. A. Mislin, P. L. Graumann, and I. J. Schalk. 2007. Real time fluorescent resonance energy transfer visualization of ferric pyoverdine uptake in Pseudomonas aeruginosa. A role for ferrous iron. *The Journal of Biological Chemistry*, 282(5):2987–2995.

A. S. Griffin, S. A. West, and A. Buckling. 2004. Cooperation and competition in pathogenic bacteria. *Nature*, 430(7003):1024–7.

W. D. Hamilton. 1964. The genetical evolution of social behaviour. I. *Journal of Theoretical Biology*, 7(1):1–16.

W. D. Hamilton. 1964. The genetical evolution of social behaviour. II. *Journal of Theoretical Biology*, 7(1):17–52.

M. Hannauer, Y. Barda, G. L. A. Mislin, A. Shanzer, and I. J. Schalk. 2010. The ferrichrome uptake pathway in Pseudomonas aeruginosa involves an iron release mechanism with acylation of the siderophore and recycling of the modified desferrichrome. *Journal of Bacteriology*, 192(5):1212–1220.

M. Hannauer, E. Yeterian, L. W. Martin, I. L. Lamont, and I. J. Schalk. 2010. An efflux pump is involved in secretion of newly synthesized siderophore by Pseudomonas aeruginosa. *FEBS Letters*, 584(23):4751–4755.

F. Harrison and A. Buckling. 2005. Hypermutability impedes cooperation in pathogenic bacteria. *Current Biology*, 15(21):1968–1971.

F. Harrison, L. E. Browning, M. Vos, and A. Buckling. 2006. Cooperation and virulence in acute Pseudomonas aeruginosa infections. *BMC Biology*, 4:21.

C. Hauert and M. Doebeli. 2004. Spatial structure often inhibits the evolution of cooperation in the snowdrift game. *Nature*, 428(6983):643–646.

J. Hofbauer and K. Sigmund. 1998. *Evolutionary Games and Population Dynamics*. Cambridge University Press.

F. Imperi, F. Tiburzi, and P. Visca. 2009. Molecular basis of pyoverdine siderophore recycling in Pseudomonas aeruginosa. *Proceedings of the National Academy of Sciences of the United States of America*, 106(48):20440–20445.

N. Jiricny, S. P. Diggle, S. A. West, B. A. Evans, G. Ballantyne, A. Ross-Gillespie, and A. S. Griffin. 2010. Fitness correlates with the extent of cheating in a bacterium. *Journal of Evolutionary Biology*.

B. Kerr, M. A. Riley, M. W. Feldman, and B. J. M. Bohannan. 2002. Local dispersal promotes biodiversity in a real-life game of rock-paper-scissors. *Nature*, 418(6894):171–4.

R. Kümmerli and S. P. Brown. 2010. Molecular and regulatory properties of a public good shape the evolution of cooperation. *Proceedings of the National Academy of Sciences of the United States of America*, 107(44):18921–18926.

R. Kümmerli, A. S. Griffin, S. A. West, A. Buckling, and F. Harrison. 2009. Viscous medium promotes cooperation in the pathogenic bacterium Pseudomonas aeruginosa. *Proceedings. Biological Sciences / The Royal Society*, 276(1672):3531–3538.

R. Kümmerli, P. van den Berg, A. S. Griffin, S. A. West, and A. Gardner. 2010. Repression of competition favours cooperation: experimental evidence from bacteria. *Journal of Evolutionary Biology*, 23(4):699–706.

I. L. Lamont and L. W. Martin. 2003. Identification and characterization of novel pyoverdine synthesis genes in Pseudomonas aeruginosa. *Microbiology*, 149(Pt 4):833–842.

I. L. Lamont, P. A. Beare, U. Ochsner, A. I. Vasil, and M. L. Vasil. 2002. Siderophore-mediated signaling regulates virulence factor production in Pseudomonasaeruginosa. *Proceedings of the National Academy of Sciences of the United States of America*, 99(10):7072–7077.

I. L. Lamont, A. F. Konings, and D. W. Reid. 2009. Iron acquisition by Pseudomonas aeruginosa in the lungs of patients with cystic fibrosis. *Biometals*, 22(1):53–60.

A. B. Lindner, R. Madden, A. Demarez, E. J. Stewart, and F. Taddei. 2008. Asymmetric segregation of protein aggregates is associated with cellular aging and rejuvenation. *Proceedings of the National Academy of Sciences*, 105(8):3076–81.

C. Loader. 1997. Locfit: an introduction. *Statistical Computing & Statistical Graphics Newsletter*, 8(1):11–17.

C. Loader and A. Liaw. Locfit, 2010. http://cran.r-project.org/web/packages/locfit/.

J. C. W. Locke and M. B. Elowitz. 2009. Using movies to analyse gene circuit dynamics in single cells. *Nature Reviews. Microbiology*, 7(5):383–392.

B. J. McMorran, M. E. Merriman, I. T. Rombel, and I. L. Lamont. 1996. Characterisation of the pvdE gene which is required for pyoverdine synthesis in Pseudomonas aeruginosa. *Gene*, 176(1-2):55–59.

W. R. Mebane and J. S. Sekhon. rgenoud: R version of GENetic Optimization Using Derivatives. http://cran.r-project.org/web/packages/rgenoud/.

A. Meksem, L. Journet, F. Hoegy, C. Reimmann, and I. J. Schalk. 2011. A role for FpvCDEF in iron release from siderophore pyoverdine in Pseudomonas aeruginosa. *In Prep.*

J. M. Meyer and M. A. Abdallah. 1978. The fluorescent pigment of Pseudomonas fluorescens: biosynthesis, purification and physicochemical properties. *Journal of General Microbiology*, 107(2):319–328.

J. M. Meyer and J. M. Hornsperger. 1978. Role of pyoverdine_Pf, the iron-binding fluorescent pigment of Pseudomonas fluorescens, in iron transport. *Journal of General Microbiology*, 107(2):329–331.

J. M. Meyer, A. Neely, A. Stintzi, C. Georges, and I. A. Holder. 1996. Pyoverdin is essential for virulence of Pseudomonas aeruginosa. *Infection and Immunity*, 64(2):518–523.

C. D. Nadell, K. R. Foster, and J. B. Xavier. 2010. Emergence of spatial structure in cell groups and the evolution of cooperation. *PLoS Computational Biology*, 6(3):e1000716.

M. Nader, L. Journet, A. Meksem, L. Guillon, and I. J. Schalk. 2011. Mechanism of ferripyoverdine uptake by Pseudomonas aeruginosa outer membrane transporter FpvA: No diffusion channel formed at any time during ferrisiderophore uptake. *Biochemistry*, 50(13):2530–2540.

M. A. Nowak. 2006. Five rules for the evolution of cooperation. *Science*, 314(5805):1560–1563.

M. A. Nowak and R. M. May. 1992. Evolutionary games and spatial chaos. *Nature*, 359 (6398):826–829.

M. A. Nowak, S. Bonhoeffer, and R. M. May. 1994. Spatial games and the maintenance of cooperation. *Proceedings of the National Academy of Sciences of the United States of America*, 91(11):4877–4881.

U. A. Ochsner, P. J. Wilderman, A. I. Vasil, and M. L. Vasil. 2002. GeneChip expression analysis of the iron starvation response in Pseudomonas aeruginosa: identification of novel pyoverdine biosynthesis genes. *Molecular Microbiology*, 45(5):1277–1287.

S. Okasha. 2006. *Evolution and the levels of selection*. Clarendon Press, first edition.

K. Poole and G. A. McKay. 2003. Iron acquisition and its control in Pseudomonas aeruginosa: many roads lead to Rome. *Frontiers in Bioscience*, 8:d661–686.

W. C. Ratcliff and R. F. Denison. 2011. Alternative actions for antibiotics. *Science*, 332 (6029):547–548.

J. Ravel and P. Cornelis. 2003. Genomics of pyoverdine-mediated iron uptake in pseudomonads. *Trends in Microbiology*, 11(5):195–200.

N. Rosenfeld, J. W. Young, U. Alon, P. S. Swain, and M. B. Elowitz. 2005. Gene regulation at the single-cell level. *Science*, 307(5717):1962–5.

A. Ross-Gillespie, A. Gardner, S. A. West, and A. S. Griffin. 2007. Frequency dependence and cooperation: theory and a test with bacteria. *The American Naturalist*, 170(3): 331–342.

K. P. Rumbaugh, S. P. Diggle, C. M. Watters, A. Ross-Gillespie, A. S. Griffin, and S. A. West. 2009. Quorum sensing and the social evolution of bacterial virulence. *Current Biology: CB*, 19(4):341–5.

I. J. Schalk, C. Hennard, C. Dugave, K. Poole, M. A. Abdallah, and F. Pattus. 2001. Iron-free pyoverdin binds to its outer membrane receptor FpvA in Pseudomonas aeruginosa: a new mechanism for membrane iron transport. *Molecular Microbiology*, 39(2):351–360.

I. J. Schalk, W. W. Yue, and S. K. Buchanan. 2004. Recognition of iron-free siderophores by TonB-dependent iron transporters. *Molecular Microbiology*, 54(1):14–22.

J. A. Shapiro. 1998. Thinking about bacterial populations as multicellular organisms. *Annual Review of Microbiology*, 52:81–104.

M. Shirley and I. L. Lamont. 2009. Role of TonB1 in pyoverdine-mediated signaling in Pseudomonas aeruginosa. *Journal of Bacteriology*, 191(18):5634–5640.

E. E. Smith, E. H. Sims, D. H. Spencer, R. Kaul, and M. V. Olson. 2005. Evidence for diversifying selection at the pyoverdine locus of Pseudomonas aeruginosa. *Journal of Bacteriology*, 187(6):2138–2147.

T. G. Spiro. 1977. Chemistry and biochemistry of iron. In E. B. Brown, P. Aisen, G. Fielding, and R. R. Crichton, editors, *Proteins of iron metabolism*, pages 23–32. Grune & Stratton, first edition. edition.

E. J. Stewart, R. Madden, G. Paul, and F. Taddei. 2005. Aging and death in an organism that reproduces by morphologically symmetric division. *PLoS biology*, 3(2):e45.

A. Stintzi, K. Evans, J. M. Meyer, and K. Poole. 1998. Quorum-sensing and siderophore biosynthesis in Pseudomonas aeruginosa: lasR/lasI mutants exhibit reduced pyoverdine biosynthesis. *FEMS Microbiology Letters*, 166(2):341–345.

H. Takase, H. Nitanai, K. Hoshino, and T. Otani. 2000. Impact of siderophore production on Pseudomonas aeruginosa infections in immunosuppressed mice. *Infection and Immunity*, 68(4):1834–1839.

F. Tiburzi, F. Imperi, and P. Visca. 2008. Intracellular levels and activity of PvdS, the major iron starvation sigma factor of Pseudomonas aeruginosa. *Molecular Microbiology*, 67(1):213–227.

B. Tümmler and P. Cornelis. 2005. Pyoverdine receptor: a case of positive Darwinian selection in Pseudomonas aeruginosa. *Journal of Bacteriology*, 187(10):3289–3292.

J. Veening, W. K. Smits, and O. P. Kuipers. 2008. Bistability, epigenetics, and bet-hedging in bacteria. *Annual Review of Microbiology*, 62:193–210.

N. Vinayavekhin and A. Saghatelian. 2009. Regulation of alkyl-dihydrothiazolecarboxylates (ATCs) by iron and the pyochelin gene cluster in Pseudomonas aeruginosa. *ACS Chemical Biology*, 4(8):617–623.

P. Visca, F. Imperi, and I. L. Lamont. 2007. Pyoverdine synthesis and its regulation in fluorescent pseudomonads. In A. Varma and S. Chincholkar, editors, *Microbial Siderophores*, pages 135–163. Springer, 1st edition.

P. Visca, F. Imperi, and I. L. Lamont. 2007. Pyoverdine siderophores: from biogenesis to biosignificance. *Trends in Microbiology*, 15(1):22–30.

D. D. Vos, M. D. Chial, C. Cochez, S. Jansen, B. Tümmler, J. M. Meyer, and P. Cornelis. 2001. Study of pyoverdine type and production by Pseudomonas aeruginosa isolated from cystic fibrosis patients: prevalence of type II pyoverdine isolates and accumulation of pyoverdine-negative mutations. *Archives of Microbiology*, 175(5):384–388.

S. A. West, A. S. Griffin, and A. Gardner. 2007. Evolutionary explanations for cooperation. *Current biology*, 17(16):R661–72.

J. Winkler, A. Seybert, L. König, S. Pruggnaller, U. Haselmann, V. Sourjik, M. Weiss, A. S. Frangakis, A. Mogk, and B. Bukau. 2010. Quantitative and spatio-temporal features of protein aggregation in Escherichia coli and consequences on protein quality control and cellular ageing. *The EMBO Journal*, 29(5):910–923.

J. B. Xavier, W. Kim, and K. R. Foster. 2011. A molecular mechanism that stabilizes cooperative secretions in Pseudomonas aeruginosa. *Molecular Microbiology*, 79(1):166–179.

E. Yeterian, L. Martin, L. Guillon, L. Journet, I. Lamont, and I. Schalk. 2010. Synthesis of the siderophore pyoverdine in Pseudomonas aeruginosa involves a periplasmic maturation. *Amino Acids*, 38(5):1447–59.

E. Yeterian, L. W. Martin, I. L. Lamont, and I. J. Schalk. 2010. An efflux pump is required for siderophore recycling by Pseudomonas aeruginosa. *Environmental Microbiology Reports*, 2(3):412–418.

APPENDICES

A.1 TECHNICAL NOTICE ON THE EVOLUTIONARY CHEMOSTAT

The project described in the first chapter is based on a chemostat specially adapted for an evolution experiment with a temperature gradient. In particular, it allows to periodically wash out biofilms from the device walls. A rapid overview of the setup is given in chapter 1 (section 1.2.2). In this appendix, I first describe the hardware features of this setup. Then, I explain the main lines of the microcontroller program used to control the hardware. The last section is a short operating guide of the device from the experimenter viewpoint.

A.1.1 HARDWARE

A.1.1.1 *Flow control*

The setup consists in two culture chambers connected to two input tanks (buffered growth medium and soda) and to a waste tank. In order to wash out biofilm from the walls, the tubing (including electrovalves) is designed so that the culture can be transfered from one chamber to the other in a sterile manner and so that all parts can be washed with soda and rinsed with air and buffer (Fig. A.1). From a functional viewpoint, we define *states*, which are a set of valves opening states, and *cycles*, which are sequences of states of predefined durations. Finally, liquids are pressurized with filtered air at 1.5 atm in the tanks in order to be moved passively in the circuits.

Tanks are large polypropylene bottles suitable for high pressure use (from Nalgene; 10 L for nutrients, 2 L for soda), with custom modifications of their caps allowing to fit tubes (Fig. A.2).

A dedicated uptake cell has been designed, based on 50 mL Falcon tube. The custom Teflon cap allow to fit Teflon tubes, and to open or close it by rotating the upper part Fig. A.3.

All tubing is in Teflon to be resistant to soda. It is 1/8" in outer diameter and 1/16" in inner diameter (from NResearch). Two-ways electrovalves in Teflon and associated Teflon fittings are from NResearch as well. Valves are solenoids and comes in two types, normally closed or normally open (default state without current, references 225T011 and 225T012 respectively).

The electrovalves are switched from one state to the other by imposing a 12 V tension. After 100 ms, the state has changed and the tension is decreased to 5 V in order to prevent valves heating. This reduces the overall power consumption and prolonges valves life. Each valve is connected to

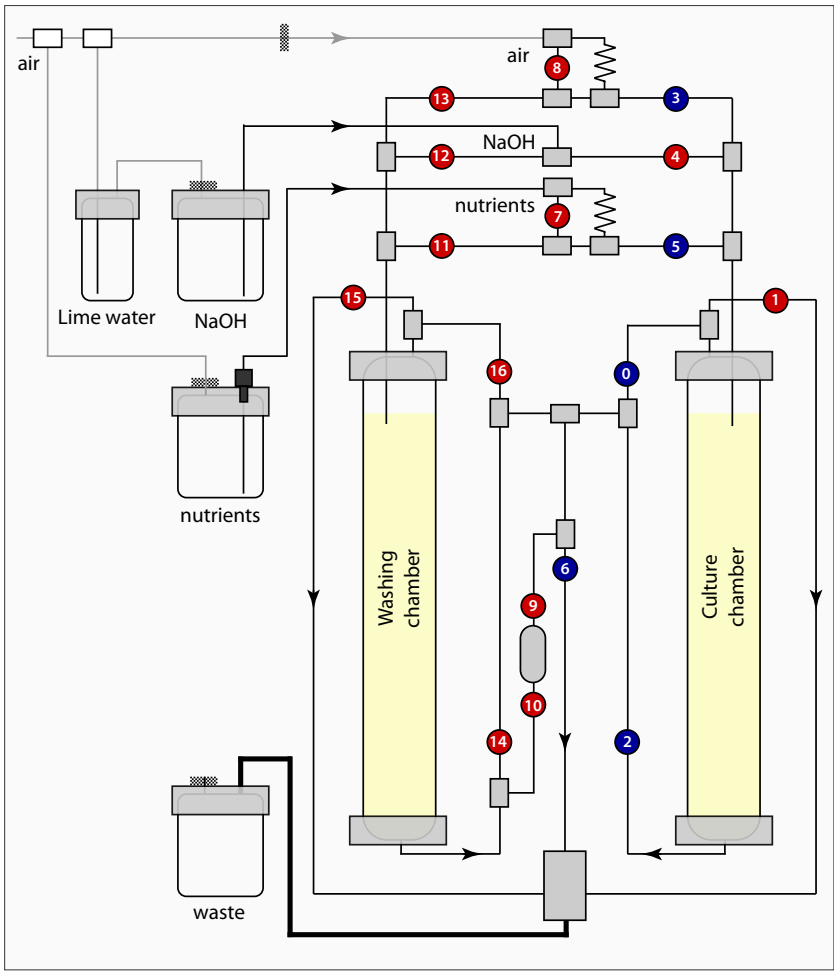

Figure A.1: Technical scheme of the chemostat tubing. Growth chamber are drawn in yellow, valves in red (normally closed) or blue (normally open), and fittings in gray. While biofilms are washed in a chamber using caustic soda, the evolving population is sequestered in the other one.

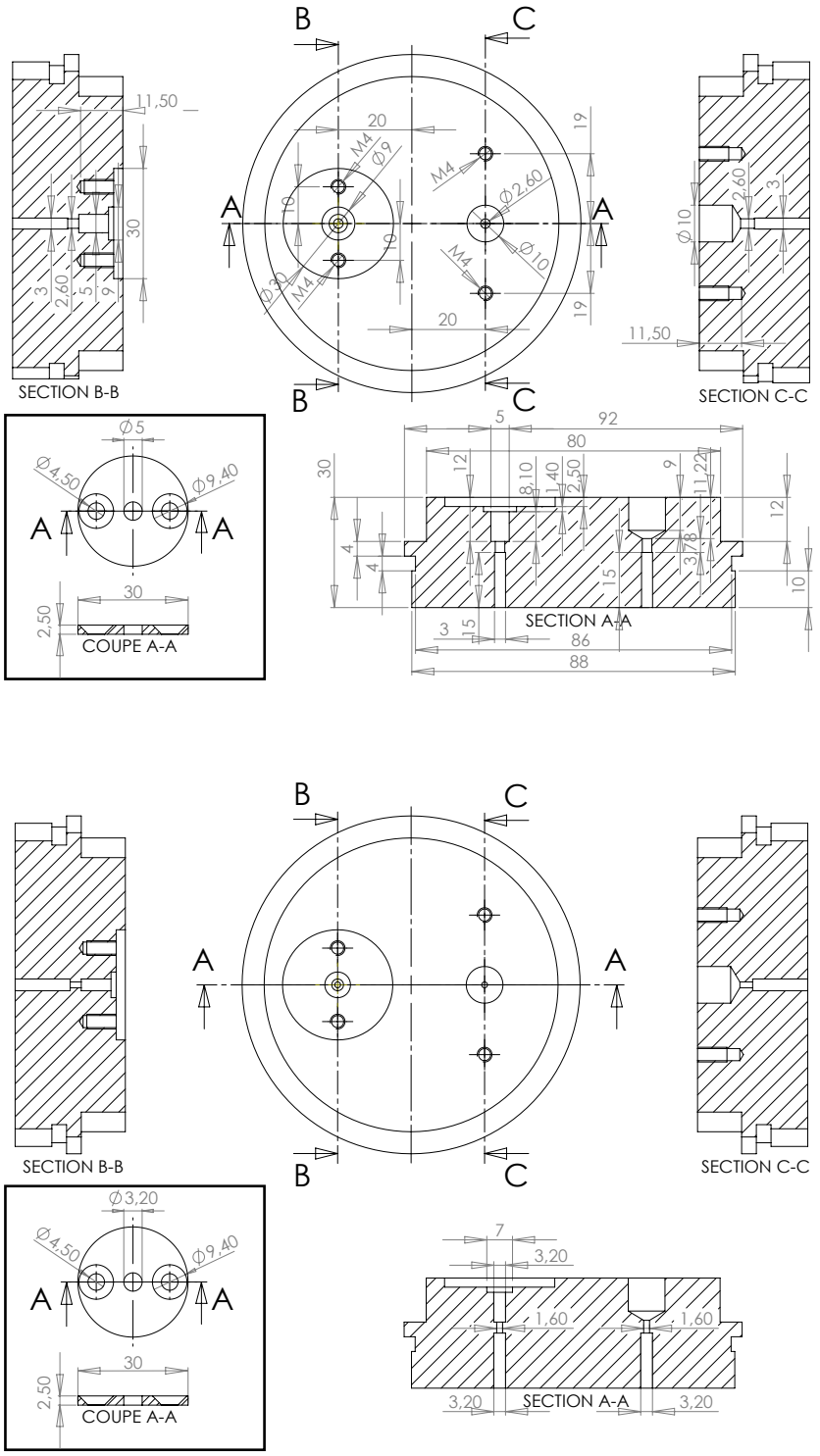

Figure A.2: Technical drawing of the Teflon caps for the nutrient tank (top) and the soda tank (bottom). Scale is 1/2.
Insets show an additional stainless steel part used to fit the output tube on the cap (section B-B). The holes on section C-C are used to hold a 0.22 µm filter through which pressured air is connected. An outer Viton O-ring is used to ensure the pressure tightness of this part, which is maintained using the hollowed out original cap.

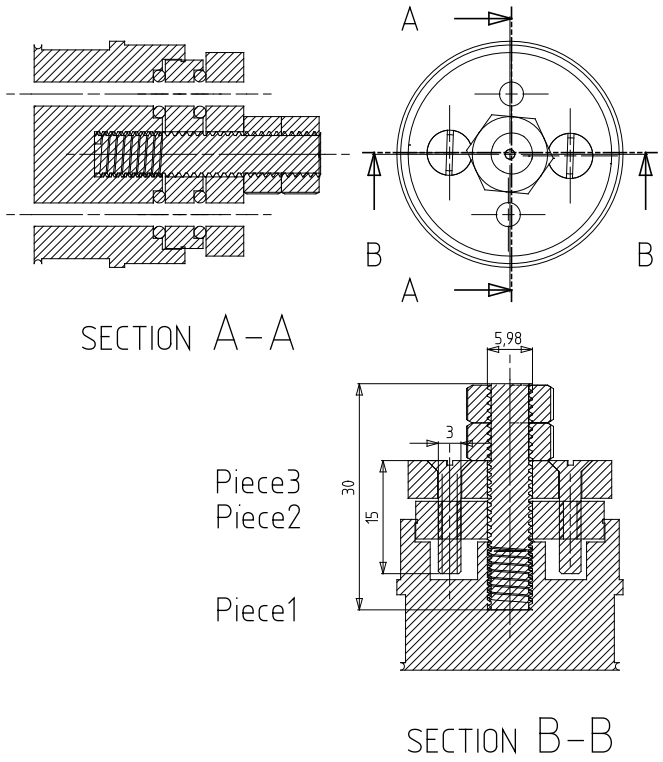

Figure A.3: Technical drawing of the cap for the uptake cell. Scale is 1. All parts are in Teflon but the threaded axe in stainless steel. Outer and inner O-rings ensure the pressure tightness of the tubes connection as well as of the cap. Rotation of pieces 2 and 3 relative to piece 1 allows to close the open holes shown on section A-A.

a microcontroller digital pin, through an inverter and a darlington pair used to amplify the logic current to 12 V. Output modulation at 1 kHz (filtered by a condenser) allows to supply 5 V after 100 ms (Listing 3).

All valves have a third wire used as a position sensor. This acts as a switch with the ground that is closed only when the valve is actually closed. A comparison between the sensor state and the program expectation allows to correct (rare) problems where the solenoid does not move when current is switched on. This feature is not yet implemented in the microcontroller code.

A.1.1.2 *Temperature control*

One of the two growth chambers features a temperature gradient. It is achieved by regulating the temperature at the two ends.

The temperature is controlled thanks to a custom proportional-integral-derivative (PID) regulation based on thermistors located close to power resistors or TECs. Temperature is measured from the thermistors by the microcontroller ADCs using a voltage divider and a fifth-order polynomial approximation of the resistance to temperature nonlinear relationship.

A.1.1.3 *General setup monitoring*

In addition to temperature regulation, circuit pressure and battery tension are measured continuously by the microcontroller ADC in order to detect environmental problems (power failure, air leaks, etc).

All the setup but the temperature regulation (microcontroller and electronics, electrovalves) are powered by a 12V lead battery (from Yuasa) in order to be able to finish washing cycle and prevent contamination in case of power failure. The battery charge is managed by a simple electronic charger. Power failure are detected using a comparator between the battery tension and the power supply tension.

In addition, a light emitting diode (LED) emitting at 592 nm is powered from the main board, and is directed through the growth chamber on a photodiode. Using a voltage divider, the current produced by the photodiode is measured by the ADC and converted into OD. The LED and photodiode are mounted on a motorized stand and can be moved together along the height of the growth chamber. At this time, motor control and data logging are operated from a computer, using a custom program written with xVin, `od_profile`. This program opens serial connections to the microcontroller and to the motor controller, and acquires vertical OD profiles at regular time intervals.

A.1.1.4 *Electronics design*

In its current version, the setup is made of two main printed circuit boards. The main board features most integrated circuits, among other regulators, valves control, temperature regulation circuit, etc. It has two connectors, one for the microcontroller board, and one for the electrovalves board. The latter has been designed as a mechanical stand, allowing to connect all electrovalves thanks to a classical parallel connector.

A.1.2 MICROCONTROLLER PROGRAM

The microcontroller used in this setup is the Silabs C8051F120. It is a classical 8051 with more analog features than the average, and reasonable

amount RAM and EPROM. The microcontroller datasheet is an invaluable source of information.

A.1.2.1 *General structure*

The program is written in C and compiled using Keil C51. The source code is available online on the lab repository `https://pimprenelle.lps.ens.fr/svn/trunk/mc8051f120/evoProto1/` (rev. 3920).

The source code is divided in shorter files. Each file (and its associated header) corresponds to the implementation of a small set of related features. A makefile is provided to build the executable from these source files. Table A.1 summarises the features implemented in each files. In addition, global switches allowing to enable/disable features are defined as macros in `evo.h`: `EVO` for valves and cycles related features, `FLASH` for parameters storage, and `LCD` for LCD-based display and setting of parameters.

FILE	DESCRIPTION
`adc12.c`	Initialization and interrupt function definition of ADC 1, based on timer 3. This interrupt function averages ADC readout and is also used to modulate electrovalves current.
`cmd.c`	Definition of command functions. Execution of the appropriate function depending on the identifier computed by `parser.c`.
`cp0.c`	Initialization and read of comparator (detect power supply failure).
`dac.c`	Initialization and control of the two digital to analog converters.
`evo.c`	Main file of the program. Valves and cycles control and definition. Treatment of recurrent tasks ("pending treatment" after ADC measurement is done: ADC averaging, PID update, cycles update, etc). Detection of user actions (through serial communication or LCD buttons).
`flash.c`	General functions for EPROM initialization, read and write.
`flashEvo.c`	Custom functions used to store and retrieve program parameters using the EPROM. A short bank of memory is used to store global parameters (PID parameters, timestamp, current cycle, etc), while the general memory is used to log important events occurring during the experiment. The storage convention is explained at the beginning of the code.

Table A.1: (continued)

FILE	DESCRIPTION
`lcd.c`	Initialization of a graphic LCD module (used in text mode). Under development.
`modules.c`	General variables and functions definitions common to all project using this microcontroller in the lab.
`osd.c`	Control of parameters using four buttons and the LCD display. Under development.
`parser.c`	Retrieve the last command from the serial port rolling buffer and compute the corresponding identifier.
`pca.c`	Initialization and interrupt function definition of the programmable counter array used in the PWM of the temperature regulation.
`port.c`	Initialization of ports states (and crossbar state).
`rtc.c`	Initialization and interrupt function definition of the real-time clock based on timer 4. `timestamp` (over one day) and `daystamp` variables are defined to keep track of the elapsed time since the last restart. Everyday, the daystamp is incremented while the timestamp is reseted.
`sysclk.c`	Initialize the crystal clock used to set the CPU frequency.
`uart0.c`	Initialization and functions definitions (including the interrupt function) of serial communication with the computer using UART0.
`vref.c`	Initialization of ADC voltage reference.
`wdt.c`	Retrieve last restart error code using the watchdog.

Table A.1: Files used for the microcontroller program.

A.1.2.2 *Serial communication*

The program handles serial communication using a classical RS-232 protocol. This is the privileged mode of user interaction.

UART0 is used for serial communication. UART interrupt functions are defined in `uart0.c`. Once received, character strings are parsed using a custom convention allowing to pass up to five characters and a numeric value (in `parser.c` and Listing 1). The corresponding custom hexadecimal identifier is compared to the list of recognized user commands to be found in `cmd.c`. A nicer implementation based on structures has been

implemented (at the end of `parser.h`) but it was not successfully compiled with C51 or SDCC.

Listing 1: Generator of custom hexadecimal identifier used in parsing. This is a standalone C program that is used during the development.

```
#include <stdio.h>

int main()
{
  char ch, cmd[6];
  int i;
  long id;

  invit: ;
  // Input command scheme
  printf("Command to convert (less than 5 char):");
  scanf("%s", cmd);

  id = 0;

  for(i = 0; cmd[i] && cmd[i] != '?' && cmd[i] != '='; i++)
  // we stop on ?,=, or end
    {
      ch = cmd[i];
      if (ch > 95) ch -= 32;          // lower case -> upper
      if (ch <= 'Z' && ch >= 'A')     // We only keep A to Z
        {
          ch = ch - ' ';
          if (i) id <<= 6;            // shift by 6 bits
          id |= (0x3F&ch);            // add the last
        }
      else if (ch == '#')             // we also accept digits
        {
          ch = '#'-' ';               // the id is compute with 0
          if (i) id <<= 6;            // shift by 6 bits
          id |= (0x3F&ch);            // add the last
        }
      else
        {
          printf("Error: command does not contain only letters or #.\r\n\n");
          return 1;
        }
    }

  printf("commandIndex is: 0x%8lx\r\n\n", id);
  goto invit;
  return 0;
}
```

Listing 2: Comparaison of a the parsed string identifier with the Led command identifier (`exec_user_cmd(void)` in `cmd.c`)

```
...
else if (id_cmd == 0x0002C964) // "LED", 3,
  {
    if (type_cmd == CMD_SET && cmd[la_cmd + 1] != 0) setLed(cmd + la_cmd +
         1);
    else if (type_cmd == CMD_GET) getLed();
```

```
    else if (type_cmd == CMD_DO) toggleLed();
  }
...
```

A.1.2.3 *Interrupts and programmable counter arrays*

ADC interrupt function is used to read the values of the ADCs, and also for some other periodic tasks. It is important to notice that to keep the interrupt short enough, a global variable `pending` can be set to 1 to indicate that calculation is to be done on CPU spare time.

For the temperature regulation, measurements are acquired at 1 kHz from the ADCs, and averaged over 1 s. This temperature value is used to adjust the power of resistors or TECs through a PID controller implemented in the pending treatment function (in `evo.c`). The actual heating power modulation is achieved using programmable counter arrays (in `pca.c`).

Other ADCs are used to measure the battery charge and the tubing pressure. They are also acquired at 1 kHz and averaged over 1 s.

Voltage control of electrovalves is achieved through a modulation of the digital output at 1 kHz. For simplicity, it is managed in the ADC interrupt (Listing 3).

Listing 3: Current modulation for electrovalves control (`adc12.c` and declarations from `evo.h`)

```
// Q: Valve active (1) / inactive (0)
// R: Modulation on (1) / off (0)
unsigned char xdata Q5 = 0x00, Q6 = 0x00, Q7 = 0x00;
unsigned char xdata R5 = 0xFF, R6 = 0xFF, R7 = 0xFF;
unsigned char xdata alt, i_alim = 0, alim[12] = {0, 1, 1, 1, 1, 1, 0, 1,
    1, 1, 1, 1};
long int xdata R_end = -1;

...

if (n_acq >= 100)  // every 0.1s
if (R_end > 0 && timestamp > R_end) // Enable modulation after 200ms
{
  R7 = 0xFF;
  R6 = 0xFF;
  R5 = 0xFF;
  R_end = -1;
}

SFRPAGE = CONFIG_PAGE;
alt = alim[i_alim]? 0xFF : 0x00;
P7 = ~Q7 | (R7 & alt);
P6 = ~Q6 | (R6 & alt);
P5 = ~Q5 | (R5 & alt);
```

```
if (++i_alim > 11) i_alim = 0;
```

A.1.2.4 *Cycles control*

An important feature of this evolutionary chemostat is that biofilms can be washed out by transferring the culture solution and cleaning all tubes with soda. In order to implement this, we define *states*, which are a set of valves opening states. For each state, an hexadecimal identifier is defined in `evo.h` (Listing 4). The function `Ecoli_state()` in `evo.c` takes this identifier as argument and open or close each electrovalve accordingly.

Although states can be changed by hand, the classical use is to run a sequence of states of predefined durations. To this purpose, we define five *cycles* in `evo.h` (Listing 5). These cycles can be started, stopped and paused using the serial communication. When a cycle is active (`currentStep` variable is not null), `execCurrentCycleStep()` is called once the current step duration as elapsed in order to start the following step (change the electrovalves state, compute the time at the end of the step, etc). In certain cases, the experimenter is expected to act on the hardware (refill tanks, uptake sample, etc). The variable `userAction` is used to pause the system until the task is completed.

A.1.3 EXPERIMENTER MANUAL

A.1.3.1 *Serial communication*

The serial communication must be configured with baudrate at 57 600 bps, 8 data bits, no parity, 1 stop bit, and no flow control. It is convenient to print the input in the console as they are not echoed by the microcontroller. Table A.2 lists all available commands using this serial communication.

COMMAND	SET (=)	GET (?)	DO (∅)
LED, L	Set LED state	Print LED state	Toggle LED state
D		Print display status	Toggle display status
DATE	Set timestamp	Print current date	
TSTP	Set timestamp	Print current timestamp	

Table A.2: (continued)

COMMAND	SET (=)	GET (?)	DO (∅)
DSTP	Set daystamp	Print current daystamp	
T#		Print current temperature	
R#	Set the temperature regulation control value	Print the temperature regulation control value	
PT#	Set the proportional parameter of the temperature regulation PID	Print the proportional parameter of the temperature regulation PID	
IT#	Set the integral parameter of the temperature regulation PID	Print the integral parameter of the temperature regulation PID	
DT#	Set the derivative parameter of the temperature regulation PID	Print the derivative parameter of the temperature regulation PID	
A#		Print current ADC value	
W#	Set heating power	Print current heating power	
P#	Set output port state	Print output port state	
V#	Set electrovalve state	Print electrovalve state	
STATE, S	Set a *state* of electrovalves		

Table A.2: (continued)

COMMAND	SET (=)	GET (?)	DO (∅)
GROWTH	Set step of growth cycle	Print current step of growth cycle	Start growth cycle
STRL	Set step of sterilization cycle	Print current step of sterilization cycle	Start sterilization cycle
UPTK	Set step of uptake cycle	Print current step of uptake cycle	Start growth uptake
INOC	Set step of inoculation cycle (first part)	Print current step of inoculation cycle (first part)	Start inoculation cycle (first part)
INOCT	Set step of inoculation cycle (second part)	Print current step of inoculation cycle (second part)	Start inoculation cycle (second part)
CYCLE, CYC		Print current cycle step	
STOP			Stop the current active cycle
PAUSE			Pause/restart the current active cycle

Table A.2: List of commands to be used in the serial communication. For each command, three variants can be defined depending whether an equal sign, a question mark or nothing occurs after the command string. # character must be replaced by a relevant number (temperature channel, electrovalve number, etc).

Regarding the temperature regulation, the PID parameters must be adjusted to each setup. In particular, the size of the device to be heated

changes very much the PID dynamics. Typically for the thin rectangular chamber, they are set to 10, 4 and 0 respectively.

A.1.3.2 *Operating cycles*

Five *cycles* are defined to run the device:

GROWTH The default state of the chemostat, that cycle the culture between the two chambers and wash all tubing afterwards.

STERILIZATION State run once before inoculation to clean all tubing with soda and rinse it. The steps are longer than in the growth cycle to ensure a better sterilization of biofilms and spores.

INOCULATION 1 First part of the inoculation cycle. Three consecutive rinsing are used to buffer the remaining soda if any.

INOCULATION 2 Second part of the inoculation cycle run automatically after the first one; the culture used to inoculate the chamber is introduced using the uptake cell.

UPTAKE Uptake a sample of the culture from the primary chamber; several transfers between the two chambers are used to homogenize the culture.

The detailed steps and durations of these cycles are shown in Listing 5. For each step, an help message can be defined (typically to explain the task expected from the experimenter). In addition, the next step is specified as well so that cycles can be run repeatedly or one after the other.

A.1.3.3 *Open issues*

Several points are to be fixed before running an evolutionary experiment with this setup. First, the new growth chamber, of rectangular shapes, are to be adapted to the setup.

In addition, transferring between the two growth chamber is done by pushing the culture solution with air. At the end, air bubbles from the bottom inlet. Since the chamber has a small section, liquid can be pushed to the top and flow out the chamber. This problem will be magnified in the new chamber design.

Lastly, it is important to test whether or not the spatial organization of a culture can be transfered to the other chamber.

Listing 4: Listing of the different states of the setup (from `evo.h`). Valves number is shown on Fig. A.1

```
// STATE                              CODES           OPEN VALVES
# define STD_GROWTH                  0x36143F        /* (    ) (    6)   (3   5   0 2)  (                ) */
# define TRANSFERT_PRI_SEC           0x331E3A        /* (    ) (8    )   (3         2)  (         15    14) */
# define WASHING_0_SOUDE_PRI         0x362D3F        /* (    ) (    6)   (  4     0  )  (                ) */
# define WASHING_1_SOUDE_PRI         0x372B3F        /* (    ) (     )   (  4   1    )  (                ) */
# define WASHING_2_SOUDE_PRI         0x362E3F        /* (    ) (    6)   (  4       2)  (                ) */
# define WASHING_0_GAZ_PRI           0x321D3F        /* (    ) (8   6)   (3       0  )  (                ) */
# define WASHING_1_GAZ_PRI           0x321B3F        /* (    ) (8   6)   (3     1    )  (                ) */
# define WASHING_2_GAZ_PRI           0x321E3F        /* (    ) (8   6)   (3         2)  (                ) */
# define WASHING_0_NUTRIMENTS_PRI    0x34153F        /* (    ) (  7 6)   (3   5   0  )  (                ) */
# define WASHING_1_NUTRIMENTS_PRI    0x35133F        /* (    ) (  7  )   (3   5 1    )  (                ) */
# define WASHING_2_NUTRIMENTS_PRI    0x34363F        /* (    ) (  7 6)   (    5     2)  (                ) */
# define TRANSFERT_SEC_PRI           0x333A1E        /* (    ) (8    )   (      1   2)  (13            14) */
# define WASHING_14_SOUDE_SEC        0x363F2E        /* (    ) (    6)   (           )  (   12          14) */
# define WASHING_15_SOUDE_SEC        0x373F2B        /* (    ) (     )   (           )  (   12    15      ) */
# define WASHING_16_SOUDE_SEC        0x363F2D        /* (    ) (    6)   (           )  (   12       16   ) */
# define WASHING_14_GAZ_SEC          0x363B1E        /* (    ) (    6)   (    5   0 2)  (13            14) */
# define WASHING_15_GAZ_SEC          0x373B1B        /* (    ) (     )   (    5   0 2)  (13       15      ) */
# define WASHING_16_GAZ_SEC          0x363B1D        /* (    ) (    6)   (    5   0 2)  (13          16   ) */
# define WASHING_14_NUTRIMENTS_SEC   0x363F36        /* (    ) (    6)   (           )  (      11        14) */
# define WASHING_15_NUTRIMENTS_SEC   0x373F33        /* (    ) (     )   (           )  (      11 15     ) */
# define WASHING_16_NUTRIMENTS_SEC   0x363F35        /* (    ) (    6)   (           )  (      11    16   ) */
# define WASHING_9_10_SOUDE          0x063F2F        /* (10 9) (    6)   (           )  (   12            ) */
# define WASHING_9_10_GAZ            0x063F1F        /* (10 9) (    6)   (           )  (13               ) */
# define WASHING_9_10_NUTRIMENTS     0x063F37        /* (10 9) (    6)   (           )  (      11         ) */

# define STERILIZE_3                 0x320F3F        /* (    ) (8   6)   (3 4         )  (                ) */
# define STERILIZE_13                0x363C0F        /* (    ) (    6)   (        0 2)  (13 12            ) */
# define STERILIZE_3_BP              0x360F3F        /* (    ) (    6)   (3 4         )  (                ) */
# define STERILIZE_11                0x363C27        /* (    ) (    6)   (        0 2)  (   12 11         ) */
```

```
# define STERILIZE_5                    0x34273F          /* (    ) (  7 6)   (  4 5      ) (                ) */
# define STERILIZE_5_BP                 0x36273F          /* (    ) (    6)   (  4 5      ) (                ) */
# define RINCE_3                        0x361C3F          /* (    ) (    6)   (3       0 2) (                ) */
# define RINCE_5                        0x36343F          /* (    ) (    6)   (    5   0 2) (                ) */

# define ADD_NUTRIMENTS_1               0x34153F          /* (    ) (  7 6)   (3   5   0  ) (                ) */
# define TRANSFERT_PRI_SEC_VIA_CELL     0x031E3B          /* (10 9) (8    )   (3         2) (         15     ) */
# define PURGE1                         0x321E3F          /* (    ) (8   6)   (3         2) (                ) */
# define PURGE2                         0x363F1E          /* (    ) (    6)   (           ) (13            14) */
# define NO_INPUT                       0x363C3F          /* (    ) (    6)   (       0 2) (                ) */
```

Listing 5: Definitions of the different cycles (from `evo.h`)

```
typedef struct _step
{
  char cycleId;
  char stepId;
  long int state;
  long int duration;
  struct _step * nextStep;
  char *mesg;
} step;

# define NBCYCLES      5
# define GROWTH        0
# define STERILIZE     1
# define INOC          2
# define INOC2         3
# define UPTAKE        4

# define NBSTEPS_MAX  33

step code cycle[NBCYCLES][NBSTEPS_MAX] =
  {
    // Define Standard GROWTH Steps
    {
      {  0,   0,  ADD_NUTRIMENTS_1            ,    5,  &cycle[0][1] ,  NULL },
      {  0,   1,  STD_GROWTH                  ,90000,  &cycle[0][2] ,  NULL },
      {  0,   2,  TRANSFERT_PRI_SEC           ,   30,  &cycle[0][3] ,  NULL },
      {  0,   3,  WASHING_1_SOUDE_PRI         ,  120,  &cycle[0][4] ,  NULL },
      {  0,   4,  WASHING_0_SOUDE_PRI         ,   30,  &cycle[0][5] ,  NULL },
      {  0,   5,  WASHING_2_SOUDE_PRI         ,   30,  &cycle[0][6] ,  NULL },
      {  0,   6,  WASHING_1_GAZ_PRI           ,   30,  &cycle[0][7] ,  NULL },
      {  0,   7,  WASHING_0_GAZ_PRI           ,   30,  &cycle[0][8] ,  NULL },
      {  0,   8,  WASHING_2_GAZ_PRI           ,   45,  &cycle[0][9] ,  NULL },
      {  0,   9,  WASHING_1_NUTRIMENTS_PRI    ,  100,  &cycle[0][10],  NULL },
      {  0,  10,  WASHING_0_NUTRIMENTS_PRI    ,   30,  &cycle[0][11],  NULL },
      {  0,  11,  WASHING_2_NUTRIMENTS_PRI    ,   30,  &cycle[0][12],  NULL },
      {  0,  12,  WASHING_1_GAZ_PRI           ,   30,  &cycle[0][13],  NULL },
      {  0,  13,  WASHING_0_GAZ_PRI           ,   30,  &cycle[0][14],  NULL },
      {  0,  14,  WASHING_2_GAZ_PRI           ,   45,  &cycle[0][15],  NULL },
      {  0,  15,  TRANSFERT_SEC_PRI           ,   30,  &cycle[0][16],  NULL },
      {  0,  16,  WASHING_15_SOUDE_SEC        ,  270,  &cycle[0][17],  NULL },
      {  0,  17,  WASHING_16_SOUDE_SEC        ,   30,  &cycle[0][18],  NULL },
      {  0,  18,  WASHING_14_SOUDE_SEC        ,   30,  &cycle[0][19],  NULL },
      // NaOH WASHED
      {  0,  19,  WASHING_15_GAZ_SEC          ,  150,  &cycle[0][20],  NULL },
      {  0,  20,  WASHING_15_NUTRIMENTS_SEC   ,  100,  &cycle[0][21],  NULL },
      // FIRST RINCE
      {  0,  21,  WASHING_14_GAZ_SEC          ,   60,  &cycle[0][22],  NULL },
      {  0,  22,  WASHING_15_GAZ_SEC          ,  150,  &cycle[0][23],  NULL },
      {  0,  23,  WASHING_16_GAZ_SEC          ,   30,  &cycle[0][24],  NULL },
      {  0,  24,  WASHING_16_NUTRIMENTS_SEC   ,   90,  &cycle[0][25],  NULL },
      // SECOND RINCE
      {  0,  25,  WASHING_14_GAZ_SEC          ,   60,  &cycle[0][26],  NULL },
      {  0,  26,  WASHING_14_NUTRIMENTS_SEC   ,   30,  &cycle[0][27],  NULL },
      // THIRD RINCE???
      {  0,  27,  WASHING_15_GAZ_SEC          ,   40,  &cycle[0][28],  NULL },
      {  0,  28,  WASHING_16_GAZ_SEC          ,   30,  &cycle[0][29],  NULL },
      {  0,  29,  WASHING_14_GAZ_SEC          ,   60,  &cycle[0][0] ,  NULL },
      {  0,  30,  0                           ,    0,  NULL ,          NULL },
      {  0,  31,  0                           ,    0,  NULL ,          NULL },
      {  0,  32,  0                           ,    0,  NULL ,          NULL }
```

```
},
// Define STERILIZATION Steps
{
  {  1,   0,  PURGE1                      ,   40,  &cycle[1][1] ,  NULL },
  {  1,   1,  PURGE2                      ,   40,  &cycle[1][2] ,  NULL },
  {  1,   2,  WASHING_1_SOUDE_PRI         ,  240,  &cycle[1][3] ,  NULL },
  {  1,   3,  WASHING_15_SOUDE_SEC        ,  240,  &cycle[1][4] ,  NULL },
  {  1,   4,  NO_INPUT                    ,   -1,  &cycle[1][5] ,  "PUT WASTE
       TANKS AT THE AIR AND NUTRIENTS INPUTS \r\nREMOVE BYPASS"},
  {  1,   5,  STERILIZE_3                 ,   30,  &cycle[1][6] ,  NULL },
  {  1,   6,  STERILIZE_3_BP              ,   30,  &cycle[1][7] ,  NULL },
  {  1,   7,  STERILIZE_13                ,   30,  &cycle[1][8] ,  NULL },
  {  1,   8,  STERILIZE_11                ,   30,  &cycle[1][9] ,  NULL },
  {  1,   9,  STERILIZE_5                 ,   30,  &cycle[1][10],  NULL },
  {  1,  10,  STERILIZE_5_BP              ,   30,  &cycle[1][11],  NULL },
  {  1,  11,  NO_INPUT                    ,   -1,  &cycle[1][12],  "PLUG AIR
       AND NUTRIENTS INPUTS" },
  {  1,  12,  PURGE1                      ,   60,  &cycle[1][13],  NULL },
  // EMPTY VANNE 8
  {  1,  13,  RINCE_3                     ,   30,  &cycle[1][14],  NULL },
  // EMPTY VANNE 3
  {  1,  14,  WASHING_14_GAZ_SEC          ,   30,  &cycle[1][15],  NULL },
  // EMPTY VANNE 13
  {  1,  15,  WASHING_2_NUTRIMENTS_PRI    ,   60,  &cycle[1][16],  NULL },
  // EMPTY VANNE 7
  {  1,  16,  WASHING_14_NUTRIMENTS_SEC   ,   60,  &cycle[1][17],  NULL },
  // EMPTY VANNE 11
  {  1,  17,  RINCE_5                     ,   60,  &cycle[1][18],  NULL },
  // EMPTY VANNE 5
  {  1,  18,  PURGE1                      ,  100,  &cycle[1][19],  NULL },
  {  1,  19,  PURGE2                      ,  100,  &cycle[1][20],  NULL },
  {  1,  20,  NO_INPUT                    ,    0,  &cycle[2][0] ,  "PLUG BYPASS
       " },
  {  1,  21,  0                           ,    0,  NULL ,          NULL },
  {  1,  22,  0                           ,    0,  NULL ,          NULL },
  {  1,  23,  0                           ,    0,  NULL ,          NULL },
  {  1,  24,  0                           ,    0,  NULL ,          NULL },
  {  1,  25,  0                           ,    0,  NULL ,          NULL },
  {  1,  26,  0                           ,    0,  NULL ,          NULL },
  {  1,  27,  0                           ,    0,  NULL ,          NULL },
  {  1,  28,  0                           ,    0,  NULL ,          NULL },
  {  1,  29,  0                           ,    0,  NULL ,          NULL },
  {  1,  30,  0                           ,    0,  NULL ,          NULL },
  {  1,  31,  0                           ,    0,  NULL ,          NULL },
  {  1,  32,  0                           ,    0,  NULL ,          NULL }
},
// Define INOCULATION Steps (first part)
{
  {  2,   0,  PURGE1                      ,   40,  &cycle[2][1] ,  NULL },
  {  2,   1,  PURGE2                      ,   40,  &cycle[2][2] ,  NULL },
  // WASH ALL THE VANNES
  {  2,   2,  WASHING_1_SOUDE_PRI         ,  240,  &cycle[2][3] ,  NULL },
  {  2,   3,  WASHING_0_SOUDE_PRI         ,   30,  &cycle[2][4] ,  NULL },
  {  2,   4,  WASHING_2_SOUDE_PRI         ,   30,  &cycle[2][5] ,  NULL },
  // NaOH WASHED
  {  2,   5,  WASHING_2_GAZ_PRI           ,  150,  &cycle[2][6] ,  NULL },
  {  2,   6,  WASHING_1_GAZ_PRI           ,   30,  &cycle[2][7] ,  NULL },
  {  2,   7,  WASHING_0_GAZ_PRI           ,   30,  &cycle[2][8] ,  NULL },
  {  2,   8,  WASHING_1_NUTRIMENTS_PRI    ,   60,  &cycle[2][9] ,  NULL },
  // FIRST RINCE
  {  2,   9,  WASHING_2_GAZ_PRI           ,   50,  &cycle[2][10],  NULL },
  {  2,  10,  WASHING_0_NUTRIMENTS_PRI    ,   60,  &cycle[2][11],  NULL },
  // SECOND RINCE
```

```
    {  2,  11,  WASHING_2_GAZ_PRI          ,   50,  &cycle[2][12],  NULL },
    {  2,  12,  WASHING_2_NUTRIMENTS_PRI   ,   30,  &cycle[2][13],  NULL },
    // THIRD RINCE???
    {  2,  13,  WASHING_2_GAZ_PRI          ,   40,  &cycle[2][14],  NULL },
    {  2,  14,  WASHING_1_GAZ_PRI          ,   30,  &cycle[2][15],  NULL },
    {  2,  15,  WASHING_0_GAZ_PRI          ,   30,  &cycle[2][16],  NULL },
    {  2,  16,  WASHING_15_SOUDE_SEC       ,  270,  &cycle[2][17],  NULL },
    {  2,  17,  WASHING_16_SOUDE_SEC       ,   30,  &cycle[2][18],  NULL },
    {  2,  18,  WASHING_14_SOUDE_SEC       ,   30,  &cycle[2][19],  NULL },
    {  2,  19,  WASHING_9_10_SOUDE         ,   30,  &cycle[2][20],  NULL },
    // NaOH WASHED
    {  2,  20,  WASHING_9_10_GAZ           ,  150,  &cycle[2][21],  NULL },
    {  2,  21,  WASHING_15_NUTRIMENTS_SEC  ,   90,  &cycle[2][22],  NULL },
    // FIRST RINCE
    {  2,  22,  WASHING_14_GAZ_SEC         ,   60,  &cycle[2][23],  NULL },
    {  2,  23,  WASHING_15_GAZ_SEC         ,   30,  &cycle[2][24],  NULL },
    {  2,  24,  WASHING_16_GAZ_SEC         ,   30,  &cycle[2][25],  NULL },
    {  2,  25,  WASHING_16_NUTRIMENTS_SEC  ,   90,  &cycle[2][26],  NULL },
    // SECOND RINCE
    {  2,  26,  WASHING_14_GAZ_SEC         ,   60,  &cycle[2][27],  NULL },
    {  2,  27,  WASHING_14_NUTRIMENTS_SEC  ,   30,  &cycle[2][28],  NULL },
    {  2,  28,  WASHING_9_10_NUTRIMENTS    ,   30,  &cycle[2][29],  NULL },
    // THIRD RINCE???
    {  2,  29,  WASHING_9_10_GAZ           ,   30,  &cycle[2][30],  NULL },
    {  2,  30,  WASHING_14_GAZ_SEC         ,   60,  &cycle[2][31],  NULL },
    {  2,  31,  WASHING_15_GAZ_SEC         ,   30,  &cycle[2][32],  NULL },
    {  2,  32,  WASHING_16_GAZ_SEC         ,   30,  &cycle[3][0],   NULL }
  },
  // Define INOCULATION Steps (second and last part)
  {
    // INOCULATION
    {  3,   0,  ADD_NUTRIMENTS_1           ,   35,  &cycle[3][1],   NULL },
    // DO NOT FILL UP TO THE TOP (40" for 10mL)
    {  3,   1,  NO_INPUT                   ,   -1,  &cycle[3][2],   "ADD THE
        UPTAKE CELL FILLED WITH BACTERIA" },
    {  3,   2,  TRANSFERT_PRI_SEC_VIA_CELL ,   50,  &cycle[3][3],   NULL },
    {  3,   3,  TRANSFERT_SEC_PRI          ,   40,  &cycle[3][4],   NULL },
    {  3,   4,  NO_INPUT                   ,   -1,  &cycle[3][5],   "REPLACE THE
         UPTAKE CELL BY THE CONNECTOR" },
    // WASH CELL2
    {  3,   5,  WASHING_15_SOUDE_SEC       ,  240,  &cycle[3][6],   NULL },
    {  3,   6,  WASHING_16_SOUDE_SEC       ,   30,  &cycle[3][7],   NULL },
    {  3,   7,  WASHING_14_SOUDE_SEC       ,   30,  &cycle[3][8],   NULL },
    {  3,   8,  WASHING_9_10_SOUDE         ,   30,  &cycle[3][9],   NULL },
    // NaOH WASHED
    {  3,   9,  WASHING_9_10_GAZ           ,  150,  &cycle[3][10],  NULL },
    {  3,  10,  WASHING_15_NUTRIMENTS_SEC  ,   90,  &cycle[3][11],  NULL },
    // FIRST RINCE
    {  3,  11,  WASHING_14_GAZ_SEC         ,   60,  &cycle[3][12],  NULL },
    {  3,  12,  WASHING_15_GAZ_SEC         ,   30,  &cycle[3][13],  NULL },
    {  3,  13,  WASHING_16_GAZ_SEC         ,   30,  &cycle[3][14],  NULL },
    {  3,  14,  WASHING_16_NUTRIMENTS_SEC  ,   90,  &cycle[3][15],  NULL },
    // SECOND RINCE
    {  3,  15,  WASHING_14_GAZ_SEC         ,   60,  &cycle[3][16],  NULL },
    {  3,  16,  WASHING_14_NUTRIMENTS_SEC  ,   30,  &cycle[3][17],  NULL },
    {  3,  17,  WASHING_9_10_NUTRIMENTS    ,   30,  &cycle[3][18],  NULL },
    // THIRD RINCE???
    {  3,  18,  WASHING_9_10_GAZ           ,   30,  &cycle[3][19],  NULL },
    {  3,  19,  WASHING_14_GAZ_SEC         ,   60,  &cycle[3][20],  NULL },
    {  3,  20,  WASHING_15_GAZ_SEC         ,   30,  &cycle[3][21],  NULL },
    {  3,  21,  WASHING_16_GAZ_SEC         ,   30,  &cycle[0][0],   NULL },
    {  3,  22,  0                          ,    0,  NULL ,          NULL },
    {  3,  23,  0                          ,    0,  NULL ,          NULL },
```

```
    {  3,  24,  0                          ,    0,  NULL ,          NULL },
    {  3,  25,  0                          ,    0,  NULL ,          NULL },
    {  3,  26,  0                          ,    0,  NULL ,          NULL },
    {  3,  27,  0                          ,    0,  NULL ,          NULL },
    {  3,  28,  0                          ,    0,  NULL ,          NULL },
    {  3,  29,  0                          ,    0,  NULL ,          NULL },
    {  3,  30,  0                          ,    0,  NULL ,          NULL },
    {  3,  31,  0                          ,    0,  NULL ,          NULL },
    {  3,  32,  0                          ,    0,  NULL ,          NULL }
  },
  // Define UPTAKE Steps
  {
    {  4,   0,  NO_INPUT                   ,   -1,  &cycle[4][1] ,  "PUT THE
        UPTAKE CELL" },
    // WASH THE CELL
    {  4,   1,  WASHING_9_10_SOUDE         ,  150,  &cycle[4][2] ,  NULL },
    {  4,   2,  WASHING_9_10_GAZ           ,   90,  &cycle[4][3] ,  NULL },
    {  4,   3,  PURGE2                     ,   40,  &cycle[4][4] ,  NULL },
    {  4,   4,  WASHING_9_10_NUTRIMENTS    ,  150,  &cycle[4][5] ,  NULL },
    {  4,   5,  WASHING_9_10_GAZ           ,   90,  &cycle[4][6] ,  NULL },
    {  4,   6,  PURGE2                     ,   40,  &cycle[4][7] ,  NULL },
    // UPTAKE
    {  4,   7,  TRANSFERT_PRI_SEC          ,   38,  &cycle[4][8] ,  NULL },
    {  4,   8,  TRANSFERT_SEC_PRI          ,   35,  &cycle[4][9] ,  NULL },
    {  4,   9,  TRANSFERT_PRI_SEC_VIA_CELL ,   15,  &cycle[4][10],  NULL },
    {  4,  10,  TRANSFERT_PRI_SEC          ,   23,  &cycle[4][11],  NULL },
    {  4,  11,  TRANSFERT_SEC_PRI          ,   32,  &cycle[4][12],  NULL },
    {  4,  12,  NO_INPUT                   ,   -1,  &cycle[4][13],  "REMOVE THE
        UPTAKE CELL" },
    // WASH CELL
    {  4,  13,  WASHING_15_SOUDE_SEC       ,   60,  &cycle[4][14],  NULL },
    {  4,  14,  WASHING_16_SOUDE_SEC       ,   30,  &cycle[4][15],  NULL },
    {  4,  15,  WASHING_14_SOUDE_SEC       ,   30,  &cycle[4][16],  NULL },
    {  4,  16,  WASHING_9_10_SOUDE         ,  120,  &cycle[4][17],  NULL },
    {  4,  17,  WASHING_9_10_GAZ           ,  100,  &cycle[4][18],  NULL },
    {  4,  18,  WASHING_14_GAZ_SEC         ,   40,  &cycle[4][19],  NULL },
    {  4,  19,  WASHING_15_GAZ_SEC         ,   30,  &cycle[4][20],  NULL },
    {  4,  20,  WASHING_16_GAZ_SEC         ,   30,  &cycle[4][21],  NULL },
    {  4,  21,  WASHING_15_NUTRIMENTS_SEC  ,   60,  &cycle[4][22],  NULL },
    {  4,  22,  WASHING_16_NUTRIMENTS_SEC  ,   30,  &cycle[4][23],  NULL },
    {  4,  23,  WASHING_14_NUTRIMENTS_SEC  ,   30,  &cycle[4][24],  NULL },
    {  4,  24,  WASHING_9_10_NUTRIMENTS    ,  120,  &cycle[4][25],  NULL },
    {  4,  25,  WASHING_9_10_GAZ           ,  100,  &cycle[4][26],  NULL },
    {  4,  26,  WASHING_14_GAZ_SEC         ,   40,  &cycle[4][27],  NULL },
    {  4,  27,  WASHING_15_GAZ_SEC         ,   30,  &cycle[4][28],  NULL },
    {  4,  28,  WASHING_16_GAZ_SEC         ,   30,  &cycle[0][0] ,  NULL },
    {  4,  29,  0                          ,    0,  NULL ,          NULL },
    {  4,  30,  0                          ,    0,  NULL ,          NULL },
    {  4,  31,  0                          ,    0,  NULL ,          NULL },
    {  4,  32,  0                          ,    0,  NULL ,          NULL }
  }
};
```

A.2 REVIEW ON NONLINEARITIES IN BIOLOGY

This review, published in a special issue of *Nonlinearity* in 2008, introduces nonlinear challenges in biological systems at various levels. In particular, the fifth part deals with ecological and evolutionary dynamics.

IOP PUBLISHING NONLINEARITY

Nonlinearity **21** (2008) T131–T147 doi:10.1088/0951-7715/21/8/T03

OPEN PROBLEM

Some nonlinear challenges in biology

Francesco Mosconi, Thomas Julou, Nicolas Desprat, Deepak Kumar Sinha, Jean-François Allemand, Vincent Croquette and David Bensimon

LPS, ENS, UMR 8550 CNRS, 24 rue Lhomond, 75231 Paris Cedex 05, France

E-mail: David.Bensimon@lps.ens.fr

Received 21 April 2008
Published 10 July 2008
Online at stacks.iop.org/Non/21/T131

Abstract

Driven by a deluge of data, biology is undergoing a transition to a more quantitative science. Making sense of the data, building new models, asking the right questions and designing smart experiments to answer them are becoming ever more relevant. In this endeavour, nonlinear approaches can play a fundamental role. The biochemical reactions that underlie life are very often nonlinear. The functional features exhibited by biological systems at all levels (from the activity of an enzyme to the organization of a colony of ants, via the development of an organism or a functional module like the one responsible for chemotaxis in bacteria) are dynamically robust. They are often unaffected by order of magnitude variations in the dynamical parameters, in the number or concentrations of actors (molecules, cells, organisms) or external inputs (food, temperature, pH, etc). This type of structural robustness is also a common feature of nonlinear systems, exemplified by the fundamental role played by dynamical fixed points and attractors and by the use of generic equations (logistic map, Fisher–Kolmogorov equation, the Stefan problem, etc.) in the study of a plethora of nonlinear phenomena. However, biological systems differ from these examples in two important ways: the intrinsic stochasticity arising from the often very small number of actors and the role played by evolution. On an evolutionary time scale, nothing in biology is frozen. The systems observed today have evolved from solutions adopted in the past and they will have to adapt in response to future conditions. The evolvability of biological system uniquely characterizes them and is central to biology. As the great biologist T Dobzhansky once wrote: 'nothing in biology makes sense except in the light of evolution'.

Mathematics Subject Classification: 01-02, 92-02, 92C15, 92C45, 92D15, 92D25, 92D40

(Some figures in this article are in colour only in the electronic version)

1. Introduction

Biology is essentially an experimental science, whose goal is to understand the engineering principles selected by evolution in the design of the great variety of organisms that are presently known. At all levels (from molecules to cells, from organisms to populations) the interactions between the various players are strongly nonlinear and usually saturate at sufficiently high concentrations (of molecules or cells). Molecular interactions occur at a microscopic level where Brownian motion and thermally activated processes are often a key factor in the function of the system studied (e.g. molecular motors). As a result all bio-molecular processes are (extrinsically) stochastic and should ideally be described within the framework of stochastic differential equations or via Fokker–Planck equations for the evolution of the probability density of given observables. Another fundamental element that characterizes biological processes at all levels is the intrinsic discreteness of its players: the number of bio-molecules of a given type in a cell is often very small. For micrometre size bacteria such as *E. coli*, $\mathrm{pH} = 7$ may mean less than 100 H^+ ions per bacteria. These ions, however, diffuse very rapidly in and out of the cell, so that on the time scale of enzymatic reactions (ms) their average is well-defined. It is not so for larger molecules which do not diffuse in and out of the cell, in particular DNA, mRNA and enzymes. For example in bacteria the number of mRNA coding for a given protein is often less than 1 per generation [1] and less than 20 DNA-polymerase molecules are responsible for replication [2]! Besides the fact that this small number of molecules introduces an extra (intrinsic) level of stochasticity it may also qualitatively alter the behaviour of the system: as pointed out by Solomon [3], the outcome of differential equations can be radically different if the underlying variables are discrete or continuous.

A fundamental and still largely unsolved problem is how biological systems can perform their function effectively under such constraints of extrinsic and intrinsic stochasticity. Here the contribution of nonlinear approaches could be fundamental since bifurcation theory can be used to predict the robust (topological) behaviour of complex dynamical systems for which we often do not know many important parameters (rate and affinity constants, cooperativities, saturation concentrations, etc). This weakness, however, can be turned into a strength. Indeed since these rates can be altered—by environmental changes (temperature, nutrients, pH, salt, etc), by different levels of protein expressions within the cell (a phenomenon known as phenotypic variability) and by genetic mutations—often without affecting the behaviour of the organism, a strong requirement of any modelling of biological systems is that it should be robust under major alterations of many of the parameters entering the model. When the actors of some regulation and metabolic networks and their topology are known (or reasonably guessed), a quite common trend among theoretical biologists is to write the differential equations describing their interactions and simulate them by making educated guesses of the many dozens of parameters that often enter such models (see for example [4]). Due to their large number of parameters and the often semi-quantitative predictions they make, it may, however, be difficult to falsify them (the usually accepted criterion for a good theory). Moreover, even if such models are robust to changes in their parameters and can be falsified, it is not clear that one can learn much from such detailed modelling. Beyond the 'forest' of equations are there some simple underlying principles? Extracting the 'slow' or relevant modes of such models might be more illuminating. How can the system be reduced to the dynamics of these modes only?

An answer to these questions would be particularly welcome if we are to understand the evolution of biological systems. Indeed the trade-off between robustness and evolvability (the possibility to adapt to new conditions) is a central theme of research in biology at all levels of inquiry: how is evolution constrained by the choices already made? What are its

rules, namely, can we predict how a biological/ecological system is going to evolve under a given selection pressure? The interesting case here is presented when different responses are possible: which one is selected? With which probability? Can we predict these probabilities? Finally, a third fundamental issue has to do with the mechanisms of development. These are remarkably robust to many variations (temperature, nutrients, fluctuations in gene expression and in rate constants, etc) yet are capable of evolving. How this robustness of the developmental pathways is achieved and how that robustness is restricting the evolutionary options presented to the organism are fascinating and unresolved issues where innovative nonlinear modelling and experimental approaches are required.

In the following we will sketch how the various issues of modelling, stochasticity (intrinsic and extrinsic), robustness and evolvability have been addressed in a variety of contexts: protein structure/function (section 2), gene expression networks (section 3), morphogenetic pathways (section 4) and ecological systems (section 5). The interested reader is referred to the appendices, where a detailed example for each topic is illustrated (appendix A is an exception as it contains a very short summary of relevant concepts in molecular biology). Our purpose is of course not to review these subjects (for that see the excellent book by Gerhart and Kirshner [5]), but rather to 'whet the appetite' of our readers and convince them that there are many unsolved fundamental problems in biology where tools from nonlinear system dynamics could be applied with great success.

2. Proteins, biochemistry and evolution

Protein structures and functions have been extensively studied from a variety of perspectives. Although physics and chemistry became quantitative sciences earlier than biology, at the level of small biological molecules, such as proteins, there are still many unsolved issues, involving stochasticity and nonlinearity, which demand further investigation both theoretically and experimentally. For example, the definition of the ground (or native) state of a protein is becoming more and more puzzling as new experiments explore it in detail. Not only is the prediction of the protein structure from its primary (i.e., amino-acid) sequence still unsolved (for a very recent account of structure prediction methods see [6]) but the mere question of the existence of a well-defined ground state is not clear.

Protein structures are thought to be determined by the minimization of free energy in the landscape of all possible configurations of the poly-peptidic chain. In the classical picture [7,8] the energy landscape is smooth and it has a unique minimum, the native state, which is both stable against thermal fluctuations and kinetically accessible to allow for a fast folding. Furthermore, this state is supposed to have a well-defined kinetic rate, its interaction with a substrate described by Michaelis–Menten (MM) dynamics (see appendix B). Soon after its formulation, the classical picture was questioned by experiments on myoglobin conducted by Frauenfelder and colleagues [9]. They suggested [10] that the protein energy landscape could resemble that of glassy materials, presenting many local minima separated by energy barriers of different heights. The local minima would correspond to different three-dimensional conformations assumed by the protein. With the development of high resolution experimental techniques such as x-ray crystallography, cryo-electron microscopy and nuclear magnetic resonance, evidence accumulated to support the idea that the same protein could assume different conformations. Only quite recently, though, the dynamics of hopping between states started to be assessed (see [11] for a recent account of progress on the subject).

Recent single molecule studies, in fact, opened a window on a previously unexplored area allowing us to follow the fluctuations in catalytic activity of an isolated protein for long time.

In such experiments [12–14] the catalytic rate of a single enzyme was monitored with the use of appropriate substrates which turned into fluorescent products upon catalysis by the enzyme. This method allowed the measurement of the time interval between successive reactions at high substrate concentrations (i.e., when diffusion is not the limiting factor). It appeared that such a time was not exponentially distributed (as one would expect if the enzyme had a well-defined conformation and kinetic rate). Rather its distribution could be fitted by a multi-exponential law, supporting the existence of a continuum of conformers, each characterized by different reaction kinetics (see appendix B). The time correlation of the activity of a single enzyme suggested that it spent up to seconds in each of these states, giving rise to memory effects in the enzyme conformational trajectory.

How many and how different are these conformers? Do they reflect thermal hopping between enzymatic structures of similar energy but different functionality or do they arise from the metabolic activity of the enzyme, kicked off from its native state by the reaction it catalyses and then moving chaotically on this manifold of excited states? One way to answer these questions is to study the dynamics of the protein structural fluctuations (using techniques such as single molecule fluorescence energy transfer [15]), in order to distinguish between thermal fluctuations about a well-defined state and fluctuations exhibiting long-term correlation effects. In a recent paper [16], the authors used this technique to assess the dynamics of conformational changes of the enzyme Adenylate Kinase and the influence of substrate interaction. Also, recent numerical simulations [17, 18] seem to support the picture of a large range of time scales in the dynamics of enzyme conformational changes.

The traditional picture of a homogeneous population of enzymes is no longer consistent with the amount of experimental and numerical data being gathered, and there is need for a theory taking into account the presence of a great number of different conformers. This effect introduces stochasticity (also called ‘static disorder’) across a population of enzymes. Similarly the possibility for a single enzyme to hop between different conformations introduces stochasticity (dubbed ‘dynamic disorder’) at the level of the activity of a single enzyme. These effects have to be taken into account if a satisfactory picture of enzyme catalysis has to be formulated. Yet, for the vast majority of known enzymes, and surely for those studied in the works mentioned above, the Michaelis–Menten kinetics seems to hold unperturbed, even for fluctuating single enzymes. A possible explanation was proposed in [19,20], yet one might expect departures from Michaelis–Menten-like kinetics in more general cases.

In the broader context of protein evolution, the previous results might also be related to the independent observation that proteins may evolve different functionalities by so called ‘promiscuous activity’ [21]. Since mutations are usually deleterious to the function of a given protein, it is important to understand how an enzyme with a specific function can mutate and evolve a new one. One known possibility for the gene coding is for the enzyme to be duplicated with evolution acting on one copy only, the other ensuring continuity of the vital activity; another is for the enzyme to have its main catalytic activity at one site and a weaker unrelated (‘promiscuous’) activity at another more distant one. This ‘promiscuous’ activity could then be acted upon by evolution without much interference with the main function of the protein (the ‘promiscuous’ site plays in real space the role of the duplicated gene). How is that picture altered by the existence of not one but many active states of the enzyme? Is the plasticity suggested in the previous paragraph useful for the evolution of protein function? Is it evolutionary easier to tailor these states to the needs of the organism or do they in contrast increase the constraints on the evolvability of the protein? These are fascinating issues that will require both sophisticated single molecule experiments on evolving enzymes and new theoretical approaches to these systems.

3. Gene expression and regulation, system biology

To understand the way cells operate it is not sufficient to study the structure and function of their molecular components. One has to grasp how the various molecules interact together in regulation and metabolic pathways to define the functional state of the cell (known as its phenotype, see appendix A). Although these pathways are interconnected, it has been proposed that just like man-made machines, they are composed of functional modules [22]. A functional module is a network of proteins (and possibly other molecules such as RNA, lipids and sugars) that are capable of performing a certain task: metabolizing glucose, making a flagellum, directing a bacterium to a source of food (chemotaxis), etc. A major goal of systems biology [23] is to understand the design principles of these modules. To that purpose one can adopt two approaches: analyse native modules or design modules that mimic natural ones.

For example an abrupt transition between a low and a high gene expression state can be ascribed to a bistable switch. Native switches are involved during the development of a multicellular organism [24] where the fate of cells results from complex inter-cellular interactions (see below). They are also observed in bacteria and single cell organisms (e.g. yeast) where the different phenotypes may result from multi-stable fixed points of the functional module dynamics (for a review see [25, 26]). For instance, bistability in gene expression was shown to be responsible for transitions in cell state such as cell competence [27, 28] (see appendix C) or sporulation [29] in *Bacillus subtilis* and sexual identity in yeast [30, 31].

Such a genetic switch was mimicked by introducing an artificial gene network decoupled from endogenous signalling pathways in bacteria [32, 33] and in yeast [34]. An important ingredient for these experimental models to function as a bistable switch seems to be the degree of cooperativity of the transcription factors regulating the genes of the network, namely, the requirement of strong nonlinearity in gene repression (or activation, see appendix C). One essential feature of a fate transition driven by a bistable switch is that at the transition point, the stochastic variation in the number of proteins in each bacterium allows the coexistence of two populations (phenotypes) each characterized by one of the fixed points. Consequently, while cells may be genetically identical (share the same genotype) they may exhibit a different phenotype.

The possibility of engineering desired biochemical pathways and networks in cells has given rise to a sub-domain of systems biology, known as synthetic biology. Inspired by the success of electrical solid state devices (transistors, micro-processors, memories, etc) researchers in that field are trying to develop functional modules (biochemical networks such as the just mentioned bistable switch) that perform logical functions [35], mimic cell–cell communication system [36] or exhibit oscillations [37]. Besides designing artificial networks in cells, there is also great effort to introduce metabolic pathways from one organism into another [38] (for example to graft the cellulose metabolism of the bacteria from termite guts into yeast to produce bio-ethanol). The experimental implementation of such networks is often not straightforward and a great deal is learnt on their regulation and their coupling to the general metabolism of the cell when attempting these grafts. The modelling of these networks is therefore both instructive and useful in helping to identify the key parameters that must be adjusted to get the sought after behaviour [39–41]. In particular, for oscillatory modules, the robustness of the desired response to fluctuations in the network's components and variation in its kinetic parameters is a key to its efficient implementation.

Even if a given function is successfully introduced into a cell, it has to be maintained over many generations. The evolutionary stability and evolvability of networks is a fundamental aspect of cell engineering which is still largely unexplored. In that respect, there has recently

been interesting experimental and theoretical investigations looking at the type of networks selected by evolutionary strategies to fulfil a desired function either in order to implement some artificial network *in vivo* [42] or to investigate the type of solutions arising *in silico* [43, 44]. Unravelling the rules behind the selection of certain solutions and being able to predict their probability of appearance in natural systems would represent a major advance in our understanding of the design principles of cellular networks.

The present approaches in systems biology consider the cell as a homogeneous medium where the components of a network diffuse and interact by the law of mass action. However, the spatial distribution of molecules inside a eukaryotic cell is not homogeneous: protein are targeted to specific structures (the nucleus, the membrane, etc) and they do not always diffuse freely: molecular motors actively transport molecules along the tracks of the cytoskeleton. Hence the structure of the cell appears to regulate the interaction between its constituents. How can these effects be incorporated in the theoretical framework of systems biology? What role do they play in cell differentiation where mechanical stresses on the cell membrane have been shown to influence the specialization of the cell into bone, muscle or neuronal tissue [45]?

4. Development

In multicellular organisms, cells are grouped to form tissues and organs. The foundations of morphogenesis, i.e., the developmental mechanisms by which organisms shape their form and patterns emerge can be traced back to influential works by D'Arcy Thompson in 1917 [47] and by Turing in 1952 [48]. In Turing's proposal, reaction–diffusion equations among appropriate signalling molecules (morphogens) provide a general framework for explaining the patterns observed in early development, the identity of a cell being set by the local value of the morphogen concentration [49]. However, while the existence of gradients and patterns of morphogens have now been firmly established, how these molecules interact both in space and in time to define a robust developmental programme is not fully understood. What type of nonlinear interactions among the various components of these networks (some of which may still be unknown) can explain the observed patterns and their precise spatial extent and temporal dynamics are basic questions that one has to elucidate. In this investigation of the possible mechanisms underlying morphogenesis one is helped (and constrained) by the fact that the developmental programme is surprisingly robust with respect to fluctuations in the environment (temperature, nutrients), in the concentration of morphogens and in the reaction rates (as a result of environmental fluctuations, genetic polymorphism or non-lethal mutations). For example, how do sharp boundaries of gene expression domains cope with the fluctuations of morphogens involved in the patterning of tissues [50, 51]? These observations suggest that a useful criterion to wean out theoretical models is to test their robustness to variations in concentrations, reaction rates, temperature, etc.

Appendix D illustrates some recent work where these issues were tackled and it exemplifies how the nonlinear degradation of morphogens could generate both robust and long range morphogen gradients. The mechanisms by which the degradation of morphogens might effectively be nonlinear are many. For instance the degradation of morphogens could be carried out by enzymes acting on morphogen dimers. In other cases (see for example [52]), an enzyme involved in the degradation pathway might be under control of the morphogen (the higher its concentration, the more enzyme is produced). Finally complex interactions among some components of a given pathway may give rise to non-exponential, i.e., robust, morphogen gradients. A very nice example of the use of nonlinear modelling in morphogenesis is presented

by dorso-ventral patterning in the fly. In this case Eldar *et al* [53] studied the robustness of the morphogen gradient to changes in its production rate (controlled by the number of copies of its gene). Since the topology of the regulation network was known (but not its nine kinetic parameters) they simulated the response of the network for values of the parameters varying by four orders of magnitude. Of the 66 000 tested network configurations, only 198 proved to be robust to changes in the morphogen production rate. These robust configurations were also immune to stochastic variation in the (small) number of interacting proteins. The robust networks were characterized by having a constraint on two of the network parameters, but not on the other seven. This helped identify the nonlinear mechanism responsible for the non-exponential and robust variation of the morphogen gradient. It also suggested a crucial test of the model: alter the constrained parameters and check the robustness of the response.

In these examples robustness to fluctuations in the morphogen concentration at the source was probed. However, as previously mentioned, the developmental programme is remarkably robust to many other perturbations. How these select the possible regulation networks and what constraints evolution imposes on the developmental programmes is not yet known. This brings us to an issue that is still largely unexplored: how does an organism achieve its correct size and proportion?

If a morphogen is produced at the head and degraded at the tail of an embryo, it has been proposed [54] that while its local concentration sets the cell's identity along the antero-posterior (AP) axis, its gradient determines the growth rate. When the gradient falls below a certain value growth stops. One then expects growth to stop far from the source much earlier than closer to it. This, however, is not the case. Growth stops almost instantly throughout the growing tissue. To explain what sets the mean size of organs, Shraiman [55] proposed that the local growth rate is set both by the morphogen concentration (growth increases monotonically when the morphogen concentration is above a certain threshold) and by the local stress P due to the differential growth rates (growth is maximal when the tissue is slightly under tension: $P_{\max} < 0$). The feedback provided by the local stress results in a more uniform growth rate and causes the tissue to stop growing when the cells further away from the morphogen source stop dividing. This mechanism may be used to set the size of the embryo and any other tissue, limb or in the case of the fly, its wing. The idea is appealing and merits further investigation. It is known that stresses can influence the developmental pathway of the fly [56] and are essential for proper bone development. However, little is know about how generic the use of tensile signalling in development is [56] and about what molecular mechanisms are used to couple these signals to gene expression [45]. With the existence of means to apply tensions locally in a tissue (for example optical and magnetic tweezers) these issues could now be tested and compared with robust theoretical models (see for example [57]).

5. Populations biology and evolution

Population biology has emerged as one of the first domains at the interface between mathematics and biology. From the beginning of the twentieth century, it gave rise to several fields ranging from population dynamics, to game theory and the modelling of adaptive evolution. These studies were seminal in many areas of nonlinear phenomena. The papers of Fisher in the 1930s on population dynamics [59] set the stage for nonlinear wave propagation through what became known as the Fisher–Kolmogorov equation. The seminal paper by May on the logistic map (inspired by a model of population dynamics [60]) introduced a generation of physicists to period doubling, chaos and nonlinear phenomena. Finally the rephrasing of game theory in the context of evolutionary biology has been exposed in great detail in the

excellent book by Maynard Smith [61]. In some sense, of all the contributions of nonlinear science to biology this is the most mature.

Over ecological time scales, the dynamics of a population of n individuals is a balance between its growth rate $g(n)$ and its death rate, $b(n)$: $\mathrm{d}n/\mathrm{d}t = g(n) - b(n)$. While the death rate of a population is usually assumed to grow linearly with n, $b(n) = bn$, its growth rate, while increasing with n, saturates at large n for the simple reason that the environmental resources are finite. For bacteria it has been shown by Monod [62] to be well fitted by $g(n) = an/(n_0 + n)$. However for mating populations, the growth rate at small population size may increase not linearly with n but for instance quadratically. This so called Allee effect [63] is crucial when considering the conservation of endangered species: it implies that there is a minimal size below which the population goes extinct. Spatial effects were also considered by Fisher in the case of diffusion of a bacterial population. If the death rate is sufficiently high so that the growth rate never saturates ($n \ll n_0$), it is easy to show that the Fisher–Kolmogorov equation for $x = an/n_0$ is obtained: $\mathrm{d}x/\mathrm{d}t = D\nabla^2 x + rx - x^2$ where $r = (a - bn_0)/n_0$.

Over evolutionary time scales, organisms in populations are selected on the basis of their reproductive efficiency with respect to environmental conditions. In order to assess this efficiency, Darwin introduced the concept of *fitness*. Two hundreds years later no general formulation of fitness has emerged yet, and evolutionary biologists still adapt its definition depending on the context. For instance, within clonal populations (of asexually reproducing individuals), the relative fitness w_{AB} of two sub-population (A and B, see appendix E) is defined with respect to their relative growth rates, $r_{A,B} = \mathrm{d}\ln n_{A,B}/\mathrm{d}t$, as $w_{AB} = r_A/r_B$. If A grown in competition with B outcompetes B then it is fitter than B (and $w_{AB} > 1$). Note that unlike energy, fitness is not a transitive property (see appendix E). While evolution occurs on large time scales, only instantaneous value of fitness can be deduced from the ecological dynamics of the population. This stresses the need to distinguish between ecological and evolutionary time scales in the formulation of the models.

Although most formulations of population dynamics are deterministic, several stochastic components may affect the dynamics. First, the intrinsic stochasticity caused by small numbers of individuals may lead to the extinction of the population (see appendix E). Second, genetic stochasticity may result in phenotypic variability within populations possibly affecting their dynamics. Finally, environmental fluctuations may affect differentially sub-populations. These empirical facts emphasize the need to incorporate stochasticity in the modelling of ecological and evolutionary processes. This was introduced for instance in evolutionary game theory where mixed and conditional strategies correspond to playing several pure strategies with different probabilities (see the book by Hofbauer and Sigmund [64] for a remarkable overview of game theory and population dynamics). Later on, it has been extensively done using agent-based simulations (as in cellular automata [65]), in particular to highlight the role of the interaction range (or spatial structure) on the outcome (see appendix E). The birth–death processes represent also a noteworthy attempt to rephrase population dynamics in a more stochastic manner that are, however, still confined to a few particular cases such as Lotka–Volterra dynamics [66]. Could this be extended to the study of other challenging issues like cooperation which may involve higher order nonlinearities? Which types of models (deterministic versus stochastic) are more relevant when confronted to experimental data?

On evolutionary time scales, the major challenge is to define a framework allowing the derivation of the evolutionary dynamics of a phenotype (e.g. a given trait such as height) from the ecological dynamics of the considered population. For the last two decades, adaptive dynamics (AD) has filled this gap, but their ecological relevance is still questioned (see the review by Waxman and Gavrilets [67] and the following comments in the same issue of *Journal of Evolutionary Biology*). Due to the dependence of this kind of evolutionary model

upon ecological ones, the nonlinear and stochastic features of the latter will necessarily be included in the former. More generally, is adaptation a continuous phenomena or are there abrupt first order transitions? Moreover how can one interlink the different levels of description of evolutionary models (from molecular to phenotypic descriptions)?

In fact, in these investigations, one is not hampered by the lack of theoretical approaches but by the dearth of experimentally controlled and reproducible data. Much ecological and evolutionary data is gathered from field studies in which conditions are tough to control, almost impossible to reproduce and with an outcome that is difficult to predict. Thus, even if various theoretical models fit the data, the uncertainty of the many uncontrolled parameters does not allow us to identify the most relevant one. However, while the evolution of most ecological systems is impossible to study on a human time scale, the ecology of microbial systems is still widely open for experimental investigations. One challenge is to devise long-term self-contained systems replicated many times and probing some well-defined question in evolution. Only then will we be able to compare quantitatively experimental observations and theoretical predictions, measure the probability of certain evolutionary scenarios and test issues of intrinsic stochasticity and robustness.

6. Conclusion

From proteins to genes and from organisms to populations, biological systems display recurrent themes: the nonlinearity of the interactions; the effects of fluctuations arising from environmental variations and the stochasticity inherent in the discreteness and small numbers of players (molecules, cells, individuals); the robustness of the response to these variations and to variation in many of the systems parameters (arising for example from mutations); the role played by evolution both in selecting the present systems and in their possibility to adapt in response to their environment and evolve (their evolvability). The last two themes, robustness and evolvability present contradictory requirements. While robustness implies stability with respect to external and internal perturbations, evolvability requires a measure of adaptation to these variations. How is the compromise between these constraints reached? A possible way out of this conundrum is suggested by the fact that robust processes coupled with the stochasticity arising from the small number of players can give rise to a minority of different phenotypes upon which selection can act.

Although the issues mentioned above can be addressed theoretically, they should also be tackled experimentally. Biology is witnessing a profound transition: from the essentially observational science of the last centuries to a quantitative discipline based on reverse engineering of complex systems: it aims to understand life as it is, not as it could be. The concepts of symmetry and universality which underlie the comprehension of physical systems from magnetism to chaos are of little use in biology where the devil is in the details. As a consequence generic models (e.g. a Landau–Ginzburg type of approach) elicit usually limited interest among biologists. While presenting a real challenge for a theorist, it is only by a thorough understanding of the experimental details that one may expect to build useful models from which hopefully some general evolutionary design principles will be learnt.

Acknowledgments

We acknowledge the financial support from CNRS, from ANR through the ANR-06-PCVI-0005 grant, from HFSP through the RGP003/2007 grant and from EU through a Bio-Nanoswitch grant.

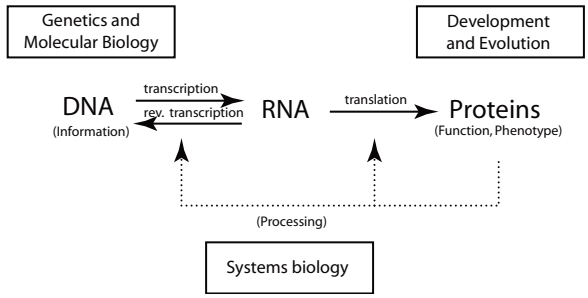

Figure A1. Central dogma of molecular biology.

Appendix A. Some biological notions

Because of their common ancestry all life forms share common motifs (enzymes, metabolic and regulation pathways, etc). The most fundamental one common to most, and dubbed 'the central dogma of molecular biology' (figure A1), is that information is encoded in the famed double helix of the DNA molecule (in the form of genes, i.e., DNA sequences encoding for proteins, regulatory sequences controlling the expression of the genes and an often large portion of DNA of unknown role). To give rise to proteins this information is first transcribed into messenger RNA, mRNA (by enzymes known as RNA-polymerases) and then translated into proteins (by a complex of tens of proteins and ribosomal RNA (rRNA), known as the ribosome). Life forms are mainly divided into two types: prokaryotes, which are single cell organisms lacking a nucleus (essentially a bag of DNA and enzymes enclosed by a lipidic membrane) that appeared about 3.5 billion years ago, and eukaryotes, which are cells with a structured environment possessing a number of so-called organelles (nucleus, mitochondria, etc) that probably evolved from prokaryotes about 1 billion years ago. Within a few hundred million years multicellular organisms appeared first as an assembly of eukaryotic cells and then as more complex organisms with cells specializing into tissues and organs. To proliferate cells divide after having replicated their DNA (with enzymes known as DNA-polymerases). In multicellular organisms, even though all the cells originate from the same initial one (a so-called monoclonal population sharing the same genotype), they specialize ('differentiate') to fill different function (i.e., adopt different phenotypes: skin, muscle, neuron, bone, etc). While the DNA molecule in these differentiated cells is the same, the pattern of expression of the encoded genes (i.e., the concentrations of the various proteins) is not. This pattern is under control of proteins known as transcription factors that bind to the regulatory sequences on the DNA and modulate gene expression. These transcription factors are themselves part of more general signalling networks that play a central role in development by coordinating the differentiation of cells within a given organism. The field in biology that studies gene networks and uses nonlinear modelling to describe them has recently acquired the name of systems biology [23].

Appendix B. Fluctuating enzymatic activity

The catalytic activity of many enzymes is well described by the Michaelis–Menten (MM) kinetics: the enzyme E binds its substrate S forming a complex ES to yield the product P while regenerating the enzyme for the next catalytic cycle (see figure B1(a)). The model assumes that the enzyme has a unique catalytic state, with

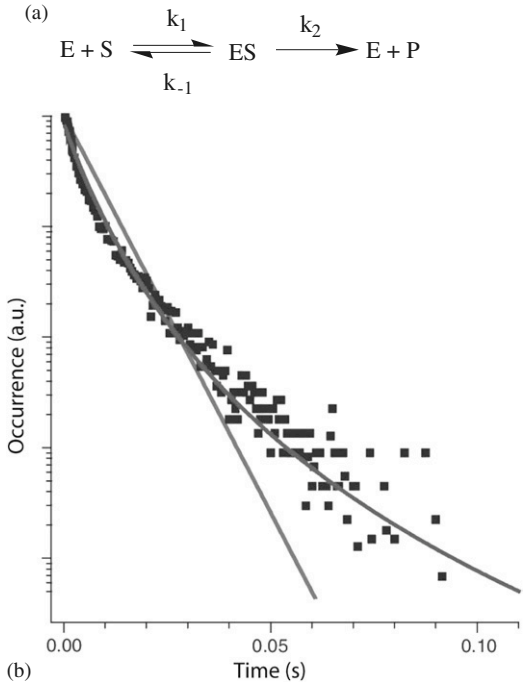

Figure B1. (*a*) Traditional interpretation of Michaelis–Menten kinetics for enzymatic reactions. (*b*) Histogram of enzymatic cycle times for a single β-galactosidase enzyme. Adapted by permission from Macmillan Publishers Ltd from [12], copyright (2006).

corresponding unique reaction rates (k_1, k_{-1}, k_2). The catalytic rate $(v = \mathrm{d}[P]/\mathrm{d}t)$ is given by

$$v = \frac{v_{\max}[S]}{[S] + K_M},$$

where the brackets [..] denote the concentration and $K_M = (k_{-1} + k_2)/k_1$ is known as the MM constant. MM dynamics is normally used to describe biochemical assays, where billions of copies of the same enzyme are involved, but a single molecule version of the Michaelis–Menten dynamics can be formulated in terms of the average time between two successive turnovers. Because the enzymatic cycle is a stochastic variable, for a MM enzyme one expects it to be exponentially distributed. However, this was not observed [12]. As shown in figure B1(*b*) the cycle time histogram for the enzyme β-galactosidase is better fit by a multi-exponential curve (curved line) than by a single exponential one (straight line). These results suggests that the catalytic (functional) conformation of an enzyme is not unique. The enzyme fluctuates between a large number of active configurations each with its own reaction rates. How general is this result? Under certain assumptions concerning the transition rates between the various states it was shown to be consistent with MM behaviour, but whether this can lead to non-MM kinetics in more general cases and how biologically, i.e., evolutionary, significant this process is, are still open questions.

Appendix C. Bistability in gene expression

Switching behaviour in biological systems is observed in many circumstances ranging from developmental biology to microbiology. The interpretation of morphogen gradients (see

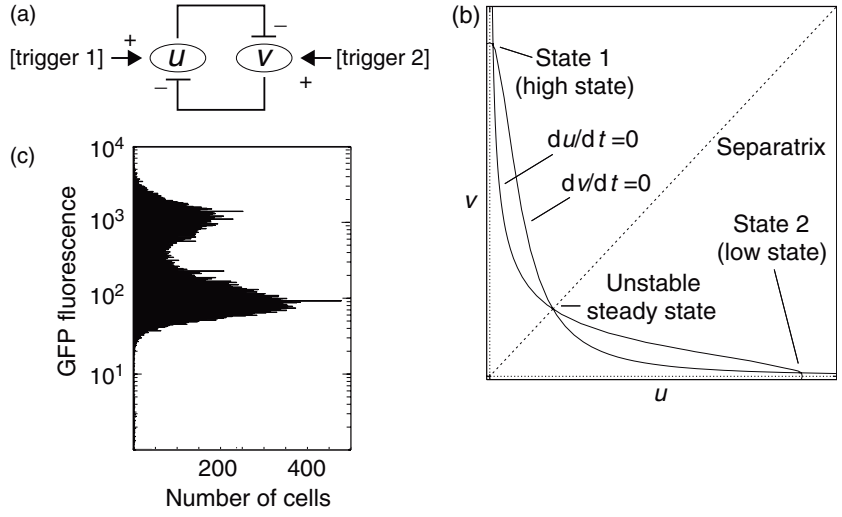

Figure C1. (*a*) Double negative feedback loop. In this circuit, two proteins A and B mutually repress each other. Reprinted from [25], Copyright (2002), with permission from Elsevier. (*b*) Phase space of the steady state solutions of the system described in (*a*). Reprinted by permission from Macmillan Publishers Ltd from [32], Copyright (2000). (*c*) Histogram of a population of cells near the bifurcation point (protein expression is monitored with fluorescent reporter). Adapted by permission from Macmillan Publishers Ltd from [32], Copyright (2000).

appendix D), which control well-defined stripe-like domains in a developing fly embryo, requires the conversion of a graded signal into an all-or-none differentiation response [46]. In the bacterium *Bacillus subtilis*, the ability to withstand stress conditions results from a switch between two states: a default non-competent state and a competent one. In the latter, the bacterium is able to incorporate DNA from the surrounding medium in the 'hope' of acquiring genetic features that will allow it to survive in the new conditions [27,28]. To model this behaviour, synthetic gene networks were engineered. Depending on the environmental conditions, which act on regulatory proteins, elementary circuits such as double-negative feedback loop (figure C1(*a*)) or positive feedback loop were shown to display bistable behaviour. In the bacterium *Escherichia coli*, a synthetic double-negative feedback circuit was engineered with two mutually repressing genes, whose products concentrations (u,v) are described by the equations [32]:

$$\frac{\mathrm{d}u}{\mathrm{d}t} = \frac{\alpha_1}{1+v^\beta} - u,$$
$$\frac{\mathrm{d}v}{\mathrm{d}t} = \frac{\alpha_2}{1+u^\gamma} - v.$$

The first term on the RH describes the repression of one gene by the product(s) (e.g. protein) of the other gene. The second term accounts for the degradation of these proteins. α_i is the effective rate of synthesis of the repressor protein i. β and γ are the degrees of cooperativity (i.e., the number of proteins required for effective gene repression). If $\beta, \gamma > 1$ and $\alpha_1 \approx \alpha_2$, this system has two stable equilibrium points (figure C1(*b*)). The capacity of achieving multiple internal states in response to a single set of external inputs is noticeable in a population of clonal (i.e., genetically identical) cells. Indeed, the noise in gene expression may often be enough to project the cell into one of the two stable states (also known as phenotypes). This is most easily demonstrated by putting a fluorescent reporter protein under the control of one of the

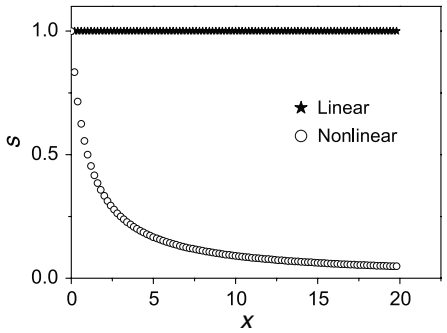

Figure D1. Sensitivity of the morphogen concentration with respect to fluctuations at the source when its degradation is linear or nonlinear.

gene products studied. As shown in figure C1(c) the distribution of fluorescence is bimodal. Thus, elementary gene network can convert graded input into a toggle switch.

Appendix D. Morphogens and development

Morphogens are molecules whose spatio-temporal concentration gradients provide positional information to the embryonic cells. The model of reference is the so-called 'french-flag' model [49] where the colours of the flag are determined by various thresholds of a putative morphogen gradient. This gradient is established via localized synthesis and subsequent diffusion as well as degradation within the embryo. As it is used to determine cell fate the gradient must be robust (with respect to fluctuation in production rate) and it must extend far enough (many cells) from its source to be useful. A simple model of localized synthesis and diffusion with linear decay rate generates an exponential gradient for the morphogen. With this type of gradient, robustness and long range cannot be achieved simultaneously (a long range gradient is not robust). If, however, the decay rate of the morphogen is nonlinear (for example if it is enzymatically degraded only in dimeric form) the gradient obtained can be both long range and robust [58]. Let us see how these conclusion can be easily derived. The diffusion equations for a morphogen whose degradation depends linearly or nonlinearly on the concentration can be written as

$$\frac{\partial L}{\partial t} = D\nabla^2 L - \alpha L \qquad \text{or} \qquad \frac{\partial L}{\partial t} = D\nabla^2 L - \beta L^n,$$

where D is the diffusion constant and α (β) is the linear (nonlinear) degradation rate. The corresponding steady-state solutions are

$$L(x) = L_0 \mathrm{e}^{\frac{-x}{\Delta_d}} \qquad \text{or} \qquad L(x) = \frac{A}{(x+\epsilon)^m},$$

where $\Delta_\mathrm{d} = \sqrt{D/\alpha}$, $m = 2/(n-1)$, $A = (Dm(m-1)/\beta)^{2/m}$, $\epsilon = (A/L_0)(1/m)$ and L_0 is the morphogen concentration at the source. A change in L_0 will modify the morphogen level everywhere, causing a shift in the cell fate boundary. One defines the sensitivity s to fluctuations in production rate as the relative change in the morphogen concentration $L(x)$ for a relative change in the concentration at the source: $s = \partial \ln L/\partial \ln L_0$. For linear decay rate the sensitivity is constant ($s = 1$). For nonlinear degradation, $s = \epsilon/(x+\epsilon)$, in other words the further away a cell is from the morphogen source the less sensitive it is to changes in its production rate and the more robust its fate is (see figure D1). Nonlinear decay of morphogen

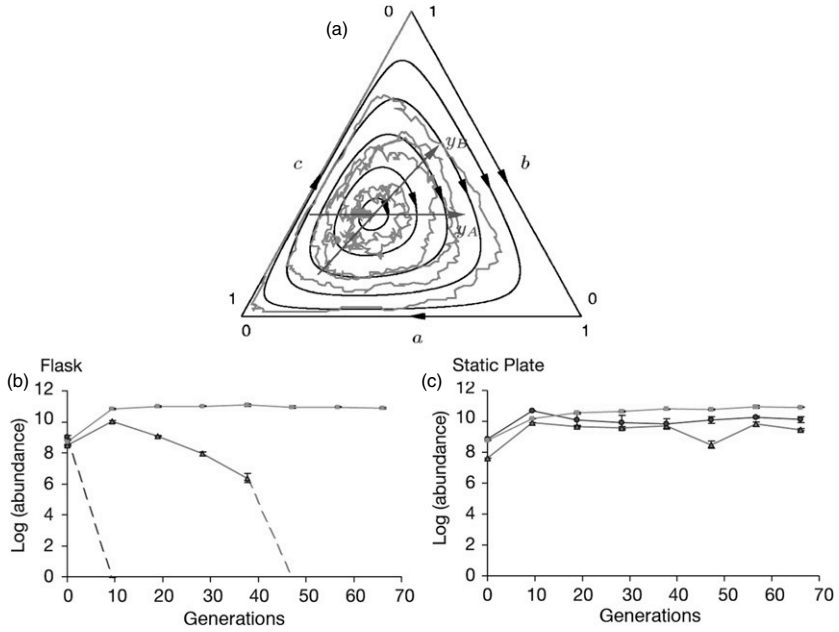

Figure E1. (*a*) Phase space diagram for the three species in a rock–paper–scissors game, showing the predicted cycles around an elliptic fixed point. The erratic flow denotes the trajectory obtained from a stochastic simulation with $N = 200$ agents: it spirals out to reach one of the three trivial fixed points (with only one population surviving). Reprinted with permission from [68]. Copyright (2006) by the American Physical Society. (*b*), (*c*) Results of an experimental realization of the game in bacteria: (*b*) when the experiment is conducted in a well-mixed flask; (*c*) when the experiment is conducted on an agar plate where the interaction range is smaller. Reprinted by permission from Macmillan Publishers Ltd from [71], Copyright (2002).

gradient has been reported in the dorso-ventral polarity of the fly and the patterning of its wing [58]. It could be crucial for establishing a long range and robust gradient of the relevant morphogens.

Appendix E. *In vivo* rock–paper–scissors game in bacteria

Consider a system of three bacterial strains where strain A outcompetes B, strain B dominates over C, and strain C in turn outperforms A, where γ, α and β are the respective competition coefficients. The dynamics of these strains densities (respectively, a, b, c) can be written as

$$\begin{aligned} \dot{a} &= a\,(\gamma b - \beta c) \qquad & A + B &\xrightarrow{\gamma} A + A, \\ \dot{b} &= b\,(\alpha c - \gamma a) \qquad & B + C &\xrightarrow{\alpha} B + B, \\ \dot{c} &= c\,(\beta a - \alpha b) \qquad & C + A &\xrightarrow{\beta} C + C. \end{aligned}$$

These equations possess three trivial stable fixed points $(1, 0, 0)$, $(0, 1, 0)$ and $(0, 0, 1)$ (only one of the three strains survives), and one elliptic fixed point (a^*, b^*, c^*) corresponding to coexistence of the three strains. Solutions for this equation can be computed for a variety of initial conditions, which yield stable cycles around (a^*, b^*, c^*) as shown in the phase space diagram (figure E1(*a*)). Using stochastic simulations, fluctuations in finite populations are shown to destabilize these orbits: single trajectories spiral out from (a^*, b^*, c^*), eventually reaching one of the three trivial fixed points. To experimentally study this type of dynamical

problems toxin secreting bacteria [69, 70] were used. Consider three types of bacteria: type A secretes a toxin (colicin) and is resistant to it; type C possesses only the resistance, while type B is not burdened by the production and secretion of the toxin nor by the production of the resistance to it. As a result, B outgrows C, which overcomes A which kills B. That ecological system has been studied when the system is well mixed (corresponding to the case where every bacterium can interact with every other) and when it grows on solid agar plates (where the bacteria interact with their neighbours). In the former case, one strain outcompetes the others in accordance with the stochastic simulations (figure E1(b)); in the later, dynamic coexistence can be observed over many generations (figure E1(c). These results emphasize the importance of the interaction range in the dynamical outcome: stochastic simulations have been widely used to show that local interactions favour cooperation but more general analytical studies are still rare (see [72]) and long-term experimental investigations almost non-existent.

References

[1] Bon M, McGowan S J and Cook P R 2006 Many expressed genes in bacteria and yeast are transcribed only once per cell cycle *FASEB J.* **20** 1721–3 (PMID: 16818468)

[2] Burgers P M and Kornberg A 1983 The cycling of *Escherichia coli* DNA polymerase iii holoenzyme in replication *J. Biol. Chem.* **258** 7669–75 (PMID: 6345527)

[3] Shnerb N M, Louzoun Y, Bettelheim E and Solomon S 2000 The importance of being discrete: life always wins on the surface *Proc. Natl Acad. Sci. USA* **97** 10322–4 (PMID: 10962027)

[4] Amonlirdviman K, Khare N A, Tree D R P, Chen W-S, Axelrod J D and Tomlin C J 2005 Mathematical modeling of planar cell polarity to understand domineering nonautonomy *Science* **307** 423–6 (PMID: 15662015)

[5] Gerhart J and Kirschner M 1997 *Cells, Embryos, and Evolution: Toward a Cellular and Developmental Understanding of Phenotypic Variation and Evolutionary Adaptability* 1st edn (Oxford: Blackwell)

[6] Helles G 2008 A comparative study of the reported performance of ab initio protein structure prediction algorithms *J. R. Soc. Interface/R. Soc.* **5** 387–96 (PMID: 18077243)

[7] Anfinsen C B, Haber E, Sela M and White F H 1961 The kinetics of formation of native ribonuclease during oxidation of the reduced polypeptide chain *Proc. Natl Acad. Sci. USA* **47** 1309–14 (PMID: 13683522)

[8] Anfinsen C B 1973 Principles that govern the folding of protein chains *Science* **181** 223–30 (PMID: 4124164)

[9] Austin R H, Beeson K W, Eisenstein L, Frauenfelder H and Gunsalus I C 1975 Dynamics of ligand binding to myoglobin *Biochemistry* **14** 5355–73 (PMID: 1191643)

[10] Frauenfelder H, Sligar S G and Wolynes P G 1991 The energy landscapes and motions of proteins *Science* **254** 1598–603 (PMID: 1749933)

[11] Henzler-Wildman K and Kern D 2007 Dynamic personalities of proteins *Nature* **450** 964–72 (PMID: 18075575)

[12] English B P, Min W, van Oijen A M, Lee K T, Luo G, Sun H, Cherayil B J, Kou S C and Xie X S 2006 Ever-fluctuating single enzyme molecules: Michaelis–Menten equation revisited *Nat. Chem. Biol.* **2** 87–94

[13] Edman L, Foldes-Papp Z, Wennmalm S and Rigler R 1999 The fluctuating enzyme: a single molecule approach *Chem. Phys.* **247** 11–22

[14] Flomenbom O *et al* 2005 Stretched exponential decay and correlations in the catalytic activity of fluctuating single lipase molecules *Proc. Natl Acad. Sci. USA* **102** 2368–72 (PMID: 15695587)

[15] Deniz A A, Dahan M, Grunwell J R, Ha T, Faulhaber A E, Chemla D S, Weiss S and Schultz P G 1999 Single-pair fluorescence resonance energy transfer on freely diffusing molecules: observation of förster distance dependence and subpopulations *Proc. Natl Acad. Sci. USA* **96** 3670–5 (PMID: 10097095)

[16] Hanson J A, Duderstadt K, Watkins L P, Bhattacharyya S, Brokaw J, Chu J-W and Yang H 2007 Illuminating the mechanistic roles of enzyme conformational dynamics *Proc. Natl Acad. Sci. USA* **104** 18055–60 (PMID: 17989222)

[17] Henzler-Wildman K A, Lei M, Thai V, Kerns S J, Karplus M and Kern D 2007 A hierarchy of timescales in protein dynamics is linked to enzyme catalysis *Nature* **450** 913–6 (PMID: 18026087)

[18] Henzler-Wildman K A *et al* 2007 Intrinsic motions along an enzymatic reaction trajectory *Nature* **450** 838–44 (PMID: 18026086)

[19] Xue X, Liu F and Ou-Yang Z-C 2006 Single molecule michaelis–menten equation beyond quasistatic disorder *Phys. Rev. E, Stat. Nonlinear Soft Matter Phys.* **74** 030902 (PMID: 17025584)

[20] Min W, Gopich I V, English B P, Kou S C, Xie X S and Szabo A 2006 When does the michaelis–menten equation hold for fluctuating enzymes? *J. Phys. Chem.* B **110** 20093–7 (PMID: 17034179)

[21] Aharoni A, Gaidukov L, Khersonsky O, McQ Gould S, Roodveldt C and Tawfik D S 2005 The 'evolvability' of promiscuous protein functions *Nature Genetics* **37** 73–6 (PMID: 15568024)
[22] Shen-Orr S S, Milo R, Mangan S and Alon U 2002 Network motifs in the transcriptional regulation network of *Escherichia coli Nature Genetics* **31** 64–8 (PMID: 11967538)
[23] Alon U 2006 *An Introduction to Systems Biology: Design Principles of Biological Circuits* 1st edn (London/Boca Raton, FL: Chapman and Hall/CRC)
[24] Ferrell J E and Machleder E M 1998 The biochemical basis of an all-or-none cell fate switch in xenopus oocytes *Science* **280** 895–8 (PMID: 9572732)
[25] Ferrell J E 2002 Self-perpetuating states in signal transduction: positive feedback, double-negative feedback and bistability *Curr. Opin. Cell Biol.* **14** 140–8 (PMID: 11891111)
[26] Dubnau D and Losick R 2006 Bistability in bacteria *Mol. Microbiol.* **61** 564–72 (PMID: 16879639)
[27] Süel G M, Kulkarni R P, Dworkin J, Garcia-Ojalvo J and Elowitz M B 2007 Tunability and noise dependence in differentiation dynamics *Science* **315** 1716–9 (PMID: 17379809)
[28] Maamar H, Raj A and Dubnau D 2007 Noise in gene expression determines cell fate in bacillus subtilis *Science* **317** 526–9 (PMID: 17569828)
[29] González-Pastor J E, Hobbs E C and Losick R 2003 Cannibalism by sporulating bacteria *Science* **301** 510–3 (PMID: 12817086)
[30] Andrews S S and Arkin A P 2007 Systems biology: a switch for sex *Curr. Biol.: CB* **17** R410–2 (PMID: 17550765)
[31] Ingolia N T and Murray A W 2007 Positive-feedback loops as a flexible biological module *Curr. Biol.: CB* **17** 668–77 (PMID: 17398098)
[32] Gardner T S, Cantor C R and Collins J J 2000 Construction of a genetic toggle switch in *Escherichia coli Nature* **403** 339–42 (PMID: 10659857)
[33] Atkinson M R, Savageau M A, Myers J T and Ninfa A J 2003 Development of genetic circuitry exhibiting toggle switch or oscillatory behavior in *Escherichia coli Cell* **113** 597–607 (PMID: 12787501)
[34] Becskei A, Séraphin B and Serrano L 2001 Positive feedback in eukaryotic gene networks: cell differentiation by graded to binary response conversion *EMBO J.* **20** 2528–35 (PMID: 11350942)
[35] Guet C C, Elowitz M B, Hsing W and Leibler S 2002 Combinatorial synthesis of genetic networks *Science* **296** 1466–70 (PMID: 12029133)
[36] Basu S, Gerchman Y, Collins C H, Arnold F H and Weiss R 2005 A synthetic multicellular system for programmed pattern formation *Nature* **434** 1130–4 (PMID: 15858574)
[37] Elowitz M B and Leibler S 2000 A synthetic oscillatory network of transcriptional regulators *Nature* **403** 335–8 (PMID: 10659856)
[38] Martin V J J, Pitera D J, Withers S T, Newman J D and Keasling J D 2003 Engineering a mevalonate pathway in *Escherichia coli* for production of terpenoids *Nature Biotechnol.* **21** 796–802 (PMID: 12778056)
[39] Thattai M and van Oudenaarden A 2001 Intrinsic noise in gene regulatory networks *Proc. Natl Acad. Sci. USA* **98** 8614–9 (PMID: 11438714)
[40] Swain P S, Elowitz M B and Siggia E D 2002 Intrinsic and extrinsic contributions to stochasticity in gene expression *Proc. Natl Acad. Sci. USA* **99** 12795–800 (PMID: 12237400)
[41] Paulsson J 2004 Summing up the noise in gene networks *Nature* **427** 415–8 (PMID: 14749823)
[42] Yokobayashi Y, Weiss R and Arnold F H 2002 Directed evolution of a genetic circuit *Proc. Natl Acad. Sci. USA* **99** 16587–91 (PMID: 12451174)
[43] François P and Hakim V 2004 Design of genetic networks with specified functions by evolution in silico *Proc. Natl Acad. Sci. USA* **101** 580–5 (PMID: 14704282)
[44] François P, Hakim V and Siggia E D 2007 Deriving structure from evolution: metazoan segmentation *Mol. Syst. Biol.* **3** 154 (PMID: 18091725)
[45] Engler A J, Sen S, Sweeney H L and Discher D E 2006 Matrix elasticity directs stem cell lineage specification *Cell* **126** 677–89 (PMID: 16923388)
[46] Clyde D E, Corado M S G, Wu X, Paré A, Papatsenko D and Small S 2003 A self-organizing system of repressor gradients establishes segmental complexity in drosophila *Nature* **426** 849–53 (PMID: 14685241)
[47] Thompson D W 1992 *On Growth and Form: The Complete Revised Edition*. (New York: Dover)
[48] Turing A M 1952 The chemical basis of morphogenesis *Phil. Trans. R. Soc. Lond.* B **237** 37–72
[49] Wolpert L, Smith J, Jessell T, Lawrence P, Robertson E and Meyerowitz E 2006 *Principles of Development* 3rd edn (New York: Oxford University Press)
[50] Gregor T, Tank D W, Wieschaus E F and Bialek W 2007 Probing the limits to positional information *Cell* **130** 153–64 (PMID: 17632062)
[51] Gregor T, Wieschaus E F, McGregor A P, Bialek W and Tank D W 2007 Stability and nuclear dynamics of the bicoid morphogen gradient *Cell* **130** 141–52 (PMID: 17632061)

[52] Eldar A, Shilo B-Z and Barkai N 2004 Elucidating mechanisms underlying robustness of morphogen gradients *Curr. Opin. Genetics Dev.* **14** 435–9 (PMID: 15261661)
[53] Eldar A, Dorfman R, Weiss D, Ashe H, Shilo B-Z and Barkai N 2002 Robustness of the bmp morphogen gradient in drosophila embryonic patterning *Nature* **419** 304–8 (PMID: 12239569)
[54] Day S J and Lawrence P A 2000 Measuring dimensions: the regulation of size and shape *Development* **127** 2977–87 (PMID: 10862736)
[55] Shraiman B I 2005 Mechanical feedback as a possible regulator of tissue growth *Proc. Natl Acad. Sci. USA* **102** 3318–23 (PMID: 15728365)
[56] Farge E 2003 Mechanical induction of twist in the drosophila foregut/stomodeal primordium *Curr. Biol.: CB* **13** 1365–77 (PMID: 12932320)
[57] Morante J, Desplan C and Celik A 2007 Generating patterned arrays of photoreceptors *Curr. Opin. Genetics Dev.* **17** 314–9 (PMID: 17616388)
[58] Eldar A, Rosin D, Shilo B-Z and Barkai N 2003 Self-enhanced ligand degradation underlies robustness of morphogen gradients *Dev. Cell* **5** 635–46 (PMID: 14536064)
[59] Fisher R A 1937 The wave of advance of advantageous genes *Ann. Eugenics* **7** 355–369
[60] May R M 1976 Simple mathematical models with very complicated dynamics *Nature* **261** 459–67 (PMID: 934280)
[61] Smith J M 1998 *Evolutionary Genetics* 2nd edn (Oxford: Oxford University Press)
[62] Monod J 1972 *Recherche sur la Croissance des Cultures Bacteriennes* (Paris: Hermann & Cie)
[63] Stephens P A, Sutherland W J and Freckleton R P 1999 What is the allee effect? *OIKOS* **87** 185–190
[64] Hofbauer J and Sigmund K 1998 *Evolutionary Games and Population Dynamics* (Cambridge: Cambridge University Press)
[65] Doebeli M and Hauert C 2005 Models of cooperation based on the prisoner's dilemma and the snowdrift game *Ecol. Lett.* **8** 748–766
[66] Gutiérrez R and Rosales M J 1998 Diffusion approximations for lotka? volterra type models *Stochastic Models* **14** 809
[67] Waxman D and Gavrilets S 2005 20 questions on adaptive dynamics *J. Evol. Biol.* **18** 1139–54 (PMID: 16135102)
[68] Reichenbach T, Mobilia M and Frey E 2006 Coexistence versus extinction in the stochastic cyclic lotka-volterra model *Phys. Rev. E, Stat. Nonlinear Soft Matter Phys.* **74** 051907 (PMID: 17279939)
[69] James R, Kleanthous C and Moore G R 1996 The biology of e colicins: paradigms and paradoxes *Microbiology* **142** 1569–80 (PMID: 8757721)
[70] Riley M A and Gordon D M 1999 The ecological role of bacteriocins in bacterial competition *Trends Microbiol.* **7** 129–33 (PMID: 10203843)
[71] Kerr B, Riley M A, Feldman M W and Bohannan B J M 2002 Local dispersal promotes biodiversity in a real-life game of rock-paper-scissors *Nature* **418** 171–4 (PMID: 12110887)
[72] Le Galliard J-F, Ferrière R and Dieckmann U 2003 The adaptive dynamics of altruism in spatially heterogeneous populations *Evolution* **57** 1–17 (PMID: 12643563)

A.3 ARTICLE DRAFT ON PYOVERDINE

This article draft summarises our most significant results obtained with *P. aeruginosa*. It is shown in a very preliminary stage of work since recent efforts have been focused on confirming the interpretation of pyoverdine concentration fluctuations in terms of stochastic switch.

Stochastic phenotypic fluctuations in a clonal population of *Pseudomonas aeruginosa*

Thomas Julou, Laurent Guillon, Isabelle Schalk, Vincent Croquette, David Bensimon, and Nicolas Desprat

(Dated: April 25, 2011)

ABSTRACT

Microorganisms secrete siderophores, small chelating peptides, as a mean to acquire iron from the environment. In bulk co-culture experiments, this situation is prone to exploitation by mutants that do not bear the metabolic costs of production. Here, we study the variability of siderophore distribution in a clonal population of the bacterium *Pseudmomonas aeruginosa* grown on an agar gel. The endogenous fluorescence of pyoverdine, the main siderophore, allow us to investigate its dynamics across different cells and over eight generations initiated from a single clone. Surprisingly we observe that bacteria switch stochastically between two phenotypes: a pyoverdine hoarding one exhibiting increasing fluorescence and a pyoverdine dumping one displaying decreasing internal fluorescence. The switching probability appears to depend on the relative concentration of pyoverdine. As a result the distribution of free internal siderophores is very broad with a mean and variance increasing proportionately with time.

INTRODUCTION

The dynamics of usage of public goods in a bacterial population is a problem of importance in order to understand the robustness of various evolutionary strategies. A central idea behind the maintenance of cooperation (e.g. production of a public good) in a bacterial population has been formulated by Hamilton [4]. It explains the stability of cooperation in spite of its cost by the advantage it confers on genetically related organisms. A common assumption is that bacteria adopt a given strategy (”cooperator” (producer) or ”cheater” (non-producer)). In batch cultures, while Hamilton's rule predict that the population will collapse due to its susceptibility to invasion by cheaters, a stable mixed population of producers and non-producers can be achieved if the benefits and costs are non-linear functions of the frequency [1, 3]. In spatially structured environment such as agar plates, a population of producers can also be stable towards invasion by non-producers if the public good diffuses over a small range, so that the mutual benefits of cooperation are limited to the immediate neighborhood (i.e. with individuals that are likely to be related) of the producers.

In that respect, bacterial populations studies at the single-cell level present a case model for a controlled investigation of these issues, in particular with respect to the dynamics of iron usage. Life needs iron as a co-factor for many enzymatic reactions, such as photosynthesis, N_2 fixation, methanogenesis, H_2 production and consumption, respiration, the trichloroacetic acid (TCA) cycle, oxygen transport, gene regulation and DNA biosynthesis (Andrews (2003)). However iron under its prevalent oxidized (ferric) form Fe^{3+} is insoluble ($c \simeq 10^{-18}$M at pH=7). To be imported into bacteria to a physiological level (on the order of the micromolar) it has to form complexes with specific iron chelators known as siderophores. These are most often low molecular mass peptides assembled via non-ribosomal peptide synthetases and secreted and imported through specific channels. Since siderophores produced and secreted by a given bacteria can be used by all (even sometimes by other species) their usage present a typical case of a public good. In the case of *P. aeruginosa*, the main secreted siderophore pyoverdine (Pvd) is fluorescent when not complexed with iron, which is convenient for monitoring its dynamics (a minor one pyocheline has lower affinity for iron).

Pyoverdines are oligopeptides assembled by a non-ribosomal peptide synthetase (NRPS) chain of reactions. The maturation of Pvd begins in the cytoplasm and ends in the periplasm where it becomes fluorescent. Whereas pyoverdine synthesis and its uptake channel are by now well characterized [10], the pathway controlling its export remains unclear. It is likely to be then

secreted in the environment mainly through the efflux pump PvdRT-OpmQ [5]. Once released in solution Pvd binds to iron and its fluorescence is quenched. Upon diffusion, the Pvd-Fe complex is imported through two channels: FpvA, the main import channel and FpvB. Upon entering the periplasm, iron is dissociated from its complex with Pvd and imported in the cytoplasm through an ABC transporter. Pvd is then recycled and re-exported outside the cell for another round of iron binding [6, 8]. Pvd uptake triggers the binding of an anti-sigma factor (FpvR) to FpvA, which enables two extracytoplasmic function sigma factors, to trigger the transcription of Pvd import and synthesis genes. The whole regulation module can be seen as a positive feedback on pyoverdine synthesis.

The genes involved in pyoverdine mediated iron uptake are part of a genome region coding for the enzymes required for Pvd synthesis (NRPS), an efflux pump for Pvd secretion and an import channel (FpvA) for its uptake[7]. Their expression is controlled by the two sigma factors mentioned above, PvdS and FpvI. PvdS controls production by initiating transcription of the NRPS-genes and FpvI controls uptake by initiating transcription of FpvA. As intracellular iron concentration increases, iron binds to Fur (a master repressor), which inhibits the transcription initiated by the two sigma factors.

In this work we have studied the dynamics of pyoverdine usage in a clonal population of PAO1 the laboratory strain of P.Aeruginosa growing in 2D on an agar plate, in conditions where growth was either iron limited or not. Contrary to expectations, in both cases we observed that the bacteria did not adopt a fixed strategy with respect to pyoverdine usage, but rather stochastically switched between two phenotypes: hoarding pyoverdine inside the cell and dumping it in the environment. We have observed that the probability of changing strategies depends non-linearly on the pyoverdine relative concentration in the colony (sensibly at low relative concentrations bacteria hoard pyoverdine while at high relative concentrations they dump it). This random phenotypic switch leads to a population displaying a huge variance in its free internal pyoverdine concentration. A simple, parameter-free analytically soluble model of that switch reproduces the main features of our observations, namely the distribution of pyoverdine concentrations and the dynamical spectrum of phenotypic fluctuations. While we see no evidence for spatio-temporal correlations in the colony, suggesting that the strategy adopted by the bacteria is cell-autonomous, i.e. uncorreleated with the neighbors, we do see a weak (few percent) asymmetry between sister bacteria: the younger one on average hoard (dump) pyoverdine at a rate larger (smaller) than the older one. This asymmetry is much stronger than the asymmetry between growth rates, which we do not observe

here but was reported for E-coli.

RESULTS

Liquid stationary phase cultures of *P. aeruginosa* in succinate medium were diluted, plated on an agar patch and covered with a glass coverslip. Colonies originating from a single cell were monitored under a microscope with time-lapse imaging. We used phase contrast microscopy to observe the cells and fluorescent imaging to visualize the concentration of iron-free pyoverdine in the cells and the surrounding medium. We were struck by the very large variations in pyoverdine concentration between bacteria, see Fig. 1 and movie in supplementary material.

The distribution of pyoverdine concentration in a bacteria (normalized by the mean across the colony) is shown in Fig.2(a). Its coefficient of variation ($\sim 30\%$) is about 10 times larger than the statistical fluctuations expected from an estimation of the amount of pyoverdine molecules in the bacteria: $10^3 - 10^4$. As more siderophores are produced the average concentration (fluorescent intensity) of iron-free pyoverdine outside and within bacteria increases with time. However contrary to expectations the standard deviation of the fluctuations among bacteria increases linearly with the mean intensity (Fig.fig:distribution (c)).

When monitoring the fluorescent of a given cell we observe large temporal fluctuations in the concentration of iron-free pyoverdine, whith a roughly $1/f^2$ power-law spectrum, see Fig.3(b). The individual bacterium appears to switch randomly between periods of increasing pyoverdine concentration (hoarding) and periods of decreasing concentration (pyoverdine dumping). Surprisingly the probability of switching between phenotypes appears to depend on the relative not absolute concentration of pyoverdine in the bacterium ($x = c/ < c >$ where $< c >$ is the colony average), see Fig.4: it is the same at early stages of colony development (when the concentration is low) as at later ones (when the average bacterial fluorescence is high)! The switching rate k_{hd} from a hoarding to a dumping phenotype can be fitted to a Hill curve:

$$k_{hd} = \frac{k_h^0}{1 + (x/x_h^0)^m}$$

with $k_h^0 = 0.24\text{min}^{-1}$, $x_h^0 = 3.80$ and $m = 1.26$. Similarly the switching rate from dumping to hoarding phenotype can be fitted by:

$$k_{dh} = \frac{k_d^0}{1 + (x_d^0/x)^n}$$

with $k_d^0 = 0.09\text{min}^{-1}$, $x_d^0 = 0.86$ and $n = 2.86$ (Fig. 4). The dependence of the phenotypic switching behaviour on the relative not absolute concentration of Pvd is reminescent of perfect adaptation in chemotaxis, where *E. coli*'s probability of switching between swimming and tumbling is independent of the absolute concentration of nutrients. In the present case the switching mechanism must involve a sensing of the relative difference between the internal and external pyoverdine concentrations, but how that is done has not been identified yet.

In order to investigate whether the phenotypic switching behaviour was cell autonomous or depended on the behaviour of neighboring bacteria, we measured the spatio-temporal correlations between bacteria. Our results (see supp.material) are consistent with uncorrelated behaviour of the bacteria in the colony, i.e. cell autonomous switching. What we uncovered however was a weak (few percent) asymmetry between sister bacteria following cell division, see Fig.5. We observed that the older sister (the one inheriting the older pole) accumulates pyoverdine at a higher smaller than the younger one. That might possibly be due to an asymmetric distribution of iron storage in the bacteria (slightly more probable at the old pole). It is however interesting to notice that in contrast with E.coli, no asymmetry was observed in the growth rate of the sister bacteria.

DISCUSSION

Our observations suggest that *P. aeruginosa* switches stochastically, with an average time of about 0.5 generation, between two phenotypes: a siderophore hoarding one (with probability $P_h(c)$) and a siderophore dumping one (with probability $P_d(c)$). A simple analytically soluble model incorporating the measured rates of switching (k_{hd}, k_{dh}) as a function of the relative concentration $x = c/ < c >$ as well as the measured rates of hoarding $k_h = 0.0063\text{min}^{-1}$ and dumping $k_d = -0.0065\text{min}^{-1}$, reproduces our results for the distribution of siderophores and the fluctuation spectrum. The model describes the evolution of the probabilities of being in either state as:

$$\begin{aligned} \frac{\partial P_h}{\partial t} + k_h c \frac{\partial P_h}{\partial c} &= -k_{hd} P_h + k_{dh} P_d \\ \frac{\partial P_d}{\partial t} - k_d c \frac{\partial P_d}{\partial c} &= +k_{hd} P_h - k_{dh} P_d \end{aligned}$$

At steady state, we have $k_h P_h = k_d P_d$ and the probability of observing a bacteria with relative pyoverdine concentration x: $P(x) = P_h(x) + P_d(x)$ satisfies:

$$x \frac{\partial P}{\partial x} = (\frac{k_{dh}(x)}{k_d} - \frac{k_{hd}(x)}{k_h}) P$$

Since all the variables in this equation have been measured, the distribution $P(x)$ is fully determined. It is in agreement with our observations, see Fig.6. In particular, notice that the dependence of the switching rate on the relative concentration x (and not on the absolute concentration c in a given bacterium) implies that the distribution P depends only on x. Hence the ratio of the standard deviation of the pyoverdine concentration (fluorescence) to its mean is a constant (~ 0.3), as indeed observed. Finally the power spectrum of the pyoverdine fluctuations obtained from a simulation of the model described above is also in good agreement with our measurements.

Stochastic phenotypic fluctuations have been reported before [2, 9] though not in the context of public goods. The suprising observation here is that this phenotypic switching is independent of the concentration of public good.

MATERIALS AND METHODS

To be written.

[1] John S Chuang, Olivier Rivoire, and Stanislas Leibler. Simpson's paradox in a synthetic microbial system. *Science*, 323(5911):272–5, January 2009.

[2] Avigdor Eldar and Michael B Elowitz. Functional roles for noise in genetic circuits. *Nature*, 467(7312):167–173, September 2010.

[3] Jeff Gore, Hyun Youk, and Alexander van Oudenaarden. Snowdrift game dynamics and facultative cheating in yeast. *Nature*, April 2009.

[4] W D Hamilton. The genetical evolution of social behaviour. i. *Journal of Theoretical Biology*, 7(1):1–16, July 1964.

[5] MÃ©lissa Hannauer, Emilie Yeterian, Lois W. Martin, Iain L. Lamont, and Isabelle J. Schalk. An efflux pump is involved in secretion of newly synthesized siderophore by pseudomonas aeruginosa. *FEBS Letters*, 584(23):4751–4755, December 2010.

[6] Francesco Imperi, Federica Tiburzi, and Paolo Visca. Molecular basis of pyoverdine siderophore recycling in pseudomonas aeruginosa. *Proceedings of the National Academy of Sciences of the United States of America*, 106(48):20440–20445, December 2009.

[7] Jacques Ravel and Pierre Cornelis. Genomics of pyoverdine-mediated iron uptake in pseudomonads.

Trends in Microbiology, 11(5):195–200, May 2003.

[8] Isabelle J Schalk, Mohamed A Abdallah, and Franc Pattus. Recycling of pyoverdin on the FpvA receptor after ferric pyoverdin uptake and dissociation in pseudomonas aeruginosa. *Biochemistry*, 41(5):1663–1671, February 2002.

[9] Jan-Willem Veening, Wiep Klaas Smits, and Oscar P Kuipers. Bistability, epigenetics, and bet-hedging in bacteria. *Annual Review of Microbiology*, 62:193–210, 2008.

[10] Paolo Visca, Francesco Imperi, and Iain L. Lamont. Pyoverdine siderophores: from biogenesis to biosignificance. *Trends in Microbiology*, 15(1):22–30, January 2007.

FIGURES

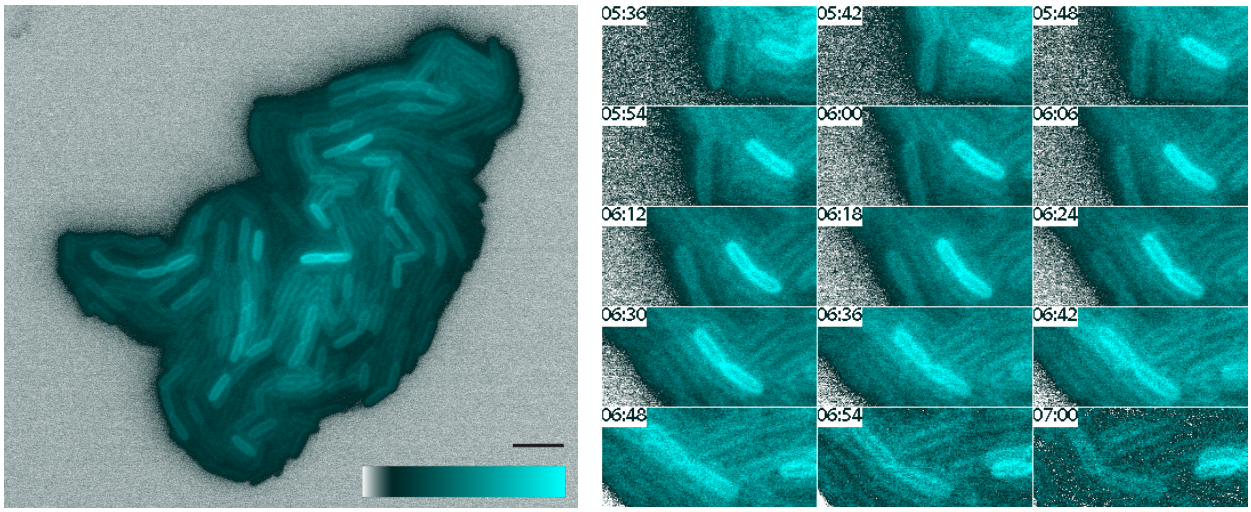

FIG. 1: (a) A colony of P. aeruginosa grown from a single clone. Notice the large variation in pyoverdine fluorescence (concentration) between bacteria. (b) Time lapse of fluorescence for a bursting cell. 3 min between frames.

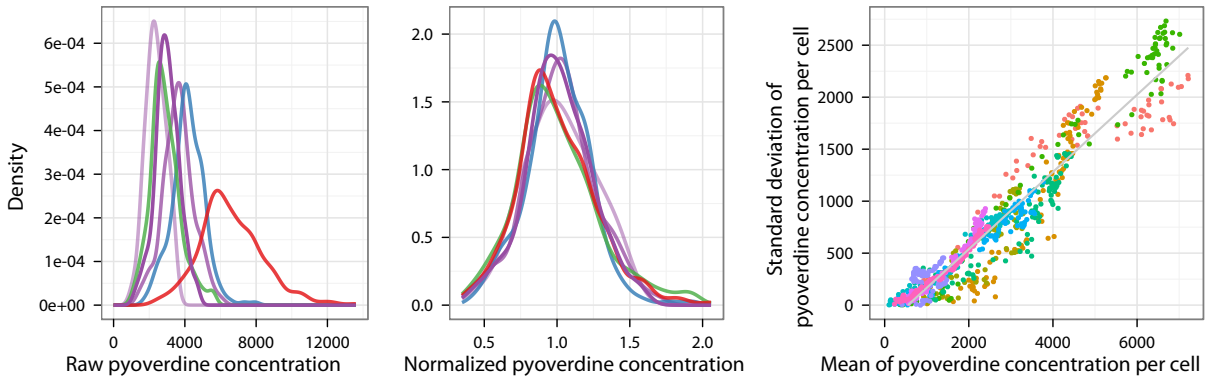

FIG. 2: (a) Pyoverdine concentrations distribution at different times for one colony. Different colors represent different movies at the stage of 300 cells; three purple lines represents the distribution of the same movie at the stages 50, 250 and 415 cells (light, medium and dark purple respectively). (b) Normalized pyoverdine concentrations distribution. (c) Standard deviation vs. mean of concentration within the colony.

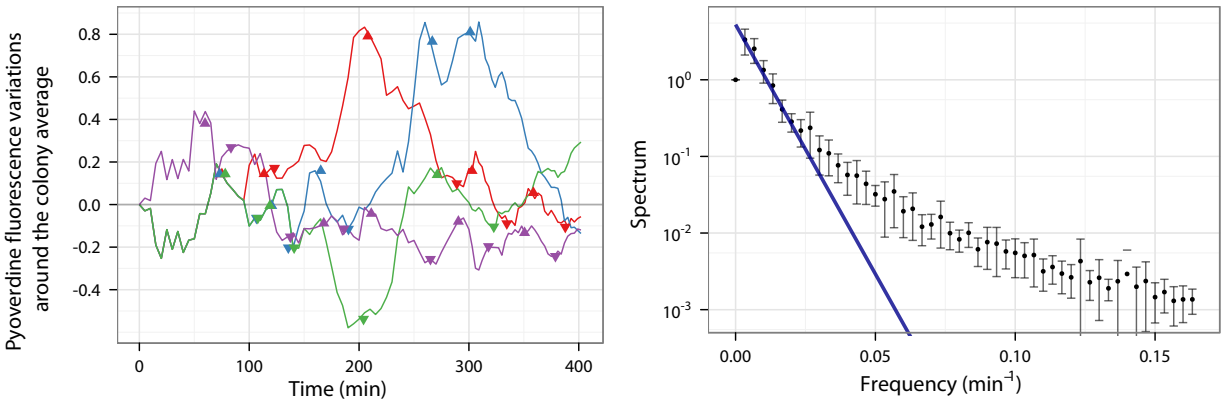

FIG. 3: (a) Typical fluorescence trace over tree branches. (b) Power spectrum of pyoverdinee fluctuations in a given bacterium. Average over 10 replicates.

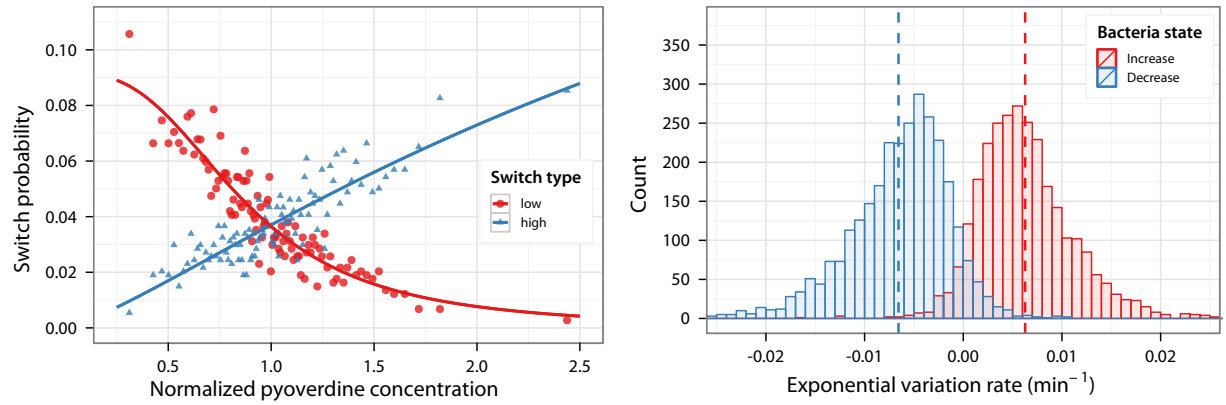

FIG. 4: (a)The probability of switching from hoarding to dumping phenotype (blue) and vice-versa (red) as a function of the normalized pyoverdine concentration (the fluorescence in a single bacterium divided by the mean of the colony). (b) Exponential variation rates in hoarding (red) and dumping phenotype (blue).

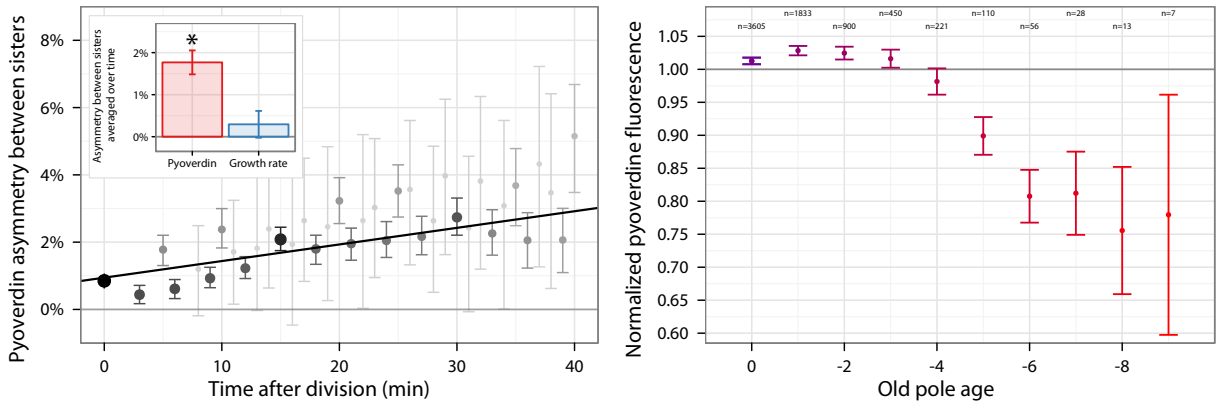

FIG. 5: (a) Asymmetry in pyoverdine fluorescence intensity I between sister bacteria $((I_{new} - I_{old})/I_{new} + I_{old})$ as a function of the time following cell division (at $t = 0$). (b) Average normalized pyoverdine fluorescence as a function of pole age. Negative values indicate old poles and 0 stands for new pole.

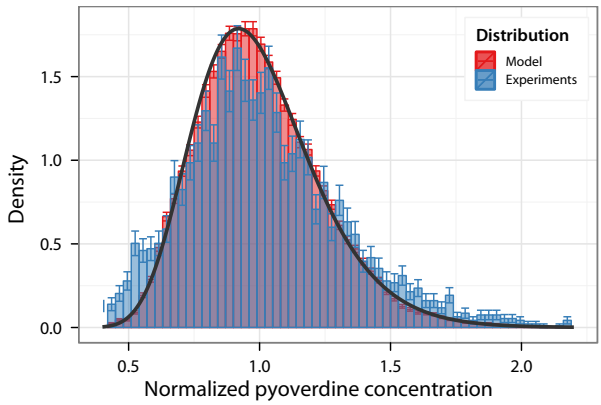

FIG. 6: Comparison of a simple model of phenotypic switching with normalized pyoverdine concentration (computed over all replicates).

SUPPLEMENTARY FIGURES

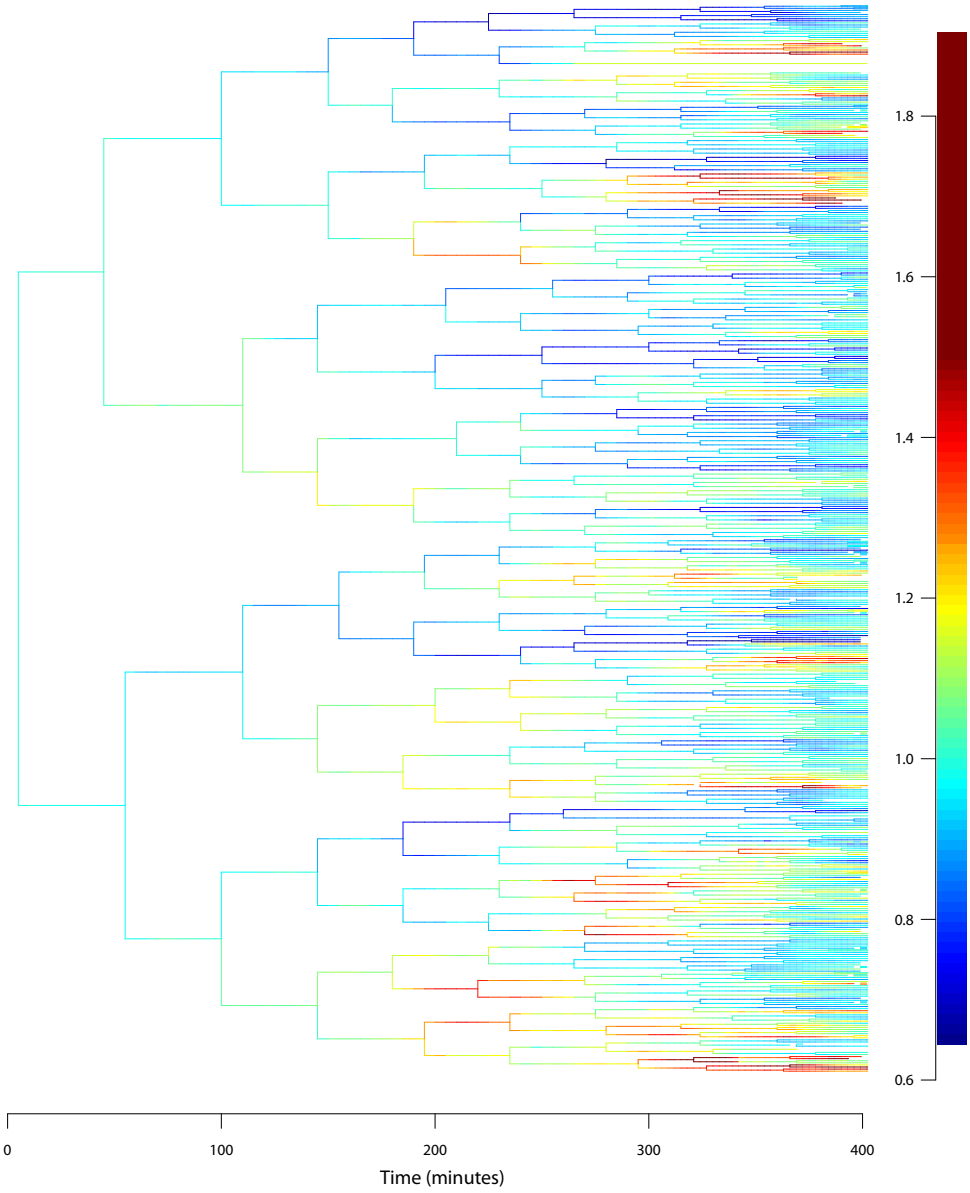

FIG. S1: The genealogical tree of an observed colony. The color of the branches code for the intensity of the pyoverdine concentration in each bacteria. Notice the intensity fluctuations as one proceeds down a given branch.

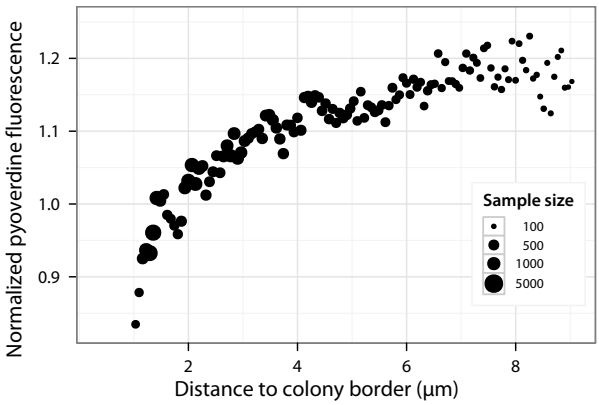

FIG. S2: Pyoverdine fluorescence as a function of cell distance to colony border.

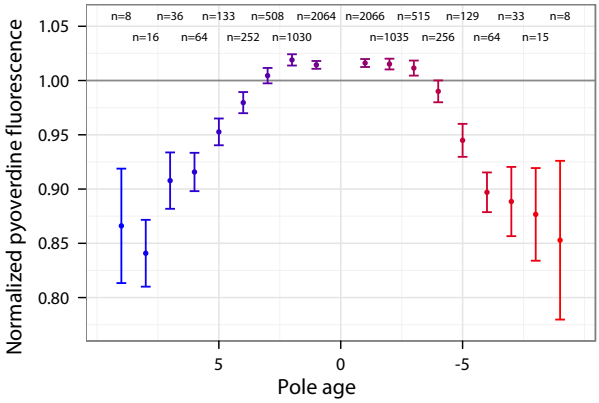

FIG. S3: Average normalized pyoverdine fluorescence as a function of pole age. Negative and positive values stand for old and new poles (respectively).

A.4 COMMENT ON DARWIN & WALLACE ORIGINAL ARTICLE

This article (written in french and published online on Bibnum) is a comment on Darwin and Wallace communications to the Linnean Society on July 1858, i.e. on the year preceding the publication of Darwin's book *On the Origin of Species*.

It is targeted to the general public, and in particular to high school teachers and pupils. It has been written in the context the graduate school lecture "History of science" by M. Morange.

La théorie de la sélection naturelle présentée par Darwin et Wallace

par
Timothée Flutre, doctorant en bioinformatique (INRA – Université Paris Diderot),
Thomas Julou, doctorant en biologie de l'évolution (École Normale Supérieure),
Livio Riboli-Sasco, doctorant en biologie théorique (Université Paris Descartes)

en collaboration avec Michel Morange,
professeur d'histoire et philosophie des sciences à l'École Normale Supérieure

Les textes commentés ici sont extraits du *Journal of Proceedings of the Linnean Society* (vol. III, 1859) ; ce sont quatre textes consécutifs :
- Lettre du 30 juin 1858 de Charles Lyell et Joshua Hooker présentant les documents qui suivent.
- Extrait d'un travail non publié sur les Espèces par C. Darwin.
- Extrait d'une lettre de Charles Darwin à A. Gray (Boston), 5 septembre 1857.
- Article de février 1858 d'Alfred Wallace.

Introduction

Le premier juillet 1858, lors d'une réunion de la Société Linéenne de Londres, les vues novatrices de deux naturalistes, Charles Darwin et Alfred Wallace, sont présentées dans trois textes introduits par une lettre de Charles Lyell et Joshua D. Hooker, éminents scientifiques de l'époque. Cette lettre explique que la nouvelle théorie, la sélection naturelle, concerne la production de variétés, races et espèces, et a été indépendamment découverte par les deux scientifiques. Cependant, l'accent est subtilement mis sur la contribution de Darwin. Pourquoi donc cette théorie suscite-t-elle aujourd'hui encore tant d'attention ? Et pourquoi le nom de Darwin est-il si connu à notre époque ? Si les hommes ont toujours cherché à comprendre l'origine de l'éblouissante diversité d'êtres vivants qui les entourent, c'est principalement au XVIII^{e} siècle que les premiers travaux systématiques furent menés. La pensée dominante est exprimée alors par Linné : les êtres vivants sont regroupés en espèces, celles-ci étant fixes, identiques depuis leur création par Dieu. Cependant, cette théorie va subir les assauts répétés des naturalistes de l'époque pour finalement céder devant la puissance explicative de la fameuse théorie

dite de la « sélection naturelle ». Cette journée de l'été 1858 est donc bien un évènement majeur dans l'histoire de la science en général et de la biologie en particulier. Pour la première fois, une théorie rationnelle détaillant un mécanisme concis expliquant l'origine et la diversité des espèces observées est présentée devant une assemblée de scientifiques.

Nous proposons ici d'analyser l'argumentaire de Darwin et Wallace, tel qu'énoncé lors de cette première publication. Bien que l'histoire ait retenu ces théories, leur formulation a changé au cours du temps : par exemple, le mot « évolution » relevait à l'époque du vocabulaire militaire et désignait le mouvement des troupes qui changeaient de position stratégique et le terme « sélection naturelle » ne sera introduit que plus tard. Relire ces textes permet de mieux comprendre le contexte social et théorique qui a permis l'émergence de cette pensée. Nous présenterons dans un premier temps les concepts scientifiques tels qu'énoncés par les deux auteurs. Nous replacerons ensuite cette pensée dans le contexte des avancées scientifiques qui ont pu inspirer Darwin et Wallace ainsi que dans le contexte social du monde de la science de l'époque.

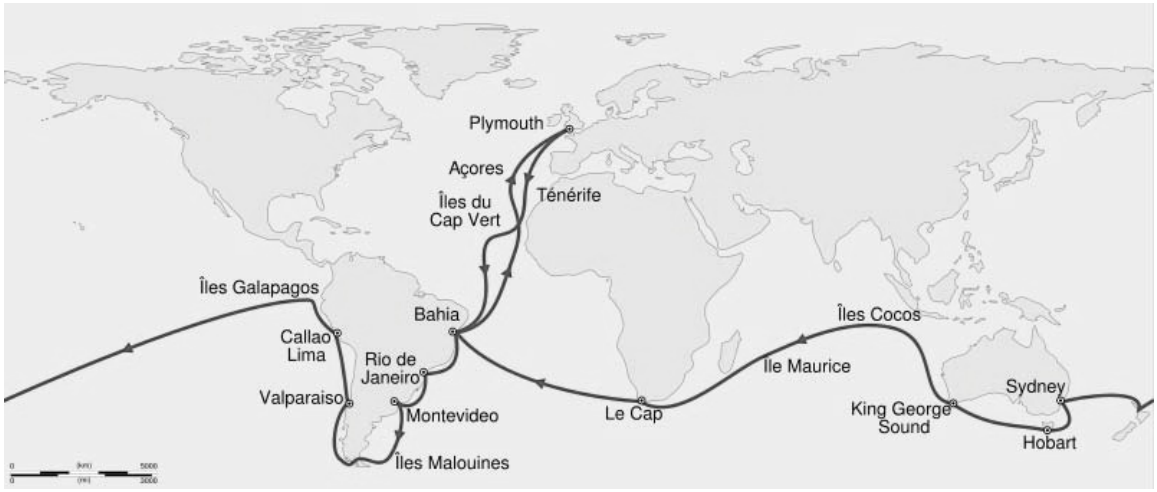

Figure 1 : ***Le voyage de Darwin sur le H.M.S Beagle*** *(décembre 1831 – octobre 1836).*

Darwin, Wallace et la sélection naturelle

La contribution majeure de ce document est la théorie de la sélection naturelle. Exprimée dans sa forme la plus claire par Darwin, cette théorie considère que l'évolution des espèces se fait par des variations aléatoires d'une génération à la suivante, variations héréditaires sur lesquelles opère ensuite une sélection par les conditions

environnementales (p. 49):

> *Dès lors, peut-on mettre en doute, à partir de la lutte que mène chaque individu pour sa survie, que chaque variation minime dans sa structure, ses habitudes ou ses instincts, qui résulte dans leur meilleure adaptation à de nouvelles conditions, pourrait révéler sa vigueur et bonne santé ? En luttant, il aurait une meilleure* chance *de survie ; et ceux de sa descendance qui auraient hérité de cette modification, même très légère, auraient également une meilleure chance de survivre.*

Par souci de clarté, nous présenterons la structure argumentative utilisée dans le deuxième document, d'une clarté et d'une concision exceptionnelles, en enrichissant certains points avec des extraits des deux autres documents. Nous allons également étudier en quoi le discours de Wallace défend le même point de vue ou présente des divergences.

PRESENTATION ET JUSTIFICATION DE LA SELECTION NATURELLE

À partir de ses observations sur les pratiques agronomiques dites « d'élevage sélectif » (« *[…] alors que nous nous souvenons de ce que Bakewell a réalisé sur les bovins et Western sur les moutons en utilisant le même principe de sélection* »), Darwin affirme que « la sélection agit seulement par accumulation de variations plus ou moins importantes produites par les conditions externes, ou par le simple fait que, au cours des générations, les descendants ne sont pas exactement semblables à leurs parents ». Darwin insiste sur le caractère externe des éléments qui conditionnent la sélection, les conditions environnementales dans la nature, le choix du sélectionneur dans le cas de la sélection artificielle, et qui dans certains cas aussi induisent les variations:

> *Le « désherbage », comme les pépiniéristes appellent le fait de détruire les variétés de plantes qui ne correspondent pas à celles qu'ils désirent faire pousser, est une forme de sélection.*

Bien que l'argumentaire de Darwin repose essentiellement sur des pratiques agronomiques, il a l'audace d'étendre ses conclusions à l'ensemble du vivant. Ces pratiques d'élevage ont très fortement contribué à la compréhension par Darwin des mécanismes de sélection naturelle, on peut également supposer qu'elles ont déterminé la terminologie employée. Pour différencier les pratiques agronomiques des mécanismes naturels on parlera plus tard de « sélection artificielle »[1] et de « sélection naturelle ». Darwin applique ainsi les mécanismes utilisés dans l'élevage et l'agriculture aux espèces

[1] Le terme « sélection artificielle » désigne l'intervention de l'homme dans la modification des conditions environnementales qui conditionnent l'évolution d'une espèce.

sauvages, en faisant deux hypothèses déterminantes: un sélectionneur omniscient et un temps très long.

Concernant la sélection, Darwin hausse sa proposition théorique à l'état de « principe » et, pour se justifier, s'appuie sur deux références. D'un côté, la sélection naturelle serait une extension de la vision du combat pour la vie proposée par Candolle (p.46) ainsi que Lyell et Herbert (p.51). Chez ces auteurs, ce concept renvoie à des variations démographiques en fonction des conditions environnementales et de la compétition entre espèces, pour autant l'impact en termes évolutifs n'est pas soupçonné. La sélection par les contraintes de l'environnement, d'une certaine façon *réduit* l'ensemble de ces variations possibles. D'un autre côté, la pensée de Malthus, développée pour décrire les populations humaines, est étendue aux autres espèces. Darwin conclut que la démographie serait très différente sans sélection puisque la croissance d'une population, fût-elle faible, est géométrique. Il donne à ce propos de nombreux exemples (p.47-49) :

> *Supposons dans un endroit déterminé qu'il y ait huit paires d'oiseaux, et que seulement quatre d'entre elles, donnent naissance annuellement (en incluant les doubles pontes), à seulement quatre oisillons, et que ceux-ci continuent à donner naissance selon le même taux de progression, alors au bout de sept ans (…) il y aura 2048 oiseaux, au lieu des seize initiaux.*

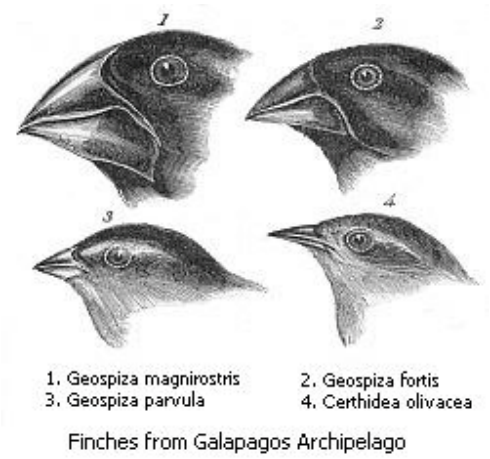

Figure 2 : Les pinsons de Darwin*. (Darwin, 1845 :* Journal of researches into the natural history and geology of the countries visited during the voyage of H.M.S. Beagle round the world, under the Command of Capt. Fitz Roy, R.N. 2d edition*).*
C'est le nom donné à une douzaine d'espèces différentes mais apparentées que Charles Darwin a recensées dans la faune des îles Galápagos durant son voyage sur l'HMS Beagle. Ces oiseaux sont tous de la même taille : entre 10 et 20 cm. Les plus importantes différences entre ces espèces se trouvent dans la taille et la forme de leurs becs. Darwin prendra conscience que chaque espèce occupe une île différente et que l'isolement géographique a pu mener à la formation d'espèces distinctes à partir d'ancêtres communs. Il établira un lien direct entre la végétation et donc le régime

alimentaire de chaque espèce et leurs caractéristiques morphologiques, la forme du bec notamment.

Concernant le facteur temporel, s'il est possible d'envisager les effets des pratiques des éleveurs, il peut être plus difficile dans le contexte historique d'envisager l'impact de la sélection sur les espèces naturelles. Darwin essaie donc de faciliter la compréhension de ce processus par analogie avec les mécanismes géologiques mis en lumière par Lyell. Ce dernier a proposé que des structures vastes et apparemment immuables comme les massifs montagneux étaient en fait en évolution (par exemple que les vallées se forment sous l'action des glaciers et des cours d'eau). Darwin parle donc d'un « temps quasi-illimité » et de « millions de générations » au cours desquelles les variations s'accumulent et sont transmises :

> *La notion de temps est quasi illimitée, seul un géologue de terrain peut comprendre cela tout à fait. Pensez à l'ère Glaciaire lors de laquelle la même espèce de coquillages a existé ; il y a dû avoir pendant cette période des millions et des millions de générations.*

Finalement, Darwin récapitule et met en scène son scénario d'évolution : étant donné l'immense diversité des formes vivantes observées, il ne peut pas ne pas y avoir de variations – remarquer la relation de causalité qui est en fait postulée – en particulier quelques variations qui confèrent un avantage par rapport à l'environnement (p.52). Les individus ainsi formés remplaceront ceux qui ont gardé les caractères de leurs parents : c'est la sélection naturelle.

LES VUES D'UN PRECURSEUR

Dans ses deux textes, Darwin présente des idées qui se révéleront particulièrement clairvoyantes et ont sans doute contribué à sa renommée. La fin du premier texte (p.50), pourtant assez précoce, présente déjà la distinction entre sélection naturelle et sélection sexuelle. Darwin y fait un contraste entre l'impact sélectif de conditions externes, environnementales, et l'impact sélectif de pratiques liées au choix des partenaires reproductifs.

> *Ce type de sélection, cependant, est moins sévère que la précédente ; elle n'implique pas la mort des moins chanceux, mais ne leur assure qu'une moindre descendance.*

De plus, dans le dernier paragraphe du deuxième texte (p.53), Darwin évoque une possible représentation de l'évolution sous forme d'arbre qui va bien au-delà de la hiérarchie fixiste :

[…] car les êtres organiques semblent toujours se diviser en branches et en sous-branches, comme les ramifications d'un arbre qui partiraient d'un tronc commun, les brindilles qui fleurissent et qui divergent détruisant les moins vigoureuses, et les branches mortes représentant grossièrement les genres et les familles disparus.

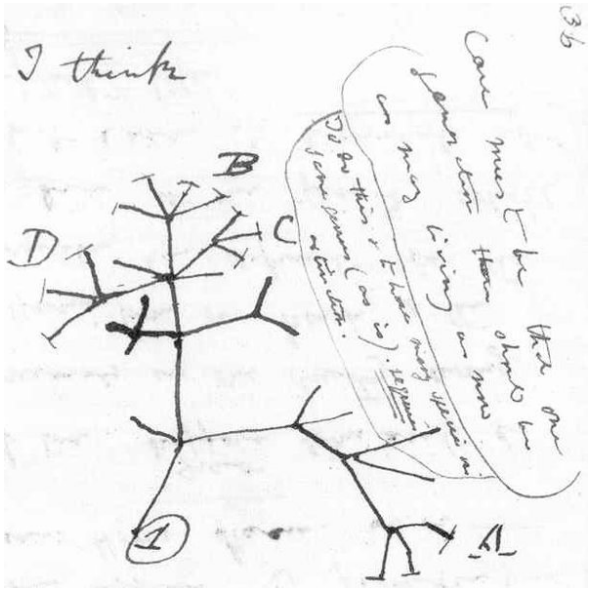

Figure 3 : Croquis de Darwin, 1837. *Son premier croquis d'un arbre de l'évolution, issu du* First Notebook on Transmutation of Species *(1837) [Museum of Natural History, New-York].*

La classification sous forme d'arbre représente désormais les liens historiques entre espèces, leur phylogénie. Il dépasse par ces concepts les hiérarchies décrites par Linné et intègre la parenté entre espèces, c'est-à-dire l'histoire évolutive, dans un nouveau mode de classification du vivant. Cette idée fera l'objet d'une des rares figures du livre « L'Origine des Espèces » mais sera surtout reprise et développée par Haeckel après 1860. Il est également intéressant de noter que Darwin porte une attention particulière à l'impact de l'environnement sur les organes reproducteurs (p.49) :

Il a été montré précédemment que de tels changements, par leur action sur le système de reproduction, pousseraient probablement l'organisation des êtres vivants qui ont été les plus touchés à se modifier, comme s'ils avaient été domestiqués.

Aurait-il l'intuition que ce sont les modifications dans les cellules germinales qui sont seules transmises? En effet il sera bien confirmé plus tard par Weismann à la fin du XIXe siècle que les modifications acquises dans la lignée somatique ne peuvent être transmises à la descendance. Finalement, Darwin propose une vision très souple de la

sélection naturelle dans laquelle le taux de variation pourrait changer en fonction des conditions environnementales (p.49). Sa formulation bien qu'imprécise sur ce point a l'avantage de laisser une place aux concepts de « mutateurs » et d'« évolvabilité » développés récemment (voir encadré):

> *de tels changements, par leur action sur le système de reproduction, pousseraient probablement l'organisation des êtres vivants qui ont été les plus touchés à se modifier[2], comme s'ils avaient été domestiqués.*

Mutateurs et évolvabilité

Ces concepts modernes explicitent des mécanismes évolutifs dits de second ordre. Dans certaines conditions, sous l'influence d'allèles dits « mutateurs », un organisme voit son taux de mutation génétique augmenter ou diminuer. Ces allèles mutateurs correspondent à des altérations des systèmes de copie ou de réparation de l'ADN dont la fidélité diminue. De nombreuses erreurs vont subsister suite à leur passage.
Ce mécanisme découvert chez les bactéries a révolutionné la façon de considérer le rapport du vivant à l'évolution. On doit considérer que dans des conditions de stress environnemental par exemple, la variabilité des individus d'une espèce donnée sur laquelle va s'effectuer la sélection naturelle peut elle-même varier. L'amplitude de ces mécanisme est alors traduite en terme « d'évolvabilité ».

Si la pensée de Wallace sur ces questions n'a pas, à coup sûr, la même portée, on notera l'analogie étonnamment moderne entre la sélection naturelle et le système de régulation de la machine à vapeur (p.62) :

> *L'action de ce principe est exactement analogue à celle du gouvernail centrifuge d'un moteur à vapeur, qui constate et corrige toute irrégularité pratiquement avant qu'elle devienne notable.*

De plus, Wallace introduit un concept absent chez Darwin et qui sera souvent repris, celui de tendance à la complexification des espèces du fait de la sélection naturelle. Cette question est aujourd'hui toujours sujette à débat.

[2] « se modifier » est exprimé dans le texte par « become plastic », qui sous entend que Darwin ne considère pas que la plasticité est nécessairement constante.

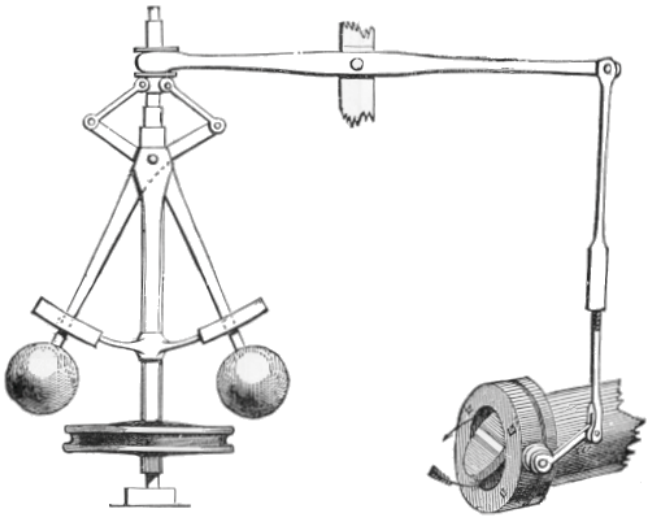

***Figure 4 :* le régulateur centrifuge (1788) de la machine à vapeur de Watt.**
C'est un mécanisme de rétroaction : plus l'arbre du moteur tourne vite à gauche, plus les boules s'écartent, et viennent obturer le mécanisme d'admission de vapeur à droite, ce qui régule la vitesse de l'arbre moteur.

LES DIFFICULTES DU TEXTE

Tout en reconnaissant l'excellence des avancées conceptuelles que l'on trouve dans l'argumentaire de Darwin et de Wallace, il est important d'identifier certaines faiblesses du texte, notamment les éléments qui seront par la suite modifiés par ces mêmes auteurs et par les générations à venir d'évolutionnistes.

Darwin construit toute son argumentation à partir de ses observations sur ce qui sera appelé la « sélection artificielle » et en postulant que des changements d'importance semblable doivent pouvoir être engendrés par la sélection naturelle. Pourtant, il ne pousse pas l'analogie jusqu'à imaginer que les vitesses d'évolution puissent être comparables, auquel cas des changements importants pourraient être observés par des êtres humains chez des espèces à reproduction rapide, comme des microorganismes. Au contraire, il insiste à plusieurs reprises sur la très grande durée nécessaire en se retranchant implicitement derrière le crédit de Lyell. On pourrait y voir là une incohérence avec son raisonnement, considérant que les deux processus sont de natures différentes. Par ailleurs, malgré l'attention portée par Darwin à la démographie, il ne veut pas envisager que les individus éliminés par la sélection naturelle puissent être observés (« *[…] il ne faut pas être surpris de ne pas être capable de déterminer le frein à la croissance aussi bien pour les animaux que pour les plantes*. »). Ce point de vue et le précédent rendent ses vues impossibles à tester car trop lentes et sans effet

démographiques visibles. Pourtant quelques décennies plus tard, Dallinger démontrera la sélection à l'œuvre sur des algues unicellulaires dans une expérience qui durera sept ans, de 1880 à 1887.

Cependant, le point le plus faible de la théorie de la sélection naturelle telle que présentée ici par Darwin et Wallace concerne l'hérédité. Aucun des deux auteurs n'a de théorie de l'hérédité et ils discutent donc sur cette sélection qui crible les organismes, favorisant ceux qui héritent de leurs parents de caractéristiques avantageuses sans que l'on sache comment ces caractéristiques sont transmises d'une génération à l'autre. À la même époque, le tchèque Gregor Mendel (1822-1884) a proposé une explication mais Darwin n'eut pas connaissance de ses travaux. Il faudra attendre le XX^{e} siècle pour voir l'avènement de la génétique, proposant des explications solides des mécanismes d'hérédité en jeu et permettant d'unifier ces points de vue dans un cadre conceptuel global.

Dans la vision de Darwin émerge l'idée que les espèces peuvent atteindre un optimum évolutif dans un environnement donné. Pour autant, il considère qu'une espèce adaptée à un contexte donné peut perdre sa place « optimale » si l'environnement est altéré. Il n'existe donc des espèces de « qualité » que dans un contexte donné. Les formulations modernes de la sélection naturelle considèreront de la même façon des optimisations locales tant d'un point de vue environnemental que temporel. Aussi, depuis, des études comparatives et expérimentales ont montré que la sélection n'était pas dirigée et pouvait aboutir à des solutions qui ne sont pas forcément avantageuses sur le long terme.

De même, Darwin mentionne que des « petites » et des « grandes » modifications peuvent intervenir mais il n'est pas clairement explicité si elles peuvent avoir des rôles différents. Rien n'est non plus dit sur le taux auquel ces modifications surviennent: les petites sont-elles plus fréquentes que les grandes ? Ces questions font encore l'objet de recherches actuelles.

Une théorie qui s’inscrit dans son histoire

La pensée de Darwin et Wallace ne s'est pas forgée dans l'isolement mais plutôt dans un contexte scientifique très prolixe. A cette époque, de nombreuses propositions théoriques tentent d'expliquer de façon plus ou moins solide la diversité des êtres vivants

et parfois leur évolution. D'une certaine façon, Darwin réussit à combiner de nombreuses idées énoncées séparément par différents scientifiques. De manière générale, il est aujourd'hui considéré que les grandes innovations scientifiques émergent du fait de la combinaison d'un petit nombre d'idées préexistantes mais séparées dans des champs disciplinaires distincts. Ainsi, pour mieux comprendre les avancées conceptuelles exprimées dans ce document, il est important de comprendre l'étendue des idées sur lesquelles Darwin et Wallace ont pu s'appuyer.

DE LA FIXITE OU DE L'EVOLUTION DES ESPECES

La théorie de la sélection naturelle, par essence, est une théorie évolutionniste. Mais avant elle, bien d'autres théories ont été proposées, chacune avec l'ambition d'expliquer la diversité des espèces naturelles.

Le fixisme considère que chaque être vivant n'appartient qu'à une et une seule espèce et que ces espèces sont fixes : pas de transformation et donc pas de spéciation. Les espèces n'évoluent pas et ce depuis leur création. Par conséquent, il existe une classification du monde vivant tel qu'il a été conçu, la mettre à jour augmentera notre connaissance du vivant. La taxinomie du suédois Linné (1707-1778) est la référence au sein de cette théorie. Il établit une hiérarchie (classes, ordres, genres, espèces, variétés) ainsi qu'une nomenclature binomiale, encore utilisées aujourd'hui, dans son ouvrage *Systema naturae* dont la première édition paraît en 1735. Linné considère ainsi que « nomina si nescis, perit et cognitio rerum », *si tu ignores le nom des choses, même leur connaissance disparaît*. Le botaniste français Jussieu (1748-1836) poursuit ce travail en améliorant la classification linéenne. Pour cela, il utilise un plus grand nombre de caractères.

Aux observations qui lui posent problème telles les variétés de plantes agricoles qui diffèrent des espèces trouvées dans la nature, le fixisme répond en les envisageant comme des changements accidentels mais réversibles permettant selon l'environnement de revenir à l'espèce initialement conçue. Cependant, les arguments fixistes sont parfois plus artificiels, *ad hoc*, voire déistes, que rationnels. Par exemple, Linné statue en 1737 dans son livre *Genera plantarum* qu'« il existe autant d'espèces différentes que l'Être infini a créé de formes différentes au commencement ». De plus, dans son travail de classification, il sera amené à diviser l'espèce humaine en différentes « races ». Pour ces idées, il sera combattu par des philosophes et naturalistes français, parmi lesquels

Diderot, Buffon et Maupertuis.

Certains scientifiques ressentirent le besoin d'amender la théorie fixiste, mais n'osèrent pas l'ébranler plus en avant. Dans ses études d'anatomie comparée, Cuvier (1769-1832) observe que les fossiles des couches profondes diffèrent plus des espèces actuelles que ceux des couches récentes. Il remarque également que des formes d'organismes ne sont plus observées dans les couches supérieures. Il envisage ainsi plusieurs épisodes de création entrecoupés de catastrophes pendant lesquelles certaines espèces disparaissent. Cependant, au sein de chaque épisode il maintient le cadre de pensée fixiste.

D'autres penseurs n'hésitent pas à attaquer le fixisme suggérant que les espèces évoluent dans le temps, notamment Maupertuis (1698-1759) qui s'intéresse à l'hérédité. Ses idées, remarquables pour l'époque, en font un précurseur lointain de la génétique : une série de mutations fortuites et répétées peut engendrer de nouvelles espèces. Il énonce ses intuitions dans *Vénus physique* en 1745 :

> *C'est ainsi que dans une carrière profonde, lorsque la veine de marbre blanc est épuisée, l'on ne trouve plus que des pierres de différentes couleurs qui se succèdent les unes aux autres. C'est ainsi que des races nouvelles d'hommes peuvent paroître sur la terre, & que les anciennes peuvent s'éteindre.*

Buffon (1707-1788), quant à lui, propose une théorie de la dégénération. Certaines espèces sont issues de la dégradation d'espèces initiales « de qualité », comme l'âne peut être issu du cheval. Les espèces dégénérées peuvent néanmoins revenir à l'espèce initiale lorsqu'on les place dans des conditions adéquates.

C'est avec Lamarck (1744-1829) que l'idée d'évolution des espèces se précise nettement. Ses nombreux travaux apporteront beaucoup aux sciences du vivant. Outre la création du mot « biologie », il propose une théorie de l'évolution basée sur deux principes, qui sont la tendance à la complexification et l'influence du milieu. Les espèces évoluent par transmission des modifications acquises au cours de la vie – c'est l'hérédité des caractères acquis (*Recherches sur l'organisation des corps vivants*, 1802) :

> *Or, chaque changement acquis dans un organe par une habitude d'emploi suffisante pour l'avoir opéré, se conserve ensuite par la génération, s'il est commun aux individus qui dans la fécondation concourent ensemble à la reproduction de leur espèce. Enfin ce changement se propage et passe ainsi dans tous les individus qui se succèdent et qui sont soumis aux mêmes circonstances, sans qu'ils aient été obligés de l'acquérir par la voie qui l'a réellement créé.*

Dans cette voie, il sera notamment suivi par Geoffroy Saint-Hilaire (1772-1844) qui

affrontera Cuvier dans des discussions épiques devant l'Académie des Sciences.

Outre-Manche également les scientifiques s'interrogent sur ces questions. En 1795, le géologue écossais James Hutton (1726-1797) propose que la Terre se soit formée graduellement, par couches successives. Pour le gradualisme, tout changement profond est le résultat de l'accumulation de processus lents, par petites étapes; cette conception s'oppose donc au catastrophisme. Charles Lyell (1797-1875) incorpore cette idée dans sa théorie de l'uniformitarisme, théorie selon laquelle les processus géologiques à l'œuvre dans un passé lointain s'exercent encore à l'heure actuelle.

LE COMBAT POUR LA VIE

Un autre argument essentiel à la théorie de la sélection naturelle est l'impitoyable lutte pour la vie observée par de nombreux naturalistes, bien loin de la vision harmonieuse présentée par certains. Le botaniste Augustin de Candolle (1778-1841) travaille avec Lamarck sur la *Flore française*.

Figure 5 : Le botaniste suisse Augustin Pyrame de Candolle (1778-1841). *Il est cité à plusieurs reprises par Darwin.*

Il étudie notamment les effets de l'environnement physique (sol, température, soleil, eau, altitude) sur la distribution géographique des plantes ainsi que le rôle de la compétition inter-espèces pour les ressources (*Essai élémentaire de géographie botanique*,1820):

> *[...] considérons sous ce rapport les plantes d'un même pays qui offre une grande variété de localités; toutes ces plantes sont dans un état de guerre continuel; les premières qui s'établissent dans un lieu en excluent les autres, les grandes étouffent les petites, les vivaces étouffent celles dont la durée est plus courte, les plus fécondes chassent celles qui se multiplient plus difficilement [...]*

Pour autant il reste fixiste:

> *Il est facile de voir que toutes ces discussions sur les lois de la distribution des végétaux dans le monde reposent essentiellement sur l'opinion de la permanence des espèces, opinion qu'appuyent de nombreux arguments et qu'on ne peut attaquer qu'en négligeant les faits bien connus et en se rejetant dans les faits mal connus.*

Dans la même veine, influencé par les mauvaises récoltes de 1794 et 1800 en Angleterre, l'économiste Malthus (1766-1834) s'est fait connaître par ses travaux sur le rapport entre croissance de la population et croissance de la production. Il exposa ses réflexions dans son livre « *An Essay on the Principle of* Population » publié anonymement en 1798 et dont l'édition finale, la sixième parue en 1826, influença Darwin et Wallace. Il y écrit notamment:

> *La croissance de la population, sans contrainte, est géométrique. La croissance des moyens de subsistance, quant à elle, est arithmétique. [...] Selon la loi de la nature qui rend la nourriture nécessaire à la vie humaine, les effets de ces deux phénomènes inégaux doivent être gardés égaux. Cela implique une contrainte forte et constante qui opère sur la population relative à la difficulté de subvenir à ses besoins.*

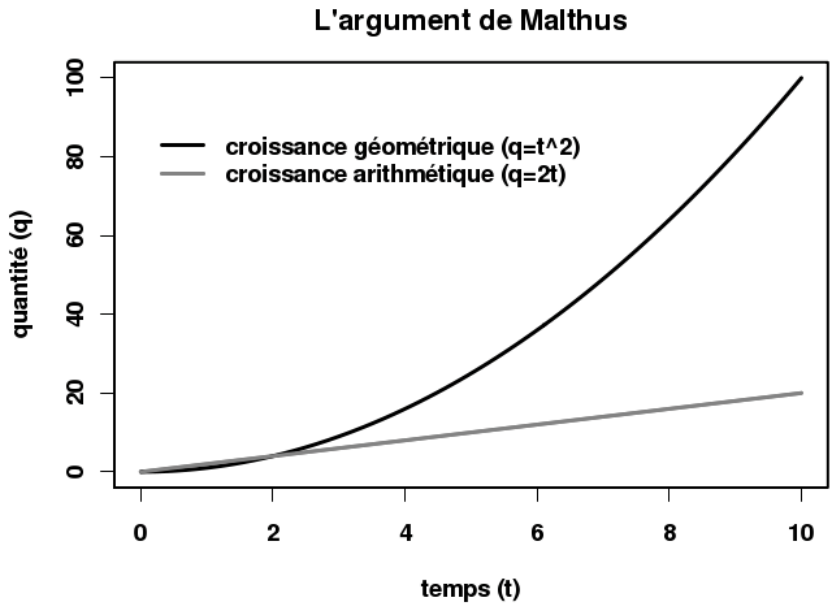

Figure 6 : ***L'argument de Malthus.*** *La croissance arithmétique (droite rouge) décrit selon Malthus la croissance des moyens de subsistance alors que la croissance géométrique (courbe noire) décrit celle de la population.*

UNE PENSEE QUI RASSEMBLE

Les idées de Darwin que nous avons exposées dans le premier paragraphe se nourrissent naturellement des concepts présentés ci-dessus et des observations qui en étaient à la base. Il est par exemple évident que Darwin importe les idées de Candolle concernant la lutte entre individus pour leur survie puis il y ajoute les idées évolutionnistes de Maupertuis et Buffon, et combine finalement le tout à la façon de Malthus. Lorsqu'il ajoute à cela l'observation des pratiques dites « d'élevage sélectif », on conçoit aisément *a posteriori* qu'il soit arrivé à énoncer le principe de la sélection naturelle.

Darwin a également su réunir des observations *in situ*, des interprétations de fossiles, des concepts mathématiques, des théories concernant les animaux, d'autres concernant les végétaux, tous ces apports venant de penseurs travaillant dans des contextes différents, voir écrivant dans des langues différentes. C'est ensuite à sa réflexion inlassable et à sa capacité d'abstraction qu'il revient d'accorder le mérite de synthétiser une multitude d'observations et d'idées éparses en une théorie concise et limpide.

Des postures scientifiques différentes

Le travail d'ancrage dans un contexte de savoirs ne peut se passer pour autant d'un ancrage dans la société des scientifiques de l'époque. Aujourd'hui, un chercheur peut difficilement aller de l'avant sans dédier un temps considérable à la discussion avec ses pairs, à l'évaluation du travail d'autrui. La science est un monde avec ses règles et ses valeurs. Il est ainsi fondamental de savoir exprimer des formes de gratitude envers les scientifiques sans lesquels nous ne pourrions faire d'ultérieures recherches. Il est bon aussi de savoir critiquer le travail d'autrui, en se basant sur des argumentaires solides et tout en ne manquant jamais de respect. Le monde académique peut parfois être cruel envers ceux qui dévient des normes sociales et ceci quelle que soit la valeur scientifique de leurs idées.

La portée des propositions mises en avant par un scientifique et leur acceptation va dépendre en grande partie de sa place au sein de la communauté scientifique, de la façon de s'exprimer, et ce quelle que soit l'époque ou la discipline. Ainsi, au delà des questions liées à l'argumentation scientifique, Darwin et Wallace diffèrent de façon importante pour ce qui a trait à leur posture scientifique, ce qui a pu avoir un impact

significatif sur la perception de leurs théories.

PLACE SOCIALE AU SEIN DE LA COMMUNAUTE SCIENTIFIQUE.

Darwin à travers son texte s'intègre dans une lignée de grands scientifiques. Il fait référence non pas directement aux conclusions de leurs travaux mais importe métaphoriquement les dimensions conceptuelles issues des travaux de ses pairs. Il réinjecte par exemple en biologie une nouvelle dimension temporelle, formulée par Lyell en géologie, expliquant que les paysages observés résultent de millions d'années d'action de l'eau et du vent. Il en est de même au sein du vivant, les formes observées ne peuvent être comprises qu'à travers de telles échelles temporelles.

Le champ des disciplines invoquées par Darwin est bien plus large que dans le texte de Wallace (géologie, épidémiologie, biologie, agronomie, etc.). Darwin se place ainsi directement sur une dimension théorique qui tire sa puissance de principes qui vont au delà de l'observation dans le domaine du vivant. Il intègre ensuite ces principes dans une nouvelle façon de penser les systèmes naturels.

Wallace attaque de façon directe Lamarck, sans diplomatie, ce que Darwin ne s'aventure pas à faire:

> [Wallace] *L'hypothèse de Lamarck selon laquelle les changements progressifs dans les espèces sont produits par les tentatives des animaux d'augmenter le développement de leurs organes, et ainsi modifier leur structure et leurs habitudes - a été réfutée de manière répétée et sans difficulté par tous les écrivains attelés au sujet des variétés et des espèces.*

Figure 7 : Alfred Russell Wallace (1823-1913)

Wallace, certes en confiance avec ses propositions, ressent pour autant le besoin de s'opposer à d'autres conceptions. Darwin lui, ne cherche pas à contester qui que ce soit. On ressent, au travers de la forme de son discours, qu'il propose ses concepts comme allant de soit, ce que certains pourraient interpréter comme une forme de prétention, qui sera d'une certaine façon justifiée par l'histoire.

Figure 8 : La médaille (recto-verso) Darwin-Wallace, 1908. *Elle est émise par la Société Linéenne cinquante ans après la présentation de leurs travaux en 1858 (textes de la Société Linéenne commentés ici)*

DES STYLES CONTRASTES

Les deux auteurs peuvent également être contrastés en terme de style d'écriture, reflétant là encore leur posture scientifique. Darwin est concis, voir elliptique, les enchaînement logiques sont mis en avant par une numérotation claire (numérotation des arguments, dont la structure sera d'ailleurs reprise dans *L'origine des espèces*, 1859). Le texte est extrêmement fluide. On ressent une profonde maîtrise du sujet. On ressent également qu'il pourrait dire bien plus, que les conséquences théoriques des éléments apportés vont bien au delà des domaines à partir desquels Darwin forge sa théorie. Alors que Wallace se cantonne dans une analyse rigoureuse basée pour l'essentiel sur des observations des variétés utilisées en élevage, Darwin expose des observations faites

chez différents animaux ainsi que des végétaux.

En outre, il est important de remarquer que Darwin utilise des métaphores, à ce que nous pourrions imaginer en dehors de ce qui est dit dans le texte. Aussi, il fait appel à des modèles mathématiques (modèle de croissance géométrique) et donne des exemples numériques (« 2048 oiseaux » p.47), pratique jusqu'alors peu courante dans les sciences du vivant.

Il est intéressant de se demander s'il serait possible de trouver aujourd'hui dans la littérature scientifique un texte avec une portée comparable à celui de Darwin. Aucun auteur scientifique ne pourrait ainsi exposer de façon si elliptique une théorie radicalement nouvelle tout en admettant en avoir parlé avec de nombreuses personnes et n'avoir rien publié depuis des années. Aussi l'on demanderait à ce que cela soit basé sur des observations expérimentales plus rigoureuses ou que du moins l'auteur fasse des prédictions des résultats de futures expériences qui viendraient corroborer ou non les propositions théoriques. On pourrait toutefois trouver ce genre de propositions théoriques dans des livres, mais avec de plus nombreuses citations se référant à des travaux expérimentaux.

POURQUOI LA POSTERITE RETIENT-ELLE DARWIN ?

À la lecture de ces trois textes on peut d'une certaine façon se rassurer du fait que l'histoire a pour l'essentiel retenu les propositions de Darwin. Retenir Darwin c'est retenir une puissance de pensée théorique qui s'embarrasse bien peu des contraintes d'un formalisme scientifique naissant. C'est retenir également une pensée scientifique qui s'aventure au delà des seuls domaines dans lesquels elle s'est forgée. Si Darwin est naturaliste, il comprend la géologie ou la démographie et s'attache à bâtir une cohérence entre les bases théoriques de ces disciplines. Il ne voit pas en quoi il y aurait des fonctionnements radicalement différents.

Conclusion

Au XX^{e} siècle, la biologie voit l'unification de plusieurs sous-disciplines en ce qui forme désormais la synthèse évolutive moderne, afin d'expliquer le plus complètement possible l'évolution des organismes vivants. La sélection naturelle y occupe une place importante, confirmée notamment par les travaux en génétique des populations et en

écologie. Les prémisses de la conception actuelle de l'évolution, énoncés au XIX^{e} siècle, sont donc toujours d'actualité.

Cependant, bien qu'ayant proposé une théorie solide de l'origine et de la diversité des espèces, Darwin a laissé à ses successeurs une tâche immense et posé quantité de nouvelles questions. Comment mesurer les effets de la sélection, notamment comment changent-ils au cours du temps ainsi qu'en fonction de la taille de la population ? Quels sont les liens entre l'impact des variations (les mutations) et leur taux d'occurrence ? Comment la sélection opère-t-elle à chaque niveau d'organisation d'un système dit « complexe »?

Le XXI^{e} siècle arrivant avec son lot d'innovations technologiques permettra sûrement d'aller encore un peu plus loin dans notre compréhension de ces phénomènes, en suivant la voie ouverte autour de Darwin.

■

(décembre 2009)